**David Stíbal**
Titulaire d'un *Master of Science in Chemical Technology*
de l'Ecole Polytechnique des Sciences Chimiques de Prague

UNIVERSITÉ DE NEUCHÂTEL

# Thiolato-Bridged Arene Ruthenium Complexes as Anticancer Agents

Thèse présentée à la Faculté des sciences,
Pour l'obtention du grade de Docteur ès sciences

**Membres du jury :**

| | |
|---|---|
| **Prof. Georg Süss-Fink** | Directeur de thèse, Université de Neuchâtel |
| **Prof. Reinhard Neier** | Rapporteur interne, Université de Neuchâtel |
| **Prof. Paul J. Dyson** | Rapporteur externe, EPF Lausanne |

Institut de Chimie de l'Université de Neuchâtel
Soutenue le 25.09.2015

Faculté des sciences
Secrétariat-décanat de Faculté
Rue Emile-Argand 11
2000 Neuchâtel - Suisse
Tél: + 41 (0)32 718 2100
E-mail: secretariat.sciences@unine.ch

# IMPRIMATUR POUR THESE DE DOCTORAT

**La Faculté des sciences de l'Université de Neuchâtel autorise l'impression de la présente thèse soutenue par**

## Monsieur David STIBAL

Titre:

## "Thiolato-bridged Arene Ruthenium Complexes as Anticancer Agents"

**sur le rapport des membres du jury composé comme suit:**

- Prof. Georg Süss-Fink, Université de Neuchâtel, directeur de thèse
- Prof. Reinhard Neier, Université de Neuchâtel
- Prof. Paul J Dyson, EPF Lausanne

Neuchâtel, le 7 octobre 2015

Le Doyen, Prof. B. Colbois

# Acknowledgements

The presented PhD thesis describes the results of the three years of research in the group of organometallic chemistry and molecular catalysis at the University of Neuchâtel, under the supervision of Professor Süss-Fink. Although most of the experimental work was done in a chemical laboratory, a rather solitary environment, this thesis would not have seen the light of day without the support, aid and input of mentors, colleagues and friends, all of whom had a profound impact on my performance, perseverance and overall mental health. All of the people named below will be thanked in person (in due time), but I would nonetheless like to mention them here, in a slightly more official manner, to acknowledge their contributions to this thesis.

First of all, I want to thank my thesis supervisor and mentor, Professor Georg Süss-Fink, who was a vital part of my PhD from the very beginning to the very end and played an essential role in my success in my doctorate studies. I have to thank Prof. Süss-Fink for offering me the position of PhD assistant and guiding me through the whole process of the doctorate studies, knowing very well from his considerable experience when to leave me to struggle with the problems at hand on my own, when to pressure me into working harder and when to allow me to relax a little before the next surge of effort. He also compelled me from the very beginning to use French over English, which was invaluable in the laboratory courses that I taught. I am grateful to him for all the scientific as well as the non-scientific discussions and for all the ways in which he helped develop my sense of scientific rigor, attention to detail and personal appreciation of good science, good food and the history of both.

I had the pleasure to discuss, on several occasions, with Professor Reinhard Neier, who did not hesitate to spend his valuable time to help me with problems in the organic chemistry part of my research and to offer the much needed and much appreciated mental support. I am also thankful for the time he devoted to reading my thesis and, particularly, for revealing some of the well-guarded secrets of the inner workings of the SNSF that might very well prove to be essential in my future career as a scientist.

I am grateful to Prof. Bruno Therrien for his expertise in X-ray crystallography and, especially in the last part of my studies, for his assistance with all aspects of the scientific research. The fruitful collaboration with PD Dr. Julien Furrer throughout the three years of my studies resulted in intellectually stimulating moments spent at the University of Bern and in several scientific publications, for which I am grateful to Julien and to the members of his group. I would further like to thank Prof. Paul J. Dyson for his help with the biological part of the thesis and for the time that he devoted to be a part of the jury of my thesis. I am thankful to Dr. Pavel Tomšík and everyone in the group of Prof. Martina Řezáčová in Hradec Králové for the pleasant three weeks I spent in their

group and especially to Pavel for introducing me to the art of *in vivo* experiments, as well as for the professional contacts he helped me obtain during my time in Hradec Králové.

The help I got from Federico, Lydia, Dr. Patrycja Nowak-Sliwinska and Dr. Tina Riedel is also highly appreciated.

Besides the official weekly group meetings, the most of the discussions regarding chemistry, publications or research in general happened in a less formal settings, either in the office or, better yet, in the pleasant environment of one of Neuchâtel bars over a beer. I have to stress here the importance of such discussions (the work-related ones, at least) and the beneficial effect they had on my motivation and on my passion for research. I have to thank people who participated in those discussions and who offered advice and support concerning difficult scientific as well as interpersonal problems. My thanks go especially to Thomas, my office mate, lab mate and for a brief period of time also a flat mate, for all the memorable moments, for the amusing and at times highly improbable discussions and notably for his patience and perseverance in improving my spoken and written French. I would further like to thank the members of the chemistry department, each of whom had an impact on my thesis in their own way – I am thankful to the past and present group members Jirka, Manu, Bing, Balázs, Minghui, Julien, Amine, Wassila, Raja, Gupta, Raja and Justin, my friends and colleagues from the other groups of the chemistry department William, Damien, Christian, Steeve, Yovana, Virginie, Pauline, Sara, Ewa, Luyen and Christelle, my apprentices Aurélie, Sébastien, Csilla and Tracy, also my ProVoc students Élodie, Marie-Nöelle, Dakota and David, and, importantly, all of the students (especially the pharmacy students) of the chemistry laboratory course that I taught during the course of my PhD.

I need to thank Armelle for the MS analyses of my compounds and her advice in this regard, Claudio and Diego for their help with NMR characterizations and the other employees of the university that were responsible for the smooth running of the institute, especially Mme Tissot and Mme Auclair for their assistance with the administrative part of everyday life at the University.

I was lucky enough to encounter a lot of very interesting people during my doctorate, both scientists and people outside my line of work, and I am happy to say that many of them became my friends. I have spent great moments with James, Eli and Marcello, for which I am grateful and I hope that our friendship will last beyond my stay in Switzerland. My teammates from the Marin squash club also played an important part in my life in Neuchâtel and I am thankful most importantly to Alex, for the lengthy semi-philosophical discussions that showed me the possibilities and depths of the French language and also to Claudio, my club mate and frequent supporter on squash tournaments. The people from the Toastmasters International shaped quite importantly my ability to present and to speak in front of an audience, a very important skill that I would have had

trouble mastering without their help; I highly value their advice and feedback. I also had the luck of meeting interesting and sympathetic people at scientific conferences and I hope that some of these contacts can extend beyond our professional interests.

I cannot forget to thank Prof. Petr Kačer and Ing. Jan Přech from the University of Chemistry and Technology in Prague and Prof. Jeroen A. van Bokhoven and Prof. Jacinto Sá from ETH Zurich, for my early formation during bachelor and master studies. The skills and knowledge that I obtained in their respective laboratories have served me as an extremely good basis for my doctorate studies.

Saving the best (the most important) for last, I have to thank my family, my brother and particularly my parents for their unending support during my studies, both personal and financial. Since these acknowledgements should probably stay relevant to my thesis and my stay in Neuchâtel, I will not (and cannot, possibly) mention all the things I would want to thank them for. I would, however, like to dedicate this thesis to my parents, to show my appreciation at least in this modest manner.

## Summary

Cancer is a major cause of morbidity and mortality in today's world, affecting populations in all countries and all regions. Although no drug or treatment able to cure cancer in all of its forms and variations was found so far, the clinical advancements of 20$^{th}$ and 21$^{st}$ century provided a number of effective drugs for specific types of cancers and had a significant effect on the survival and the quality of life of patients. One of these drugs, the platinum-based complex cisplatin, achieved almost 100% cure rate of testicular cancer, not only saving lives of thousands of patients every year but also overturning a paradigm of medicinal chemistry – it was the first metal-based anticancer drug used in the clinic. The success of cisplatin encouraged the search for new metal-based anticancer agents, which soon expanded to other metals, such as ruthenium. During the last three decades, numerous ruthenium-based compounds with interesting anticancer properties were prepared and thoroughly investigated, two of which (NAMI-A and KP1019) were ultimately introduced into clinical trials, showing the potential of ruthenium complexes in cancer therapy.

The goal of the presented thesis was to investigate the properties of dinuclear arene ruthenium thiolato-bridged complexes and to establish their potential as anticancer drugs. In the first part of the thesis, several monothiolato, dithiolato and trithiolato complexes were synthesized and evaluated for their stability and reactivity with biological substrates. The results were correlated with the *in vitro* anticancer activity of the three types of complexes and showed the most stable trithiolato complexes to be the most active against ovarian cancer cell lines. Subsequently, the most active trithiolato derivative, *diruthenium-1*, was thoroughly investigated *in vitro* and *in vivo* to establish the mode of action of this complex, showing its promising ability to influence the tumor growth and to prolong the survival of tumor-bearing mice.

In the second part of this thesis, three series of conjugates of the mixed trithiolato complexes were synthesized to demonstrate the potential of the coupling of dinuclear arene ruthenium complexes with biologically active organic molecules. Thus, the thiolato-bridged complexes were coupled with propargyl bromide, the resulting conjugates being available for the 1,3-Huisgen addition with tumor targeting compounds. Conjugates with ibuprofen were synthesized to investigate the effect of the antiinflamatory agent on the activity and selectivity of the resulting complexes towards cancer cells. Finally, conjugates of dinuclear trithiolato arene ruthenium complexes with alkylating agent chlorambucil were synthesized to show the effect of the two different modes of action of the conjugates on their activity *in vitro* and *in vivo*.

These results demonstrate the potential of the dinuclear thiolato-bridged arene ruthenium complexes as a versatile platform for the synthesis of anticancer agents with variable biological properties and modes of action.

## Key Words

Organometallic complexes, dinuclear arene ruthenium complexes, thiolato ligands, cytotoxicity, anticancer activity.

## Mots Clés

Complexes organométalliques, complexes dinucléaires arène ruthénium, ligands thiolato, cytotoxicité, activité anticancéreuse.

*…to those who made my childhood memories possible.*

# Table of Contents

# Chapter 1: Introduction

## 1.1 Cancer

*"… the renegade cells that form a tumor are the result of normal development gone awry. In spite of extraordinary safeguards taken by the organism to prevent their appearance, cancer cells somehow learn to thrive. Normal cells are carefully programmed to collaborate with one another in constructing the diverse tissues that make possible organismic survival. Cancer cells have a quite different and more focused agenda. They appear to be motivated by only one consideration: making more copies of themselves."*

From The Biology of Cancer, R. Weinberg, Garland Science, 2nd edition, 2014.

The adult human body is composed of approximately $10^{15}$ cells, many of which are required to divide and differentiate rapidly, in order to sustain their population and preserve the function of the tissue they form. Cells that have the capacity for division and differentiation are called stem cells. It can be calculated that there are about $10^{12}$ divisions per day in these stem cell compartments. Yet in spite of this enormous production of new cells, the majority of divisions proceeds without errors, owing to hundreds of genes that intricately control the process. Normal tissue growth requires a balance between the activity of the genes that promote cell proliferation and those that suppress it. It also relies on the activities of genes that signal when damaged cells should undergo apoptosis. In cancer cells, however, genetic mutations accumulated over time in their DNA are the cause of the suppression of some of those control mechanisms and signaling pathways, leading to malignant cells that grow and divide in an uncontrolled manner, invading normal tissues and organs and eventually spreading throughout the body. This growth and spreading of malignant cells is called cancer [1-4].

Cancer is a major cause of morbidity and mortality in today's world, with approximately 14 million new cases and 8 million cancer-related deaths in 2012, affecting populations in all countries and all regions. Among men, the five most common sites of cancer diagnosed in 2012 were lung (16.7% of the total), prostate (15.0%), colorectum (10.0%), stomach (8.5%) and liver (7.5%). Among women, the most common incident sites of cancer were breast (25.2%), colorectum (9.2%),

lung (8.7%), cervix (7.9%) and stomach (4.8%) [5-6]. Figure 1 shows the incidence and mortality of the most common cancers in the world [5].

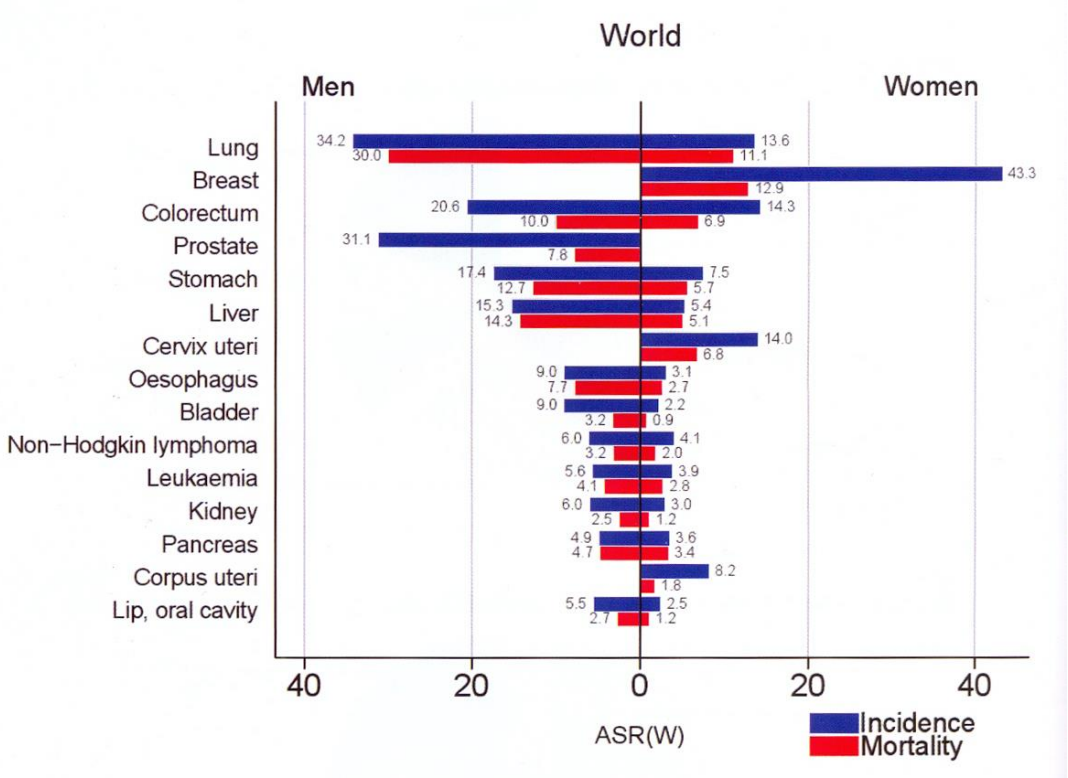


**Figure 1** - Cancer incidence and mortality rates per 100 000 by major sites in 2012 [5]

Since cancer can result from abnormal proliferation of any of the different kinds of cells in the body, there are more than a hundred distinct types of cancer, which can vary substantially in their behavior and response to treatment [4]. A summary of the overall pathological classification scheme of tumor types is presented in Figure 2. However, the entire spectrum of tumors that appear in various organs and tissues is difficult to capture in a single classification scheme, since it requires the use of histological features of tumors together with information about their tissues of origin, differentiation states and biological behavior. The scheme presented here allows the classification of the majority of human tumors [1].

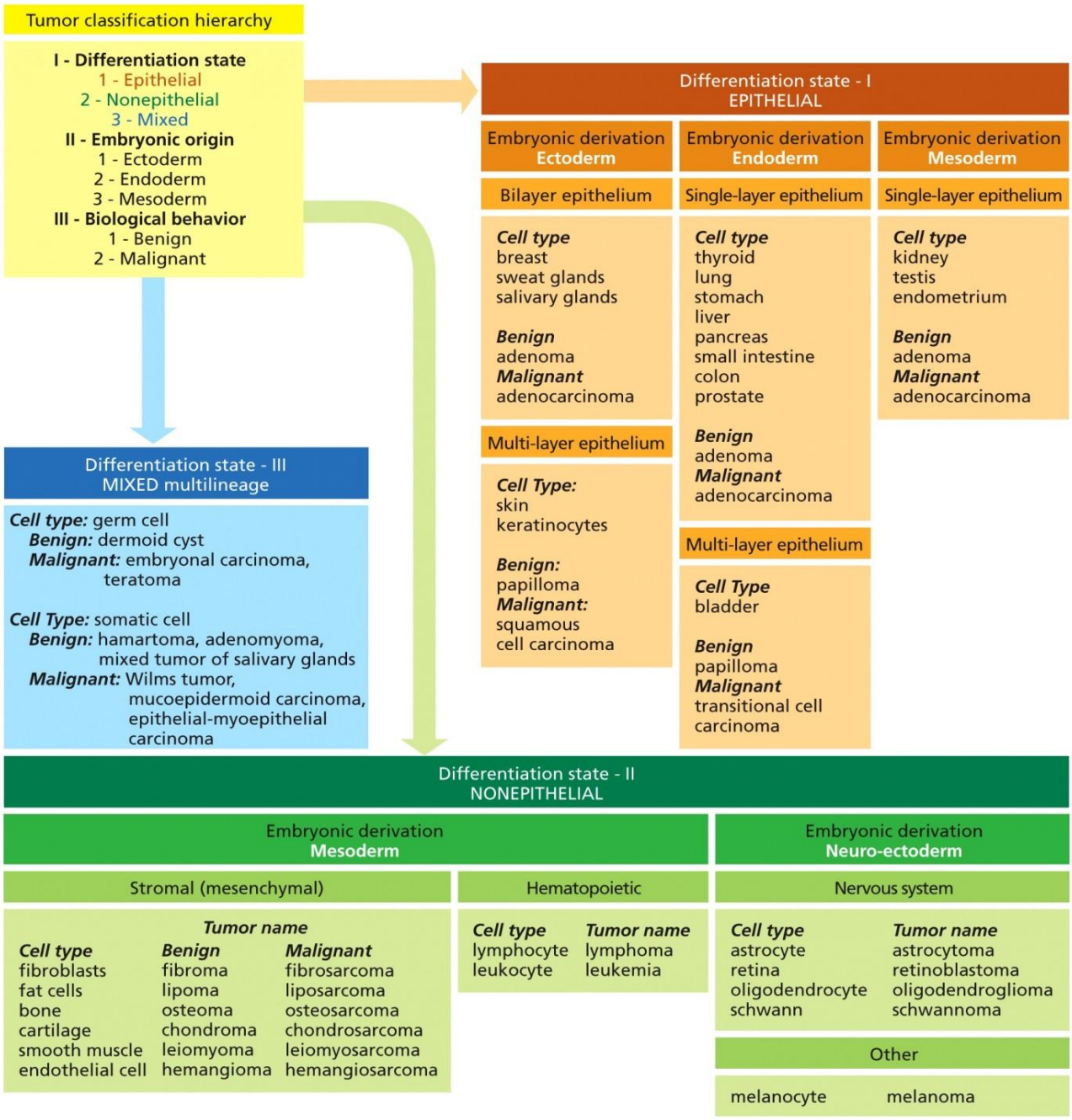


**Figure 2** - Classification of human tumors

The great majority of the commonly occurring cancers are caused by factors or agents that are external to the body and that somehow attack and corrupt its tissues. Those factors include lifestyle, diet, occupational exposure, viruses and carcinogens (substances causing cancer) [1].

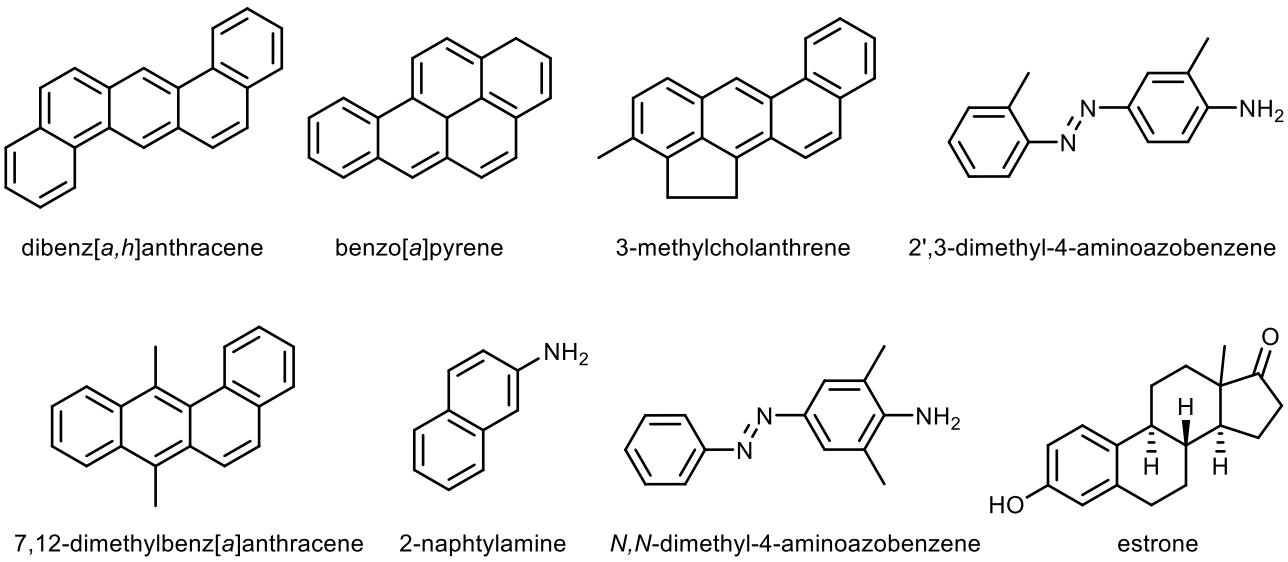


**Figure 3** – Examples of carcinogenic compounds

The development of cancer proceeds in three stages - initiation, promotion and malignant transformation. The initiators, such as some alkylating agents or polycyclic hydrocarbons, induce the first mutagenic changes to the cell, which then needs to undergo multiple other mutations before the cancer really develops. Agents called promoters are usually responsible for this. Promoters do not cause cancer by themselves; they increase cell division, which is required for the outgrowth of a proliferative cell population during early stages of tumor development. Promotion has no effect on cells that have not undergone initiation. Thus, several factors, often the combination of a susceptible cell and a carcinogen, are needed to cause cancer. Examples of tumor promoters are free radicals, hormones or immune system suppressors. The malignant transformation is then the process by which the first lesions, caused by initiators and promoters, are transformed into malignant cancers. This step can be caused by the same agents as the initiation. Some agents, such as certain polycyclic hydrocarbons or aromatic amines (Figure 3) are complete carcinogens, that is to say they are both initiators and promoters, being able to start cancer on their own [1,4,8].

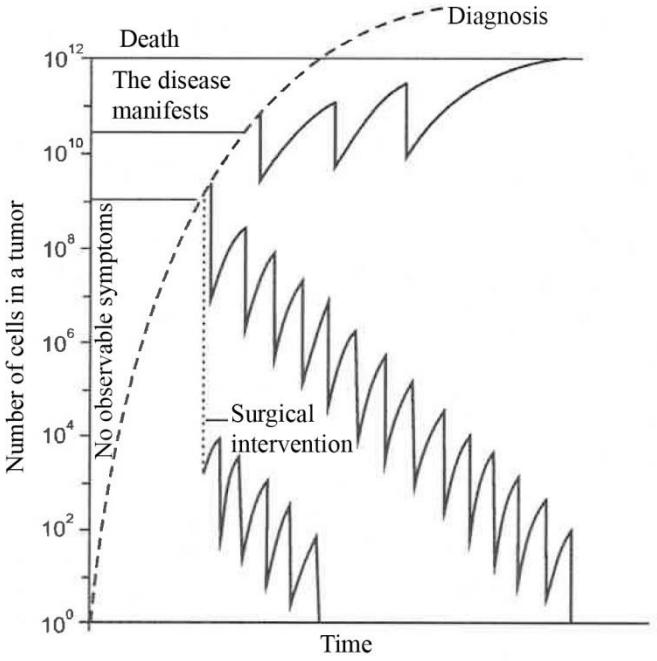


**Figure 4** - Progression of cancer depending on different treatment approaches [9]

In order to successfully cure cancer, it is necessary eliminate all of the cancerous cells in the body of the host (patient) and to eliminate any possibility of recurrence. To achieve this, a combination of approaches is often adopted – at first, surgical intervention is used to remove as much of the solid tumor as possible, followed by radiation therapy and several cycles of chemotherapy to kill all the remaining cancer cells in the body. The effectiveness of this approach, largely dependent on the early diagnosis of the disease, is demonstrated in Figure 4.

## 1.2 Chemotherapy

The term *chemotherapy* was coined at the beginning of 20$^{th}$ century by the famous German clinician Paul Ehrlich, who defined it as the use of chemicals to treat disease [10]. The original meaning of the world was rather broad, referring to the treatment of any disease by a chemical agent. In today's usage, chemotherapy refers mainly to the treatment of cancer, the original meaning is expressed by the word *pharmacotherapy*.

The first anticancer chemotherapeutic agents were developed based on the observation made during the World War II – the troops that were exposed to mustard gas showed notably depleted bone marrow and lymph nodes. This encouraged pharmacologists Alfred Gilman and Louis Goodman in 1943 to examine the potential therapeutic effects of the nitrogen mustard (Figure 5) on mice bearing transplanted lymphoid tumor. They observed clear regression of the tumor and followed up with an experiment on a human patient, obtaining the same surprising result.

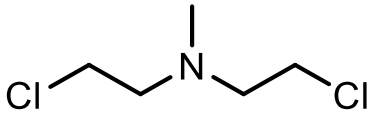


**Figure 5** - Nitrogen mustard HN2, mechlorethamine

This discovery led to the development of structural analogues of nitrogen mustards, with the aim of designing agents with lower general toxicity while preserving the anticancer effect of the compounds, at the time unparalleled. Several related alkylating agents were thus developed, including modern orally available drugs such as chlorambucil or cyclophosphamide [10].

The success of alkylating agents in 1940s followed by studies on tetrahydrofolate metabolism inhibitors proved for the first time that a chemical compound can be used to treat and possibly even cure cancer, an achievement many scientists at the time considered improbable at best [10]. Soon after, new targets for chemotherapeutic drugs started to be discovered and new families of cytotoxic compounds were developed, some of which ultimately proved highly efficient in treatment of various cancers. The overview of different types of chemotherapeutic agent in current clinical use is given below [11-12].

***Alkylating Agents***

Alkylating agents, in a medicinal sense, are compounds capable of interacting with DNA nucleobases. They are either electrophiles or generate electrophiles *in vivo* to produce polarized molecules that bind to the nucleophilic nitrogen of a nucleobase. This binding results in cross-linking or strand-breaking reactions that hinder the correct DNA replication and bring about, by various cellular mechanisms, the programmed death of the cell – apoptosis. Chlorambucil, cyclophosphamide or busulfan are examples of alkylating agents, the platinum chemotherapeutics cisplatin, oxaliplatin and carboplatin also belong to this group.

***Antimetabolites***

Low-molecular-weight compounds that exert their effect by virtue of their similarity with naturally occurring metabolites involved in nucleic acid synthesis are called anti–metabolites. Their similarity allows them to be incorporated in the nucleic acid and produce errors that inhibit DNA replication, other antimetabolites can influence critical enzymes involved in nucleic acid synthesis. The most often used antimetabolites are purine or pyrimidine analogs such as mercaptopurine, fludarabine or fluorouracil, or folic acid analogs such as methotrexate [1].

***Natural Products***

The natural products include mitotic inhibitors vincristine and vinblastine, found in the plant *Cataranthus roseus*, products from *Podophyllum peltatum* and *Camphoteca accuminata* affecting enzymes topoisomerase I and II, antitumor antibiotics, or antimicrobial compounds produced by *Streptomyces* species affecting the function and synthesis of nucleic acids. Examples of clinically used drugs include doxorubicin, paclitaxel, vincristine or topotecan.

***Hormones and Hormone Antagonists***

Clinically active anticancer hormones and hormone antagonists include steroid estrogens, progestins, androgens, corticoids and their synthetic derivatives, nonsteroidal synthetic compounds with steroid or steroid-antagonist activity, hypothalamic-pituitary analogs, and thyroid hormones. Each agent has diverse effects, whose relative roles are only partially

understood and can vary between tumor types. Examples of hormones and hormone antagonists are prednisone, tamoxifen or letrozole.

***Molecularly Targeted Agents***

Recent advances in oncology and the increased understanding of molecular events that are responsible for the development of cancer have made possible the development of new drugs with specific molecular targets. These highly specific drugs take advantage of the modern drug development approaches and are able to selectively influence specific enzymes in cancer cells or induce an immunological response of the organism against cancer cells. Imatinib or cetuximab are examples of molecularly targeted agents.

***Other Chemotherapeutic Drugs***

Other chemical agents with various ways of influencing cancer cells have been used in clinic, for example growth factor binding inhibitors (suramin), cytoprotectors (amifostine), somatostatin analogs (octreotide) or photosensitizing agents (porfimer).

In order to completely cure a patient of cancer, it is necessary to eradicate all the cancer cells present in the body, since even a single remaining cell is able to continue the uncontrolled division that defines cancer and can therefore cause a complete relapse of the disease [10]. Unfortunately, most tumors are heterogeneous, meaning that they contain populations of different cells, each population possessing different sensitivity to given chemotherapy treatment. This presents a significant problem inasmuch as, even if the majority of the tumor cells is killed by a chemotherapeutic agent, the remaining cells that are resistant to this treatment will continue to grow and the tumor will no longer respond to the treatment. As a measure to overcome this natural drug resistance, multidrug protocols were developed and applied with success. The first multidrug protocol was used in 1960s and was called '*VAMP*' – an abbreviation of four anticancer drugs *v*incristine, *a*methopterin, 6-*m*ercaptopurine and *p*rednisone that constituted the treatment. This program increased the remission rate of acute lymphotic leukemia to 60%, proving that combinations of drugs with different cellular targets can be beneficial for the success of chemotherapy [13].

As the understanding of cancer biology increases, new multi-drug treatment programs are developed, clearly showing the superiority of this approach over single-drug treatments. In order to address the issue of drug resistance of many cancers and to successfully fight all the existing types of the disease, new drugs with novel modes of action need to be developed and applied in the clinic, possibly in combination with other, already known agents [14].

## 1.3 Metal-Based Chemotherapeutics

Inorganic compounds have been used in medicine for almost 5000 years. As far back as 3000 years before Christ, the Egyptians used copper to sterilize water. Other precious metals such as gold and silver were used by Chinese, Egyptian, Greek, Indian and Arabic healers in cures of various sorts. Iron and zinc remedies were used since around 1500 BC. During the Renaissance period in Europe, mercurous chloride found use as a diuretic and was widely utilized along with other mercurial diuretics until 1950s. It was only at the beginning of the 19$^{th}$ century, however, that a more rational development of medicinal applications of inorganic compounds started to flourish. In 1908, Paul Ehrlich was the first to document the effectiveness of animal models in screening series of compounds to establish their activity against diseases. Using a rabbit model to screen compounds against syphilis, he discovered compound 606 (arsphenamine, marketed as Salvarsan), which was then used as a successful antisyphilitic, replacing the toxic mercury compounds used previously. Other metal-containing compounds of value were discovered and used in medicine during the 19$^{th}$ century, such as $K[Au(CN)_2]$ for the treatment of tuberculosis, pentavalent antimony compounds for the treatment of leishmaniasis [15] or gold complexes (mostly thiolates) against rheumatoid arthritis [16-18].

The first metal complex ever to be used in the field of anticancer chemotherapy was *cis*-diamminedichloridoplatinum(II), or cisplatin, whose anticancer properties were discovered serendipitously in 1965 [19] and which was approved for clinical use in 1978 [20]. Since then, platinum complexes are the most widely studied metal complexes in the field of cancer chemotherapy, but complexes of other platinum metals such as ruthenium, rhodium, palladium, osmium and iridium are also subject to detailed studies [21-22]. Only platinum complexes have so far been applied in the clinical practice, although several complexes of ruthenium as well as of some other metals (Fe, Zn, Ga, Mo, or Au) are currently undergoing clinical trials [23-24].

### 1.3.1 Platinum Compounds

Although platinum was probably known and used already in ancient times [25], the first European reference to the element 78 appears in 1557 in the works of the Julius Caesar Scaliger as a description of an unknown noble metal found near Mexico, *"which no fire nor any Spanish artifice has yet been able to liquefy"*. Pre-Columbian Indians apparently used white alloys of gold and

platinum, from which they made many little artifacts [26]. Being a subject of intensive studies in 18$^{th}$ and 19$^{th}$ century, platinum gradually found applications in jewelry, in the production of laboratory ware, in fuel cell electrodes [27] and later also as part of chemical catalysts and catalytic converters in cars. Currently, over 46% of the world production of platinum is used in vehicle emission control devices, 31% in jewelry and the rest in other applications, such as electrodes, catalysts in chemical industry or anticancer drugs [28].

Since the discovery of the biological properties of cisplatin by Rosenberg in 1965 [19], this simple inorganic complex has gradually found its way into the clinical practice and has become one of the most important drugs in cancer chemotherapy. Today, cisplatin is used in 32 of 78 treatment regimens listed in Martindale reference book in combination with a wide variety of other drugs including topoisomerase II inhibitors (doxorubicin, etoposide, mytomycin, bleomycin and epirubicin), nitrogen mustards (cyclophosphamide, melphalan and ifosfamide), antimetabolites (gemcitabine, 5-fluorouracil and methotrexate), vinca alkaloids (vinblastine and vinorelbine) and taxols (paclitaxel) [29]. Cisplatin has a central role in the treatment of testicular cancer, for which it has a 90% cure rate, with nearly a 100% cure rate for the early stage disease. It is also used in the treatment of ovarian, bladder, non-small cell lung and small cell lung cancer, melanoma, lymphomas and myelomas [30-31]. The limitations of cisplatin stem from the toxic side-effects of the drug, which arise from its indiscriminate uptake into all rapidly dividing cells. These side-effects include nephrotoxicity, neurotoxicity, myelosuppression, emetogenesis and ototoxicity. Some of these problems can be mitigated by supplementary drugs or treatments, such as antiemetics or hydration by saline solution [11,32].

Since 1970s, a plethora of structural analogs of cisplatin has been synthesized in order to find compounds with higher selectivity and therefore less severe side-effects as well as compounds active against different types of cancer. Insofar only two platinum compounds other than cisplatin (carboplatin and oxaliplatin) were approved for the use in the clinic worldwide; three other complexes of platinum ledaplatin, lobaplatin and heptaplatin (Figure 6) are used locally in Japan, China and Korea, respectively [32].

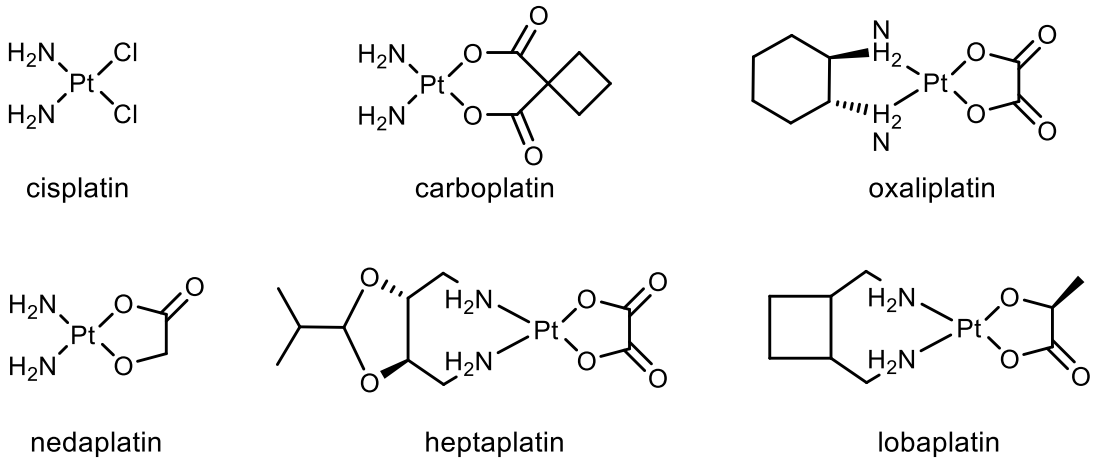


**Figure 6** - Structures of clinically used platinum(II) complexes

Apart from square-planar platinum(II) complexes, a large part of the research on platinum anticancer drugs concentrated on octahedral platinum(IV) complexes. The rationale is the following: The octahedral geometry allows the introduction of two additional ligands, providing further tuning of physico-chemical properties and the attachment of targeting ligands. Platinum(IV) complexes are also substantially more inert than the platinum(II) complexes and do not bind to intracellular proteins or thiols, which can lead to their increased bioavailability compared to platinum(II) compounds. Due to their inertness, platinum(IV) drugs are able to get internalized into the cancer cells before being reduced to the active platinum(II) species that ultimately bind to the DNA. An elegant description of the structure-activity relationship and drug design of platinum(IV) drugs based on the recent scientific discoveries is shown in Figure 7 [33].

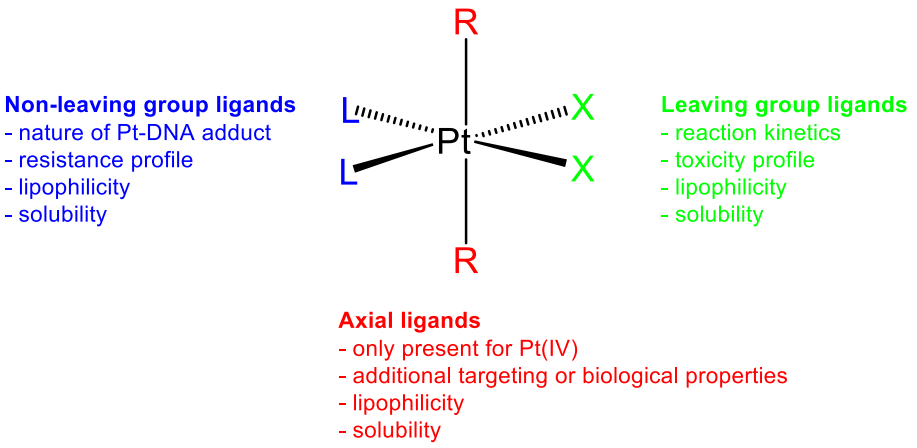


**Figure 7** - Influence of ligands on the behavior and activity of platinum(IV) complexes [33].

Despite the number of new platinum complexes that have been synthesized and tested for their anticancer activity, the problems mentioned previously for cisplatin still remain – the side effects, although significantly reduced in modern drugs such as carboplatin, are still an issue and the resistance (inherent as well as acquired) of certain cancer cells limit the scope of application of platinum drugs [34-36]. Therefore, many research groups have rather focused their efforts on other metals then platinum, in order to overcome the aforementioned problems [36].

One of the most successful metals in recent anticancer research is ruthenium [37].

### 1.3.2 Ruthenium Compounds

Discovered by Karl Ernst Claus (Karl Karlovich Klaus) in 1844 and named after Ruthenia (the latinised name for Russia) in the honor of the country where it was first identified [38], ruthenium was in fact the last one of the platinum metals to be discovered. Ruthenium is the element 44 of Mendeleev's periodic table, its molecular weight is 101.07 $g \cdot mol^{-1}$, its density is 12.41 $g \cdot cm^{-3}$ at 20°C, and seven isotopes are naturally occurring. The electronic configuration of ruthenium is Kr [$4d^7$] [$5s^1$] [39-40]. Ruthenium is a rare element, contained in the earth's crust in the concentration of about 1 ppb [41], but is relatively inexpensive compared with other group 8 metals [42]. Its isolation from platinum group metal ores is described in Figure 8.

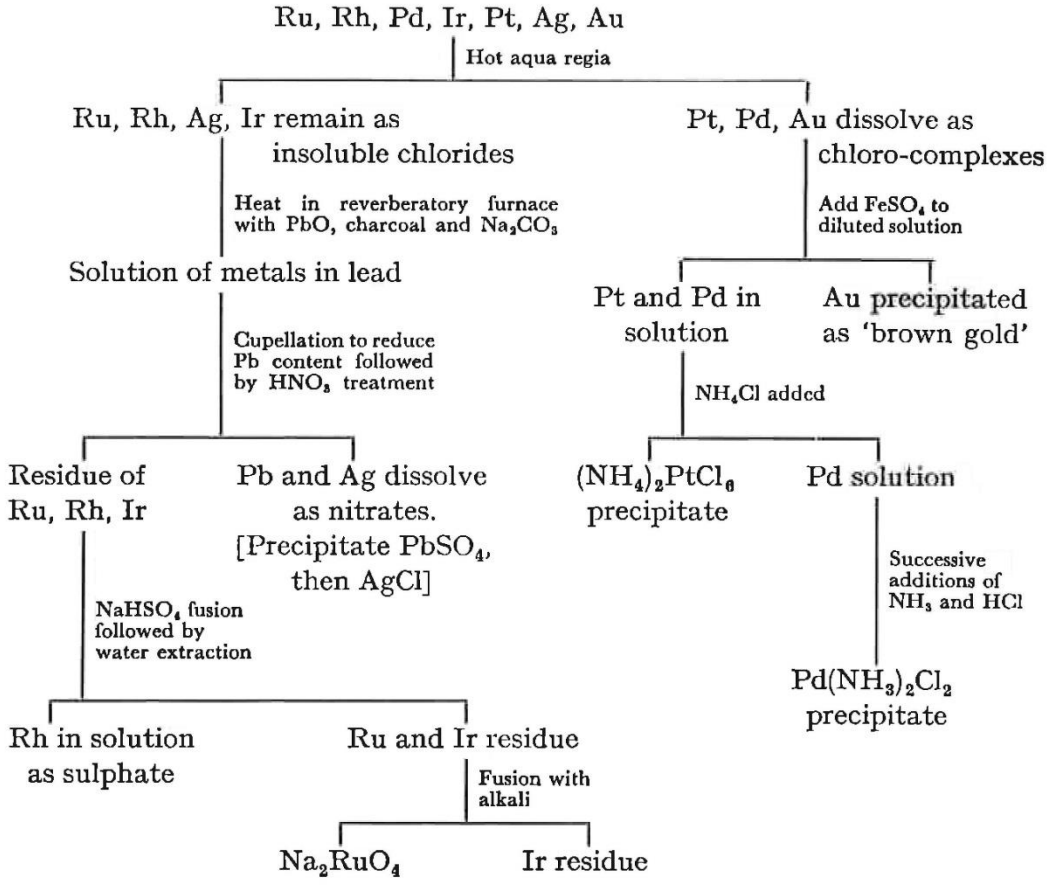


**Figure 8** - Isolation of platinum metals from metal ores [43]

The biological effects of ruthenium compounds have been studied since the mid-1950s [44], but these compounds have generally remained disregarded, partly because of their poor water solubility. Another reason was the discovery of the anticancer properties of cisplatin in 1965, which has inclined the research towards platinum compounds [45]. We can probably consider the pioneering work of Clarke in 1980 [46] as the impulse that started the thorough investigations on ruthenium complexes and their anticancer properties that last to this day. The main arguments in favor of ruthenium are the non-toxicity of the metal, the low general toxicity of most of its compounds, a wide range of oxidation state that ruthenium can access under physiological conditions and a very similar ligand exchange rate of platinum and ruthenium compounds (in both cases the ligand exchange processes are quite slow and may take hours, rates of exchange ranging from $10^{-3}$ to $10^{-2}$ $s^{-1}$, see Figure 9) [41,47].

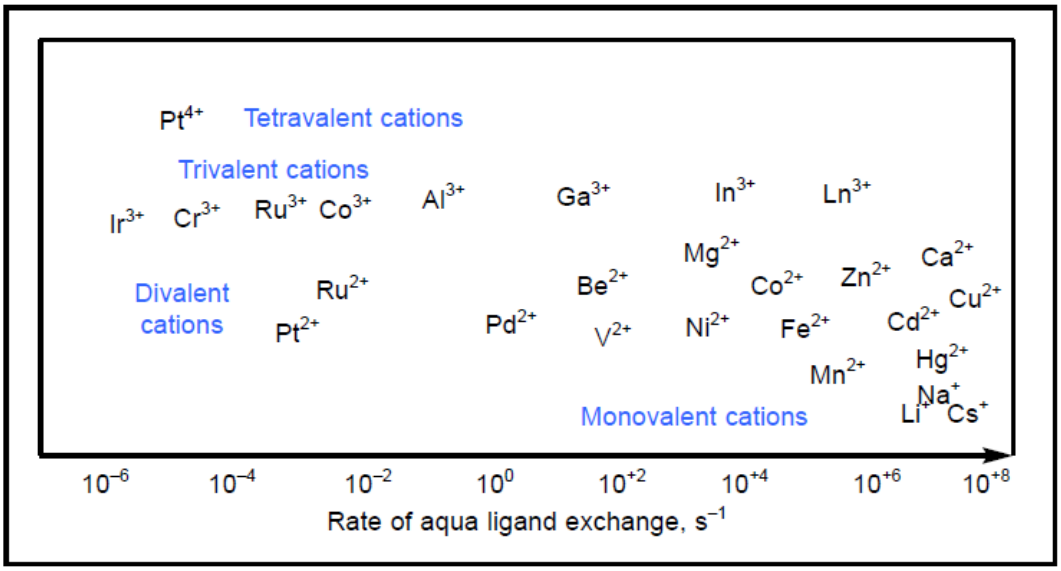


**Figure 9** - Ligand exchange of some metal ions [48]

As with platinum, a plethora of coordination complexes of ruthenium have been synthesized and studied. Among them, two complexes are currently undergoing clinical trials and can be therefore considered to be at the forefront of ruthenium chemotherapy. Those two complexes (Figure 10) are [indH]*trans*-[Ru(*N*-ind)$_2$Cl$_4$] named KP1019 and [imiH]trans-[Ru(N-imi)(S-dmso)Cl$_4$] named NAMI-A (imi being imidazole, dmso dimethyl sulfoxide and ind indazole) [49].

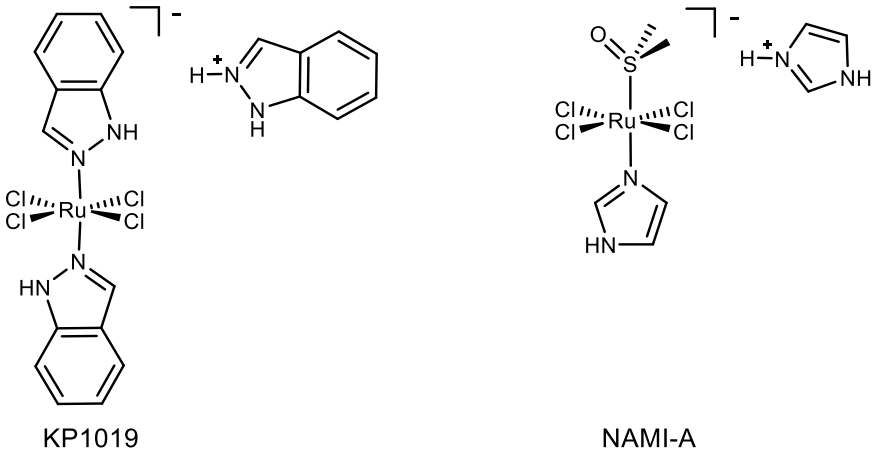


**Figure 10** - Structures of NAMI-A and KP1019

The mode of action of these two potential drugs differs from established platinum-based chemotherapeutic agents. The theory of activation by reduction, already postulated by Clarke in

1980 [46], states that ruthenium(III) complexes act as prodrugs, being little active and non-toxic. It is assumed that once they are delivered into the tumor, the physiological differences between the cancerous and healthy tissue (most importantly the reducing environment caused by the increased metabolic rate of the tumor cells) lead to the reduction of the Ru(III) complexes to the active Ru(II) species [45,50-51].

It is now well-recognized that immediately after intravenous administration, ruthenium-based anticancer drugs interact with serum proteins, such as albumin and transferrin. Transferrin, which is responsible for transporting iron through the body to supply the cells, may particularly serve as a natural route for the delivery of the cytotoxic Ru agents to tumor cells as a result of their higher demand for iron. Along with transferrin, the most abundant human plasma protein, albumin, displays high binding affinity and may contribute to the drug's cellular uptake via the enhanced permeability and retention (EPR) effect, but might also act as a reservoir for the transferrin cycle. The binding to proteins and the cellular uptake of the two drugs is followed by the activation by reduction, whereupon the compounds exhibit their anticancer properties in cancer cells (Figure 11) [50].

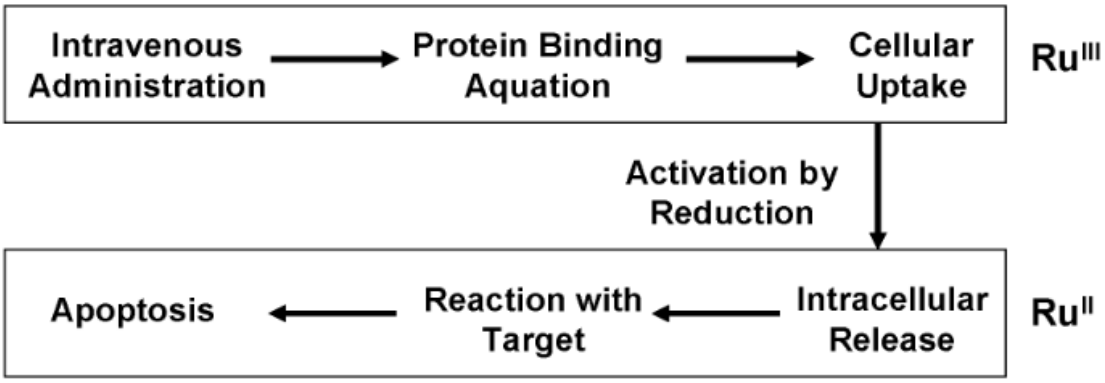


**Figure 11** - Mode of action of NAMI-A and KP1019 [50]

Although structurally similar (Figure 10), NAMI-A and KP1019 differ largely in their effects on primary solid tumors and metastases. NAMI-A, the first ruthenium anticancer compound to ever reach clinical trials [37], failed the usual screenings of putative anticancer agents, such as the National Cancer Institute (NCI, USA) screen against a panel of 60 cell lines. On the other hand it has been shown to prevent the development and growth of pulmonary metastases in all the solid tumors on which it has been tested. Metastases were inhibited independently of their stage of

growth. Such behavior is observed in the absence of activity against primary tumors [52]. Importantly, NAMI-A is active on lung metastases also when it is dosed by the per oral (p.o.) route. Metastases spawned by malignant tumors are responsible for about 90% of deaths from cancer [1], NAMI-A was therefore abandoned as a conventional chemotherapeutic agent in favor of its development as a selective antimetastatic compound [53]. The investigation of mode of action of NAMI-A showed that it undergoes aquation and hydrolysis within minutes in aqueous media at pH = 7.4 and 37°C [54], and is practically non-cytotoxic in common cancer cell lines [55]. These findings suggest that its activity is not related to DNA binding in the cell nucleus [56-57]. Interactions with actin-type proteins on the cell surface [58-59] or with collagens of the extracellular matrix [60-61], which preserves it from elimination and gives it prolonged contact with the metastatic cells in the lungs, have been suggested as possible mechanisms of anti-metastatic action of NAMI-A [61]. The recent results of combined phase I/II study of NAMI-A in combination with gemcitabine showed rather severe side-effects that were not discovered in the preclinical evaluations. The doses of 300 $mg/m^2$ and 450 $mg/m^2$ caused neutropenia, anemia, elevated liver enzymes, transient creatinine elevation, nausea, vomiting, constipation, diarrhea, fatigue, and renal toxicity. The combination of NAMI-A with gemcitabine was shown to be less active in non-small cell lung cancer patients than gemcitabine alone [62].

Contrary to NAMI-A, KP1019 is active against a wide range of primary tumors, in particular against platinum-resistant colorectal autochthonous tumors [63-64], its $IC_{50}$ value (50% inhibitory concentration) against SW480 cell line being 58.2 μM [65]. KP1019 induces apoptosis predominantly by the intrinsic mitochondrial pathway (loss of mitochondrial membrane potential in a high percentage of cells) and shows an activity superior to that of 5-fluorouracil in experimental therapy of autochthonous colorectal carcinoma. In early clinical trials, no dose-limiting toxicity was found, and the state of five out of six patients either stabilized or improved after the treatment with KP1019 [66]. Based on the recent results of the clinical evaluations of KP1019, its sodium analog NKP-1339 (sodium *trans*-[tetrachloridobis(1H-indazole)ruthenate(III)]), has been proposed as the lead compound in the further trials. The main reason for the use of NKP-1339 was its higher water solubility, which not only facilitates manufacturing and handling of the drug, but also allows clinical application of larger doses [67].

## 1.4 Arene Metal Complexes

The history of arene metal complexes starts with the discovery of ferrocene. In 1952, the groups of Ernst Otto Fisher and Geoffrey Wilkinson independently reported the structure of bis–(cyclopentadienyl) iron, previously prepared by Pauson, for which Mark C. Whiting suggested the name ferrocene (Figure 12) [68]. It was the first example of a so-called molecular sandwich complex, a type of structure hitherto unknown to chemists. The structure was not immediately accepted by the general scientific community (a reviewer of the Journal of the American Chemical Society wrote to Woodward in 1952: *"We have dispatched your communication to the printers but I cannot help feeling that you have been at the hashish again."* [69]), but when other groups confirmed the veracity of the structure by X-ray crystallography and molecular orbital theory studies, the skepticism disappeared.

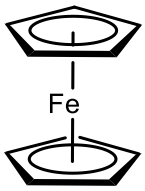


**Figure 12** - Structure of ferrocene

The first arene metal complex was presumably prepared by Franz Hein in 1918. With the intention of preparing triphenylchromium, Hein reacted phenylmagnesium bromide with $CrCl_3$ and obtained a mixture of products with surprising properties and of unknown structures. He then spent years of work trying to rationalize the unexpected behavior of his phenylchromium compounds, which, peculiarly, did not fit his theories. It was only after the discovery of ferrocene, and after the general acceptance of sandwich structure, that Harold H. Zeiss and Minoru Tsutsui proposed in 1953 the following sandwich structure for Heins' compounds (Figure 13).

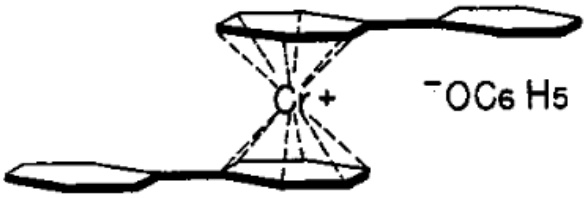


**Figure 13** – Sandwich structure of Heins' compound proposed by Zeiss and Tsutsui

As with ferrocene, the proposed structure did not convince the scientific community and it was not until 1957 that the full paper of Zeiss and Tsutsui was finally accepted. What made the publication possible was the synthesis of bis(benzene) chromium (Figure 14) by Ernst Otto Fischer and Water Hafner [70] by reacting $CrCl_3$, Al and $AlCl_3$ and reducing the resulting orange solid with sodium dithionite in aqueous NaOH [71-72].

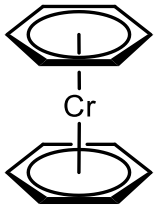


**Figure 14** - Structures of bis(benzene) chromium

The discovery of ferrocene, bis(benzene) chromium, and the work on the chemistry of sandwich complexes earned Ernst Otto Fisher and Geoffrey Wilkinson a 1973 Nobel Prize in Chemistry [73].

### 1.4.1 Arene Ruthenium Complexes

The first arene ruthenium complex was prepared by Winkhaus and Singer in 1967 by reduction of ruthenium trichloride hydrate in the presence of 1,3-cyclohexadiene. This neutral diamagnetic complex was obtained as a brown precipitate, for which a polymeric structure (Scheme 1) was first proposed [74].

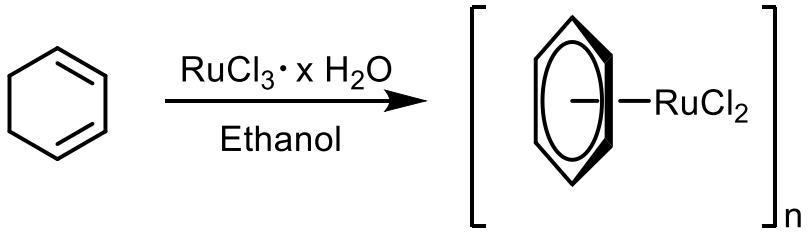


**Scheme 1** – Synthesis of benzene ruthenium dichloride dimer and its proposed polymeric structure

In 1972 Baird and Zelonka showed this polymeric formula to be erroneous and suggested a dimeric structure [75], analogous to the complexes $[(\eta^5\text{-}C_5H_5)M(\mu^2\text{-}Cl)Cl]_2$ (M = Ir, Rh) published

by Maitlis in 1969 [76]. Eventually, in 1974, Bennett confirmed this dimeric structure $[(\eta^6\text{-}C_6H_6)Ru(\mu^2\text{-}Cl)Cl]_2$, in which each ruthenium atom has the oxidation state +II, the two ruthenium centers are linked by two chlorido bridges and where the arene is a $L_3$ ligand (Figure 15) [77].

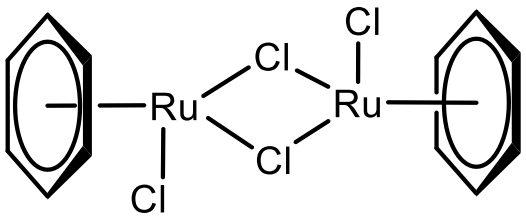


**Figure 15** – Structure of benzene ruthenium dichloride dimer

The robust nature of the organometallic scaffold of ruthenium arene compounds presents an ideal template for rational drug design. The hydrophilic nature of the metal and the hydrophobic nature of the arene ligand make those complexes highly versatile. The arene can be functionalized with many types of groups in order to change the solubility of the complex or even to deliver the final compound to specific cellular targets, whereas the σ-ligands can be tuned to change the hydrolysis behavior or to achieve charged complexes with increased solubility in water [47,78].

The first anticancer arene ruthenium complex was synthetized by Tocher in 1992 by coordinating metronidazole [1-β-(hydroxyethyl)-2-methyl-5-nitro-imidazole] to a benzene ruthe–nium dichlorido fragment, which resulted in a cytotoxicity enhancement [79]. Later on, the field of arene ruthenium anticancer complexes was pioneered individually by the groups of Dyson and Sadler with their respective prototype compounds $[(\eta^6\text{-}p\text{-}MeC_6H_4Pr^i)Ru(P\text{-pta})Cl_2]$ (pta is 1,3,5-triaza-7-phosphatricyclo[3.3.1.1$^{3,7}$]decane), named RAPTA-C [80], and $[(\eta^6\text{-}PhC_6H_5)Ru(en)Cl]^+$ (en is 1,2-diaminoethane), named RM175 [81] (Figures 16 and 17).

RAPTA compounds are characterized by a monodentate 1,3,5-triaza-7-phosphatricyclo-[3.3.1.1$^{3,7}$]decane ligand and a $\eta^6$-arene ligand bound facially to the metal center (Figure 16). They are generally air-stable complexes with good thermodynamic stability. Two lead compounds in the series are RAPTA-T, $[RuCl_2(\eta^6\text{-toluene})(pta)]$ and RAPTA-C $[RuCl_2(\eta^6\text{-}p\text{-cymene})(pta)]$. Both compounds were found to be only poorly toxic towards cancer cells and completely non-toxic to non-tumorigenic (healthy) cells *in vitro*. Like NAMI-A, RAPTA compounds failed the NCI screening process [82]. *In vivo*, RAPTA-T was found to inhibit lung metastases in mice bearing the MCa mammary carcinoma, although again with only mild effects on primary tumors. Like

NAMI-A, extremely low general toxicity combined with excellent clearance rates was observed [52]. RAPTA-C also displays antimetastatic activity [82] and also increases the survival of mice bearing Ehrlich Ascites Carcinoma [83]. Further studies of RAPTA-C i*n vivo* showed that it inhibits cell growth by triggering G2/M phase arrest leading to apoptosis. Treatment with RAPTA-C also upregulates p53, triggering the mitochondrial apoptotic pathway. Moreover, increased cytochrome c levels induced by RAPTA-C suggest the activation of procaspase-9, an effect that has been linked to apoptosis. These facts indicate that RAPTA-C acts on various molecular pathways and does not bind to a single target. Such conclusion is perhaps not unexpected given the relatively simple structures of RAPTA complexes, which can bind to many different biomolecules [83].

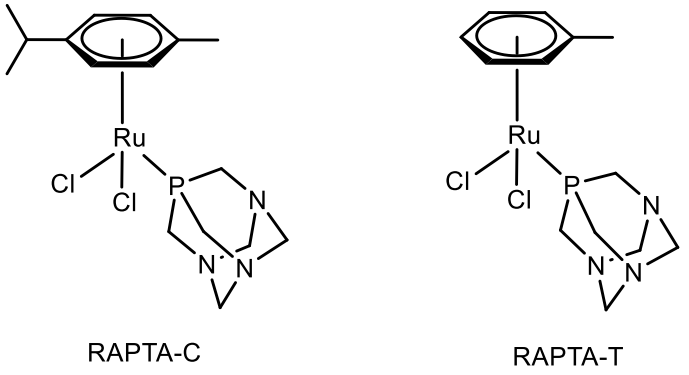


**Figure 16** – Structures of RAPTA-C and RAPTA-T

A number of parameters have been varied in the RAPTA series, using approaches characte–ristic to medicinal chemistry, in order to improve their efficacy and to test various hypotheses regarding their mode of action [52]. Replacement of *p*-cymene in the RAPTA-C complex with different arene ligands such as benzene, toluene and hexamethylbenzene only slightly changes the cytotoxic activity [84]. By contrast, the insertion of a cyclopentadienyl system as aromatic ligand shows a remarkable cytotoxicity dependence on the substituents at the ring [85]. Substitution of the hydrolysis-susceptible chlorido ligands with other anionic ligands such as bromido, iodido and isothiocyanato ligands does not result in large differences in terms of cytotoxicity [86]. However, certain aquation-resistant RAPTA complexes with chelating diketone (acac) ligands exhibit cytotoxicity profiles different to classical RAPTA complexes [87-88]. These observations indicate that the speed of aquation is not essential for reactions of RAPTA complexes with biomolecules, although it influences their behavior in some cancer cell lines [89]. The replacement of the pta ligand by the *N*-methylated pta-$Me^+$ causes the loss of selectivity for cancerous and non-

tumorigenic cell lines, showing that the water-soluble phosphine pta ligand plays an important role for the selectivity of RAPTA compounds [82]. Functionalization of the arene ligand in RAPTA complexes has also been used for tumor targeting. The RAPTA scaffold was functionalized by a benzaldehyde moiety that can be conjugated to specific target groups and was used to tether RAPTA derivatives to human serum albumin via a hydrazone bond that may be cleaved at low pH [90]. The significant enhancement in the cytotoxicity of the RAPTA structure following attachment to human serum albumin, which leads to increased internalization of the compound, indicates that the antimetastatic effect of RAPTA compounds may be due to extracellular events, and that once inside the cell, RAPTA compounds are quite cytotoxic. The importance of the extra- and intracellular effects of these compounds has yet to be quantified [89].

The studies of the Sadler group focused on monofunctional ruthenium(II) arene anticancer complexes of the type $[(\eta^6\text{-arene})Ru(ethylenediamine)(X)]^{n+}$, where X is a leaving group (e.g. Cl). In these pseudooctahedral ‘‘piano-stool’’ Ru(II) complexes, a π-bonded arene occupies three coordination sites, and the ethylenediamine (en) and X fill the remaining three sites (Figure 17). In contrast to the phosphine complexes of the RAPTA family that exhibit only low cytotoxicity *in vitro* but a high metastatic activity *in vivo* [82], the cationic arene ruthenium complexes containing ethylenediamine chelating ligands show very high cytotoxicities *in vitro* as hexafluorophosphate salts, and they are also very active *in vivo* [47].

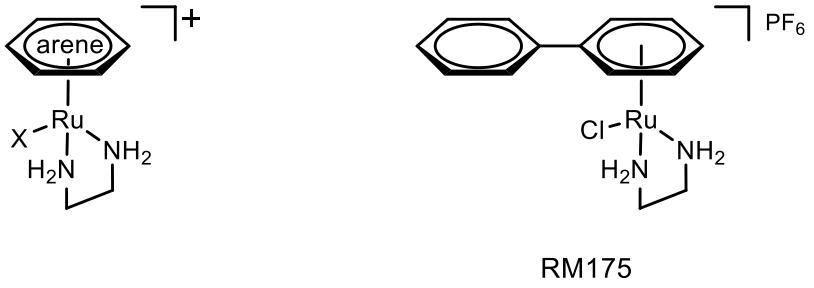


**Figure 17** – General structure of Ru(en) complexes and the structure of the RM175

The investigation of the mode of action of these Ru(en) complexes showed that, similarly to cisplatin, those complexes bind specifically to guanines of the DNA double-helix and form G7- or G8- monoruthenated species as well as G7, G8-diruthenated species [91]. The π-π stacking between multiring (biphenyl, dihydroanthracene or tetrahydridoanthracene) arene ligand and the DNA nucleobase was also shown to take place and was confirmed by X-ray crystallography [92],

although the guanine binding is preferential [93]. Interactions with other biomolecules, such as amino acids [94-95], peptides [96], proteins [95], and DNA bases [97] were also observed. These interactions were shown to involve, as the first step, the hydrolysis of the ruthenium-halide bond, the aqua ligand being then much more reactive towards biomolecules. The influence of structural variations on the rate of hydrolysis was therefore extensively studied using different arenes (hexamethylbenzene = hmb, *para*-cymene = *p*-cym, indane = inda, biphenyl = bip, benzene = bz, tetrahydroanthracene = tha and dihydroanthracene = dha) and different leaving groups X (Br, Cl, I, $N_3$). The variations of arene ligand showed that the hydrolysis rate decreases with increase in the electron accepting ability of the arene (hmb < *p*-cym < inda ≈ tha ≈ dha < bip < bz), whereas the rates of the hydrolysis of the halide and azide complexes followed the order Br ≈ Cl > I > $N_3$. This correlated with the cytotoxicities of the studied complexes, generally showing that the complexes that readily hydrolyze exhibit high cytotoxicities, those that do not hydrolyze are inactive or weakly active [98]. The variations of the bidentate ligand showed that it is vital for the anticancer activity, analogs containing two monodentate N-donor ligands instead of the en ligand showed almost no activity towards the A2780 ovarian cancer cell line [91].

### 1.4.2 Dinuclear Arene Ruthenium Thiolato-Bridged Complexes – State of the Art

The versatility of arene ruthenium complexes can be exploited to produce a plethora of complexes with diverse structural features, which are not limited to classical mononuclear piano-stool complexes - multinuclear arene ruthenium complexes are also frequently studied. Dinuclear complexes with pyridone-derived linkers were synthesized by Hartinger *et al*. and showed to be active against ovarian and colon cancer cell lines [99]. Sadlers' dinuclear arene ruthenium complexes containing 2,3-bis(2-pyridyl)pyrazine (dpp) as doubly chelating ligands have been studied for their potential in photodynamic therapy [100]. Water-soluble chloride or tetrafluoroborate salts of the cationic trinuclear arene ruthenium clusters $[(\eta^6\text{-}C_6Me_6)_2(\eta^6\text{-}C_6H_6)Ru_3(\mu^2\text{-}H)_3(\mu^3\text{-}O)]^+$ and $[(\eta^6\text{-}C_6Me_6)(\eta^6\text{-}p\text{-}MeC_6H_4Pr^i)(\mu^6\text{-}C_6H_6)Ru_3(\mu^2\text{-}H)_3(\mu^3\text{-}O)]^+$ were found to be cytotoxic against human ovarian cancer cells [101]. Biological properties of other tetranuclear ruthenium clusters [102-103], as well as of supramolecular arene ruthenium assemblies of various geometries were also investigated [45].

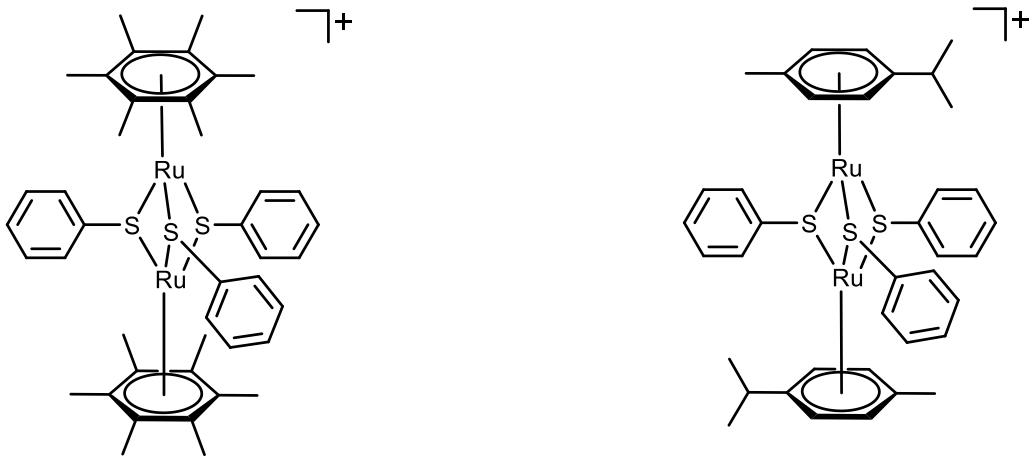


**Figure 18** – First two examples of dinuclear thiolato-bridged arene ruthenium complexes [104-105]

In 1992, the reaction of the dimeric arene ruthenium dichloride dimers $[(\eta^6\text{-arene})_2Ru_2Cl_4]$ with thiols gave rise to the cationic trithiolato complexes of the type $[(\eta^6\text{-arene})_2Ru_2(\mu\text{-SR})_3]^+$, the first examples being the hexamethylbenzene derivative $[(\eta^6\text{-}C_6Me_6)_2Ru(\mu\text{-}SC_6H_5)_3]^+$ reported by H. T. Schacht *et al.* [104] and the *p*-cymene derivative $[(\eta^6\text{-}p\text{-}MeC_6H_4Pr^i)_2Ru(\mu\text{-}SC_6H_5)_3]^+$, reported by K. Mashima *et al.* [105], both containing three thiophenolato bridges. The series was completed in 2003 by the synthesis of the *p*-bromothiophenolato derivative $[(\eta^6\text{-}p\text{-}MeC_6H_4Pr^i)_2Ru_2(\mu\text{-S-}p\text{-}C_6H_4Br)_3]^+$ [106-107], the *p*-methylthiophenolato and *p*-hydroxythiophenolato derivatives $[(\eta^6\text{-arene})_2Ru_2(\mu\text{-S-}p\text{-}C_6H_4X)_3]^+$ (arene = $C_6H_6$, $p\text{-}MeC_6H_4Pr^i$, $C_6Me_6$; X = Me, OH) [107], as well as the 2-hydroxyethylthiolato derivatives $[(\eta^6\text{-arene})_2Ru_2(\mu\text{-}SCH_2CH_2OH)_3]^+$ (arene = $C_6H_6$, $p\text{-}MeC_6H_4Pr^i$, $C_6Me_6$) [108]. The chloride salts of the trithiolato complexes $[(\eta^6\text{-arene})_2Ru_2(\mu\text{-SR})_3]^+$ were found to be highly cytotoxic for human ovarian cancer cells [109], they are in fact among the most active ruthenium anticancer compounds [37,45,84,110]. The $IC_{50}$ values of these compounds are in the nanomolar range for A2780 human ovarian cancer cells and for their cisplatin-resistant mutant A2780cisR [111-113]. It was shown that these complexes, the most active derivative being the $[(\eta^6\text{-}p\text{-}MeC_6H_4Pr^i)_2Ru_2(\mu\text{-S-}p\text{-}C_6H_4Bu^t)_3]^+$ ($IC_{50}$ = 30 nM for both A2780 and A2780cisR cell lines) [111], are highly efficient catalysts for the oxidation of glutathione in aqueous solution, which may at least partly explain their high cytotoxicity [114].

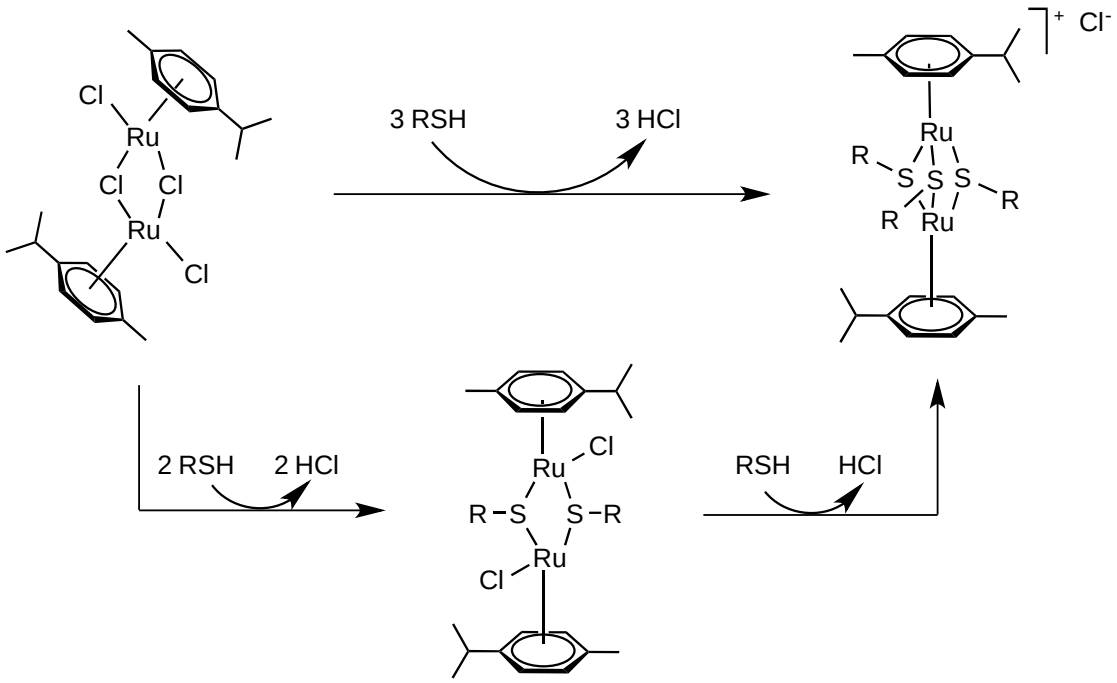


**Scheme 2** - Intermediacy of dithiolato complexes in the formation of trithiolato complexes [115]

The synthesis of the trithiolato complexes $[(\eta^6\text{-arene})_2Ru_2(\mu\text{-SR})_3]^+$ was recently shown to proceed through the intermediacy of the dithiolato complexes $[(\eta^6\text{-arene})_2Ru_2(\mu\text{-SR})_2Cl_2]$, several representatives of which could be isolated and structurally characterized in the case of aliphatic thiolato ligands [115] (see Scheme 2).

## 1.5 Aim of this Work

This thesis aims to investigate the properties of the thiolato-bridged dinuclear arene ruthenium complexes synthesized previously in our group. In order to understand the fate of a compound in a biological system, the behavior of this compound must be thoroughly studied, starting at first by experiments under laboratory conditions, then by *in vitro* tests on cell lines or specific isolated receptors, followed by *in vivo* studies on animal models, such as mice, rats or rabbits. The knowledge of the precise interactions and chemical changes that the complexes undergo in biological system is vital to design a successful selective anticancer agent. Therefore, with the assistance of research groups from Switzerland (Paul J. Dyson at EPFL, Julien Furrer at the University of Bern) and the Czech Republic (Martina Řezáčová at the Charles University in Hradec Králové), an effort will be made to study the mode of action of trithiolato complexes, as the reason for their high anticancer activity is so far unknown.

The second goal of the presented PhD thesis is to investigate the effect of the coupling of well-established organic anticancer drugs as well as other molecules with known anticancer properties to ruthenium complexes. The benefits of this approach have already been demonstrated in several cases, proving that organic compounds with well-defined molecular targets can enhance the anticancer activity and selectivity of ruthenium complexes. Conjugates of thiolato-bridged arene ruthenium complexes with chemotherapeutic drugs or bioactive molecules will thus be synthesized and their biological properties and modes of action will be investigated.

# Chapter 2: Properties of Dinuclear Arene Ruthenium Thiolato Complexes

The trithiolato dinuclear arene ruthenium complexes were first synthesized in our group in 2003, originally for their use as precursors of star-like oligophenylene dendrimers [116]. It was only in 2010 that their anticancer properties were evaluated *in vitro* and their high cytotoxicity against ovarian cancer cells A2780 and A2780cisR was discovered [117]. Since then, several series of the complexes of the general formula $[(\eta^6\text{-arene})_2Ru_2(\mu\text{-SR})_3]^+$ were prepared and their anticancer activity assessed. The $IC_{50}$ values of all the derivatives are systematically in the nanomolar range for both cisplatin-sensitive and cisplatin-resistant cancer cells [111-115,117]. The recently discovered dithiolato complexes [115] are less cytotoxic, their $IC_{50}$ values being in the micromolar range.

Despite the number of synthesized compounds, the reason for the high cytotoxicity of dinuclear thiolato arene ruthenium complexes is not yet understood. The only indication for the possible mode of action is their ability to catalyze the oxidation of glutathione, an important intracellular antioxidant. The ratio between the reduced (GSH) and the oxidized (GSSG) form of the glutathione was found to differ in cancer cells and in healthy cells [118] and the depletion of GSH is believed to have an effect on the efficacy of the cancer treatment [119], the catalytic activity of the complexes could therefore offer a partial explanation for their high anticancer activity.

In this chapter, the chemical properties, the stability, the reactivity and the *in vitro* and *in vivo* behavior of the thiolato-bridged arene ruthenium complexes are investigated, with the goal of learning the reasons for their cytotoxic properties.

## 2.1 Stepwise Synthesis of Dinuclear Trithiolato Arene Ruthenium Complexes

**Adapted from:** D. Stíbal, B. Therrien, F. Giannini, L.E.H. Paul, J. Furrer, G. Süss-Fink, Monothiolato-Bridged Dinuclear Arene Ruthenium Complexes: The Missing Link in the Reaction of Arene Ruthenium Dichloride Dimers with Thiols, *European Journal of Inorganic Chemistry*, **2014,** 34, 5925-5931.

### 2.1.1 General

The dithiolato complexes reported in 2012 [115] showed that it is possible to isolate intermediates in the synthesis of trithiolato complexes, if the conditions and the chemical properties of thiols are carefully chosen. Although monothiolato complexes are also expected as intermediates, they have never been isolated or observed so far from this reaction. Apart from the chelating amino-thiolato complexes $[(\eta^6\text{-}p\text{-}MeC_6H_4Pr^i)_2Ru_2(\mu\text{-}N,S\text{-}L)(\mu\text{-}Cl)]^+$ (LH = 2-mercapto-1-methylimidazole or 4,5-diphenyl-2-mercaptoimidazole) [120] and $[(\eta^6\text{-}C_6Me_6)_2Ru_2(\mu\text{-}N,S\text{-}L)(\mu\text{-}Cl)]^+$ (LH = 2-aminoethylthiol or 2-dimethylaminoethanethiol) [121], the only dinuclear monothiolato arene ruthenium complexes known so far are the dihydrido complexes $[(\eta^6\text{-arene})_2Ru_2(\mu\text{-S-}p\text{-}C_6H_4\text{-X})(\mu\text{-H})_2]^+$ (arene = $C_6Me_6$, 1,2,4,5-$Me_4C_6H_2$; X = Me or Br) [122].

### 2.1.2 Results

When we tried to synthesize the known [115] dithiolato complex $[(\eta^6\text{-}p\text{-}MeC_6H_4Pr^i)_2Ru_2Cl_2(\mu\text{-}SCH_2C_6H_5)_2]$, we found the product to be contaminated by another compound that appeared to be the predicted monothiolato intermediate $[(\eta^6\text{-}p\text{-}MeC_6H_4Pr^i)_2Ru_2Cl_2(\mu\text{-Cl})(\mu\text{-}SCH_2C_6H_5)]$ (**1**). By modifying the reaction conditions, it was possible to obtain this complex as the main product; however, in our hands it was not possible to separate the mono- and the dithiolato complexes by chromatographic methods. We therefore decreased the reactivity of the thiol by introducing electron-withdrawing or sterically demanding substituents. Using the modified reaction conditions, monothiolato derivatives **1** – **4** $[(\eta^6\text{-}p\text{-}MeC_6H_4Pr^i)_2Ru_2Cl_2(\mu\text{-Cl})(\mu\text{-SR})]$, (R = $CH_2C_6H_5$, **1**, *p*-$CH_2C_6H_4NO_2$, **2**, $C_{10}H_{15}$, **3**, *m*-9-$B_{10}C_2H_{11}$, **4**) were synthesized. Complexes **1** and **2** are formed in a mixture with the corresponding dithiolato complex, while complexes **3** and **4** are obtained free of the corresponding dithiolato complex; **3**, however, being contaminated with the starting ruthenium

*para*-cymene dichloride dimer. In our hands, it was not possible to eliminate the contaminations of **1** and **3** by chromatographic methods. Although we managed to grow a single crystal of **1** by vapor diffusion, we did not succeed in isolating larger quantities by crystallization. Therefore, only **2** and **4** could be obtained in an analytically pure form. Complexes **1** – **4** (Figure 19) are orange to red solids that are stable in air and well soluble in dichloromethane, methanol and ethanol.

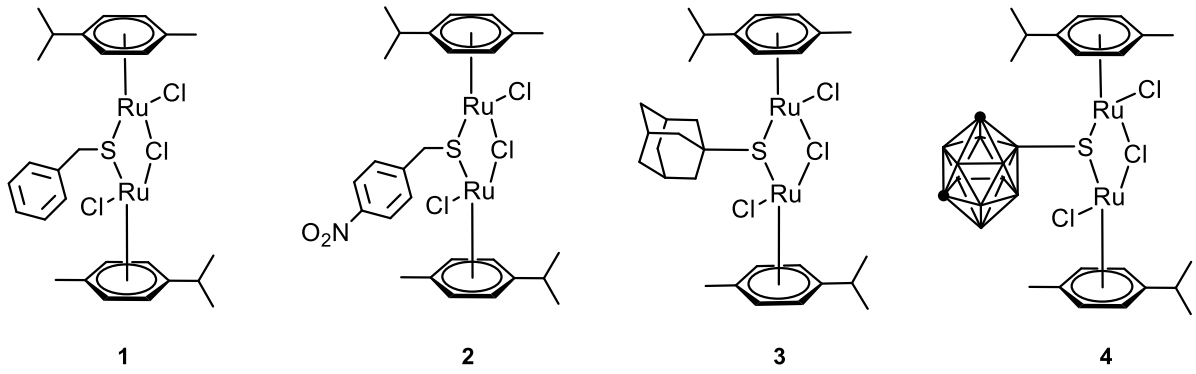


**Figure 19** - Monothiolato complexes **1** – **4**, the symbols • in the formula of **4** representing the CH groups of the carborane

Complexes **1** – **4** have been characterized by $^{1}H$ and $^{13}C$ NMR and mass spectroscopy, **2** and **4** also by correct micro-analytical data, the molecular structure of **1** and **2** was solved by X-ray crystallography. The spectroscopic and analytical data are given in the Chapter 9.4.1. Suitable crystals for X-ray analysis were obtained for the benzylthiolato derivative **1** and for the 4-nitrobenzylthiolato derivative **2** by vapor diffusion of diethylether into the dichloromethane solution of the complex. The molecular structures shown in Figure 20 can be described in terms of two *p*-cymene ruthenium units held together by one μ-bridging thiolato unit and one μ-bridging chlorido unit. Selected bond lengths and angles are listed in Table 1. In accordance with the electron count of 36, there is no metal-metal bond, the distance between the two ruthenium atoms being 3.6617(6) Å and 3.6555(4) Å, respectively. Both structures compare well with those of the dithiolato complex $[(\eta^6\text{-}p\text{-}MeC_6H_4Pr^i)_2Ru_2Cl_2(\mu\text{-}p\text{-}SCH_2C_6H_4Bu^t)_2]$ [115] and of the trithiolato complex $[(\eta^6\text{-}p\text{-}MeC_6H_4Pr^i)_2Ru_2(\mu\text{-}SCH_2C_6H_5)_3]^+$ [105], where the ruthenium-ruthenium separations are 3.674(2) Å and 3.3489(8) Å, respectively. This is in contrast to the dinuclear pentamethylcyclopentadienyl ruthenium monothiolato complexes, in which there is a metal-metal bond: $[(\eta^5\text{-}C_5Me_5)_2Ru_2Cl_2(\mu\text{-}SPr^i)(\mu\text{-}PMe_2)]$ [Ru-Ru 2.8839(5) Å] [123], and $[(\eta^5\text{-}C_5Me_5)_2Ru_2(\mu\text{-}SPr^i)\{\mu\text{-}\eta^2\text{:}\eta^2\text{-}C(CO_2Bu^t)=CH\text{-}SPr^i\}]$[(Ru-Ru 2.747(1) Å] [124].

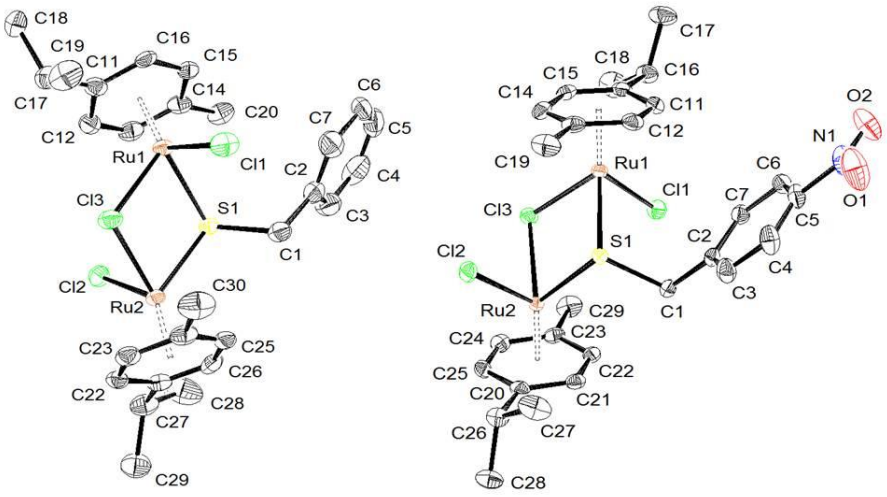


**Figure 20** - Molecular structures of **1** (left) and **2** (right) at 50% probability level ellipsoids hydrogen atoms were omitted for clarity.

**Table 1** - Selected bond lengths (Å) and angles (°) for complexes **1** and **2.**

| | **1** | **2** |
|---|---|---|
| Interatomic distances | | |
| Ru1···Ru2 | 3.6617(6) | 3.6555(4) |
| Ru1-Cl1 | 2.4000(14) | 2.4144(8) |
| Ru2-Cl2 | 2.4202(13) | 2.4267(8) |
| Ru1-Cl3 | 2.4549(13) | 2.4342(8) |
| Ru2-Cl3 | 2.4408(15) | 2.4438(8) |
| Ru1-S1 | 2.4167(14) | 2.4173(8) |
| Ru2-S1 | 2.4052(13) | 2.4088(8) |
| Angles | | |
| Ru1-S1-Ru2 | 98.82(5) | 98.48(3) |
| Ru1-Cl3-Ru2 | 96.83(5) | 97.07(3) |
| S1-Ru1-Cl3 | 81.78(5) | 81.90(3) |
| S1-Ru2-Cl3 | 82.31(5) | 81.87(3) |
| Cl1-Ru1-Cl3 | 85.92(5) | 85.63(3) |
| Cl2-Ru2-Cl3 | 86.23(5) | 86.03(3) |

In order to prove the step-wise formation of trithiolato-bridged complexes as suggested in Scheme 3, we attempted the synthesis of a mixed dithiolato complex starting from a monothiolato complex. Thus, we reacted the monothiolato complex **2** with the 4-fluorobenzylthiol. However, the reaction yielded not only the expected mixed dithiolato product $[(\eta^6\text{-}p\text{-}MeC_6H_4Pr^i)_2Ru_2Cl_2(\mu\text{-}S\text{-}p\text{-}CH_2C_6H_4NO_2)(\mu\text{-}S\text{-}p\text{-}CH_2C_6H_4F)]$, but a complex mixture of products. By monitoring the reaction by $^{19}F$ NMR spectroscopy (Figure 21), we observed the formation of the mixed complex $[(\eta^6\text{-}p\text{-}MeC_6H_4Pr^i)_2Ru_2Cl_2(\mu\text{-}S\text{-}p\text{-}CH_2C_6H_4NO_2)(\mu\text{-}S\text{-}p\text{-}CH_2C_6H_4F)]$ during the first minutes of the reaction, followed by the formation of the exchanged monothiolato complex $[(\eta^6\text{-}p\text{-}MeC_6H_4Pr^i)_2Ru_2Cl_2(\mu\text{-}S\text{-}p\text{-}CH_2C_6H_4F)(\mu\text{-}Cl)]$ as well as of the homoleptic dithiolato complexes $[(\eta^6\text{-}p\text{-}MeC_6H_4Pr^i)_2Ru_2Cl_2(\mu\text{-}S\text{-}p\text{-}CH_2C_6H_4F)_2]$ and $[(\eta^6\text{-}p\text{-}MeC_6H_4Pr^i)_2Ru_2Cl_2(\mu\text{-}S\text{-}p\text{-}CH_2C_6H_4NO_2)_2]$, the latter one being NMR-silent in the $^{19}F$ NMR spectra but being identified in the $^1H$ NMR and ESI-MS spectra. A further product showing up at $\delta(^{19}F)$ = -114.4 ppm is believed to be bis(4-fluorobenzyl) disulfide, arising from the oxidation of 4-fluorobenzylthiol. In a similar fashion, complex **1** reacts with 4-nitrobenzylthiol to give a mixture of the expected mixed dithiolato complex, the exchanged monothiolato complex and the two homoleptic dithiolato complexes.

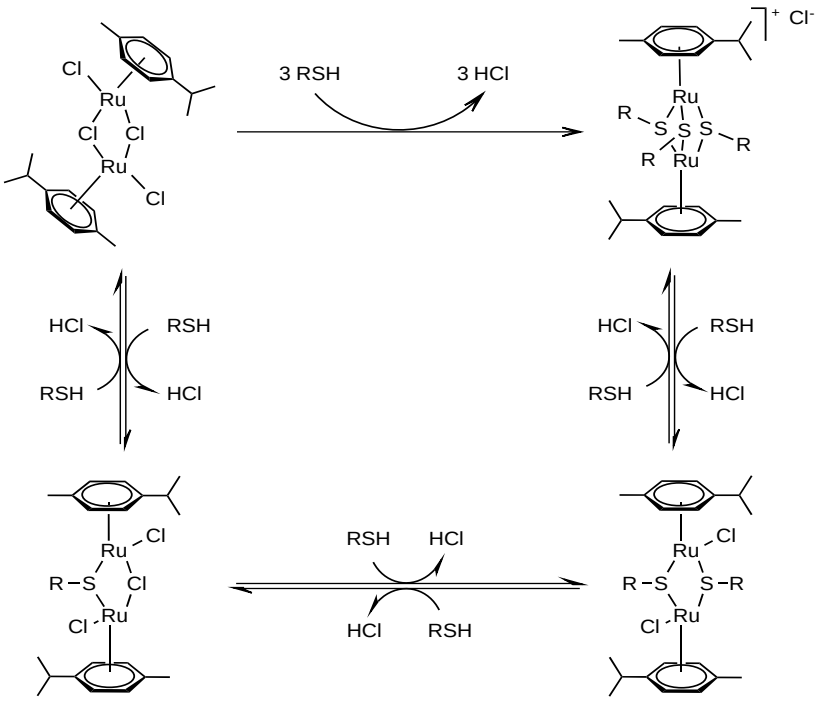


**Scheme 3** - The reaction of *p*-cymene ruthenium dichloride dimer with thiols

These results confirm the existence of equilibria between the thiolato complexes and the thiols. The coordinated thiolato bridge can come off as free thiol to be replaced by a thiolato bridge derived from another thiol in the solution, which leads to a mixture of thiolato complexes. These equilibria are governed mostly by the reactivity of the thiols and to a lesser extent by the choice of the solvent and reaction conditions.

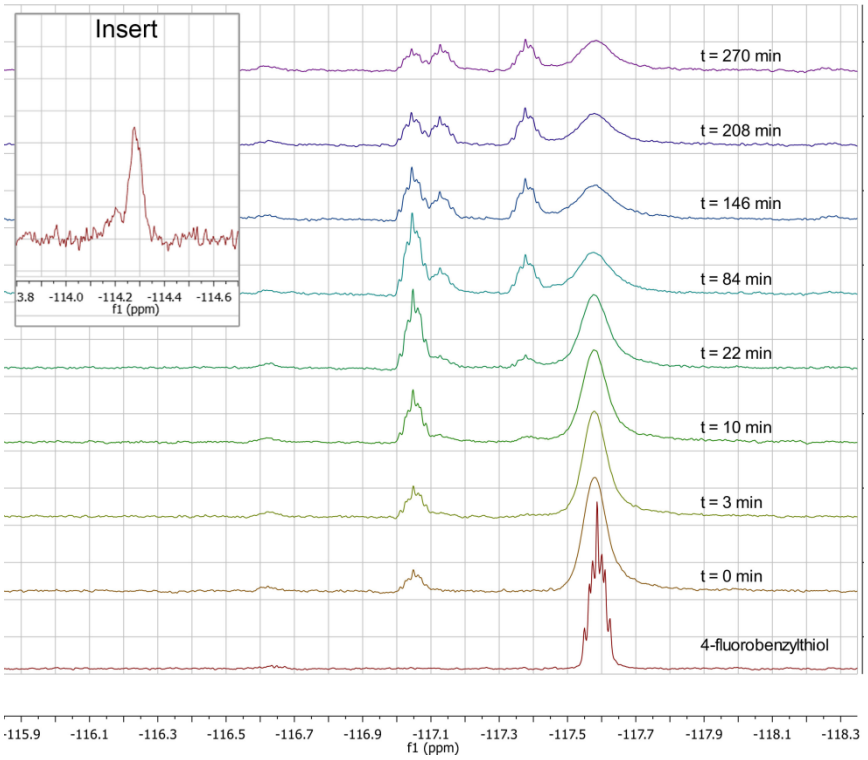


**Figure 21** - Time-dependent $^{19}F$ NMR spectra of the reaction of **2** with 4-fluorobenzylthiol

Since the derivatives **1** and **3** could not be isolated in a pure form because of these equilibria, the biological activities of the new monothiolato complexes were studied only with the derivatives **2** and **4**. Both complexes were found to be cytotoxic for human ovarian cancer cells (96 h of incubation), the $IC_{50}$ values for the A2780 cell line being in the lower micromolar range (5.42 ± 0.55 μM for **2** and 2.59 ± 0.15 μM for **4**). The *in vitro* anticancer activity of the monothiolato complexes is comparable to that of the dithiolato complexes [115], but considerably lower than that of the trithiolato complexes, the $IC_{50}$ values of which are in the nanomolar range [111-113]. Thus, the number of thiolato bridges seems to play a critical role for the cytotoxicity. We also studied the

catalytic activity of **2** and **4** for the oxidation of the tripeptide glutathione (GSH) to the oxidized form GSSG, since the catalytic oxidation of this endogenous antioxidant has been supposed to be at the origin of the biological activity of certain arene ruthenium complexes [125], and was shown to be at least partially responsible for the high cytotoxicity of the trithiolato complex $[(\eta^6\text{-}p\text{-}MeC_6H_4\text{-}Pr^i)_2Ru_2(\mu\text{-}S\text{-}p\text{-}C_6H_4Me)_3]^+$ [111]. Surprisingly, only **2** was found to catalyze the oxidation of GSH in a $D_2O/(CD_3)_2CO$ (95 : 5) solution at 37°C in the presence of air, while **4** was completely inactive under these conditions. The catalytic reaction was monitored by $^1H$ NMR spectroscopy, showing the disappearance of the signal at 3.0 ppm ($\beta$-$CH_2$ resonances of GSH) to be accompanied by the simultaneous appearance of the GSSG $\beta$-$CH_2$ resonances at 3.2 and 3.5 ppm. The catalytic turnover frequency at the time when half of the glutathione is converted ($TOF_{50}$) for **2** was determined to be 0.145 $h^{-1}$, which means that the monothiolato complex **2** is catalytically much more active than the trithiolato complexes [111].

Thus, the tendency in the $TOF_{50}$ values is in contrast to that of the $IC_{50}$ values, indicating that the catalytic GSH oxidation activity cannot be the main mode of action of the *in vitro* anticancer activity of dinuclear arene ruthenium complexes with thiolato bridges. This is also supported by the findings for complex **4**, which is cytotoxic (comparable to cisplatin) but inactive for the catalytic oxidation of GSH.

### 2.1.3 Conclusion

In conclusion, we have synthesized and characterized four complexes of the type $[(\eta^6\text{-}p\text{-}MeC_6H_4Pr^i)_2Ru_2Cl_2(\mu\text{-}Cl)(\mu\text{-}SR)]$ containing one thiolato and one chlorido bridge. These monothiolato complexes represent the missing link in the three-step synthesis of the well-known trithiolato complexes. The reaction of these monothiolato complexes with thiols to give the corresponding dithiolato complexes was shown to be reversible. The monothiolato complexes **2** and **4** are cytotoxic for human ovarian cancer cells, but only complex **2** catalyzes the oxidation of glutathione.

## 2.2 Interactions of Mono-, Di- and Trithiolato Dinuclear Arene Ruthenium Complexes with Biological Ligands

### 2.2.1 General

The studies of the stability and the reactivity of some of the recently synthesized trithiolato complexes with various amino acids, peptides, nucleotides and DNA have revealed that the complexes are very stable in physiological conditions as well as under acidic and basic conditions and that they are particularly inert towards substitution. Only sulphur-containing biomolecules such as the amino acid cysteine (Cys) and the tripeptide glutathione (GSH) were found to interact with the complexes. Surprisingly, no adducts were identified, but Cys and GSH undergo a catalytic oxidation in the presence of trithiolato complexes, forming cystine and GSSG [111]. Such a mode of action has already been proposed for arene ruthenium azopyridine iodo complexes, which are surprisingly cytotoxic despite their inertness to ligand substitution: In a pioneering study, Sadler and co-workers demonstrated that these complexes act as catalysts for the oxidation of the tripeptide glutathione, supposed to be at the origin of their anticancer activity [125]. For our dinuclear trithiolato arene ruthenium complexes, no direct correlation between their cytotoxicity and catalytic activity for the oxidation of glutathione was found. Although a decrease in the glutathione levels with increasing concentration of the complex $[(\eta^6\text{-}p\text{-}MeC_6H_4Pr^i)_2Ru_2(\mu\text{-}S\text{-}p\text{-}C_6H_4{}^tBu)_3]Cl$ was observed both *in vitro* and *in vivo* (see Chapter 2.3), we assume other mechanisms to be mainly responsible for the high cytotoxicity of the trithiolato complexes.

In an effort to rationalize the relationship between reactivity and the *in vitro* cytotoxicity of thiolato-bridged arene ruthenium complexes, we set out to investigate the hydrolysis of two monothiolato complexes **2** and **4** and two dithiolato complexes **5** and **6** (Figure 22) as well as their interactions with selected amino acids and a DNA 20-mer and to compare the results with those of trithiolato complexes.

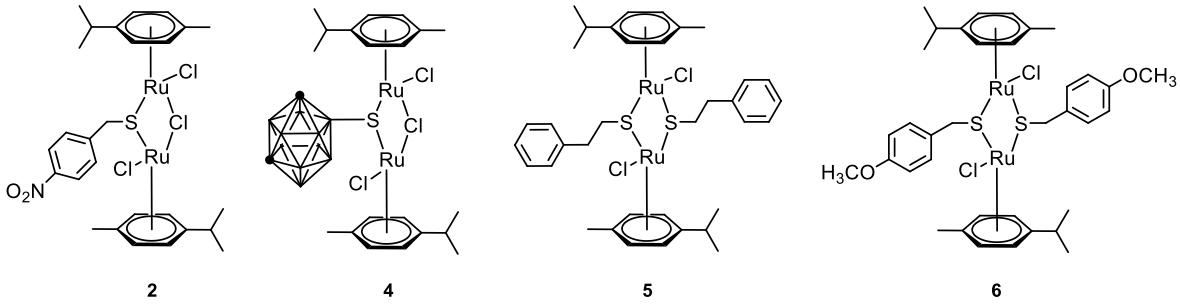


**Figure 22 -** Structures of complexes **2**, **4**, **5** and **6**, the symbols • in the formula of **4** representing CH groups of the carborane

### 2.2.2 Results

#### Synthesis and molecular structure of the dithiolato complex 6

The new dithiolato complex **6** was synthesized by a slight variation of the reaction conditions published previously for other dithiolato complexes [115]. The *p*-cymene ruthenium dichloride dimer was dissolved in ethanol, the 4-methoxy-α-toluenthiol was added dropwise and the solution was stirred at room temperature for 3 hours. The product was precipitated with hexane, filtered and dried *in vacuo*. The resulting yellow crystalline powder was completely characterized. The X-ray quality crystals for **6** were obtained by the slow diffusion of diethylether into the solution of **6** in dichloromethane. The molecular structure shown in Figure 23 can be described in terms of two *p*-cymene ruthenium units held together by two μ-bridging thiolato units. Selected bond lengths and angles are listed in Table 2. In accordance with the electron count of 36, there is no metal-metal bond, the distance between the two ruthenium atoms being 3.6555(9). The structure compares well with those of the previously published dithiolato complex $[(\eta^6\text{-}p\text{-}MeC_6H_4Pr^i)_2Ru_2Cl_2(\mu\text{-}p\text{-}SCH_2\text{-}C_6H_4Bu^t)_2]$ [115] and of the trithiolato complex $[(\eta^6\text{-}p\text{-}MeC_6H_4Pr^i)_2Ru_2(\mu\text{-}SCH_2C_6H_5)_3]^+$ [105], where the ruthenium-ruthenium distances are 3.674(2) Å and 3.3489(8) Å, respectively.

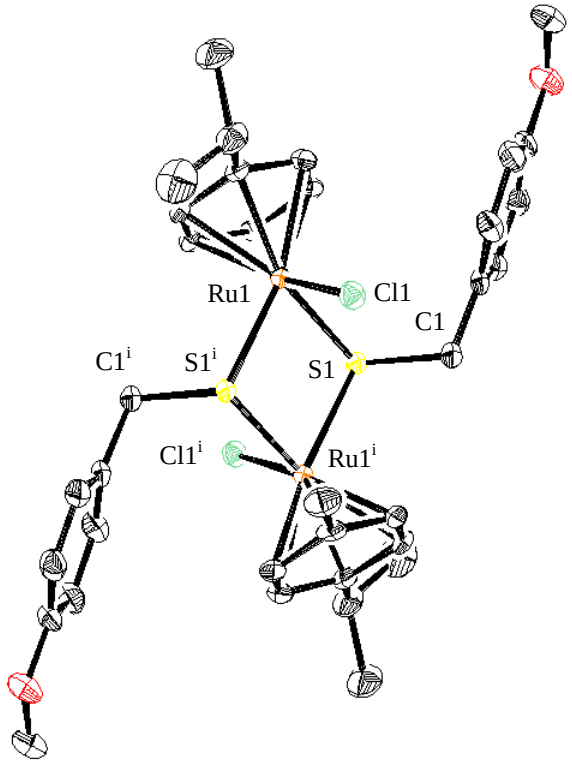


**Figure 23 -** Molecular structure of **6** at 50% probability level ellipsoids. Hydrogen atoms are omitted for clarity.

**Table 2 -** Selected bond lengths (Å) and angles (°) for complex 4 *(i = 1-x, 1-y. –z)*

| | **6** |
|---|---|
| Interatomic distances | |
| Ru1···Ru1$^{i}$ | 3.6555(9) |
| Ru1-Cl1 | 2.4293(9) |
| Ru1-S1 | 2.3931(8) |
| Ru1-S1$^{i}$ | 2.3783(8) |
| S1-C1 | 1.845(3) |
| Angles | |
| Ru1-S1-Ru1$^{i}$ | 99.99(3) |
| S1-Ru1-Cl1 | 90.49(3) |
| S1-Ru1-S1$^{i}$ | 80.01(3) |
| S1-Ru1$^{i}$-Cl1$^{i}$ | 81.69(3) |
| Ru1-S1-C1 | 109.67(10) |
| Ru1$^{i}$-S1$^{i}$-C1$^{i}$ | 111.26(11) |

**Stability of complexes 2, 4, 5 and 6 in aqueous solutions and in DMSO**

The stability of the monothiolato and dithiolato complexes in solution and in DMSO was studied by 1D $^{1}$H NMR and ESI-MS spectroscopy. Figure 24 shows 1D $^{1}$H-NMR spectra of complex **4** dissolved in a mixture acetone-$d_6$/$D_2O$ (ratio 7 : 3) recorded at 37°C between 5 and 1440 minutes together with the 1D $^{1}$H-NMR spectrum of complex **4** dissolved in acetone-$d_6$. As is obvious from the spectra, additional resonances appeared already 5 minutes after dissolution; the hydrolysis reached a steady state after 1 hour and did not continue further. The two sets of two new doublets appearing at 5.44 ppm and 5.28 ppm and at 5.89 ppm and 5.80 ppm, respectively, prove the formation of at least two new species. Similar results were obtained for complex **2**, which hydrolyzes significantly faster; the steady state is already achieved after 5 minutes, at the time of the first NMR measurement (Figure 24). ESI-MS spectra of the solutions of both **2** and **4** reveal the presence of three species corresponding to dinuclear complexes. In both spectra, the starting complex $[(\eta^6\text{-}p\text{-}MeC_6H_4Pr^i)_2Ru_2Cl_2(\mu\text{-}Cl)(\mu\text{-}SR)]$ at *m/z* = 709.1 and 717.12, respectively (Figure 25), is still present, while new peaks (fragment *m/z* = 692.01 for **2** and *m/z* = 699.16 for **4,** Figure 25), corresponding to the hydrolyzed complex $[(\eta^6\text{-}p\text{-}MeC_6H_4Pr^i)_2Ru_2Cl(OH)(\mu\text{-}Cl)(\mu\text{-}SR)]$ where one chlorido ligand has been replaced by a hydroxo ligand, are clearly observed. The third species observed by NMR presumably corresponds to the second hydrolyzed complex, $[(\eta^6\text{-}p\text{-}MeC_6H_4\text{-}Pr^i)_2Ru_2(OH)_2(\mu\text{-}Cl)(\mu\text{-}SR)]$, but this product could not be confirmed, as it would show at the same *m/z* ratio as the first hydrolyzed complex. Therefore, we assume that these products of the hydrolysis to the second degree are present but we were not able to prove it by the employed methods. The last species in the ESI-MS spectra of **2** and **4** corresponds to the dithiolato complexes $[(\eta^6\text{-}p\text{-}MeC_6H_4Pr^i)_2Ru_2Cl_2(\mu\text{-}SR)_2]$, as indicated by the peaks at *m/z* = 842.2 and 857.3, respectively (Figure 25), in accordance with the previously reported thiol exchange in solution (Chapter 2.1). The stability of the two monothiolato complexes in DMSO is low. NMR and ESI-MS demonstrate that the complex **2** degrades into mononuclear fragments already after 5 minutes of incubation at 37°C, complex **4** degrading more slowly, in accordance with their hydrolytic stability (Figure 26).

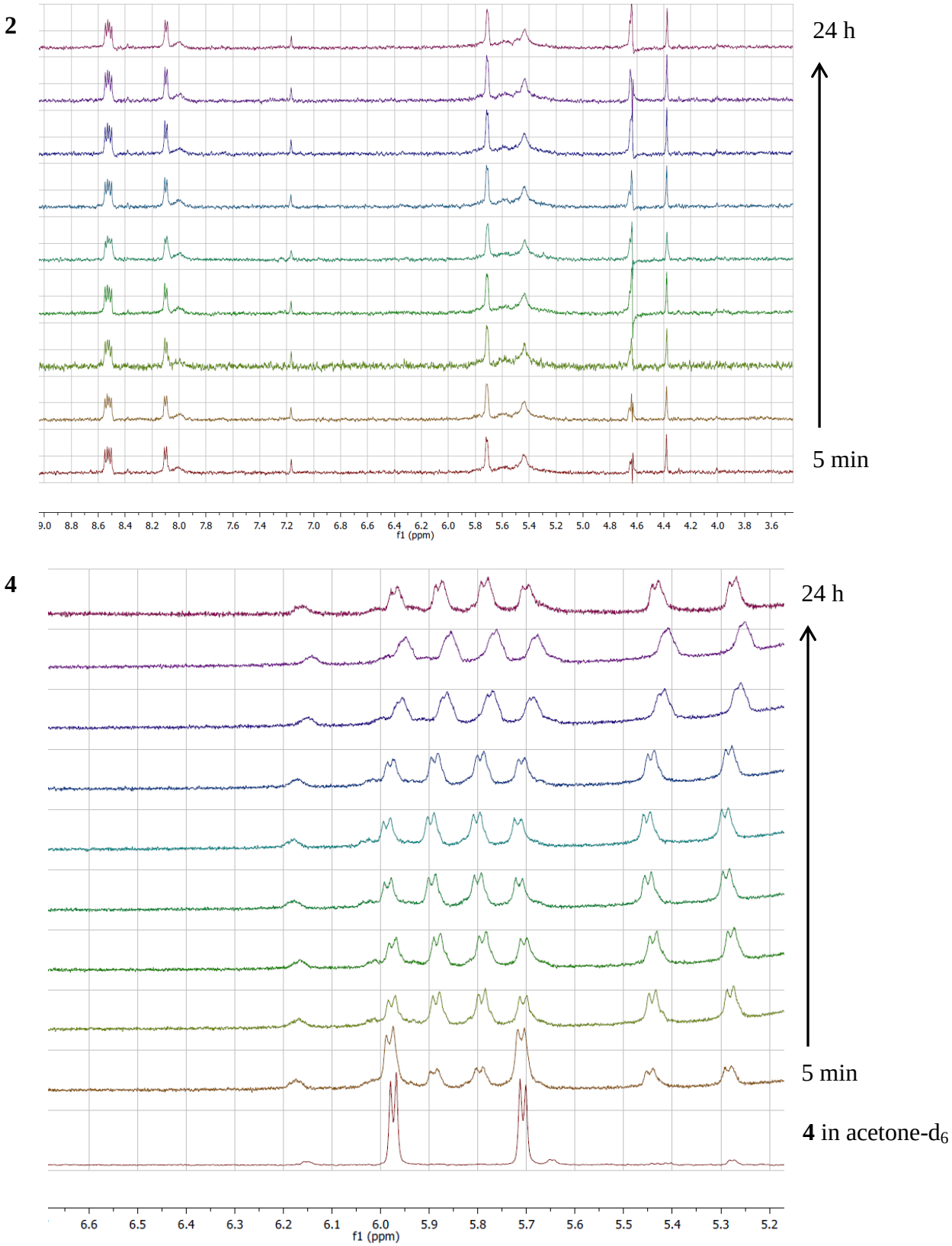


**Figure 24** - Hydrolysis of **2** and **4** in acetone-$d_6$/$D_2O$ mixtures followed by NMR

**2**

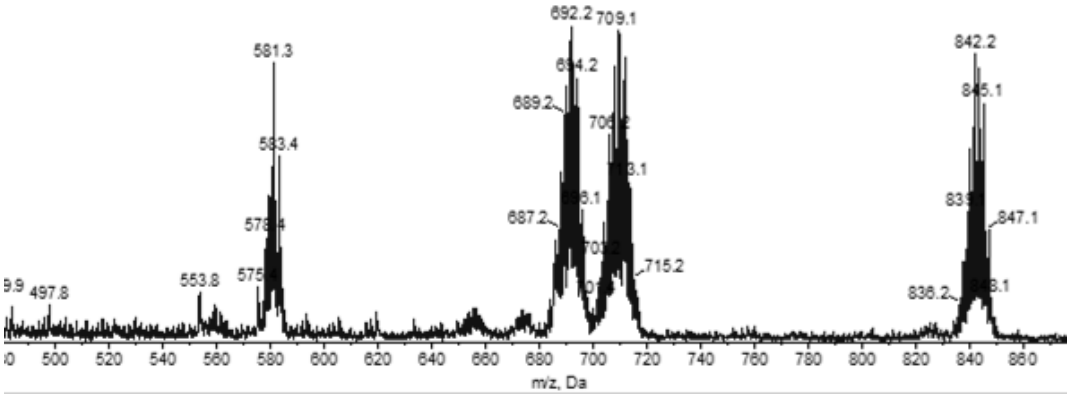


**4**

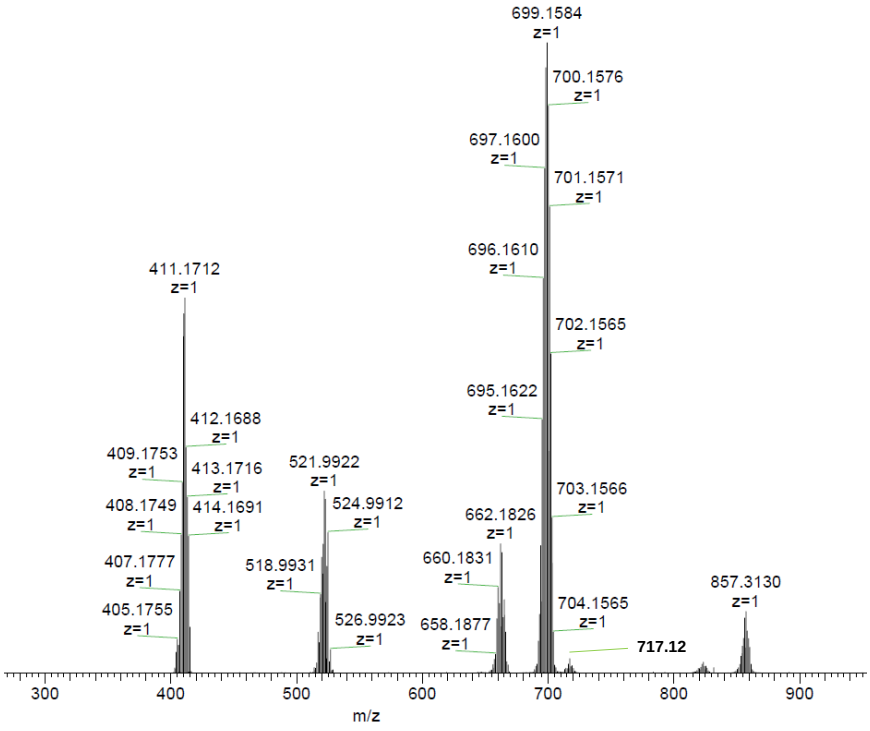


**Figure 25** - ESI-MS spectra of the hydrolysis of **2** and **4** in acetone-$d_6$/$D_2O$ mixtures

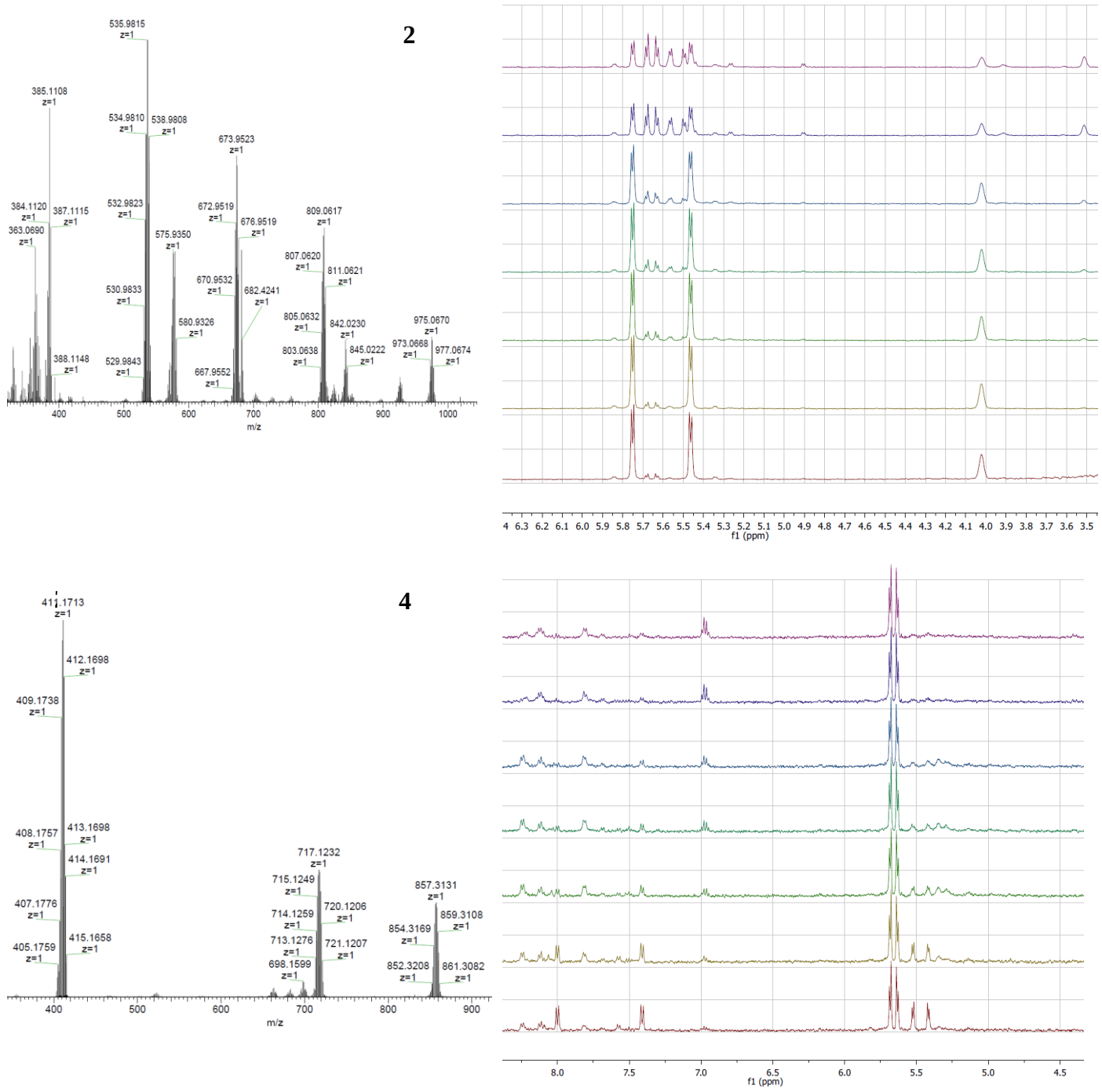


**Figure 26** - Stability of **2** and **4** in DMSO

The dithiolato complexes proved to be more stable in aqueous solutions. Under neutral (no addition of buffer) and acidic (pH = 2) conditions, the complexes are stable, no changes in NMR spectra are observed after 24 hours at 37°C. On the other hand, at basic pH (pH = 10), additional peaks appeared in the 1D $^{1}$H NMR spectrum after 4 hours at 37°C for complex **5** and after24 hours for **6** (Figure 27). For both complexes **5** and **6**, ESI-MS spectra show fragments at *m/z* = 763.12 and

795.11, respectively, corresponding to the hydrolyzed hydroxo complexes [($\eta^6$-*p*-$MeC_6H_4$-$Pr^i$)$_2$$Ru_2$Cl(OH)(μ-SR)$_2$], which is confirmed by the new resonances appearing in the $^1$H NMR spectra. The hydrolysis to the second degree is expected to take place, but, similarly to monothiolato complexes **2** and **4** could not be proven. In accordance with the results for the two monothiolato complexes **2** and **4**, the two dithiolato complexes **5** and **6** are also not very stable in DMSO. NMR and ESI-MS spectra demonstrate that the dithiolato complexes degrade into mononuclear ruthenium complexes already after 15 minutes of incubation at 37°C. The instability of both mono- and dithiolato complexes in DMSO strongly contrasts with the high stability of the trithiolato complexes, which are stable for at least 24 h. The Ru-Cl bond is therefore the reactive part of the mono- and dithiolato complexes, the Ru-S bond being highly stable, as is evidenced by the inertness of the trithiolato complexes [114].

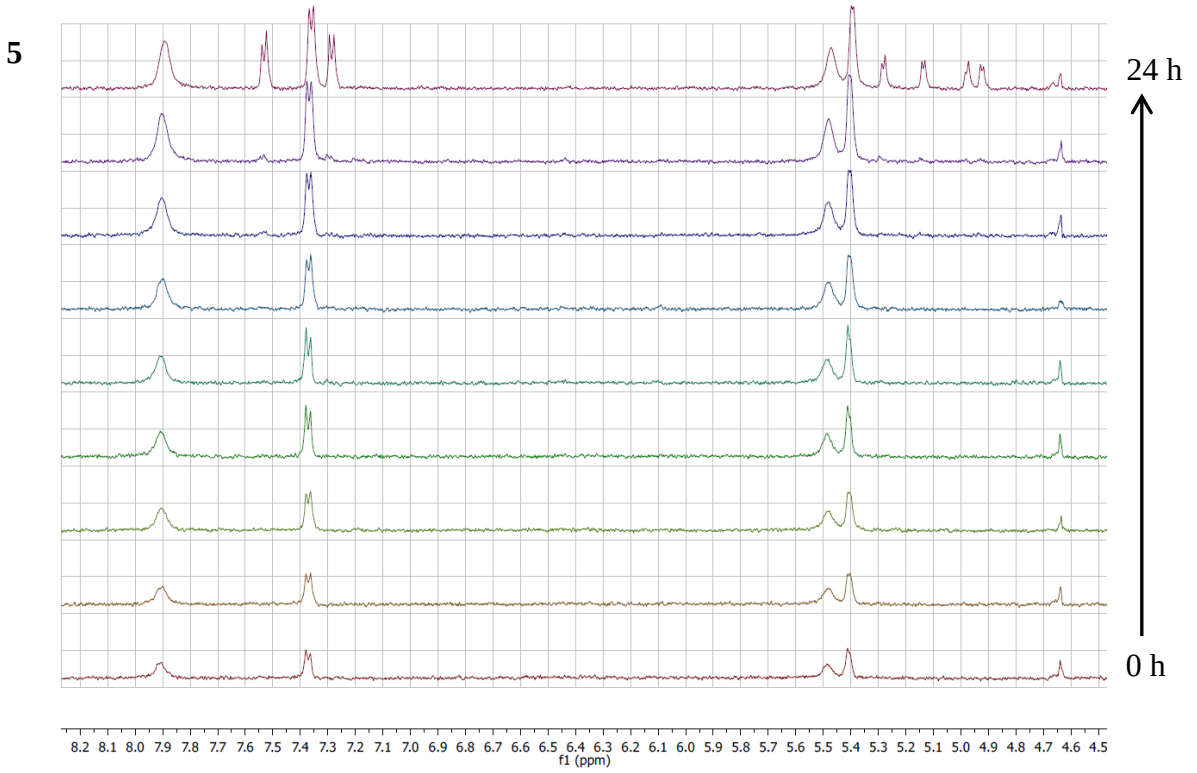

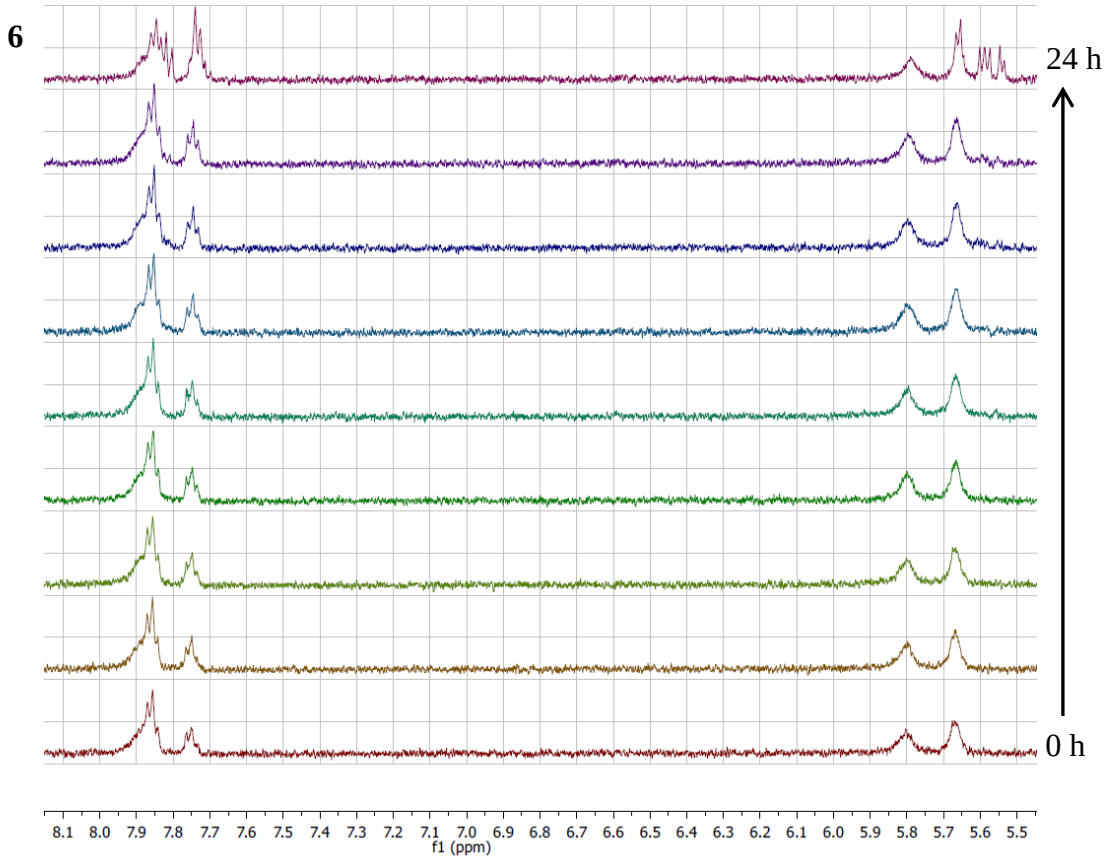


**Figure 27 -** Hydrolysis of **5** and **6** in the aqueous solution at pH = 10 over 24 hours

### Reactivity of 2, 4, 5 and 6 with the DNA 20-mer

In order to investigate the possible binding of the complexes **2, 4, 5** and **6** to DNA, we incubated the complexes at 37°C together with the single-stranded DNA 20-mer CGCGATCGCGGCGCTAGCGC. We assumed that once the complexes hydrolyzed, they would bind to the nucleophilic nitrogen of DNA nucleobases, in analogy with platinum complexes and some other ruthenium compounds [126-128]. However, even though the hydrolysis of the complexes **2** and **4** occurred in the same way as in aqueous solution, no adduct of either monothiolato or dithiolato complexes with DNA was observed by ESI mass spectroscopy in negative or positive mode. The inertness of both mono- and dithiolato complexes towards DNA is in line with the results obtained with trithiolato complexes. It appears therefore that DNA is not a target of these arene ruthenium thiolato-bridged complexes and that they exert their cytotoxicity through other mechanisms.

**Reactivity of 2, 4, 5 and 6 with aspartic acid, alanine and histidine**

Most of the metallodrugs currently used in antitumor therapy, such as carboplatin and cisplatin, are administered intravenously and can therefore encounter various reactive biomolecules in the bloodstream. Interactions with peptides and serum proteins can have a pronounced influence on the drug distribution, bioavailability and target or off-target effects [127-128]. To investigate some of these possible interactions, four different amino acids were chosen in order to account for the effects of pH and of various side chains. The neutral amino acid L-alanine, the acidic L-aspartic acid and the basic L-histidine were used to see the effect of the pH of amino acids. L-histidine was also chosen to see a possible binding between the imidazole side chain and ruthenium complexes, since it was already shown to strongly and rapidly interact with ruthenium compounds [129-132]. L-cysteine was used to evaluate the reactivity of the SH group towards the complexes. No buffers were used, to avoid the introduction of other ions into the solutions, which could influence the hydrolysis of the complexes. The pH values of the solutions, measured right after the mixing of the complex and the amino acid, are given in Table 3.

**Table 3** - pH values of aqueous solutions of complexes **2, 4, 5** and **6** and various amino acids

| | Ala | Cys | His | Asp |
|---|---|---|---|---|
| **2** | 4.45 | 3.20 | 6.72 | 3.41 |
| **4** | 4.28 | 3.48 | 5.99 | 3.60 |
| **5** | 6.05 | 3.92 | 7.42 | 4.02 |
| **6** | 6.86 | 4.45 | 7.70 | 4.08 |

Alanine is not known to react with ruthenium complexes, although it was shown to slowly degrade a hexacationic arene ruthenium assembly possessing an oxalato linker to give mononuclear ruthenium-alanine adducts [132]. Upon addition of 3 eq of Ala, no adduct formation was observed for the four complexes **2, 4, 5** and **6**. NMR and ESI-MS spectra showed the same hydrolysis products for **2** and **4** that were observed in aqueous solutions (Figure 25), the spectra of **5** and **6** did not show any change. The same result was observed with aspartic acid – the compounds **2** and **4** underwent hydrolysis upon addition of 3 eq of Asp, while with **5** and **6** no adduct formation was observed and the compounds remained stable after 24 hours at 37°C.

Many ruthenium complexes are known to react with the basic imidazole ring of His. For instance, with arene ruthenium assemblies, the reactions with His were always complete and were finished within hours [131-132]. Surprisingly, it appears that none of the four complexes investigated in this study reacts with His, in line with the results for trithiolato complexes. In the mixture with histidine, **2** and **4** hydrolyzed in the same way as in aqueous solution (Figure 25). Complexes **5** and **6** also slowly hydrolyzed, forming the corresponding hydroxo complexes, evidenced by the peak at *m/z* = 763.12 for **5** and *m/z* = 795.11 for **6**. After 24 hours of NMR monitoring, the reactions did not reach steady state. No adducts of histidine to the complexes were observed by NMR of by ESI-MS spectroscopy. We assume that the difference in the stability of complexes **5** and **6** in solution with histidine compared to their stability in aqueous solution is caused solely by the slight difference in the pH of the mixture (see Table 3).

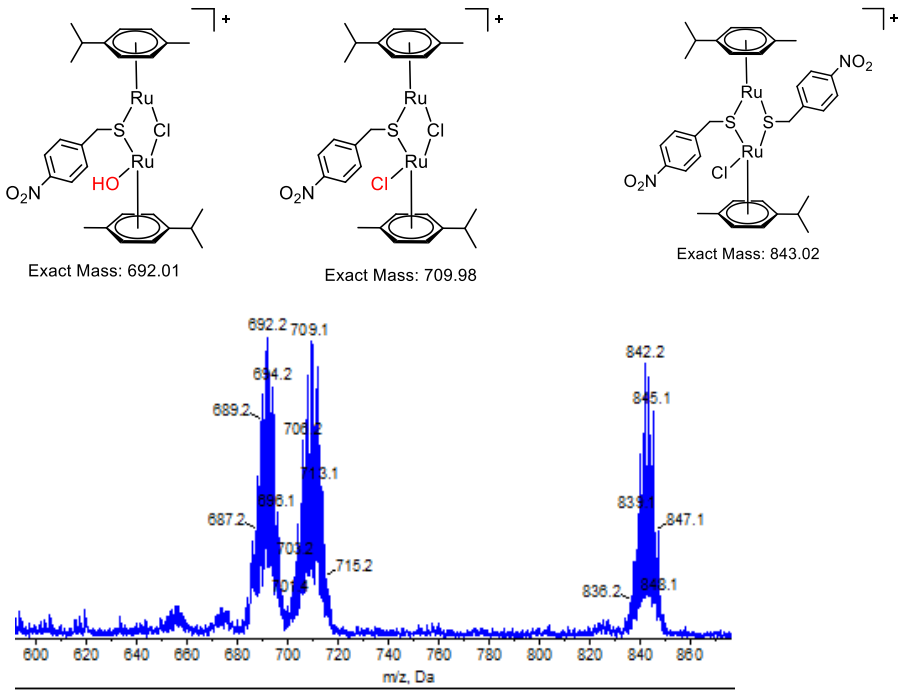


**Figure 28 –** Fragments of the three products detected by ESI-MS in the mixture of **2** with histidine after 24 hours

### Reactivity of 2, 4, 5 and 6 with cysteine

Unlike Ala, Asp, and His, Cys reacts rapidly with the four complexes. In all four cases, the only product detected after 24 hours at 37°C was a trithiolato cationic complex, where the cysteinato unit occupies the position of the third (in the case of **5** and **6**) or both second and third (in **2** and **4**)

bridging thiolato ligands. This finding was surprising, since our previous attempts to synthesize cysteinato-containing trithiolato complexes by standard methods resulted in the degradation of the arene ruthenium unit and no trithiolato complexes could be isolated. Since the DOSY and ESI-MS data proved the formation of these cysteinato-containing complexes as the only species in the mixture after 24 hours (shown for **4** in Figure 29), we decided to modify the synthetic conditions and attempt the synthesis and isolation of cysteinato-containing trithiolato complexes by mimicking the conditions of our NMR experiments. Thus, the dithiolato precursor **7** was dissolved in a small amount of methanol and the excess of cysteine was added dropwise as a solution in distilled water. This mixture was allowed to stir at ambient temperature for two days, its color changing gradually from orange to yellow. The product proved to be highly unstable at higher temperature, not allowing even the evaporation at 40°C on the rotary evaporator. It also degraded rapidly in purely organic solutions. The product was therefore purified by size exclusion chromatography on Sephadex® LH20 with MeOH/$H_2O$ 9 : 1 mixture, evaporated at room temperature and dried *in vacuo*. Spectroscopy methods and elemental analysis proved the structure of the cysteinato-containing product (Scheme 4). Because of its low stability, it was not possible to obtain X-ray quality crystals. The synthesis of other cysteinato-containing complexes from dithiolato precursors **5** and **6** was also attempted, but the products degraded rapidly and it was not possible to obtain analytically pure samples.

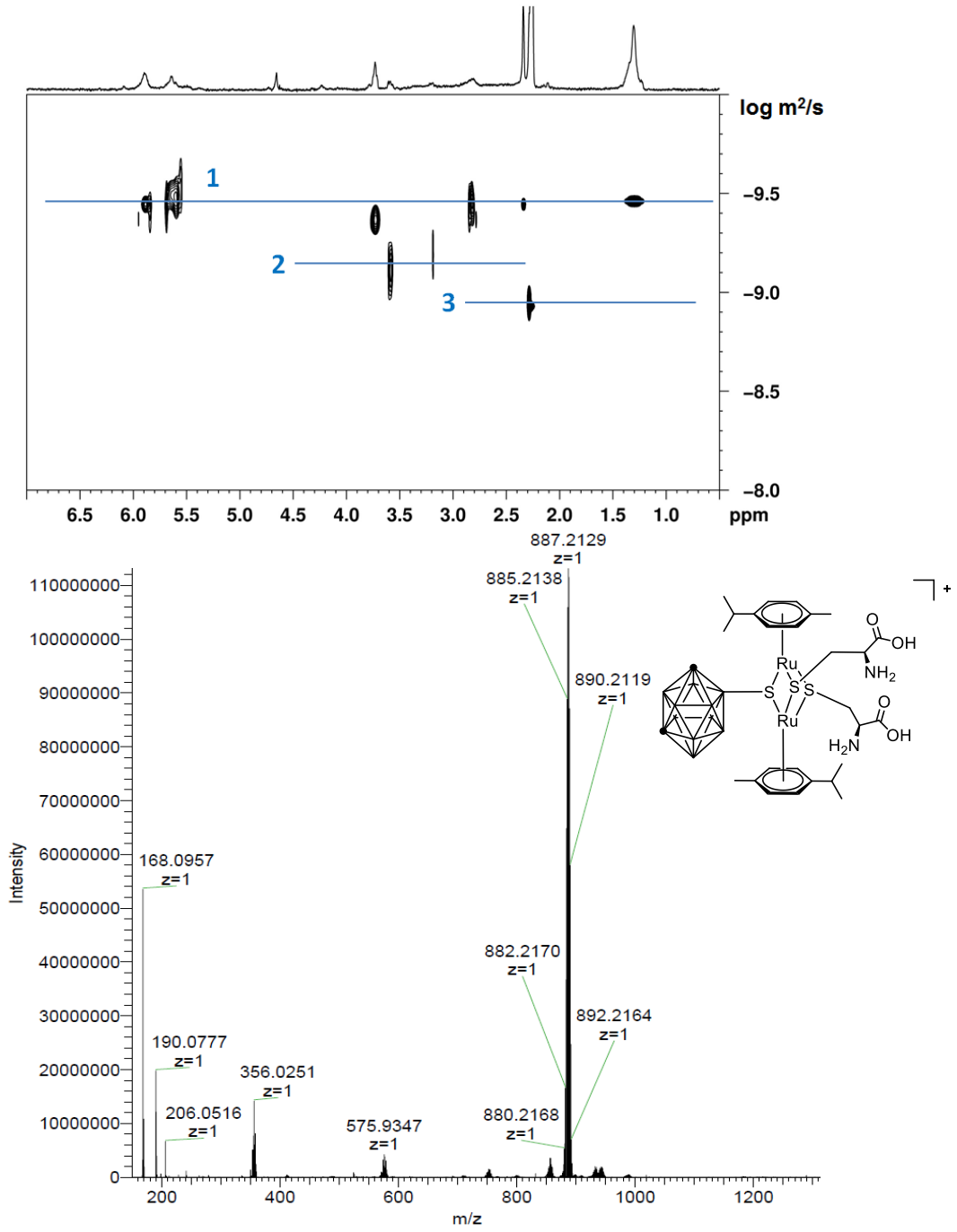


**Figure 29 –** Top: 2D 1H-DOSY NMR spectrum of the mixture **4**/Cys (molar ratio 1:3) recorded at t = 24 h in a mixture $D_2O$/acetone-$d_6$ (7 : 3). Line 1: adduct with the presumed structure $\{(\eta^6\text{-}p\text{-}MeC_6H_4Pr^i)_2Ru_2[\mu\text{-}SCH_2CH(NH_2)COOH]_2(\mu\text{-}S\text{-}m\text{-}9\text{-}B_{10}C_2H_{11})]\}^+$, line 2: free Cys, line 3: acetone. Bottom: ESI mass spectrum of the mixture **4**/Cys dissolved in $H_2O$ recorded at t = 24 h. The adduct exhibits as a peak at *m/z* = 887.21.

In view of the general lower stability of monothiolato complexes and the low stability of the synthesized complex **8**, the isolation of cysteinato-containing trithiolato complexes corresponding to **2** and **4** was not attempted.

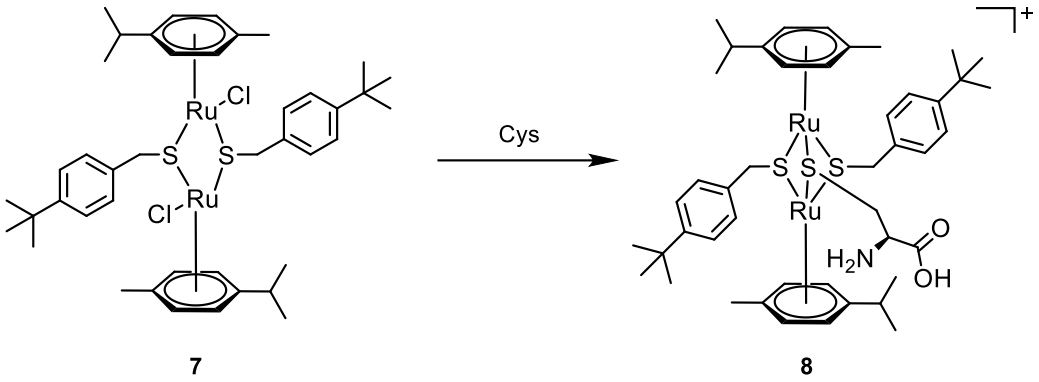


7 8

**Scheme 4** – Synthesis of cysteinato-containing complex **8**, isolated as tetrafluoroborate salt

Many proteins, in particular serum proteins such as albumin and transferrin, were already shown to bind to metal complexes and influence their activity [128-129]. We assume that this is the main reasons for the lower cytotoxicity of mono- and dithiolato complexes as compared to the trithiolato ones [111-115]. The high stability of trithiolato arene ruthenium complexes allows them to accumulate inside the cells of a tumor (see Chapter 2.3), where they can reach their molecular target and exhibit their anticancer activity. The monothiolato and dithiolato complexes can, on the other hand, bind to proteins and other molecules containing the sulfhydryl group, which we assume impedes their accumulation in cancer cells in sufficient concentrations.

### 2.2.3 Conclusion

The stability of monothiolato and dithiolato complexes was studied in aqueous solutions and in DMSO. The results confirmed the hypothesis that the presence of chlorido ligands renders the complexes less stable. Monothiolato complexes were found to undergo hydrolysis, forming the corresponding hydroxo complexes. Dithiolato complexes are stable under acidic and neutral conditions, forming hydroxo complexes only at elevated pH. The hydrolysis to the second degree could not be observed by the employed analytical methods, but is presumed to proceed in the case of all four studied complexes. The complexes **2, 4, 5** and **6** do not interact with amino acids L-alanine, L-aspartic acid or L-histidine. With L-cysteine, they form cationic trithiolato complexes, where the cysteinato unit forms the second and third thiolato bridge. One of the cysteinato-bridged complexes could be isolated and completely characterized. No interactions with a DNA fragment were observed. We propose that these results partially explain the difference between the

cytotoxicity of the previously studied trithiolato complexes and the more reactive, but an order of magnitude less cytotoxic mono- and dithiolato complexes.

## 2.3 *In Vivo* Study of [(*p*-MeC$_6$H$_4$Pr$^i$)$_2$Ru$_2$(SC$_6$H$_4$-*p*-Bu$^t$)$_3$]Cl (*diruthenium-1*)

**Adapted from:** P. Tomšík, D. Muthná, M. Řezáčová, S. Mičuda, J. Ćmielová, M. Hroch, R. Endlicher, Z. Červinková, E. Rudolf, S. Hanne, D. Stíbal, B. Therrien, G. Süss-Fink, [(*p*-MeC$_6$H$_4$Pr$^i$)$_2$Ru$_2$(SC$_6$H$_4$-*p*-Bu$^t$)$_3$]Cl (*diruthenium-1*), a dinuclear arene ruthenium compound with very high anticancer activity: An *in vitro* and *in vivo* study, *Journal of Organometallic Chemistry*, **2015**, 782, 42–51.

### 2.3.1 General

*In vitro* studies offer a rapid and largely accessible means to assess the anticancer potential of novel molecules. Their cytotoxicity on a wide range of cancer cell lines and their selectivity towards cancerous versus healthy cells can be established this way. However, as was clearly demonstrated by NAMI-A and RAPTA-C [52,82], it is not an approach without limitations. The cellular cultures used in *in vitro* studies are populations of single-phenotype cells extracted originally from a tumor of a patient. The tumors found in animal models or in human patients are, on the other hand, heterogeneous and contain a large variety of phenotypically different cells with possibly different responses towards the tested chemical agent [1]. It is therefore imperative to study the potential of anticancer drugs *in vivo*, to gain a more in-depth understanding of the behavior of the studied compound in an organism.

Herein we report the *in vitro* and *in vivo* investigation of the *tert*-butyl derivative [(*p*-MeC$_6$H$_4$-Pr$^i$)$_2$Ru$_2$(SC$_6$H$_4$-*p*-Bu$^t$)$_3$]Cl (*diruthenium-1*, [**9**]Cl, Figure 30), which was selected from 21 compounds of the three series [(*p*-MeC$_6$H$_4$Pr$^i$)$_2$Ru$_2$(SC$_6$H$_4$-*p*-X)$_3$]Cl (X = H, Me, Ph, Br, OH, NO$_2$, OMe, CF$_3$, F, Pr$^i$, Bu$^t$), [(*p*-MeC$_6$H$_4$Pr$^i$)$_2$Ru$_2$(SC$_6$H$_4$-*m*-X)$_3$]Cl (X = Me, OMe, OEt, CF$_3$, NH$_2$, Cl) and [(*p*-MeC$_6$H$_4$Pr$^i$)$_2$Ru$_2$(SC$_6$H$_4$-*o*-X)$_3$]Cl (X = Me, OMe, Pr$^i$, CF$_3$) as the most active one *in vitro* [111,113].

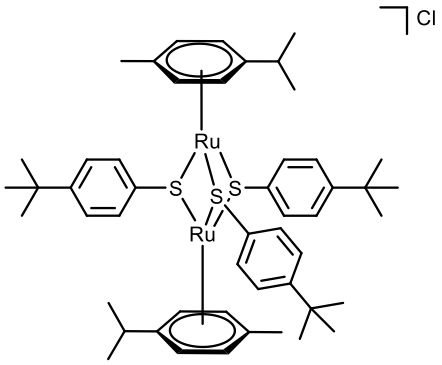


**Figure 30** - Structure of *diruthenium-1*

### 2.3.2 Results

The complex $[(p\text{-}MeC_6H_4Pr^i)_2Ru_2(SC_6H_4\text{-}p\text{-}Bu^t)_3]^+$ was prepared by a simple one-step synthetic process from the commercially available *p*-cymene ruthenium dichloride dimer and *p-tert*-butylthiophenol in refluxing ethanol; it was obtained as the chloride salt in high yield by a slight variation of the published method (Chapter 9.4.5.) [111].

The *diruthenium-1* shows anticancer activity *in vitro* and *in vivo*. The antiproliferative effect was evaluated towards the human ovarian cancer cell line A2780 and its cisplatin-resistant mutant A2780cisR using the MTT assay which measures the mitochondrial dehydrogenase activity as an indication of cell viability. The $IC_{50}$ values for *diruthenium-1* were determined to be 30 ± 10 nM for A2780 and 30 ± 10 nM for A2780cisR [111]. Thus, *diruthenium-1* is with $IC_{50}$ values in the lower nanomolar range for both cell lines, to the best of our knowledge, the ruthenium compound with the highest *in vitro* anticancer activity reported so far.

The *in vivo* anticancer effect of *diruthenium-1* was studied using a mouse model: Initially, the maximum tolerated dose (MTD) was assessed as the maximum dose of *diruthenium-1*, dissolved in water/propane-1,2-diol, that could be administered i.p. (by intraperitoneal injection) to healthy mice without causing toxic deaths or body weight loss of more than 15%. The MTD for healthy animals was estimated on this basis to be 2 mg/kg. For the *in vivo* anticancer study, a total of 98 female NMRI mice (average weight 33.5 g) were inoculated subcutaneously with a solid breast cancer Ehrlich tumor. The tumor-bearing mice, divided into 7 groups of 14 animals, were administered with the water/propane-1,2-diol solution of *diruthenium-1*, in doses of 0.2, 0.4, 0.6, 1.0, or 2.0 mg/kg i.p. on days 1 and 7, in volumes of 0.2 ml per 20 g body weight. A control group was treated with the

pure solvent and a positive control group received a standard cisplatin treatment (5.0 mg/kg cisplatin i.p.). The mice were weighed on the first, fourth, sixth and seventh day. On the eighth day, half of the mice were sacrificed; the remaining animals were kept in order to observe their survival. In addition to the total body weight, the tumor weight was also determined.

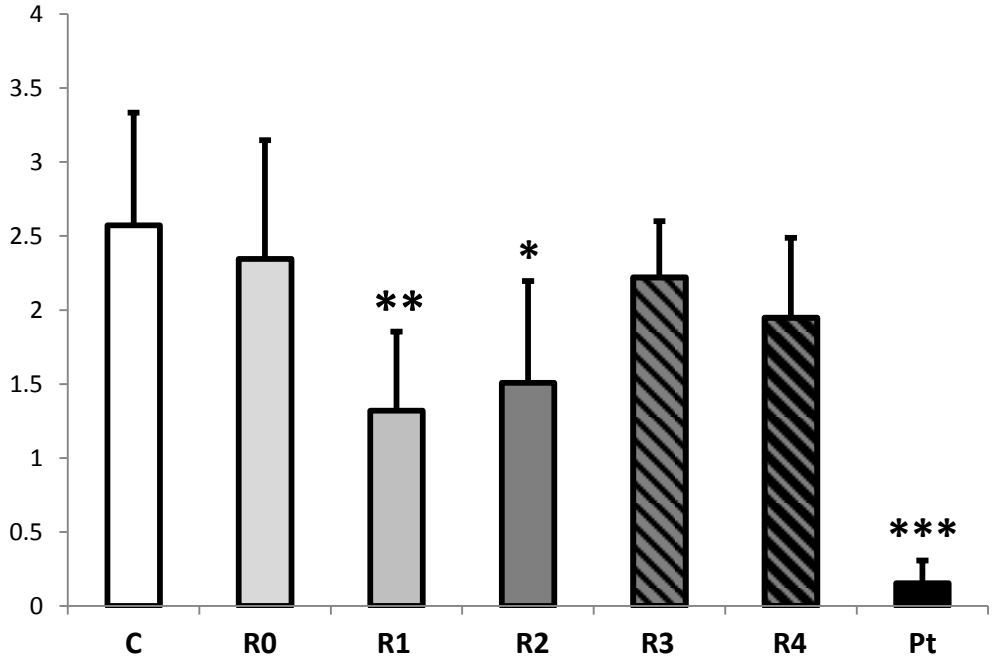


**Figure 31 -** Weight of the solid Ehrlich tumor (in grams) on day 8 of the sacrificed mice injected on days 1 and 7 i.p. with pure solvent, *diruthenium-1* or cisplatin. Values are the means ± SD (n = 7 in each group). C = tumor-bearing control treated with pure solvent; R: *diruthenium-1*, R0 = 0.2 mg/kg i.p.; R1 = 0.4 mg/kg i.p.; R2 = 0.6 mg/kg i.p.; R3 = 1.0 mg/kg i.p.; R4 = 2.0 mg/kg i.p.; Pt = cisplatin 5.0 mg/kg i.v. Significantly different from the control: $^{*}P < 0.05$, $^{**}P < 0.01$, $^{***}P < 0.001$.

No macroscopic metastases were found in the organs. Figure 31 shows the weight of the tumors in mice treated with the pure solvent, with *diruthenium-1* in various doses, and with cisplatin measured on day 8. It documents the inhibitory effect of *diruthenium-1* at 0.4 and 0.6 mg/kg, although it is inferior compared to cisplatin in high dose (5.0 mg/kg). Tumor-bearing mice showed symptoms of acute intoxication (especially weight loss) already after the first injection of 1.0 or 2.0 mg/kg of *diruthenium-1*, doses which were tolerated in healthy mice during the previous acute toxicity study. This is why only the dose groups from 0.2 to 0.6 were included in the survival study. The administration of *diruthenium-1* 0.6 mg/kg prolonged significantly the survival time of tumor-bearing mice, when compared with untreated tumor-bearing control mice ($P < 0.01$). It was also

effective compared to cisplatin ($P < 0.05$), which itself did not exert a significant effect on the survival ($P = 0.068$), see Figure 32.

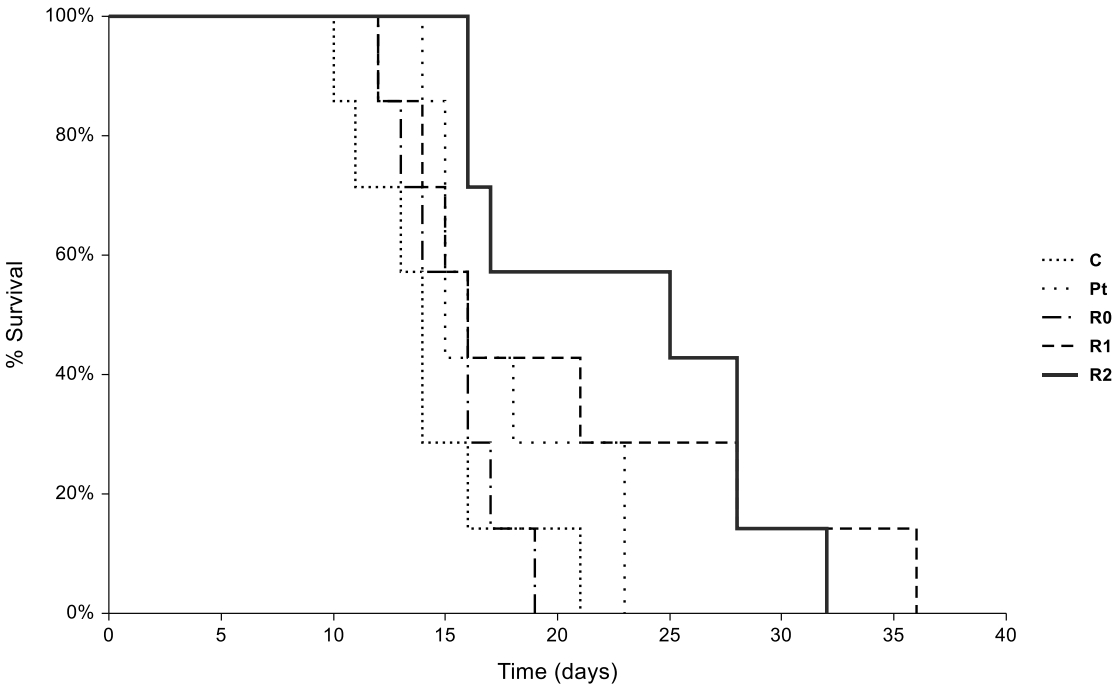


**Figure 32 -** Kaplan-Meier analysis of survival: The i.p. administration of *diruthenium-1* 0.6 mg/kg (R2) on days 1 and 7 significantly prolonged the survival of tumor-bearing mice compared to the tumor-bearing control group treated with the pure solvent (C). The injection of cisplatin 5 mg/kg (Pt) had the second largest effect, although this was not statistically significant. R0 = 0.2 mg/kg, R1 = 0.4 mg/kg (n = 7 in each group).

The tumor homogenates from mice treated with cisplatin showed significant decrease in the amount of PCNA (proliferating cell nuclear antigen), a marker of cell proliferation, contrary to those from the mice injected with *diruthenium-1*, in which we did not observe any changes in PCNA. Investigating the effect on the anticancer immune response mediated by T-lymphocytes, we did not detect a significant change in the expression of the CD3 antigen, an indicator of T-lymphocytes, after either *diruthenium-1* or cisplatin therapy (Figure 33).

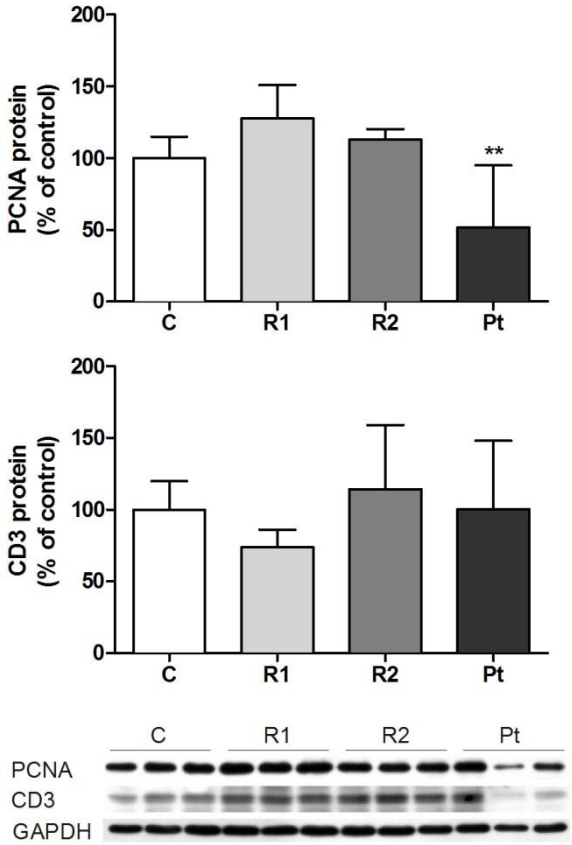


**Figure 33 -** Western blot analysis to detect the presence of the proliferation-related marker PCNA and CD3 (indicator of T-lymphocytes) antigens in tumor homogenates from mice treated i.p. with pure solvent (C), [(*p*-$MeC_6H_4$-$Pr^i$)$_2$$Ru_2$($SC_6H_4$-*p*-X)$_3$]Cl, 0.4 mg/kg (R1) and 0.6 mg/kg (R2), or cisplatin 5.0 mg/kg (Pt). Apart from the inhibitory effect of cisplatin to PCNA, no significant changes in expression of these proteins were detected. Values are the means ± SD (n = 7 in each group, exemplified by 3 samples for each group). Significantly different from the control: $^{**}P < 0.01$.

In addition to the core results focused on the anticancer effect of *diruthenium-1*, we also performed a preliminary evaluation of its pharmacokinetics using four mice from the sacrificed R2 group. ICP-MS measurements at *m/z* = 101 were done in plasma and selected tissues (tumor, brain, liver, and kidney) from the mice 48 hours after the second administration, when we anticipated (based on similar studies with other ruthenium- or platinum-based compounds [133-134]) the terminal excretory period with finished distribution (Table 4). High ruthenium concentrations were observed in liver and kidneys, but ruthenium also accumulated at high levels in the tumor. The levels in the tumor were well above the previously assessed $IC_{50}$ values [111,113]. No ruthenium

was detected in the brain, indicating that *diruthenium-1* does not cross the blood-brain barrier. Calculations of tissue content showed that at least 31.6% of the administered dose still persisted in the organism, which corresponds to an elimination half-life of 30 hours.

**Table 4** - Biodistribution of *diruthenium-1* into different organs after repeated administration of 2.0 mg/kg i.p. on days 1 and 7, studied by ICP-MS of $^{101}$Ru. The ruthenium concentration (conc.) is given in ng/g wet weight, the total uncertainty being approximately 10%. The weight of the organs is in grams. Number of animals n = 4.

| | 1 | | 2 | | 3 | | 4 | |
|---|---|---|---|---|---|---|---|---|
| Organ | Organ weight | Conc. | Organ weight | Conc. | Organ weight | Conc. | Organ weight | Conc. |
| Tumor | 1.4 | 320 | 1.3 | 310 | 1.1 | 150 | 1.4 | 200 |
| Brain | 0.4 | 3.5 | 0.4 | 2.3 | 0.4 | 1.4 | 0.4 | 1.3 |
| Liver | 1.5 | 270 | 1.5 | 290 | 1.9 | 900 | 1.5 | 100 |
| Kidney L | 0.1 | 570 | 0.1 | 890 | 0.1 | 760 | 0.1 | 620 |
| Kidney R | 0.1 | 670 | 0.1 | 760 | 0.1 | 610 | 0.1 | 580 |
| Plasma | 0.5 | 53 | 0.6 | 55 | 0.5 | 18 | 0.6 | 25 |

Figure 34a shows that *diruthenium-1* at the concentration of 200 nM and higher significantly decreased the proliferation of MCF-7 cells. Interestingly, after treatment with low concentrations (50 and 100 nM), the proliferation of BT-549 cells was stimulated. The quantity of LDH (lactate dehydrogenase) as a marker of cytotoxicity significantly increased after the treatment with 100 nM *diruthenium-1* and its release occurred in a concentration dependent manner in both cell lines.

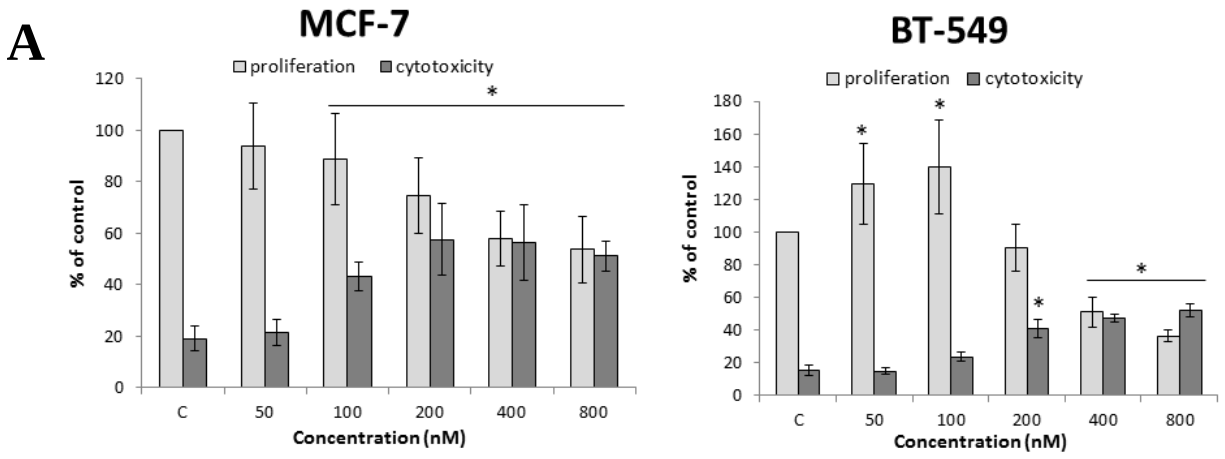

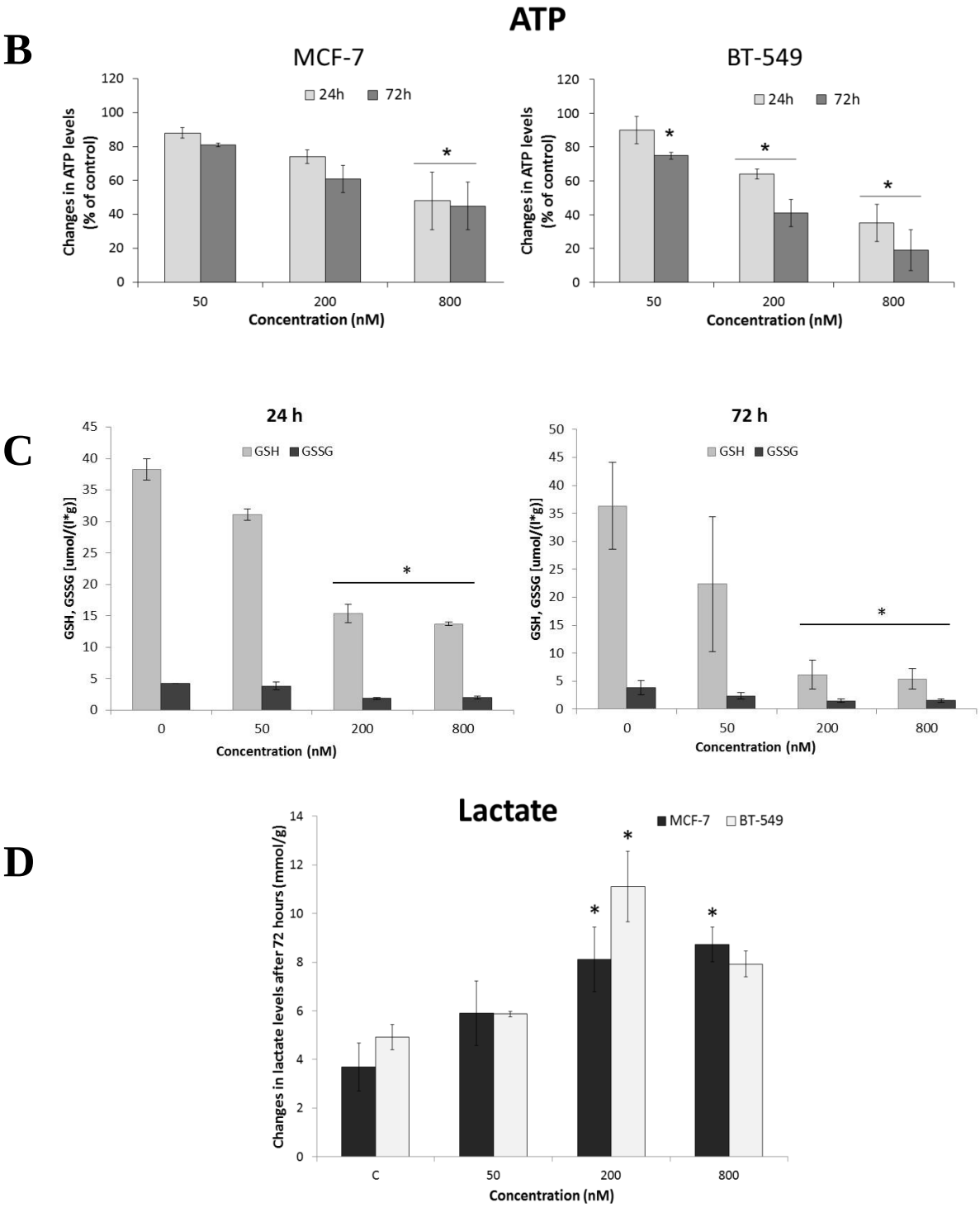


**Figure 34** – A: The influence of *diruthenium-1* on cell proliferation (WST-1 assay) and its cytotoxic effect (LDH cytotoxicity detection assay) in MCF-7 and BT-549 cells. Values represent means of 3 independent experiments, P values < 0.05 are considered significant, * indicate values significantly different from control. B: The effect of *diruthenium-1* on ATP levels in MCF-7 and BT-549 cells. Values represent means of 3 independent experiments, P values < 0.05 are considered significant, * indicate values significantly different from control. C: The influence of

*diruthenium-1* on intracellular levels of reduced (GSH) and oxidized (GSSG) glutathione in MCF-7 cells. The levels of GSH and GSSG were related to the protein amount in the appropriate sample. Values represent means of 3 independent experiments, P values < 0.05 are considered significant, * indicate values significantly different from control. D: The effect of *diruthenium-1* on levels of lactate in the cultivation medium of MCF-7 and BT-549 cells. The levels of lactate were divided by the concentration of protein in the appropriate sample. Values represent means of 3 independent experiments, P values < 0.05 are considered significant, * indicate values significantly different from control.

*Diruthenium-1* caused a decrease of ATP levels in the cells, as shown in Figure 34b. In MCF-7 cells, a significant decrease of ATP was observed after the treatment with 800 nM of *diruthenium-1*, as the ATP level dropped to the half of the control in both time intervals. BT-549 cells appear to be more sensitive. After 72 hours of treatment with 200 nM of *diruthenium-1*, the level of ATP decreased to 41% of the control, and 800 nM caused a decline to 19%. MCF-7 cells incubated with *diruthenium-1* showed a drop in the intracellular levels of both reduced (GSH) and oxidized (GSSG) glutathione, the latter being less impacted (Figure 34c). It may imply an interaction of *diruthenium-1* with glutathione other than its oxidation. We observed the same GSH and GSSG decrease in BT-549 cells, but without statistical significance (data not shown). An increase in the concentration of lactate in the cultivation medium was observed after 72 hours of incubation (Figure 34d). In MCF-7 cells it rose in a concentration dependent manner, whereas in BT-549 it peaked at 200 nM of *diruthenium-1*. In BT-549 cells, we observed an increase in the expression of protein p53 after 24 hours of treatment with 800 nM *diruthenium-1*. This increase was accompanied by the phosphorylation of p53 at serine 15 which was also present in MCF-7 cells. We further examined the expression of selected MAP (mitogen-activated protein) kinases. In an early interval of treatment, no changes were observed in the case of MCF-7 cells, whereas in BT-549 a decrease in phosphorylation occurred in a concentration dependent manner. In both cell lines, treatment with 50 nM *diruthenium-1* for 72 hours led to an enhanced phosphorylation of ERK (extracellular signal-regulated kinases) and p38. This phosphorylation surprisingly declined with increasing concentration of *diruthenium-1* (Figure 35).

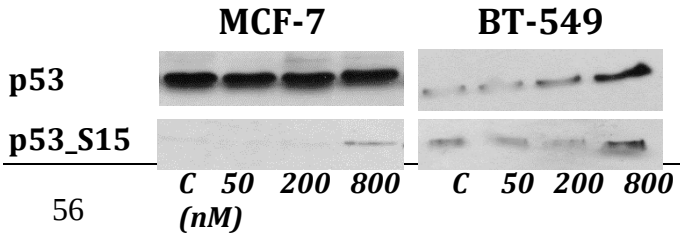

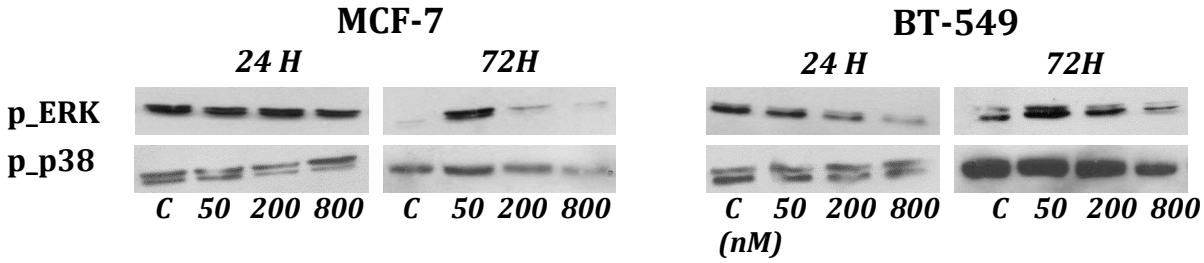


**Figure 35** - Changes in the expression of protein p53 and its phosphorylation at serine 15 after 24 hours treatment with *diruthenium-1* at the indicated concentrations (top). Changes in the expression of ERK phosphorylated at T202/Y204 and p38 phosphorylated at T180/Y182 after 24 and 72 hours treatment with *diruthenium-1* at the indicated concentrations (bottom).

The measurement of oxygen consumption in rat liver mitochondria (Figure 36) revealed a significant inhibition of both the complex I and II upon the addition of *diruthenium-1*. The respiration after addition of complex I substrates (glutamate + malate) was 47% after 5 minutes and only 32% after 10 minutes of incubation with *diruthenium-1* when compared with the control. The respiration after addition of succinate, which is the substrate of complex II, was 59% of that of the control after 5 minutes of exposure to *diruthenium-1* and 40% after 10 minutes. Significant recovery of the respiration of mitochondria incubated with *diruthenium-1* was observed after the addition of cytochrome *c*, a marker of the status of the mitochondrial outer membrane. This increase was observed both for complex I and complex II, indicating a disintegration of the outer membrane by *diruthenium-1*.

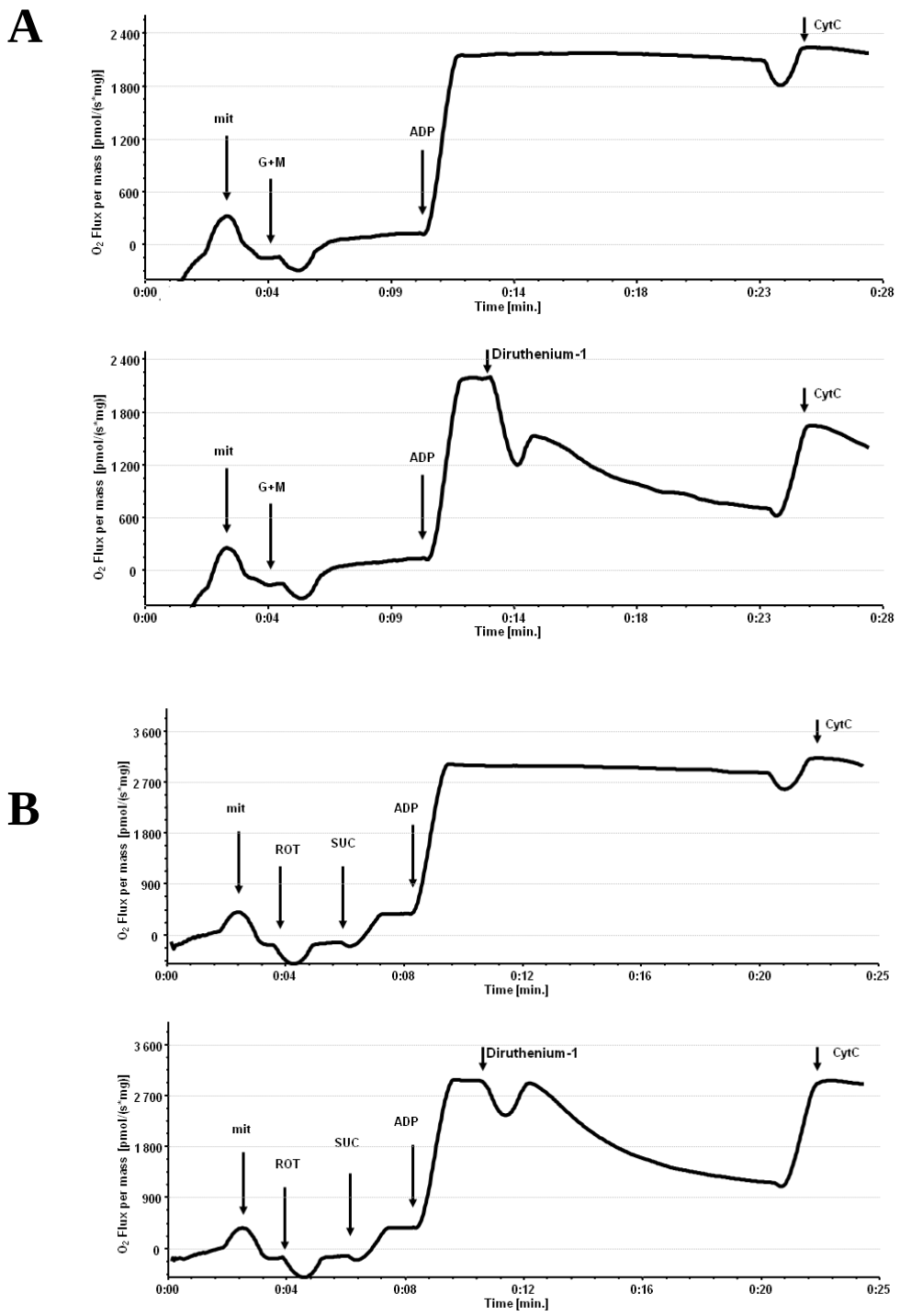


**Figure 36** - Respiration of rat liver mitochondria, with a special focus on complex I (A) and II (B). To the 2 ml of K-medium (30°C), mitochondria (mit) 0.2 mg protein/ml were added followed by 10 mM glutamate + 2.5 mM malate (G+M) for complex I or 10 mM succinate for complex II, further 1.5 mM ADP, 0.8 μM *diruthenium-1* and 20 μM cytochrome *c* (CytC). In both A and B, *diruthenium-1* decreased the oxygen consumption which was reversible by the addition of cytochrome *c*.

### 2.3.3 Conclusion

For the study of the anticancer activity of *diruthenium-1 in vivo*, a solid Ehrlich tumor in immunocompetent mice was employed as a model of mammary adenocarcinoma sensitive to cisplatin, which was used as a positive control drug. The study revealed that *diruthenium-1* at doses of 0.4 and 0.6 mg/kg administered twice within 8 days inhibits the tumor growth in tumor-bearing mice, although this effect was somewhat less pronounced than for cisplatin. On the other hand, it was only *diruthenium-1* at the dose of 0.6 mg/kg that significantly prolonged the survival rate of tumor-bearing mice. In terms of post-treatment survival, *diruthenium-1* was in fact more effective than cisplatin, which can be considered a clinically valuable marker [135]. A possible explanation could be a mode of action that produces a longer lasting inhibition of the tumor regrowth rather than a significantly longer persistence of *diruthenium-1* in the body.

The elimination half-life predicted in our preliminary study correlates with the data formerly reported for other ruthenium-containing compounds in mice [136-137], and points toward a more rapid excretion than that detected for cisplatin [138-139]. Although we are aware of the limitations of such a prediction, overall pharmacokinetics similar to other heavy metal containing cytostatic agents can be anticipated, although a more detailed study is highly desirable. Due to the supposed elimination half-life, the influence of the first dose given 192 h before the sample collection seems to be negligible. Repeated administration was chosen in order to assess the concentrations of ruthenium in the tumor tissue during our *in vivo* study. Since the concentrations in tumor were more than one order of magnitude higher than the $IC_{50}$ values [111,113], the inhibitory concentrations should be reached even if a considerable part of the compound were in an inactive state.

The dose of cisplatin was chosen near the reported MTD [140], since the dose range of *diruthenium-1* was also adjacent to the MTD assessed in our study. However, at the doses of 1.0 and 2.0 mg/kg, which had been at the upper range of tolerance in healthy mice, *diruthenium-1* did not display any anticancer activity and instead caused severe acute toxicity to tumor-bearing mice. The use of the selected tumor model allows the observation of the effect on anticancer immune response [141-142]. The observed absence of changes in T-cell-infiltration into the tumor may refer to the mechanism of action of cisplatin, since alkylating agents were reported to impair the immune response [143]. The disproportion between the distinct tumor-inhibitory effect of *diruthenium-1* and the absence of any changes in PCNA expression could also support the hypothesis of rapid cell death.

We studied cellular mechanisms of action of *diruthenium-1* in human MCF-7 and BT-549 breast cancer cells. It exhibited antiproliferative and cytotoxic effects against both cell lines, the MCF-7 cells seem to be more sensitive than BT-549. Both cell lines produced higher levels of lactate after *diruthenium-1* treatment. The increase in lactate production was accompanied by a decrease in the level of ATP, which could indicate a switch to anaerobic glucose metabolism. In order to investigate this hypothesis, we measured the consumption of oxygen by the electron transfer chain in rat liver mitochondria. *Diruthenium-1* was found to inhibit both the complex I and II of the electron transfer chain. In addition, it disrupts the outer mitochondrial membrane. Such mitochondrial dysfunction typically augments the formation of reactive oxygen species (ROS) [144]. This is why we expected an increased oxidation of GSH, in addition to the previously demonstrated catalytic GSH oxidation under cell-free conditions [111,113]. During the incubation of cells with *diruthenium-1*, the intracellular levels of GSH indeed decreased. However, since GSSG dropped rather than rose, we conclude that another type of interaction with glutathione prevails in living cells than the oxidation of GSH to GSSG. It might well be that *diruthenium-1* interacts with sulphur-containing peptides and proteins including the components of the electron transfer chain.

Chen *et al*. [145] and Zhao *et al*. [146] described mitochondrial dysfunction and an increase in p53 in cells treated with other ruthenium complexes. The p53 protein, a key player in apoptosis, was also increased and activated by the phosphorylation at serine 15 in our study after the treatment with 800 nM *diruthenium-1*. The balance between MAPK members ERK1 and p38 is critical in terms of cell death or survival. In *diruthenium-1* treated cells, we observed increased amount of phosphorylated ERK and p38 protein after 72 hours; interestingly it decreased with increasing concentration of *diruthenium-1*. Zhao *et al*. [146] associated the slight suppression of ERK after treatment with ruthenium polypyridyl complexes with an overproduction of ROS by dysfunctional electron transfer chain as a result of the regulation of Bcl-2 (B-cell lymphoma 2) family proteins.

In conclusion, our results show that *diruthenium-1*, the most cytotoxic ruthenium compound reported so far, has indeed a potential as an anticancer drug, since it significantly prolongs the survival of tumor-bearing mice. However, further studies on pharmacokinetics, on the mode of action as well as on the assessment of its indication range are required.

# Chapter 3: Trithiolato Complexes with Fluorinated Side-Chains

## 3.1 General

Large numbers of synthetic fluorine-containing compounds have been used in a variety of fields, notably in the field of medicinal chemistry. Currently, up to 20% of all pharmaceuticals contain fluorine substituents, because of the unique properties that the incorporation of fluorine atom(s) or fluorinated group(s) can provide [147-148]. It is well known that fluorine's electronegativity, size, lipophilicity, and electrostatic interactions can dramatically influence chemical and biological behavior of the resulting compounds [149]. The bioisosterism of fluorine-containing substituents with other chemical groups is therefore often exploited in the search for more active or more selective compounds in medicinal chemistry [150]. Thus, the C–F, C–OH, and C–OMe bonds can be sometimes interchanged without a major influence on the biological behavior of the compound [147], the C–$CF_3$ fragment can be used as a substitute for the C=O group [151], the $CF_3$ group is often used as a bioisoster of the $CH_3$ group or as a variation of other halide groups; the fluorovinyl group (C=CHF) has been used as a replacement for the peptide bond [152].

The lack of selectivity of most of the currently used anticancer agents manifests by their severe side-effects. In the search for more selective means of cancer treatment, many new approaches have been devised such as phototherapy, treatment with magnetic nanoparticles or thermotherapy. During these therapies, a non-toxic agent (photosensitizer, magnetic nanoparticles or thermo-responsive drug, respectively) is introduced into the tumor tissue, followed by the application of an external inducer such as light [153], magnetic field [154] or hyperthermia [155], which then activates the agent, thus increasing its cytotoxicity. Since these external inducers can be applied locally on the area containing the tumor tissue, the selectivity of such treatments is significantly increased and the side-effects are limited. In recent years, thermoresponsive properties of compounds with long fluorinated alkyl chains were investigated by the Dyson group (Figure 37) [156-157]. Fluorinated derivatives of the alkylating agent chlorambucil (Figure 37a) were shown to be non-toxic at 37°C but active against 8 different cancer cell lines under mild hyperthermia (41.5°C) [156]. Subsequently, the thermoresponsive properties of ruthenium complexes of the general formula $[(\eta^6\text{-}p\text{-}MeC_6H_4Pr^i)Ru(\mu\text{-}NC_5H_4\text{-}m\text{-}C_2H_5COOC_2H_5(CF_2)_nCF_3]$ (n = 5, 7, 9) were also studied [157]. The Ru(III) complexes with fluorinated alkyl chains on the pyridine ligand (Figure 37b) were shown to be up to two orders of magnitude more toxic to cancer cells under mild hyperthermia than under normal conditions (37°C), while being non-toxic to healthy HEK293 cells.

The fluorinated ligands were discussed as the source of the thermoresponsive properties, since they displayed marked difference in toxicity under normal conditions and under mild hyperthermia already on their own [157]. The benefits of thermotherapy with ruthenium-based drugs were later confirmed by *in vivo* studies, showing 90% decrease in tumor growth after the application of the ruthenium complex $[(\eta^6\text{-}p\text{-}MeC_6H_4Pr^i)Ru(\mu\text{-}NC_5H_4\text{-}m\text{-}C_2H_5COOC_2H_5(CF_2)_9CF_3]$ together with local hyperthermia [157].

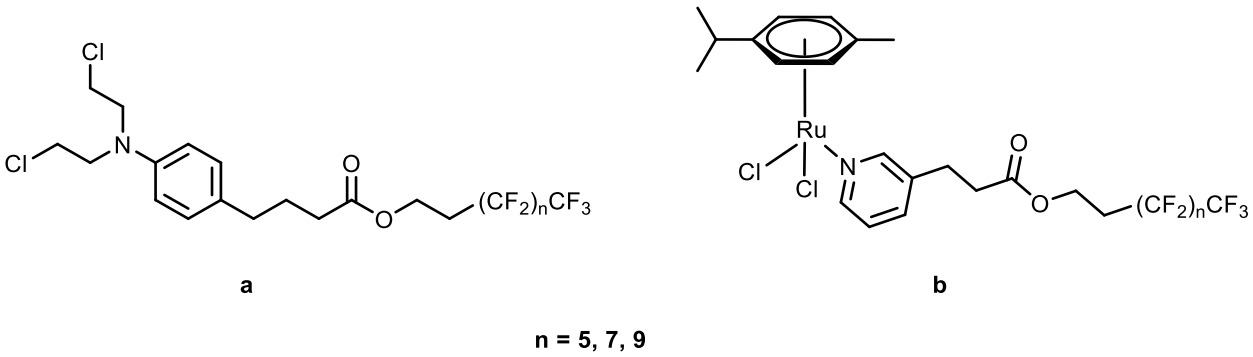


**Figure 37** - Thermoresponsive chlorambucil derivatives (a) and ruthenium(III) complexes (b)

The cytotoxicity of the arene ruthenium thiolato-bridged complexes was shown to depend on the lipophilicity of the complexes, the most active compound $[(p\text{-}MeC_6H_4Pr^i)_2Ru_2(SC_6H_4\text{-}p\text{-}Bu^t)_3]Cl$ being also one of the most lipophilic derivatives [111]. The lipophilicity of long fluorinated chains on the dinuclear ruthenium core could therefore have a positive effect on the anticancer activity of the resulting compounds. Thus, in order to investigate the effects of fluorinated alkyl chains on the solubility, cytotoxicity and thermoresponsivness of thiolato-bridged arene ruthenium complexes, we synthesized a new series of complexes of the general formula $[(\eta^6\text{-}p\text{-}MeC_6H_4Pr^i)_2Ru_2(\mu\text{-}SC_2H_4R)_3]^+$, R = $(CF_2)_7CF_3$ (**11**), $(CF_2)_5CF_3$ (**12**), $(CF_2)_3CF_3$ (**13**) and $(CH_2)_5CH_3$ (**14**). Their structure, stability and anticancer activity under normal conditions and under mild hyperthermia are reported.

### 3.2 Results

The dinuclear *p*-cymene complex $[(\eta^6\text{-}p\text{-}MeC_6H_4Pr^i)_2Ru_2Cl_2(\mu\text{-}Cl)_2]$ reacts with the thiols RSH [R = $C_2H_4(CF_2)_7CF_3$, $C_2H_4(CF_2)_5CF_3$, $C_2H_4(CF_2)_5CF_3$ and $C_2H_4(CH_2)_5CH_3$] to give cationic trithiolato arene ruthenium complexes **11** – **14** (Scheme 5). All four complexes were isolated in the form of their chloride salts as light orange crystalline powders and characterized by spectroscopic methods and correct elemental analyses. The analytical data are given in the experimental section.

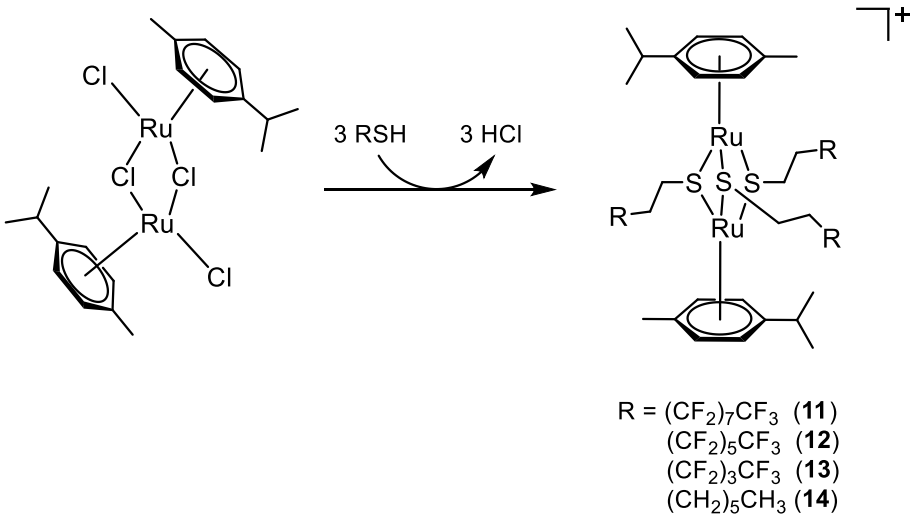


**Scheme 5** - Synthesis of trithiolato complexes **11** – **14**, isolated as chloride salts

The stability of the compounds was tested at 37°C in DMSO-$d_6$/$D_2O$ solution and followed by 1D $^1$H NMR spectroscopy. As can be seen in Figure 38, no changes were observed in the NMR spectra after a week of incubation at 37°C. We therefore considered the compounds stable and proceeded with the biological studies of their anticancer activity and thermoresponsivness.

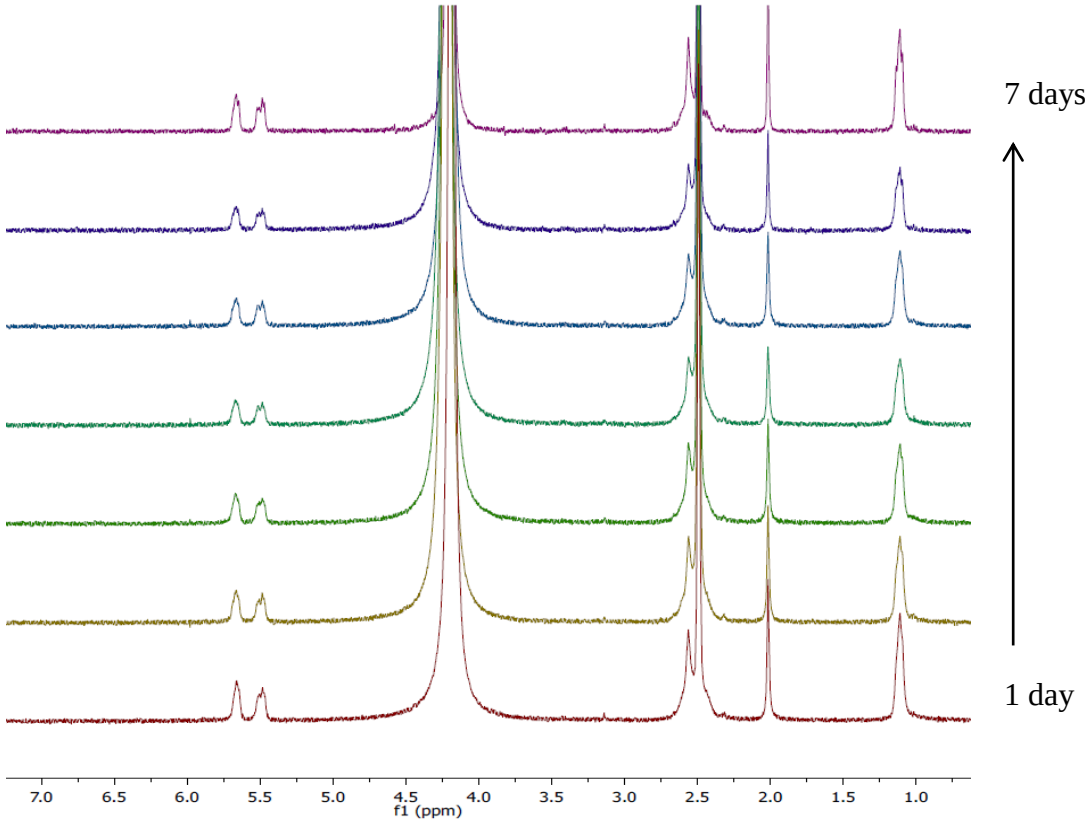


**Figure 38** – Stability of complex **12** in DMSO-$d_6$/$D_2O$ solution over 7 days

Unfortunately, compounds [**11**]Cl and [**12**]Cl had a very low solubility in $H_2O$ mixtures, due to their long fluorous chains; it was therefore not possible to prepare solutions of sufficient concentrations for *in vitro* experiments even with 1% of DMSO as co-solvent. These compounds had to be abandoned and the biological studies were performed only with compounds [**13**]Cl and [**14**]Cl.

**Table 5** – Cytotoxicity of compounds [**13**]Cl and [**14**]Cl against cancer cell lines

| Compound | A2780 (37°C) | A2780 (41°C) | A2780cisR | HEK293 |
|---|---|---|---|---|
| | μM | μM | μM | μM |
| [**13**]Cl | 0.03 ± 0.01 | 0.03 ± 0.01 | 0.04 ± 0.02 | 0.08 ± 0.05 |
| [**14**]Cl | 0.10 ± 0.02 | 0.10 ± 0.02 | 0.08 ± 0.02 | 0.17 ± 0.03 |

To study the effects of hyperthermia on the trithiolato compounds, preliminary experiments were performed with A2780 ovarian cancer cells at 37°C and 41°C. Although the $IC_{50}$ values of compounds [**13**]Cl and [**14**]Cl were in nanomolar range, no difference was observed when the experiments were performed at 41°C. These results suggest that the fluorous chains on compound [**13**]Cl have no significant effect on their thermoresponsivness, contrary to chlorambucil derivatives and Ru(III) complexes reported previously [156-158]. Therefore, the cytotoxicity for A2780cisR and HEK293 cell lines was studied only at 37°C and showed the compounds to be highly cytotoxic to both cell lines and slightly less cytotoxic (by the factor of two) to the healthy HEK293 cells (Table 5). The cytotoxicity of compounds [**13**]Cl and [**14**]Cl to A2780 and A2780cisR matches well with the observations for previously reported trithiolato complexes of the type $[(p\text{-}MeC_6H_4Pr^i)_2Ru_2(SC_6H_4\text{-}p\text{-}X)_3]^+$ (X = H, Me, Ph, Br, OH, $NO_2$, OMe, $CF_3$, F, $Pr^i$ or $Bu^t$), where the chloride salt of the most lipophilic complex $[(p\text{-}MeC_6H_4Pr^i)_2Ru_2(SC_6H_4\text{-}p\text{-}Bu^t)_3]$ (**9**) was found to be the most cytotoxic, with $IC_{50}$ value of 0.03 μM for A2780 and A2780cisR. Compound [**13**]Cl is therefore as active as **9**[Cl] for the cisplatin-sensitive cell line A2780 and only slightly less active for the cisplatin-resistant cell line A2780cisR, which makes is one of the most active ruthenium complexes discovered to date. The high activity of the complex is supposedly related to the high lipophilicity of the fluorous chains.

### 3.3 Conclusion

Four dinuclear arene ruthenium complexes **11** – **14** were synthesized and fully characterized. The long fluorous chains influenced the solubility of the complexes, not allowing to test compounds [**11**]Cl and [**12**]Cl *in vitro*. The compounds [**13**]Cl and [**14**]Cl were highly cytotoxic towards cancer cell lines, their $IC_{50}$ values being similar to those of complex **9**, most active thiolato-bridged complex synthesized so far. The lipophilicity of the compounds [**13**]Cl and [**14**]Cl is presumably the reason for this high cytotoxicity. No enhancement of the anticancer activity by hyperthermia was observed and the compounds did not exhibit any particular selectivity to cancer cells compared to healthy cells.

# Chapter 4: Mixed Trithiolato Complexes

To address the second objective of this thesis – the synthesis of conjugates of biologically relevant compounds with arene ruthenium thiolato-bridged complexes – new complexes that would allow the tethering of organic compounds had to be synthesized. Several examples of the so-called mixed trithiolato complexes were already known [112] and allowed us to use the hydroxo derivatives of the general formula $[(\eta^6\text{-}p\text{-}MeC_6H_4Pr^i)_2Ru_2(SCH_2R)_2(SC_6H_4\text{-}p\text{-}OH)]^+$ for esterification reactions (the results of which will be presented in Chapters 6 and 7). The conditions for the synthesis of mixed trithiolato complexes were also applied on the synthesis of new derivatives, intended as precursors for different coupling reactions. The reasoning behind the design of these complexes as well as the obstacles encountered during their synthesis and isolation are presented herein.

## 4.1 Trithiolato Complexes with Halido Substituents

During the investigation of the stepwise synthesis of trithiolato complexes (Chapter 2.1), various thiols were tested to find examples that form preferentially monothiolato products. During this screening, a correlation between the reactivity of the thiol of a general formula $HSCH_2\text{-}p\text{-}C_6H_4R$ and its pKa was observed, presented in the Table 5 (pKa values were obtained from the SciFinder® database).

**Table 6** – Relationship between the pKa of the thiol and product of the reaction

| R | pKa value | Product |
|---|---|---|
| $NO_2$ | 8.74 ± 0.1 | Monothiolato |
| Cl | 9.32 ± 0.1 | Monothiolato and dithiolato |
| Br | 9.32 ± 0.1 | Monothiolato and dithiolato |
| I | 9.53 ± 0.1 | Monothiolato and dithiolato |
| H | 9.68 ± 0.1 | Dithiolato |
| $Bu^t$ | 9.83 ± 0.1 | Dithiolato |
| OMe | 9.93 ± 0.1 | Dithiolato |

Thus, under the standard conditions (see Chapter 9.4.2), the three previously reported dithiolato complexes [115] were synthesized from the *p*-cymene dichloride dimer and benzenemethanethiol

(**10**), 2-phenylethanethiol (**5**, not presented in the table) and (4-*tert*-butylphenyl)methanethiol (**7**) and the fourth dithiolato complex was synthesized by the same method using (4-methoxyphenyl)methanethiol (see Chapter 9.4.3, product **6**); (4-nitrophenyl)methanethiol yielded the monothiolato complex **2** described in the Chapter 2.1.

The formation of dithiolato complexes from the reaction with (4-chlorophenyl)methanethiol, (4-bromophenyl)methanethiol and (4-fluorophenyl)methanethiol provided us with the possibility to increase the number of dithiolato precursors available for the syntheses of various conjugates. Therefore, by increasing the temperature, the reaction time and the ratio between the *p*-cymene dichloride dimer and the thiol, it was possible to synthesize the tree dithiolato complexes **15** – **17** (Figure 39) without the presence of the contamination by the monothiolato product. The complexes were significantly less soluble than the four dithiolato complexes reported previously, precipitating from the ethanolic solution already during the reaction.

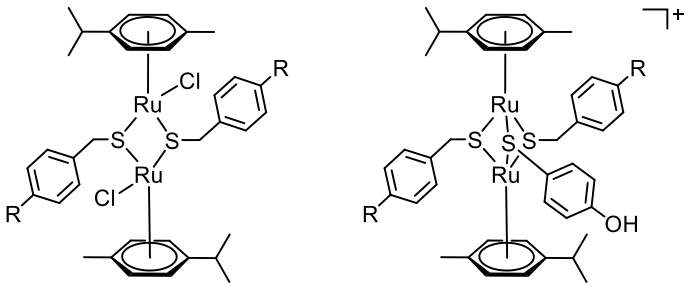


| R | Cl | Br | F |
|---|---|---|---|
| | **15** | **16** | **17** |

| R | Cl | Br | F |
|---|---|---|---|
| | **18** | **19** | **20** |

**Figure 39** – Structure of thiolato arene ruthenium complexes with halido substituents

The three complexes were then reacted with HS-*p*-$C_6H_4$-OH in order to obtain the mixed trithiolato complexes (isolated as their chloride salts) and use them as starting products in the synthesis of chlorambucil conjugates (Chapter 7). When the Steglich esterification with the trithiolato complexes **19** and **20** was attempted, however, the resulting conjugates proved unstable (already the elemental analysis of complex **19** suggests its slight instability). The NMR spectra taken directly after the synthesis showed the expected products, but the results of elemental analyses showed that no nitrogen (and therefore no bound chlorambucil) was present. We assume that the slow degradation took place during the time between the synthesis and the elemental analysis. The reasons for this instability or the precise nature of the degradation products were not

studied. The esterification of product **18** with chlorambucil gave a stable conjugate, which was fully characterized and is discussed in the Chapter 7.

### 4.2 Trithiolato Complexes with Amino Groups

The reaction of a carboxylic acid R-COOH with an amine R'-$NH_2$ forms a peptide bond R-CO-NH-R'. Since it is the basis of all peptides and proteins, peptide bond is probably one of the most abundant structural features in living organisms. As such, it is frequently used in the design of pharmaceutical agents, because of its relative stability in biological environments [159]. The synthesis of trithiolato complexes containing an $NH_2$ group would allow us to attach various biologically active compounds to the ruthenium center. Examples of such compounds include amino acids or peptides (which could be attached by their C-terminus), biologically active carboxylic acids such as ethacrynic acid, ibuprofen or chlorambucil, or compounds with tumor targeting properties, such as folic acid or biotin. Besides the formation of the peptide bond, $NH_2$ derivatives of trithiolato complexes would also allow us to explore the possibility of other organic coupling reactions, for example the Buchwald-Hartwig amination (cross-coupling reaction between amines and aryl halides or pseudohalides), thus broadening the spectrum of compounds that can be attached to the dinuclear arene ruthenium core.

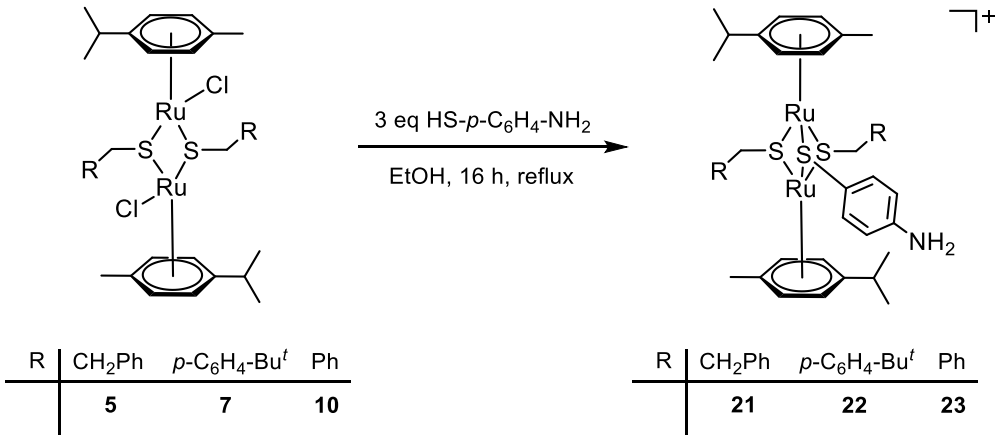


| R | $CH_2Ph$ | *p*-$C_6H_4$-$Bu^t$ | Ph |
|---|---|---|---|
| | **5** | **7** | **10** |

| R | $CH_2Ph$ | *p*-$C_6H_4$-$Bu^t$ | Ph |
|---|---|---|---|
| | **21** | **22** | **23** |

**Figure 40** - Synthesis of amino derivatives **24** – **26** isolated as chloride salts

The syntheses of products **21** – **23** were carried out using the standard reaction conditions published previously [112,115], refluxing the ethanolic solution of the dithiolato precursor and 6 equivalents of the 4-aminothiophenol for 16 hours. The resulting mixture was separated by column chromatography, yielding chloride salts of the products **21** – **23** as orange crystalline powders (Figure 40). Both NMR and ESI-MS spectra of the products contained an impurity that was

impossible to remove by any of the employed separation methods. The impurity appeared in the aromatic region of the NMR and also in the ESI-MS spectra (two doublets at 7.18 ppm and 6.57 ppm and a peak at *m/z* = 942.0 for the product **21**, see Figure 41).

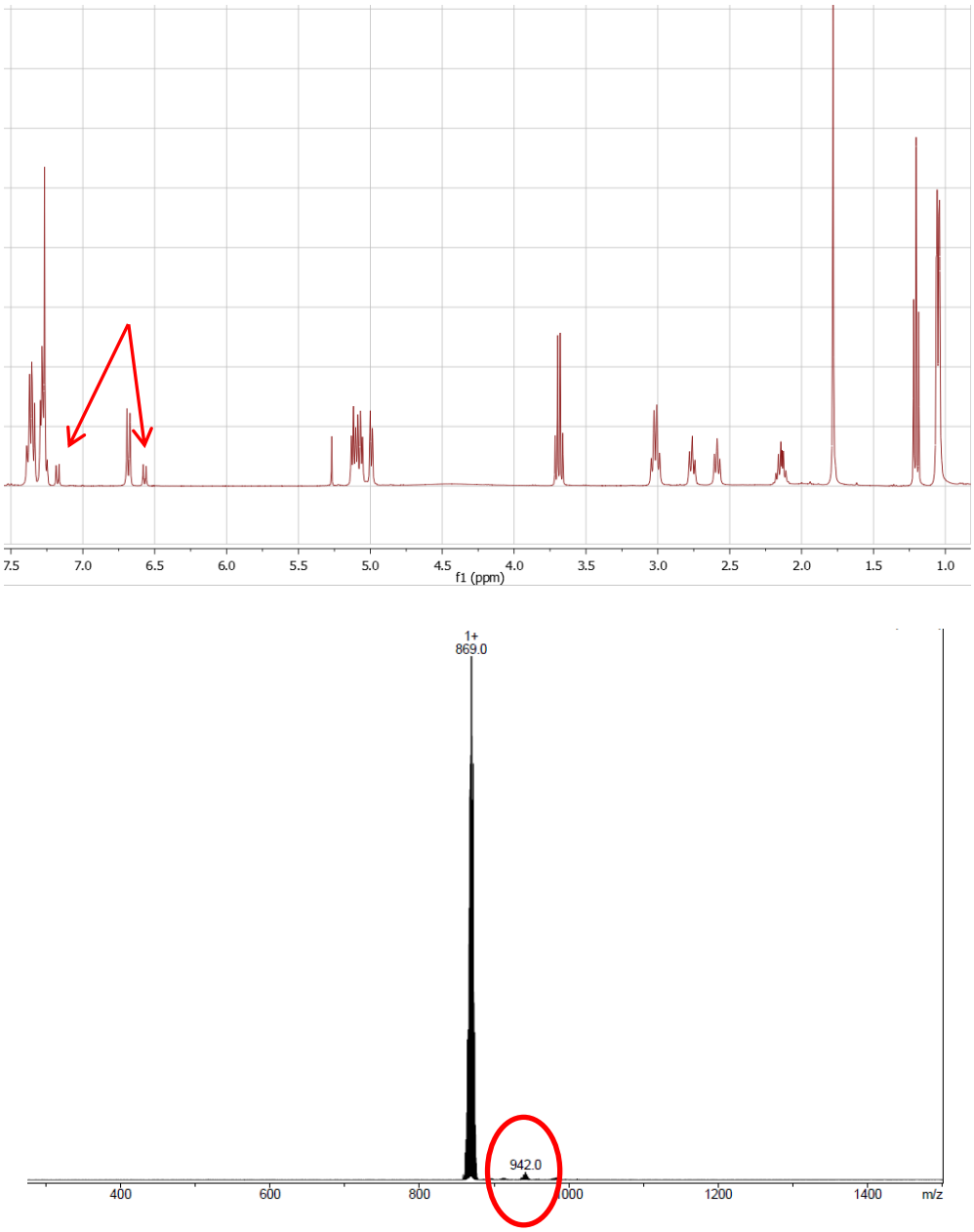


**Figure 41 -** Impurity in the product **21**, NMR and ESI-MS spectra

This impurity could not be isolated or identified and its presence did not allow the correct elemental analyses of the products. Therefore, this approach for the synthesis of conjugates of trithiolato arene ruthenium complexes had to be abandoned. NMR and ESI-MS data for the chloride salts of the three products **21** – **23** are given in the section 9.4.8.

## 4.3 Trithiolato Complexes with Carboxylic Acid Groups

Since the synthesis of $NH_2$-containg derivatives of arene ruthenium thiolato-bridged complexes was unsuccessful, we decided to approach the problem from the opposite side – the complexes containing a carboxylic acid moiety would still allow us to attach $NH_2$-containing molecules by the formation of peptide bond and would at the same time provide us with the possibility of tethering biologically interesting molecules containing OH groups, such as flavonols [160]. We therefore set out to synthesize the carboxylic acid derivatives of the mixed trithiolato complexes.

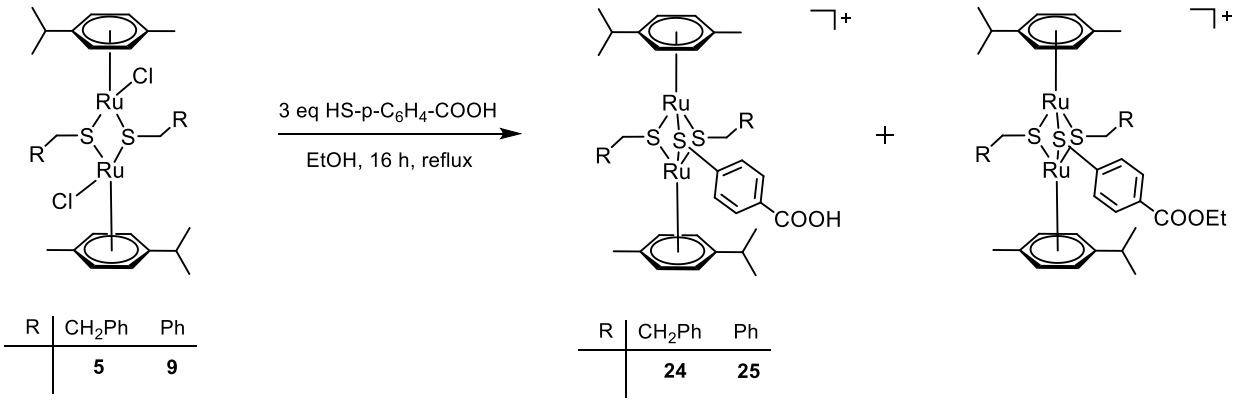


**Scheme 6** – Synthesis of trithiolato complexes with COOH functionality

When the standard reaction conditions for the synthesis of the mixed trithiolato complexes were used (3 equivalents of thiol, ethanol, reflux, 16 hours), the two dithiolato precursors **5** and **9** yielded a mixture of the COOH containing complex and its respective ethyl ester (Scheme 6). Although the majority of the ester-containing complex could be separated by column chromatography, a trace contamination was always present in the desired COOH derivative (manifested by NMR resonances at 4.40 ppm and 1.42 ppm for the derivative **24** and 4.36 ppm and 1.39 ppm for **25**) and no separation method that we tried afforded the pure product. Therefore, the correct elemental analysis of the products **24** and **25** was not obtained and it was not possible to use them in further reactions. The 1D $^1$H NMR and ESI-MS data of the two products are shown in the section 9.4.9. The attempts to run the reaction in other solvents that would not form esters (MeCN at reflux, ethyl acetate at reflux or $CH_2Cl_2$ in pressure Schlenk tube at 75°C) did not yield the desired product.

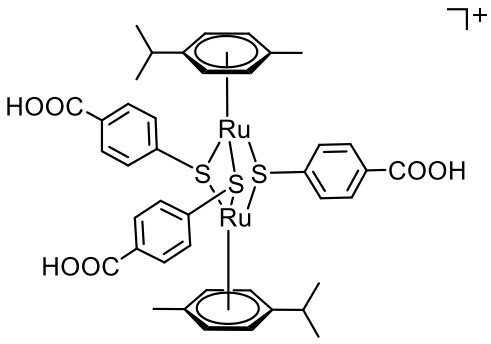


**Figure 42** – Structure of the tris(mercaptobenzoic acid) derivative **26**

Interestingly, when the *p*-cymene dichloride dimer was reacted with 6 equivalents of 4-mercaptobenzoic acid in ethanol, only the carboxylic acid derivative of the triply bridged arene ruthenium complex was obtained (Figure 42). This product ([**26**]Cl) was therefore isolated by column chromatography on silicagel using a mixture EtOH/$CH_2Cl_2$ 1 : 1 with 0.1% of formic acid and was subsequently fully characterized.

# Chapter 5: Propargyl Derivatives of Dinuclear Thiolato Ruthenium Complexes

## 5.1 General

In 2001, K. B. Sharpless *et al*. coined the term "Click chemistry", describing reactions that are useful in synthetic chemistry to generate substances by joining small structural units together. These reactions, as defined by Sharpless *et al*., have to be: "… *modular, wide in scope, give very high yields, generate only inoffensive byproducts that can be removed by nonchromatographic methods, and be stereospecific (but not necessarily enantioselective). The required process characteristics include simple reaction conditions (ideally, the process should be insensitive to oxygen and water), readily available starting materials and reagents, the use of no solvent or a solvent that is benign (such as water) or easily removed, and simple product isolation. Purification (if required) must be by nonchromatographic methods, such as crystallization or distillation, and the product must be stable under physiological conditions.*" [161]. One such reaction that has gained a remarkable amount of interest and has been frequently used in various fields of chemistry is the Huisgen 1,3-dipolar addition, named "Click reaction". In this synthetic transformation, an organic azide reacts with an alkyne in water or water/organic mixture to form a triazole [162]. The reaction, catalyzed most frequently by Cu(I) species (formed *in situ* by the reduction of $CuSO_4$ by sodium ascorbate or ascorbic acid), gives selectively 1,4-disubstituted 1,2,3-triazoles (Scheme 7) [163]. Due to its robustness, tolerance to water and air and due to the commercial availability of a large number of organic alkynes and azides, this reaction has become the basis for the synthesis of a plethora of compounds and materials, including dendrimers [164], derivatized nanoparticles [165-166] or carbon nanotubes [167]. It is also worth noting that a variation of the Click reaction that utilizes metal azides was developed for the use in bioinorganic chemistry and was termed "iClick" (= inorganic Click reaction) [168].

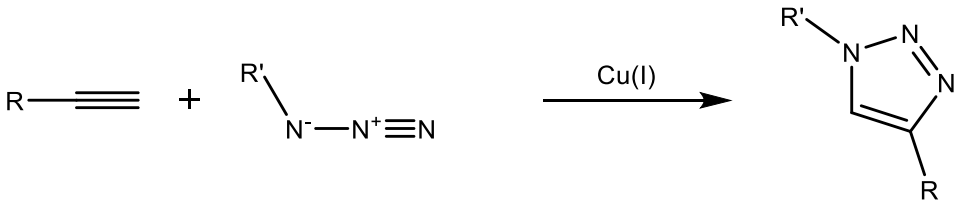


**Scheme 7** - Copper-catalyzed Huisgen 1,3-cycloaddition ("Click reaction")

The synthesis of dithiolato dinuclear ruthenium complexes in 2010 [115] provided us with the possibility to prepare the mixed trithiolato complexes, where the third bridging thiol contains a chemically modifiable substituent on the benzene ring, such as methyl, trifluoromethyl, hydroxyl, fluoride or bromide. Since azides of some biologically important substrates such as glucose, galactose or biotin are commercially available [169], we attempted the synthesis of alkyne-containing arene ruthenium complexes from the hydroxo derivatives $[(\eta^6\text{-}p\text{-}MeC_6H_4Pr^i)_2\text{-}Ru_2(SCH_2R)_2(SC_6H_4\text{-}p\text{-}OH)]^+$ (Scheme 8). The resulting complexes could then be used as a platform for the Click reaction with various azides.

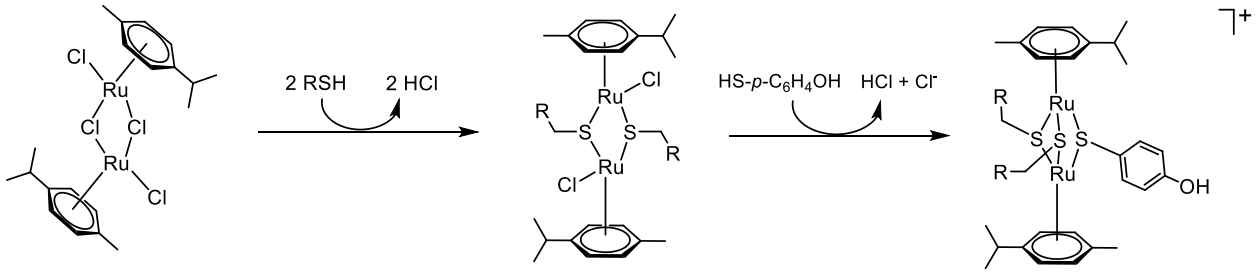


| R | Ph | $CH_2Ph$ | $C_6H_4$-*p*-$^t$Bu | $C_6H_4$-*p*-OMe |
|---|---|---|---|---|
| | **10** | **5** | **7** | **6** |

| R | Ph | $CH_2Ph$ | $C_6H_4$-*p*-$^t$Bu | $C_6H_4$-*p*-OMe |
|---|---|---|---|---|
| | **27** | **28** | **29** | **30** |

**Scheme 8 -** Synthesis of the precursor complexes **27** – **30**

## 5.2 Results

The four complexes **27** – **30** (the new complex **30** was synthesized by analogy to the previously published complexes **27** – **29**, see Chapter 9.4.3) were subjected to the Williamson reaction with propargyl bromide in the presence of $K_2SO_4$, yielding propargyl-containing complexes **31** – **34** (Scheme 9). All the four complexes were isolated as tetrafluoroborate salts and completely characterized.

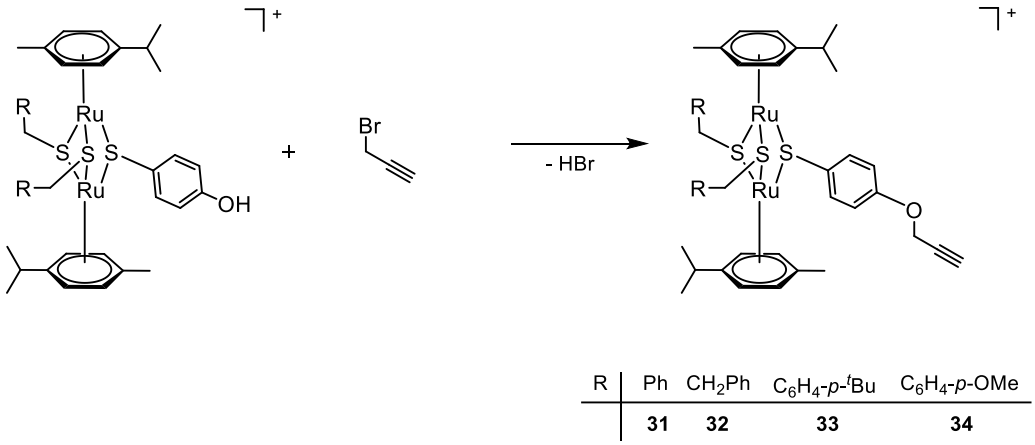


| R | Ph | $CH_2Ph$ | $C_6H_4$-*p*-$^t$Bu | $C_6H_4$-*p*-OMe |
|---|---|---|---|---|
| | **31** | **32** | **33** | **34** |

**Scheme 9 -** Synthesis of propargyl-containing complexes **31 – 34**

Due to the high number of synthetic steps needed to obtain the precursor compounds [**27** – **30**][$BF_4$] and due to low yields of the Williamson reaction, it was difficult to obtain sufficient amounts of products for further syntheses of conjugates and this approach was therefore not prioritized. However, a proof-of-concept experiment was conducted in order to see if the propargyl-containing complexes can indeed react with azide functionality and form triazoles. Thus, the compound [**33**][$BF_4$] was reacted with benzyl azide under the conditions of the Click reaction (0.4 eq sodium ascorbate, 0.1 eq $CuSO_4$, $H_2O$, $CH_2Cl_2$, rt, 24 h). The resulting mixture was extracted with $CH_2Cl_2$ and directly subjected to NMR and ESI-MS analysis. The spectra clearly show the formation of the "clicked" product, demonstrated by the fragment at *m/z* = 1126.6 and by the new resonances in the NMR spectrum belonging to the aromatic protons of *p*-cymene and aliphatic protons of $SCH_2$-*p*-$C_6H_4$-$Bu^t$ (Figure 43).

Starting material **33**[$BF_4$]

Product of the Click reaction

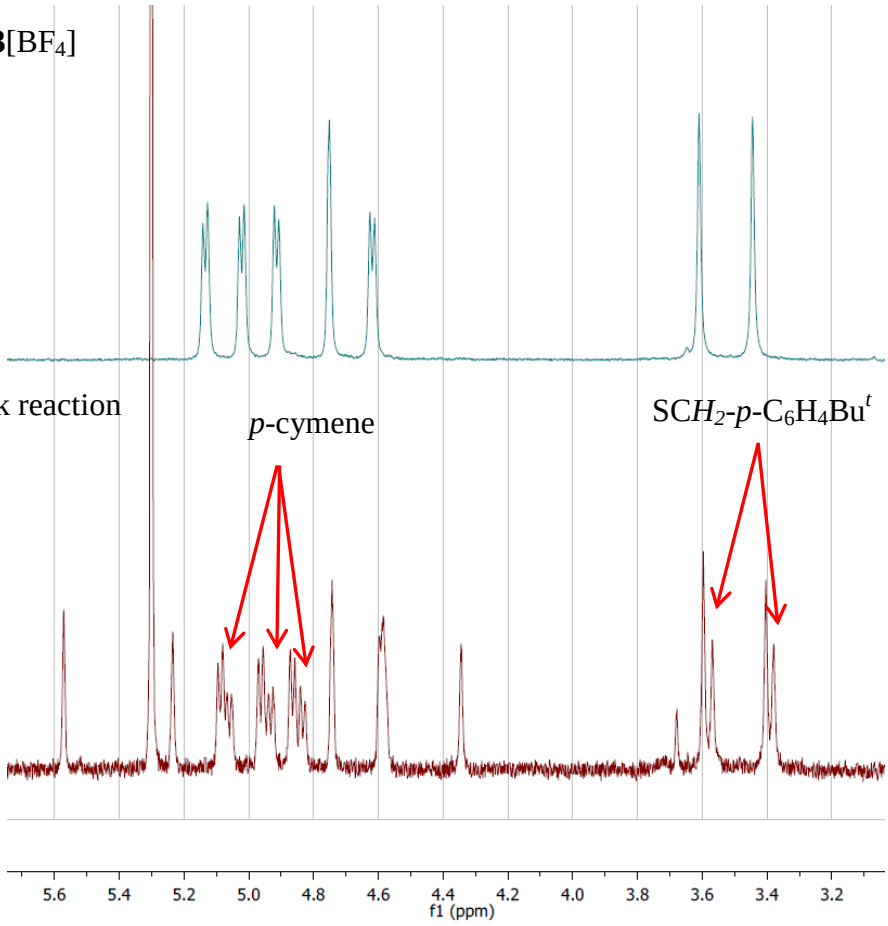


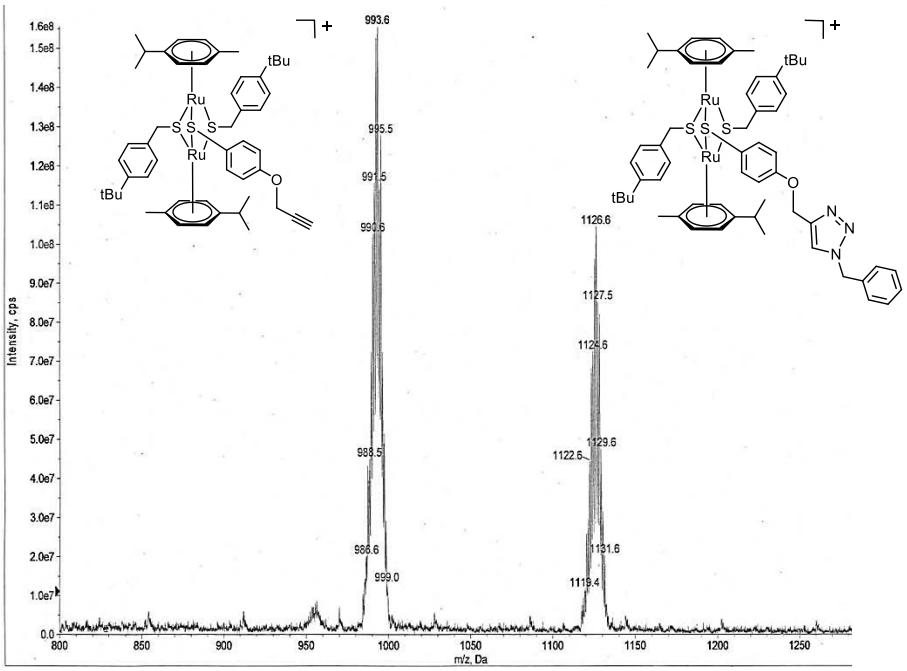


**Figure 43** - NMR and ESI-MS spectra of the triazole-containing product

Therefore, the synthesized propargyl-containing products are available for the copper-catalyzed Huisgen 1,3-cycloadition, although the reaction seems to proceed significantly slower than in the case of purely organic substrates - reaction between benzyl azide and (2-propynyloxy)benzene under the same conditions gives 95% yield in 12 hours [170].

## 5.3 Conclusion

Four propargyl-containing trithiolato complexes were synthesized and their availability for the Huisgen 1,3-cycloaddition was demonstrated. The products form selectively the 1,4-substituted triazoles, the expected product of the copper-catalyzed Click reaction. Provided that the synthetic procedure to obtain products **30** – **34** can be optimized to give better yields, the products could be coupled with commercially available azides to prepare useful conjugates with glucose, galactose, biotin (a molecule frequently used in the syntheses of targeted agents [171-172]) or other biologically relevant molecules to which the azide moiety can be synthetically attached.

# Chapter 6: Ibuprofen Conjugates of Dinuclear Thiolato Ruthenium Complexes

## 6.1 General

Tumors have been called “wounds that do not heal” [173], referring to the critical role that inflammation plays in tumorigenesis [174]. It is now well established that inflammatory microenvironment is an essential component of all tumors [175] and that the induction of inflammation, for example by bacterial and viral infection, increases cancer risk [176]. Moreover, recent work has shown that tobacco smoke is a tumor promoter because of its ability to trigger chronic inflammation [177], in addition to its high carcinogen content. Those findings encouraged the research of the effects of anti-inflammatory drugs on cancer. Thus, non-steroid anti-inflammatory drugs (NSAIDs) such as aspirin, ibuprofen, naproxen or indomethacin were studied for their influence on cancer incidence, progression and mortality. The mode of action of NSAIDs is the inhibition of the enzyme cyclooxygenase (COX), which is the effect at the origin of the analgesic, antipyretic and antirheumatic effects of NSAIDs [9]. The inducible version of the COX (COX-2) was shown to be overexpressed in tumor tissue and involved in tumor initiation and progression [178-180]. Subsequently, several large-scale epidemiologic studies showed that individuals who take NSAIDs on a regular basis have 40-50% reduction in mortality from colorectal cancer [181]. Furthermore, a direct effect on the proliferation and cell cycle of colon cancer cells was evidenced by *in vitro* studies – a series of 18 NSAIDs exhibited $IC_{50}$ values in the micromolar range for HT-29 and DLD-1 colon cancer cell lines, similar results were obtained for human breast cancer, lung cancer and melanoma cells [182]. Aspirin, indomethacin, naproxen and piroxicam increased the proportion of cancer cells in the $G_0/G_1$ phase, reduced the proportion in the S phase of the cell cycle and induced apoptosis [183]. In a different study, 7 examples of NSAIDs were found to inhibit the heat shock protein 70 (HSP70), a family of proteins that play an essential role for cell survival in stressful conditions and that is often overexpressed in cancer cells [184-185]. This finding was used to explore the effect of ibuprofen, one of the studied agents, on the cisplatin anticancer activity. The cisplatin-dependent cellular events leading to lung cancer cell apoptosis were found to be accelerated by ibuprofen, an effect that was ascribed to the HSP70 inhibition [186].

The combination studies of two different anticancer drugs can encounter problems of disparate biodistribution of the two agents, not allowing to replicate the *in vitro* results in the following *in vivo* studies [187]. This problem could be addressed by attaching the two agents by a chemical bond, forming a drug conjugate with unified biodistribution and possibly with the biological effects of the two composing parts [188]. NSAIDs were already successfully coupled with platinum anticancer drugs, yielding complexes with interesting properties. Cheng *et al*. synthesized platinum(IV) complex with aspirin as one of the axial ligands that showed up to ten-fold increase in cytotoxicity compared to cisplatin [189]. Similarly, the binding of two molecules of ibuprofen or indomethacin as the two axial ligands of the oxidized cisplatin and oxaliplatin yielded anticancer compounds with up to two orders of magnitude higher cytotoxicity to colorectal carcinoma and at the same time with the ability to inhibit COX-1 and COX-2 and to overcome cisplatin resistance [188,190]. Recently, the group of Hartinger synthesized arene ruthenium compounds with non-selective NSAID piroxicam and a preferential COX-2 inhibitor meloxicam as *O,O*-chelating ligands (Figure 44). These ruthenium-based compounds proved to be only slightly toxic to HCT116 colon carcinoma cells, the $IC_{50}$ of the most active compound being 80 μM. Docking studies with the COX-2 enzyme showed low binding affinities of the complexes, suggesting that the coordination of the arene ruthenium unit changes the mode of action of the COX inhibitor [191].

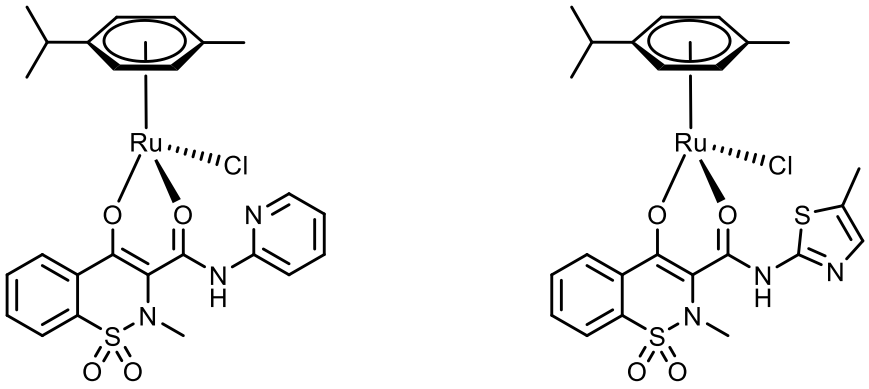


**Figure 44 -** Structure of the two Ru(III) complexes with oxicams as *O,O*-chelating ligands, synthesized by Hartinger et al. [191]

Herein we report the synthesis of a series of arene ruthenium dinuclear trithiolato conjugates with ibuprofen. The NSAID molecule is covalently bound to the ruthenium core by an ester bond, which we suppose might allow the ibuprofen moiety to preserve its anti-inflammatory effect and enhance the anticancer activity of the trithiolato ruthenium complex.

## 6.2 Results

The complexes **27** – **30** were reacted with ibuprofen using the Steglich esterification conditions, yielding ibuprofen conjugates **35** – **38** (Scheme 10). The tetrafluoroborate salts of the four ibuprofen conjugates were isolated by column chromatography as orange crystalline powders and completely characterized. They are well soluble in chlorinated solvents, lower alcohols and polar solvents such as acetonitrile and THF.

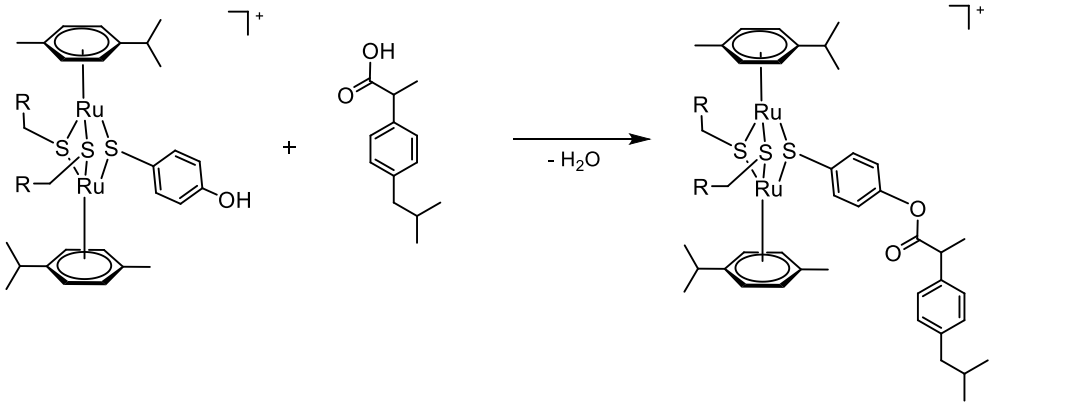


| R | Ph | $CH_2Ph$ | $C_6H_4$-*p*-$^t$Bu | $C_6H_4$-*p*-OMe |
|---|---|---|---|---|
| | **35** | **36** | **37** | **38** |

**Scheme 10 -** Synthesis of ibuprofen conjugates **35 – 38**

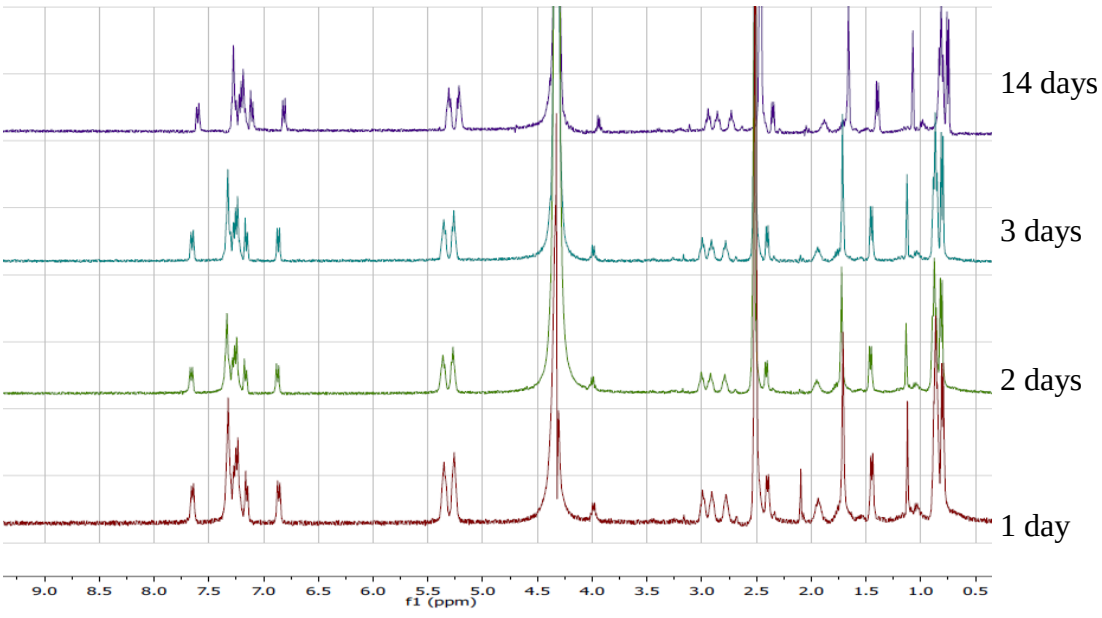


**Figure 45 –** Stability of complex **32** in DMSO-$d_6$/$D_2O$ mixture over 14 days

The stability of the conjugates in aqueous solution was investigated by NMR spectroscopy and showed the complex **32** to be stable for more than 1 week in DMSO-$d_6$/$D_2O$ mixture, as can be seen in Figure 45. The anticancer activity of the four compounds [**31 – 34**][$BF_4$] was therefore studied *in vitro* on ovarian cell line A2780 and its cisplatin-resistant mutant A2780cisR as well as in the healthy cell line HEK293. The $IC_{50}$ values of all four compounds were in the nanomolar range, matching well with those of the chloride salts of the mixed trithiolato complexes **27** – **30** that served as precursors for the ibuprofen conjugates [112]. Unfortunately, no selectivity towards cancer cells was observed and the conjugates were highly cytotoxic also towards HEK293 cell line (Table 7).

**Table 7** – *In vitro* cytotoxicity of compounds [**35** – **38**]Cl

| Compound | $IC_{50}$ (A2780) [μM] | $IC_{50}$ (A2780cisR) [μM] | $IC_{50}$ (HEK293) [μM] |
|---|---|---|---|
| [**35**][$BF_4$] | 0.21 ± 0.05 | 0.20 ± 0.04 | 0.21 ± 0.02 |
| [**36**][$BF_4$] | 0.37 ± 0.07 | 0.39 ± 0.07 | 0.34 ± 0.03 |
| [**37**][$BF_4$] | 0.29 ± 0.04 | 0.20 ± 0.06 | 0.22 ± 0.07 |
| [**38**][$BF_4$] | 0.54 ± 0.14 | 0.45 ± 0.10 | 0.49 ± 0.03 |

These results suggest that the coupling of the ibuprofen moiety does not confer any selectivity towards ovarian cancer cells. The same effect as in the case of the complexes with meloxicam and piroxicam could be the reason – the coupling of ibuprofen with the ruthenium complex might influence the binding affinity of the NSAID to the COX enzyme. The conjugates cannot therefore benefit from the anti-inflammatory properties of ibuprofen and can exert their anticancer activity solely by the mode of action already described for the trithiolato complex **9** (Chapter 2.3).

## 6.3 Conclusion

The Steglich esterification of hydroxo derivatives of trithiolato arene ruthenium complexes afforded four conjugates with ibuprofen [**31 – 34**][$BF_4$]. The complexes were fully characterized by analytical methods and found to be sufficiently stable for *in vitro* biological studies. The results show high anticancer activity of the four conjugates, the $IC_{50}$ values being in sub-micromolar range. No selectivity towards ovarian cancer cells was observed. The conjugation of ibuprofen to the

ruthenium core does not provide the expected benefits of higher anticancer activity or selectivity, presumably because of the different binding affinity of the conjugates to the COX enzyme compared to the free ibuprofen. The choice of a different cancer model, for example the colorectal or the breast cancer that responded to the treatment of ibuprofen alone [182,186] might yield new insights into the anticancer activity of the ibuprofen conjugates.

# Chapter 7: Chlorambucil Conjugates of Dinuclear Thiolato Ruthenium Complexes

## 7.1 General

Both platinum and ruthenium anticancer complexes have been shown to benefit from coupling with organic molecules that can increase their solubility, facilitate their transport into cells or enhance their selectivity for cancer cells. For instance, the ruthenium complex [($\eta^6$-*p*-$MeC_6H_4Pr^i$)Ru(pta)$Cl_2$] was coupled with ethacrynic acid, a compound that inhibits the enzyme glutathione-S-transferase. The resulting complex was found to bind to glutathione-S-transferase, whereupon the metal moiety was enzymatically cleaved and released into the sensitized cancer cell [192]. A similar approach was patented by the Lippard group for platinum(IV) complexes coupled to vitamin E precursors. These complexes act as anticancer agents with increased selectivity for cancer cells, where both the platinum moiety and vitamin E precursor attack cancer cells via a separate mode of action [193]. In a similar manner, thiolato-bridged arene ruthenium complexes were recently coupled to oligopeptides, which largely increased their solubility in water, thus facilitating their application [194].

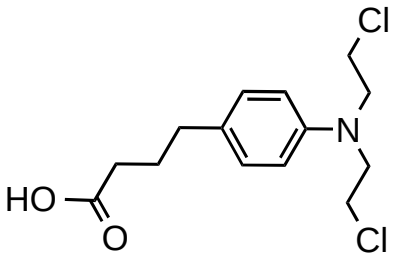


**Figure 46 -** *N*,*N*-bis(2-chloroethyl)-*p*-aminophenylbutyric acid (chlorambucil)

In this chapter we report the synthesis and *in vitro* activity of four thiolato-bridged arene ruthenium complexes coupled to the alkylating agent chlorambucil (Figure 46). Chlorambucil [*N*,*N*-bis(2-chloroethyl)-*p*-aminophenylbutyric acid] is a drug standardly employed in the treatment of chronic myeloid leukemia, myeloma and chronic lymphocytic leukemia [195]. Its anticancer properties are explained by its direct binding to DNA, specifically to N7 of guanines. Chlorambucil can form either monofunctional nucleotide adducts, or interact with DNA by both of its electro-

philic sites at once, forming either intrastrand or interstrand DNA cross-links [196]. Very recently, RAPTA-type complexes were reported, in which the arene ligand was functionalized by chlorambucil moieties; some of these chlorambucil-functionalized RAPTA complexes show superior anticancer activity to cisplatin-resistant cancer cells as compared to chlorambucil, to the parent RAPTA complex, or to the mixture of both. These conjugates are supposed to act by two disparate modes of action, namely by protein ruthenation and by DNA alkylation [197].

Dinuclear arene ruthenium trithiolato complexes can be functionalized on one of the thiolato ligands, in particular since mixed complexes of the type $[(\eta^6\text{-arene})_2Ru_2(SR^{al})_2(SR^{ar})]^+$ are easily accessible with aliphatic (al) and aromatic (ar) substituents on the thiolato bridges [112]. We therefore prepared the neutral precursors $[(\eta^6\text{-}p\text{-}MeC_6H_4Pr^i)_2Ru_2(SCH_2R)_2Cl_2]$ (R = Ph: **10**, R = $CH_2Ph$: **5**, R = $C_6H_4$-*p*-$Bu^t$: **7, R =** $C_6H_4$-*p*-OMe: **6**) from *p*-cymene ruthenium dichloride dimer and the corresponding thiol, and the mixed cationic complexes $[(\eta^6\text{-}p\text{-}MeC_6H_4Pr^i)_2Ru_2(SCH_2R)_2(SC_6H_4\text{-}p\text{-}OH)]^+$ (Ph: **27**, R = $CH_2Ph$: **28**, R = $C_6H_4$-*p*-$Bu^t$: **29**), by reaction with *p*-mercaptophenol according to published methods [112,115]; the new derivative $[(\eta^6\text{-}p\text{-}MeC_6H_4Pr^i)_2Ru_2(SCH_2C_6H_4\text{-}p\text{-}OMe)_2(SC_6H_4\text{-}p\text{-}OH)]^+$ (**30**) was synthesized by analogy. The mixed cationic complexes **27** – **30** containing a phenolic group in one of the thiolato bridges can be used for the functionalization with chlorambucil.

## 7.2 Results and Discussion

The mixed trithiolato complexes $[(\eta^6\text{-}p\text{-}MeC_6H_4Pr^i)_2Ru_2(SCH_2R)_2(SC_6H_4\text{-}p\text{-}OH)]^+$ (**27** – **30**) react in dichloromethane with chlorambucil (cabOOH) under Steglich esterification conditions to give the chlorambucil conjugates $[(\eta^6\text{-}p\text{-}MeC_6H_4Pr^i)_2Ru_2(SCH_2R)_2(SC_6H_4\text{-}p\text{-}OOCcab)]^+$ R = Ph: **39**, R = $CH_2Ph$: **40**, R = $C_6H_4$-*p*-$Bu^t$: **41**, R = $C_6H_4$-*p*-OMe: **42**), which can be isolated as tetrafluoroborate salts in the form of orange crystalline powders (Scheme 11). The compounds [**39** – **42**][$BF_4$] are well soluble in chlorinated solvents, alcohols and polar solvents such as acetonitrile, THF or DMSO. All complexes have been fully characterized by $^1H$ and $^{13}C$ NMR spectroscopy, mass spectroscopy and elemental analysis. The conjugation of product **18** (Chapter 4.1) yielded a stable complex $[(\eta^6\text{-}p\text{-}MeC_6H_4Pr^i)_2Ru_2(SCH_2C_6H_4\text{-}p\text{-}Cl)_2(SC_6H_4\text{-}p\text{-}OOCcab)]^+$ (**43**), that had significantly lower solubility in organic solvents and in water than the other four conjugates and was therefore not included in the further studies.

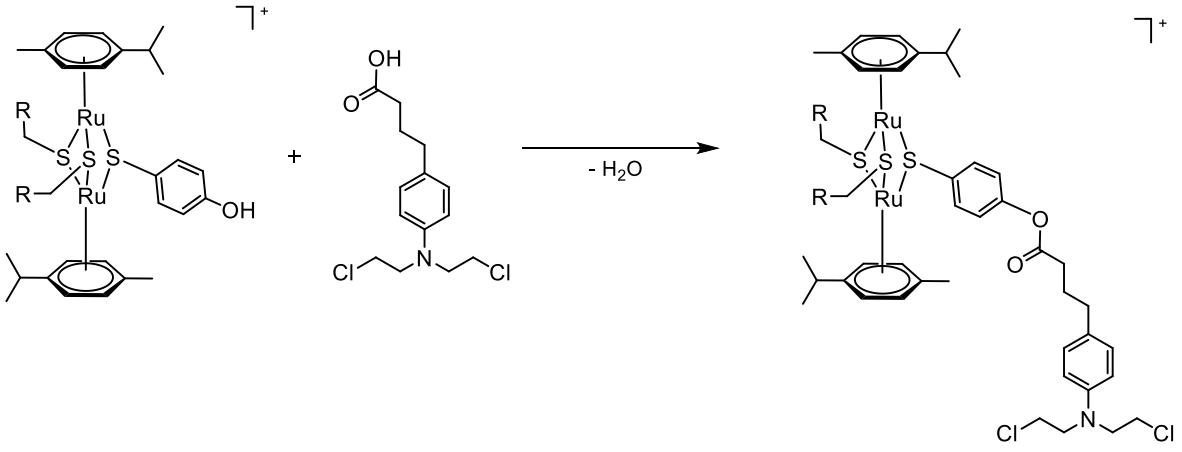


| R | Ph | $CH_2Ph$ | $C_6H_4$-*p*-$^t$Bu | $C_6H_4$-*p*-OMe | $C_6H_4$-*p*-Cl |
|---|---|---|---|---|---|
| | **27** | **28** | **29** | **30** | **18** |

| R | Ph | $CH_2Ph$ | $C_6H_4$-*p*-$^t$Bu | $C_6H_4$-*p*-OMe | $C_6H_4$-*p*-Cl |
|---|---|---|---|---|---|
| | **39** | **40** | **41** | **42** | **43** |

**Scheme 11 -** Synthesis of chlorambucil conjugates **39 – 43**

The *in vitro* anticancer activity of the chlorambucil conjugates [**39** – **42**][$BF_4$] was evaluated against the human ovarian cancer cell line A2780 and its cisplatin-resistant mutant A2780cisR, using the The CellTiter-Glo® luminescent cell viability assay (CTG) that determines the number of viable cells in culture based on quantitation of the ATP present, an indicator of metabolically active cells. As far as the neutral dithiolato precursor complexes and the cationic trithiolato precursor are concerned, the $IC_{50}$ values for the known derivatives **5, 6, 7** and **10** [115] and **27 – 30** [112] have been taken from our earlier publications (Tables 8 and 9). In general, the neutral dithiolato complexes are less cytotoxic than the cationic trithiolato complexes; the derivative **30** confirms this tendency. All cationic trithiolato complexes exhibit $IC_{50}$ values in nanomolar range.

**Table 8 -** $IC_{50}$ values of the neutral dithiolato complexes **5, 6, 7** and **10** for human ovarian carcinoma cells. Values are given as the means ± the standard error of the mean.

| Complex | $IC_{50}$ A2780 [nM] | $IC_{50}$ A2780cisR [nM] |
|---|---|---|
| **5** | 2940 ± 600 | 3600 ± 800 |
| **6** | 200 ± 50 | 310 ± 80 |
| **7** | > 5000 | > 5000 |
| **10** | 235 ± 50 | > 5000 |

**Table 9 -** $IC_{50}$ values of the cationic trithiolato complexes [**27** – **30**][$BF_4$] for human ovarian carcinoma cells. Values are given as the means ± the standard error of the mean.

| Compound | $IC_{50}$ A2780 [nM] | $IC_{50}$ A2780cisR [nM] |
|---|---|---|
| [**27**]Cl | 47.8 ± 3.0 | 42.9 ± 1.0 |
| [**28**]Cl | 74.4 ± 2.8 | 49.9 ± 1.9 |
| [**29**]Cl | 163 ± 8.0 | 59.5 ± 1.3 |
| [**30**]Cl | 320 ± 80 | 109 ± 30 |

The cytotoxicity of chlorambucil conjugates [**39** – **42**][$BF_4$] was studied using four cell lines: non-cancerous human embryonic kidney (HEK293) cells, immortalized endothelial cells (RF24), human ovarian carcinoma cell line (A2780) and cisplatin resistant human ovarian carcinoma cell line (A2780cisR). The results reveal the $IC_{50}$ values for the two ovarian cancer cell lines to be in the nanomolar range (Table 10), though being higher than those of the corresponding trithiolato complexes **27** – **30** that are not conjugated to chlorambucil (Table 9). This may be partially explained by the change in lipophilicity caused by the conjugation of chlorambucil. The lipophilicity (represented by Hammett constants $\sigma_p$ and the lipophilicity parameter log P) has been shown to be a major factor influencing the anticancer activity of trithiolato arene ruthenium complexes [111].

**Table 10 -** $IC_{50}$ values of [**39** – **42**][$BF_4$] against human carcinoma cell lines A2780 and A2780cisR determined using the CTG assay after 72 h. Values are given as the means ± the standard error of the mean.

| Compound | $IC_{50}$ A2780 [nM] | $IC_{50}$ A2780cisR [nM] | $IC_{50}$ HEK293 [nM] | $IC_{50}$ RF24 [nM] |
|---|---|---|---|---|
| [**39**][$BF_4$] | 75 ± 14 | 321 ± 44 | 335 ± 26 | 152 ± 15 |
| [**40**][$BF_4$] | 55 ± 6 | 353 ± 10 | 448 ± 40 | 325 ± 45 |
| [**41**][$BF_4$] | 183 ± 25 | 335 ± 50 | 451 ± 65 | 280 ± 36 |
| [**42**][$BF_4$] | 600 ± 72 | 591 ± 62 | 1580 ± 300 | 770 ± 100 |

The cell viability experiments conducted in the four cell lines (Figure 47) show that chlorambucil conjugates [**40**][$BF_4$] and [**42**][$BF_4$] exhibit an interesting selectivity for the A2780 cell line at the dose range 50 to 300 nM (compound [**40**][$BF_4$]) or 50 to 100 nM (compound [**42**][$BF_4$]), while being only slightly active in RF24, HEK293 or A2780cisR cells. The $IC_{50}$ value

for the chlorambucil conjugate [**40**][$BF_4$] is 55 ± 6 nM for A2780 cells, similar as for its precursor, compound [**28**]Cl (49.9 ± 1.9 nM), while for chlorambucil alone it is reported to be approximately 22-fold higher (1200 nM [198]). The $IC_{50}$ of [**39**][$BF_4$] in A2780 cells is 75 ± 14 nM and only 2-fold higher in endothelial RF24 cells. Complex [**41**][$BF_4$], at low doses (up to 70 nM), seems to be the most selective towards A2780cisR cells, which is not observed in the higher dose range.

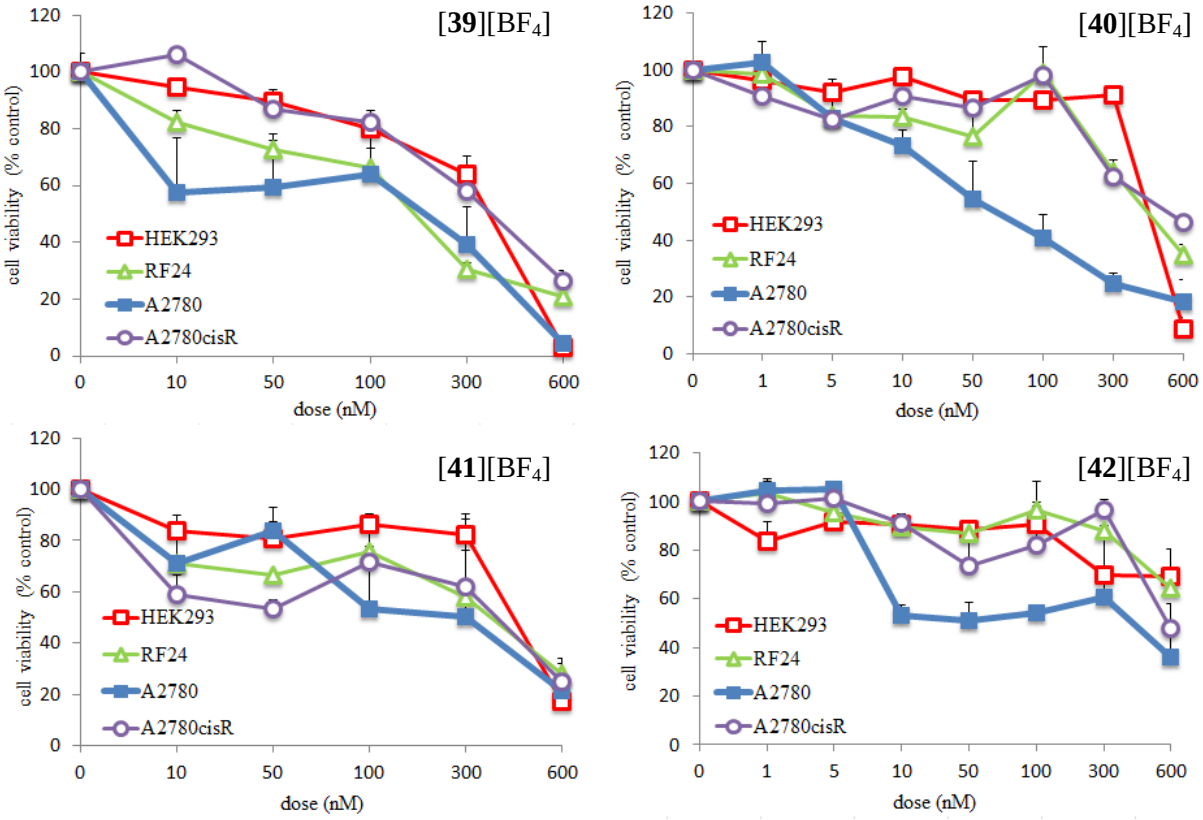


**Figure 47 -** Dose-dependent cell viability after administration of compounds [**39** – **42**][$BF_4$]. Values are presented as the means ± the standard error of the mean.

In order to study the mechanism of action of the new chlorambucil conjugates, the compound [**40**][$BF_4$] was incubated with the tripeptide glutathione and with the nucleobase 2-deoxyguanosine 5'monophosphate. The catalytic oxidation of glutathione is reported to be at least partially responsible for the high *in vitro* cytotoxicity of trithiolato dinuclear arene ruthenium complexes [112]. On the other hand, the mode of action of chlorambucil is its covalent binding to DNA nucleobases, namely to the position 7 of guanine. Both of these targets were investigated in order to see if the chlorambucil conjugates retain the mode of action of its composing parts. To our surprise, the compound [**40**][$BF_4$] does not oxidize glutathione, although its precursor [**28**]Cl has a reported

turnover frequency of 7.02 $h^{-1}$ for the catalytic glutathione oxidation [112]. After 24 hours of incubation at 37°C, the NMR spectrum shows only the peaks of glutathione, no formation of the disulfide was detected. The interaction of [**40**][$BF_4$] with 2-deoxyguanosine 5'-monophosphate (dGMP) was studied at two different pH values - at pH = 3.5 without the addition of any buffer or base, and after the addition of 0.1 M NaOH, which raised the pH to 8. According to studies of chlorambucil binding to DNA, the alkylation of guanines proceeds much faster at elevated pH [199]. However, in our case the ESI-MS spectra showed no adducts of 2-deoxyguanosine 5'-monophosphate and [**40**][$BF_4$] even at pH 8. At pH = 3.5, the only detected products aside from the original complex were the two hydrolysis products of the chlorambucil conjugate, as shown in Figure 48.

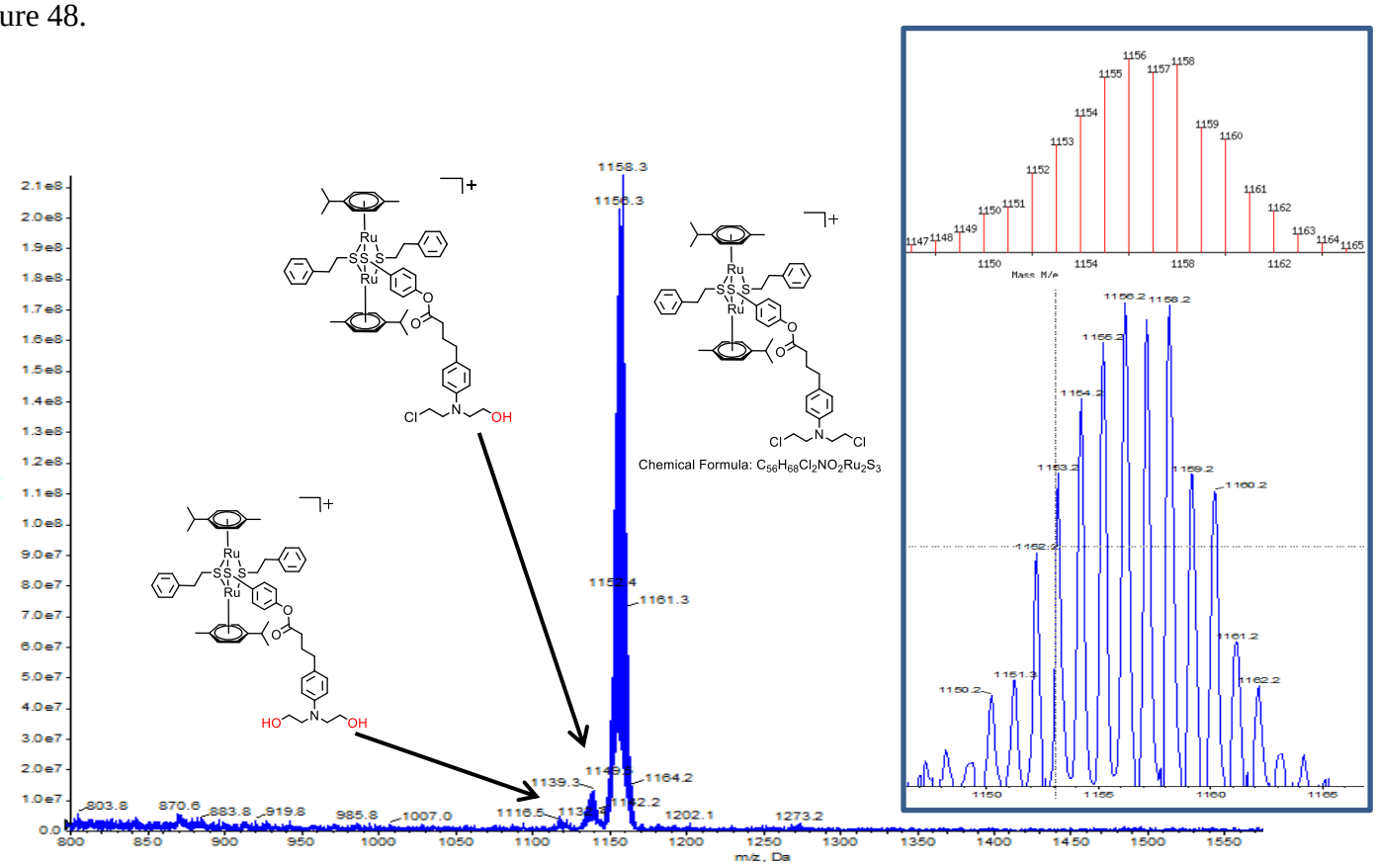


**Figure 48 -** Hydrolysis products of the complex **40** after 24 hours incubation at 37°C with 4 equivalents of 2-deoxyguanosine 5'monophosphate. Insert: Simulated (top) and measured (bottom) MS spectra.

These results demonstrate that the conjugation of the thiolato-bridged arene ruthenium complex to chlorambucil hampers the chlorambucil moiety to interact with nucleobases. Conversely, the conjugation also blocks the catalytic activity of the dinuclear trithiolato unit. We therefore assume

that these conjugates can deploy their anticancer properties in the cancer cells only after hydrolysis of the ester bond brought about by the esterases in the cells.

Compound [**40**][$BF_4$] was used to evaluate the effect of the conjugates on tumor growth and that on the survival of tumor-bearing mice of an immunocompetent strain. The doses were selected according to the dose-finding study which had revealed a maximum tolerated dose (MTD) of 20 mg/kg. Figure 49 shows the weight of tumors in mice treated with saline, [**40**][$BF_4$], chlorambucil or cisplatin measured on day 11, and significantly documents differences in the effect of the used drugs. [**40**][$BF_4$] at the dose of 15 mg/kg had a significant inhibitory effect on tumor growth ($P$ = 0.0474). The positive control, cisplatin, was the most potent. Chlorambucil itself was also effective ($P > 0.05$); interestingly, a multiple comparison revealed that its effect did not significantly differ from the one of [**40**][$BF_4$] ($P > 0.05$).

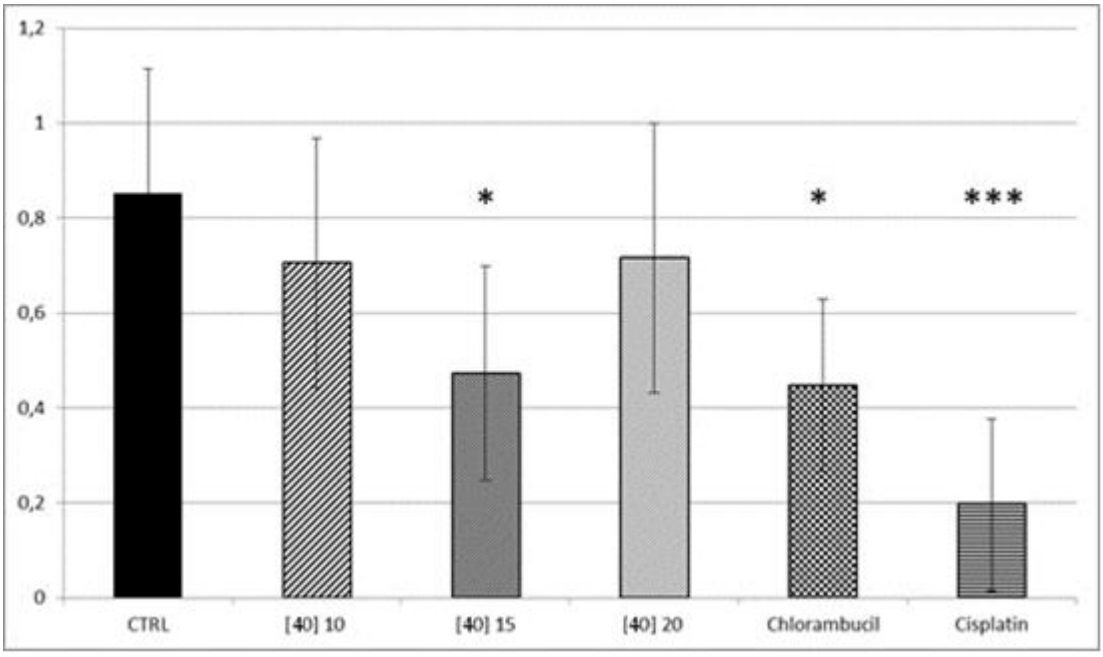


**Figure 49 -** Weight of the solid Ehrlich tumor (in grams) on day 11 of mice injected on days 1, 4 and 8 i.p. with [**40**][$BF_4$] in doses of 10, 15, or 20 mg/kg, or chlorambucil 5 mg/kg, or cisplatin 5 mg/kg. Values are the means ± SEM (n = 7 in each group). Values that are significantly different from the controls are labeled by * ($^{*}P < 0.05$, $^{***}P < 0.001$).

As for the effect on survival, the mean overall survival of tumor-bearing mice without therapy was 21.6 days. [**40**][$BF_4$] at both 10 mg/kg and 15 mg/kg showed a tendency to prolong the survival albeit the effect was not significant ($P$ = 0.458 and 0.693, respectively). The group receiving [**40**][$BF_4$] 20 mg/kg could not be evaluated because of their bad general condition. Unlike the

healthy mice in the MTD finding study, the tumor bearing mice treated with 20 mg/kg of [**40**][$BF_4$] displayed severe symptoms of intoxication and had to be euthanized. Only chlorambucil prolonged the mean survival time significantly when compared with untreated tumor-bearing control mice ($P$ = 0.0401). Chlorambucil was also more effective when compared with its conjugate [**40**][$BF_4$] at both doses evaluated ($P < 0.01$). The effect of cisplatin could not be considered significant ($P$ = 0.0869). The Kaplan-Meier analysis of survival can be seen in Figure 50.

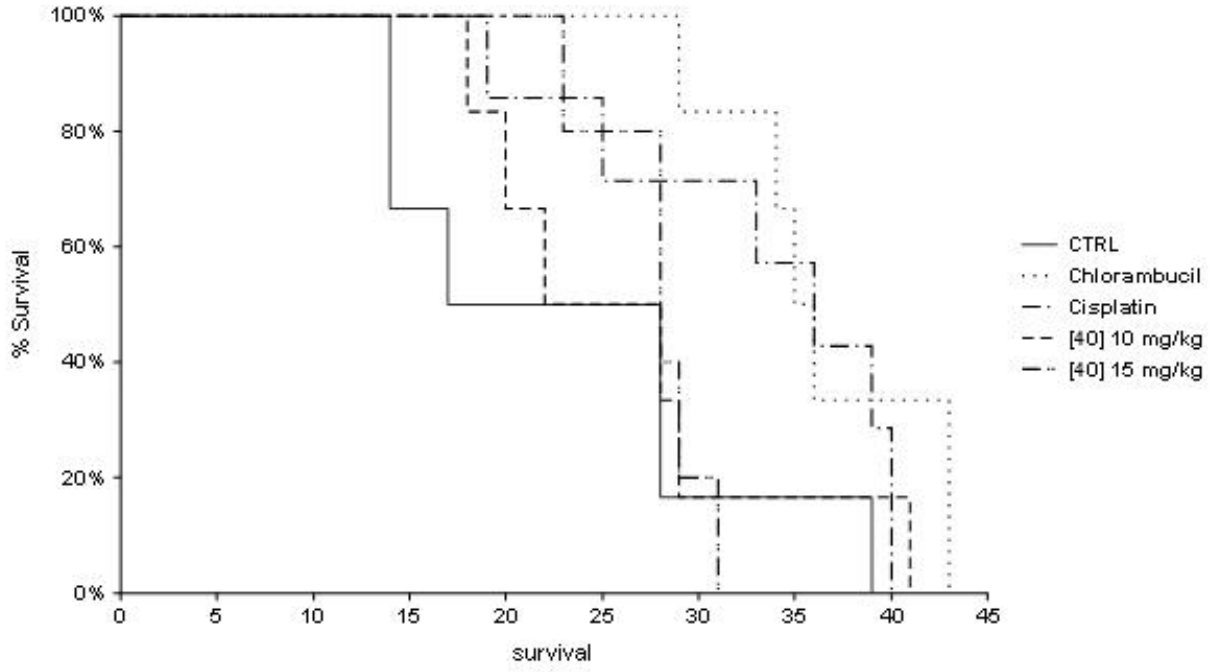


**Figure 50 -** Kaplan-Meier analysis of survival. Only the administration of chlorambucil 5 mg/kg significantly prolonged the survival of tumor-bearing mice when compared with tumor-bearing controls treated with saline i.p. (CTRL). Neither 10 mg nor 15 mg of [**40**][$BF_4$]/kg BW (body weight), nor 5 mg of cisplatin/kg BW had any statistically significant effect. The compounds were administered i.p. on days 1, 4 and 8 after tumor inoculation.

The conjugate [**40**][$BF_4$] at any dose did not have a significant therapeutic effect in comparison to chlorambucil alone. When the dose of 20 mg/kg, which is stoichiometrically almost equivalent to 5 mg/kg chlorambucil, was applied, [**40**][$BF_4$] turned out to be more systemically toxic and less potent than chlorambucil itself. It is quite possible that, even if the conjugate was completely hydrolyzed into the putatively more active components, the summation of their toxicity might hinder the body´s own defence mechanisms such as the anticancer immune surveillance. Studies in

more cancer models are needed to determine whether or not the conjugation in question increases the anticancer potential of the components.

## 7.3 Conclusions

Four chlorambucil conjugates of trithiolato arene ruthenium complexes were synthesized, fully characterized and studied for their anticancer properties. In vitro studies showed the complexes to be highly cytotoxic, their IC50 values being comparable to those of the trithiolato precursors. The difference in the cytotoxicity towards the cisplatin-resistant cell line A2780cisR shows the clear influence of the chlorambucil moiety. The cisplatin-resistant cancer cells are known to be cross-resistant to chlorambucil, [200] presumably due to the similar modes of action of the two agents. The difference in the spectrum of anticancer activity of the chlorambucil conjugates compared to their trithiolato precursors suggests that chlorambucil is cleaved after uptake into cells with both parts of the conjugate subsequently exhibiting the cytotoxic effects by their respective modes of action.

In a breast cancer model in immunocompetent mice, [**40**][$BF_4$] at the dose of 15 mg/kg shows an interesting effect on the inhibition of tumor growth. However, it did not show a statistically significant effect on the survival of tumor bearing mice, possibly due to the high systemic toxicity of **40**[$BF_4$]. It will be necessary to carry out experiments with other cancer models to assess the therapeutic potential of the chlorambucil conjugates. Since the high toxicity of the tested compound turned out to be a problem, it is possible that the conjugates that exhibited lower cytotoxicity *in vitro* might have more advantageous properties *in vivo* compared to the tested compound [**40**][$BF_4$].

# Chapter 8: General Conclusion and Perspectives

The work presented in this thesis focused on three main aspects of the research of the dinuclear thiolato-bridged arene ruthenium complexes:

1) The step-wise synthesis of the trithiolato complexes and the investigation of the properties of the three obtained types of products.
2) The *in vitro* and *in vivo* investigation of the mode of action of the trithiolato complexes.
3) The effect of the coupling of trithiolato complexes with biologically active molecules on the anticancer properties of the resulting conjugates.

The investigation of the reaction of *p*-cymene ruthenium dichloride dimer with thiols resulted in the isolation of three types of thiolato-bridged complexes: monothiolato, dithiolato and trithiolato complexes. The reactivity of the thiol was found to have major influence on the product of the reaction, followed by the reaction conditions. The influence of the pKa of the thiol on the formation of mono- or dithiolato complex was clearly demonstrated for a subset of thiols.

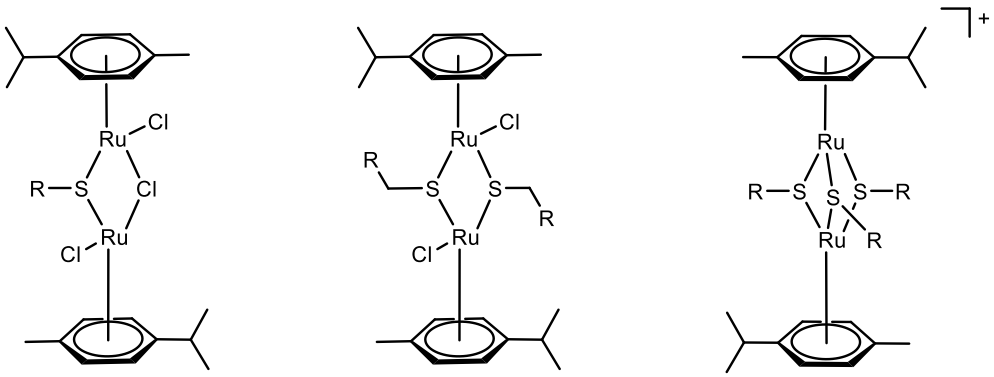


**Figure 51 –** General structures of monothiolato, dithiolato and trithiolato complexes

Differences in the anticancer activity of the three isolated species (Figure 51) prompted us to study their stability and their reactivity with biological ligands. The monothiolato complexes were found to be the least stable, hydrolyzing rapidly in aqueous solutions and reacting with amino acid cysteine to give dicysteinato-bridged cationic complexes. The dithiolato complexes are more stable towards hydrolysis, but react with cysteine in the same manner as monothiolato complexes, yielding monocysteinato-bridged cationic complexes. Interestingly, none of the studied complexes interact

with amino acids alanine, aspartic acid or histidine or with a DNA fragment. The trithiolato complexes are highly inert, not reacting with any of the tested amino acids and not interacting with DNA; however, in solution with the amino acid cysteine or the tripeptide glutathione, the trithiolato complexes catalyze the oxidation of these two compounds into the corresponding disulfides. The stability of the monothiolato, dithiolato and trithiolato complexes correlate well with their anticancer activity – the stable trithiolato complexes are highly cytotoxic towards ovarian cancer cell lines A2780 and A2780cisR, having $IC_{50}$ values in nanomolar range. The more reactive monothiolato and dithiolato complexes are by an order of magnitude less cytotoxic, having $IC_{50}$ values in micromolar range. We assume that this difference in cytotoxicity stems from the reactions of dithiolato and monothiolato complexes with extracellular and intracellular substrates, not allowing them to reach their target in sufficient concentrations. Trithiolato complexes can, on the other hand, reach their intracellular targets with high specificity, not interacting with other biological substrates.

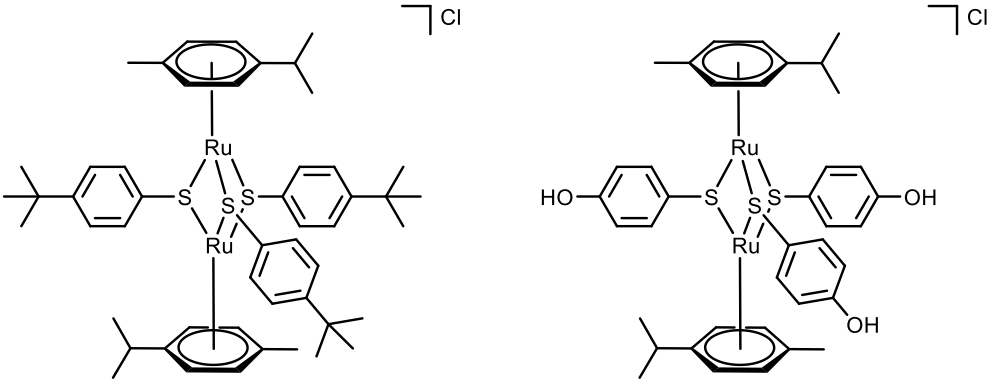


**Figure 52 –** Structure of *diruthenium-1* and *diruthenium-2*

To identify the mode of action of the trithiolato complexes, a detailed *in vitro* and *in vivo* study was performed with the most active compound of the trithiolato series, [**9**]Cl (*diruthenium-1*). The study showed its influence on the levels of ATP and lactate, suggesting an effect on the aerobic metabolism of cells. This observation was confirmed by the measurement of the mitochondrial respiration, which showed the inhibition of both complex I and complex II of the electron transfer chain by *diruthenium-1*, revealing some of the molecular bases of its mode of action. The *in vivo* study showed a marked effect of *diruthenium-1* on the survival of mice bearing a solid Ehrlich tumor. To understand the influence of chemical modifications of the trithiolato complexes on their biological properties, another compound of the series, $[(p\text{-}MeC_6H_4Pr^i)_2Ru_2(SC_6H_4\text{-}p\text{-}OH)_3]Cl$,

termed *diruthenium-2* (Figure 52), is currently undergoing *in vitro* and *in vivo* studies, the results of which will be published shortly.

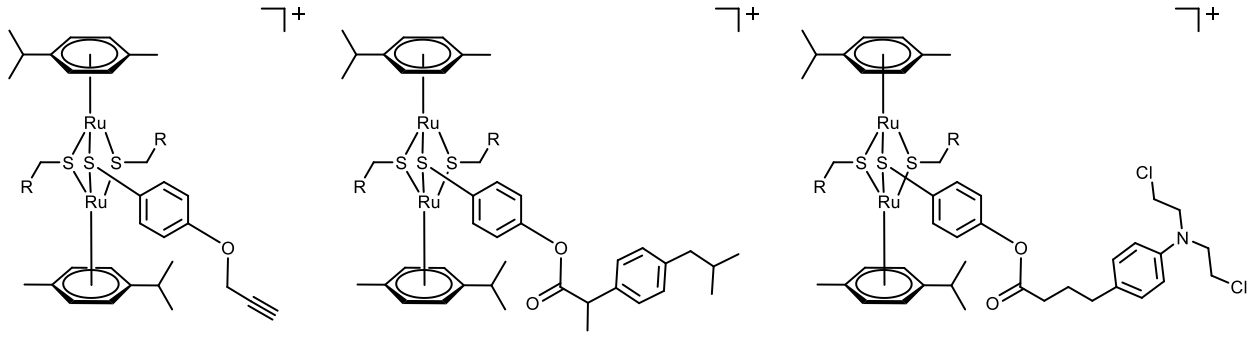

**Figure 53 –** General structures of the three series of conjugates

The synthesis of conjugates of trithiolato arene ruthenium complexes with biologically active molecules yielded three series of complexes (Figure 53). The propargyl-containing complexes were synthesized by the Williamson reaction of propargyl bromide with the hydroxo derivatives of mixed trithiolato complexes. This type of complexes was found to be available for the copper-catalyzed Huisgen 1,3-cycloaddition (Click reaction), which would allow the tethering of targeting molecules such as biotin, galactose or folic acid onto the ruthenium core. The second series, the series of conjugates with ibuprofen, was designed with the intention to influence the inflammatory microenvironment of tumors, providing the complexes with selectivity towards cancer cells. This theory was not confirmed; the resulting conjugates show no particular selectivity, presumably due to the chemical changes to the ibuprofen moiety that prevent its interaction with the cyclooxygenases. The third series of conjugates was synthesized by the esterification of the mixed trithiolato complexes with nitrogen mustard chlorambucil. The two disparate modes of action of the ruthenium complex and the alkylating agent chlorambucil were thought to provide higher anticancer activity to the resulting conjugates as well as the ability to overcome possible resistance of cancer cells. The conjugates were found to be highly cytotoxic to four different cancer cell lines, although their $IC_{50}$ values are in the same range as those of the precursor trithiolato complexes. The tetrafluoroborate salts of conjugates **39** and **40** show an interesting selectivity to A2780 cells compared to the three other cell lines. The chlorambucil moiety clearly influences the spectrum of anticancer activity, which is apparent from the lower activity of the conjugates towards the cisplatin-resistant A2780cisR cells. The *in vivo* studies of the compound [**40**][$BF_4$] showed its high

systemic toxicity, the probable cause being the summation of the toxicities of the ruthenium complex and the chlorambucil – the ester bond of the conjugate is assumed to hydrolyze in cells and to liberate the two composing parts of the conjugate.

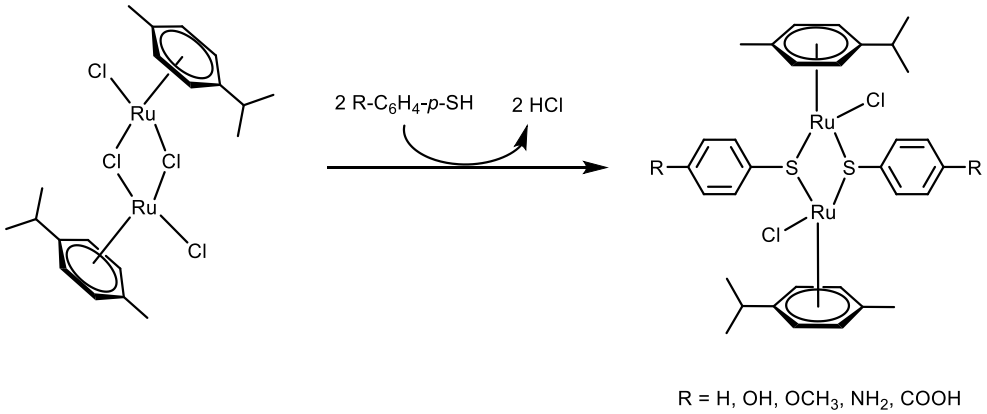


**Figure 54 –** Synthesis of "aromatic" dithiolato complexes

The presented results indicate possible directions of the future research of the subject of dinuclear thiolato-bridged arene ruthenium complexes. The preliminary results of the synthesis of new neutral "aromatic" dithiolato complexes of the type $[(p\text{-}MeC_6H_4Pr^i)_2Ru_2(SC_6H_4\text{-}p\text{-}R)_2Cl_2]$ (Figure 54) indicate the possibility to synthesize trithiolato complexes with highly variable chemical properties. The synthesis of the corresponding trithiolato complexes $[(p\text{-}MeC_6H_4Pr^i)_2Ru_2(SC_6H_4\text{-}p\text{-}R)_2(SC_6H_4\text{-}p\text{-}R')]^+$ would offer three binding positions for the attachment of biologically relevant molecules. The large variety of derivatives that could be synthesized by this approach would allow the use of a number of organic coupling reactions that are frequently employed in synthetic organic chemistry. Throughout the course of this thesis, only three organic coupling reactions were used to synthesize conjugates of arene ruthenium complexes – the Williamson reaction for the propargyl derivatives, followed by the Click reaction that was used as a proof of concept for the availability of the resulting complexes for this approach; the ibuprofen and chlorambucil conjugates were synthesized using the Steglich esterification reaction. The success of these reactions with arene ruthenium complexes suggests that with careful choice of the thiolato ligand, a vast number of coupling reactions routinely used in synthetic organic chemistry could be used in the synthesis of new arene ruthenium thiolato-bridged conjugates. For example, Sonogashira coupling of the propargyl derivatives could be employed to attach aryl or vinyl halides onto the ruthenium core. Kumada coupling reaction could be used to synthesize conjugates with bromide-containing mixed

trithiolato complexes. Other reactions, such as Heck or Suzuki coupling, could also increase the possibilities to vary the properties of the trithiolato arene ruthenium conjugates.

In conclusion, this thesis increased the understanding of the chemistry and biological properties of thiolato-bridged arene ruthenium complexes. It also proved the versatility of the dinuclear thiolato-bridged arene ruthenium platform as well as the influence that the chemical variations of the thiolato ligands can have on the biological properties of the resulting complexes. The results show that the dinuclear trithiolato arene ruthenium unit can be exploited to design novel anticancer agents with advantageous chemical and biological behavior and with variable mechanism of action, combining the benefits of both the organic part and the ruthenium core.

# Chapter 9: Experimental

## 9.1 General

Solvents of analytical grade purchased from Acros Organics, Honeywell or VWR International S.A.S were used for syntheses and not degassed or distilled prior to use, unless stated otherwise. All organic starting materials were purchased from Acros Organics, Sigma-Aldrich, Fluka, Alfa Aesar or TCI-Europe and used as received. The silicagel used for column chromatography (32-64, 60 Å) was purchased from Brunschwig. The starting material $[(\eta^6\text{-}p\text{-}MeC_6H_4Pr^i)_2Ru_2Cl_2(\mu\text{-}Cl)_2]$ was prepared according to published methods [201]. All other reagents were bought from commercial sources and were used without further purification.

### 9.1.1 X-Ray Structure Analyses

**Single-Crystal X-Ray Structure Analysis of 1 and 2:** Crystals of **1** and **2** were mounted on a Stoe Image Plate Diffraction system equipped with a $\phi$ circle goniometer, using Mo-K$\alpha$ graphite monochromated radiation ($\lambda$ = 0.71073 Å) with $\phi$ range 0-200º. The structures were solved by direct methods using the program SHELXS-97, while the refinement and all further calculations were carried out using SHELXL-97 [202]. The H-atoms were included in calculated positions and treated as riding atoms using the SHELXL default parameters. The non-H atoms were refined anisotropically, using weighted full-matrix least-square on $F^2$. Crystallographic details are summarized in Table 11. Figure 20 was drawn with ORTEP [203]. CCDC 1016530 (**1**) and 1016531 (**2**) contain the supplementary crystallographic data for these compounds. This data can be obtained free of charge from the Cambridge Crystallographic Data Centre via www.ccdc.cam.ac.uk/data_request/cif.

**Table 11 -** Crystallographic data and structure refinement parameters for **1** and **2**.

| | **1** | **2** |
|---|---|---|
| Chemical formula | $C_{27}H_{35}Cl_3Ru_2S$ | $C_{27}H_{34}Cl_3NO_2Ru_2S$ |
| Formula weight | 700.10 | 745.10 |
| Crystal system | Monoclinic | Monoclinic |
| Space group | *P* $2_1/n$ (no. 14) | *P* $2_1/c$ (no. 14) |
| Crystal color and shape | Orange block | Orange block |
| Crystal size | 0.22 x 0.18 x 0.18 | 0.21 x 0.20 x 0.16 |
| *a* (Å) | 10.7440(5) | 12.6397(5) |
| *b* (Å) | 13.0281(6) | 14.5768(5) |
| *c* (Å) | 19.8652(9) | 15.5388(6) |
| *β* (°) | 102.819(4) | 98.077(3) |
| *V* (Å$^3$) | 2711.3(2) | 2834.57(18) |
| *Z* | 4 | 4 |
| *T* (K) | 173(2) | 173(2) |
| $D_c$ (g·cm$^{-3}$) | 1.715 | 1.746 |
| μ (mm$^{-1}$) | 1.502 | 1.448 |
| Scan range (°) | $1.88 < \theta < 29.26$ | $1.63 < \theta < 29.21$ |
| Unique reflections | 7331 | 7661 |
| Observed refls [I>2σ(I)] | 4703 | 5927 |
| $R_{int}$ | 0.1318 | 0.0826 |
| Final *R* indices [I>2σ(I)]* | 0.0577, $wR_2$ 0.1009 | 0.0443, $wR_2$ 0.0614 |
| *R* indices (all data) | 0.1087, $wR_2$ 0.1146 | 0.0696, $wR_2$ 0.0656 |
| Goodness-of-fit | 0.975 | 1.079 |
| Max, Min Δρ/e (Å$^{-3}$) | 0.984, -1.358 | 0.668, -0.719 |

* Structures were refined on $F_0^2$: $wR_2 = [\Sigma[w (F_0^2 - F_c^2)^2] / \Sigma w (F_0^2)^2]^{1/2}$, where $w^{-1} = [\Sigma(F_0^2) + (aP)^2 + bP]$ and $P = [\max(F_0^2, 0) + 2F_c^2]/3$

**Single-Crystal X-Ray Structure Analysis of 6:**

Crystal of complex **6** · 2 $CHCl_3$ was mounted on a Stoe Image Plate Diffraction system equipped with a $\phi$ circle goniometer, using Mo-Kα graphite monochromated radiation (λ = 0.71073 Å) with $\phi$ range 0 – 180º. The structure was solved by direct methods using the program SHELXS–97 [204]. Refinement and all further calculations were carried out using SHELXL–97 [205]. The H-atoms were included in calculated positions and treated as riding atoms using the SHELXL default

parameters. The non-H atoms were refined anisotropically, using weighted full-matrix least-square on $F^2$. Crystallographic details are summarized in Table 12.

**Table 12 -** Crystallographic and structure refinement parameters for complex **6** · 2 $CHCl_3$.

| | **6** · 2 $CHCl_3$ |
|---|---|
| Chemical formula | $C_{38}H_{48}Cl_8O_2Ru_2S_2$ |
| Formula weight | 1086.62 |
| Crystal system | Triclinic |
| Space group | *P* -1 (no. 2) |
| Crystal color and shape | Orange block |
| Crystal size | 0.24 x 0.21 x 0.19 |
| *a* (Å) | 10.034(2) |
| *b* (Å) | 10.070(2) |
| *c* (Å) | 12.124(2) |
| *α* (°) | 112.75(3) |
| *β* (°) | 95.58(3) |
| *γ* (°) | 98.51(3) |
| *V* (Å$^3$) | 1101.2(4) |
| *Z* | 1 |
| *T* (K) | 173(2) |
| $D_c$ (g·cm$^{-3}$) | 1.639 |
| μ (mm$^{-1}$) | 1.299 |
| Scan range (°) | 1.85 < θ < 29.31 |
| Unique reflections | 5787 |
| Observed refls [I>2σ(I)] | 4504 |
| $R_{int}$ | 0.0575 |
| Final *R* indices [I>2σ(I)]* | 0.0386, $wR_2$ 0.0868 |
| *R* indices (all data) | 0.0530, $wR_2$ 0.0917 |
| Goodness-of-fit | 0.965 |
| Max, Min Δρ/e (Å$^{-3}$) | 0.941, - 1.470 |

Structures were refined on $F_0^2$: $wR_2 = [\Sigma[w (F_0^2 - F_c^2)^2] / \Sigma w (F_0^2)^2]^{1/2}$, where $w^{-1} = [\Sigma(F_0^2) + (aP)^2 + bP]$ and $P = [\max(F_0^2, 0) + 2F_c^2]/3$

### 9.1.2 NMR Experiments

The $^{1}H$, $^{13}C$, COSY, HSQC and HMBC NMR spectra were recorded on a Bruker Avance II 400 spectrometer using the residual protonated solvent as internal standard.

For the stability and reactivity study of mono- and dithiolato complexes (Chapter 2.2), the spectra were recorded using a Bruker Avance II 500-MHz NMR spectrometer equipped with an inverse triple channel ($^{1}H$, $^{13}C$, $^{31}P$) *z*-gradient 1.7 mm microprobehead. One-dimensional $^{1}H$ NMR data were measured with 16 – 64 transients into 32 k data points over the width of 12 ppm using a classic presaturation to eliminate the water resonance. A relaxation delay of 4 s was applied between the transients. Two-dimensional $^{1}H$ – $^{1}H$ NMR correlation spectroscopy data were acquired over a frequency width of 12 ppm in both $F_2$ and $F_1$ into 2 k complex data points in $F_2$ (acquisition time 213 or 170 ms) using 128 $t_1$ increments. The water resonance was suppressed by means of a presaturation routine. Two-dimensional $^{1}H$ diffusion-ordered spectroscopy (DOSY) NMR data were acquired with a standard longitudinal encode – decode pulsed-field-gradient stimulated echo sequence containing bipolar gradients [206-207]. For all experiments, the airflow was increased to 670 l/min, and the NMR tube was not spun. Experimental parameters were $\Delta$ = 100 ms (diffusion delay), $\tau$ = 1 ms (gradient recovery delay) and $T$ = 5 ms (eddy current recovery delay). For each data set, 4 k complex points were collected, and the gradient dimension was sampled by means of 32 experiments in which the gradient strength was linearly increased from 1.0 to 50.8 G/cm. The gradient duration $\delta/2$ was adjusted to observe a near-complete signal loss at 50.8 G/cm. A 2-s recycle delay was used between scans for the data shown. For each data set, the spectral axis was processed with an exponential function (3 – 5 Hz line broadening), and a Fourier transform was applied to obtain 8 k real points. The DOSY reconstruction was realized with 8 k complex points in the detection dimension and with 256 points in the diffusion dimension. 32 scans were used for each sample. All NMR data were processed using TopSpin (versions 2.1 or 3.0, Bruker, Switzerland).

**Catalytic Glutathione Oxidation**: Each compound (approximately 0.1 mg) was incubated with 10 equivalents of glutathione in a $D_2O/(CD_3)_2CO$ (95 : 5) solution (0.5 mL), the same solution without the complex being inactive for glutathione oxidation. The resulting mixture was subsequently analyzed by $^{1}H$-NMR at 37°C every hour for a total of 24 hours on a Bruker Avance II 400MHz spectrometer equipped with an inverse dual channel ($^{1}H$, X) *z*-gradient probehead (BBI). 1D $^{1}H$-NMR data were acquired with 16 to 64 transients into 32K data points over a width of

12 ppm using a classical presaturation to eliminate the residual water resonance. All NMR data were processed using Topspin (version 3.0, Bruker Switzerland). Turnover numbers (TON) were calculated from the integrals (I) relative to the corresponding resonances of glutathione in its reduced (GSH) and oxidized forms (GSSG), according to the following equation: $\frac{I(GSSG)}{I(GSH)+I(GSSG)} * \frac{[GSH]^\circ}{[complex]}$ . Turnover frequencies for the GSH conversion (TOF) were obtained by fitting the TONs as a function of time using the exponential function $y = a - bc^x$.

**Stability of complexes 11 – 13 and 35 – 38**

The stability of complexes **11 – 13** and **35 – 38** in aqueous solutions was studied by dissolving 1 mg of the complexes in the $D_2O$/DMSO-$d_6$ 1 : 1 mixture and incubating the solutions at 37°C. 1D $^1$H-NMR spectra were recorded every 24 hours.

### 9.1.3 Other Analytical Instruments

Electrospray mass spectra in the Chapter 2.2 were recorded with an LTQ Orbitrap XL mass spectrometer (Thermo Fisher Scientific, Bremen, Germany) equipped with a nanoelectrospray ion source. The samples were analysed in the positive or negative ion mode with a voltage of +700 V applied to the glass emitter (New Objective, Woburn, MA, USA). The tube lens was at +150 V and the transfer capillary was held at 200°C. Spectra were acquired in Fourier transform mass spectrometry mode over an *m/z* range from 100 to 2,000 with a resolution of 100,000 at *m/z* = 400. Calibration of the instrument was performed with ProteoMass LTQ/FT-Hybrid electrospray ionization (ESI) positive mode calibration mix (Supelco Analytical, Bellefonte, PA, USA). The Xcalibur software package (version 2.0.7, Thermo Fisher Scientific) was used for instrument control and data processing. All the other ESI-MS spectra were recorded on a Bruker APEX II 9.4-tesla FT-ICR-MS equipped with an Apollo II electrospray ion source: sample condition 10-50 μmol/l in methanol or in methanol/dichloromethane mixture at 30ºC, end plate voltage being 3500 V and capillary voltage - 4000 V.

Infrared spectra were recorded as KBr pellets on a Perkin-Elmer FTIR 1720-X spectrometer. Elemental analyses were done by Mikroelementar-analytisches Laboratorium de ETH Zürich or by the Schürch group at the University of Bern.

## 9.2 Studies of Interactions with Biological Ligands

All reactions were monitored by 1D $^{1}$H NMR spectroscopy. Two-dimensional homonuclear $^{1}$H–$^{1}$H and DOSY experiments were performed after 24 hours of incubation at 37°C. All experiments were carried out in aqueous solutions without the addition of any buffers. The pD values of solutions were obtained by use of a glass electrode and by addition of 0.4 to the pH meter reading [208-209]. Oxygen was not excluded from the solutions.

**Stability of 2, 4, 5 and 6 in aqueous solution**

The stability of complexes **2, 4, 5** and **6** in aqueous solutions was studied by dissolving 1 mg of the complexes in the mixture of an appropriate deuterated solvent and water ($D_2O$/acetone-$d_6$ 6 : 4 for **2**, $D_2O$/acetone-$d_6$ 7 : 3 for **4** and $D_2O$/MeCN-$d_3$ 7 : 3 for **5** and **6**,). The pH of the solutions was varied by the addition of NaOD or DCl. The solutions were subsequently transferred to 1.7 mm NMR tubes and 1D $^{1}$H-NMR experiments were recorded at 37°C after 5, 15, 45, 75, 105, 135, 195, 255 and 1440 minutes. Between the measurements, the NMR tubes were stored in an incubator at 37°C.

**Stability of 2, 4, 5 and 6 in DMSO**

The stability in DMSO was studied by dissolving the complexes **2, 4, 5** and **6** in DMSO-$d_6$ and recording 1D $^{1}$H-NMR experiments according to the protocol for investigating the stability in aqueous solutions described above.

**Interactions of 2, 4, 5 and 6 with amino acids**

1 mg of the respective complex was dissolved in the appropriate aqueous solution (vide supra). When the hydrolysis reactions had reached a steady state, 3 equivalents of amino acid (Ala, Asp, Cys or His) were added. The solutions were then transferred into NMR tubes and 1D $^{1}$H-NMR experiments were measured after 5, 15, 45, 75, 105, 135, 195, 255 and 1440 minutes at 37°C. Between the measurements, the tubes were stored in the incubator at 37°C. ESI-MS, 2D $^{1}$H – $^{1}$H COSY and 2D $^{1}$H-DOSY spectra were recorded after the last 1D $^{1}$H-NMR experiment.

**Interactions of 2, 4, 5 and 6 with the DNA 20-mer**

Interaction of complexes with the DNA 20-mer was studied by dissolving the complexes in appropriate aqueous solution (vide supra), adding 1 mg of DNA fragment (Mw = 6119.2) and incubating the mixture at 37°C. ESI-MS measurements were performed after 2 h and 24 h of incubation.

## 9.3 Biological Studies

### 9.3.1 *In Vitro* Cytotoxicity Studies

The *in vitro* cytotoxicity studies for monothiolato compounds **2** and **4** were carried out by the Furrer group at the University of Bern. All the other *in vitro* studies (except for the in-depth study of diruthenium-1) were carried out in the group of Paul J. Dyson at the EPFL.

**Complexes 2 and 4**

Human A2780 ovarian carcinoma cells were obtained from the European Centre of Cell Cultures (ECACC, Salisbury, UK) and maintained in culture as described by the provider. The cells were routinely grown in RPMI-1640 medium which contained fetal calf serum (FCS) (10%), 2 mM Gln, and 1% antibiotics (penicillin/streptomycin) at 37°C and $CO_2$ (5%). The cytotoxicity was determined using the cell counting kit 8 (Dojindo). Therefore, the cells were seeded in 96-well plates as monolayers with 100 μL of cell solution (approximately 10'000 cells) per well. The compounds were dissolved in DMSO, then added to the culture medium and serially diluted with water to the appropriate concentration, to give a final DMSO concentration of 1%. 100 μL of drug solution were added to each well and the plates were incubated for 96 h. After incubation the culture medium was removed completely and subsequently, 10 μL kit solution and 100 μL fresh medium were added to the cells. The plates were incubated for a further 90 minutes. The optical density, directly proportional to the number of surviving cells, was quantified at 450 nm using a multiwell plate reader and the fraction of surviving cells was calculated from the absorbance of untreated control cells. The evaluation is based on means from four independent experiments, each comprising four micro-cultures per concentration level.

**Complexes 6, 30 and 39 – 42**

Human A2780 and A2780cisR ovarian carcinoma cells were obtained from the European Centre of Cell Cultures (ECACC, UK). Non-cancerous human embryonic kidney HEK293 cells were provided by the Institute of Pathology, CHUV, Lausanne, Switzerland. Immortalized human endothelial cells RF24 were kindly provided by the Angiogenesis Laboratory of VU Medical Center, Amsterdam, Netherlands. A2780 and A2780cisR cells were routinely grown in RPMI 1640 medium supplemented with GlutaMAX (Gibco), 10% fetal calf serum and 1% antibiotics (Penicillin/Streptomycin, Sigma), while HEK293 cells were grown in DMEM medium, both containing heat-inactivated fetal calf serum (FCS, Sigma, USA) (10%) and 1% antibiotics at 37°C

and $CO_2$ (5%). RF24 cells were maintained in RPMI 1640/DMEM (1 : 1) supplemented as above. $10x10^4$ cells/well were seeded in 96-well cell culture plates as described previously [210]. Briefly, 24 h after seeding, culture medium with or without compounds was added and cells were grown for an additional 72 hours. Cell viability was assessed using the CellTiter-Glo®. Luminescent Cell Viability Assay (Promega, Madison, WI) according to the manufacturer's instructions. Evaluation is based on means from two independent experiments, each comprising three microcultures per concentration level. 0.1% DMSO in 0.9% NaCl was used as the control.

**Complexes 11 – 14 and 35 – 38**

Human A2780 and A2780cisR ovarian carcinoma cells were obtained from the European Centre of Cell Cultures (ECACC, Salisbury, UK). Nontumorigenic HEK293 cells were obtained from ATCC (Sigma, Switzerland). A2780 and A2780cisR cells were routinely grown in RPMI 1640 medium with GlutaMAX containing 5% fetal bovine serum (FBS) and 1 % antibiotics (penicillin and streptomycin) at 37°C and 5% $CO_2$. HEK293 cells were grown in DMEM medium containing 5% fetal bovine serum (FBS) and 1% antibiotics (penicillin and streptomycin) at 37°C and 5% $CO_2$. In order to keep the A2780cisR cells resistant to cisplatin the cells were monthly treated with 2 μM cisplatin for one passage. Cytotoxicity was determined using the MTT assay [MTT = 3(4,5-dimethyl-2-thiazolyl)-2,5-diphenyl-2H-tetrazolium bromide)]. Briefly, the cells were seeded in 96-well plates (10'000 cells per well) and grown for 24 h in complete medium. For each testing, compounds were freshly prepared as DMSO stock solution, then dissolved in the culture medium and immediately serially diluted to the appropriate concentration, to give a final DMSO concentration of 0.5% v/v. Drug solution (100 μL) was added to each well and the plates were incubated at 37°C for 72 h or 2 h at 41.5°C followed by a 68 h incubation at 37°C. Following drug exposure, 20 μL of MTT (5 mg/mL solution in PBS) were added to the cells and incubated for 4 h, then the culture medium was aspirated and the violet formazan crystals were dissolved in DMSO (100 μL). The optical density of each well (96-well plates) was quantified at 590 nm using a multiwell plate reader (Molecular Devices, UK), and the percentage of surviving cells was calculated from the ratio of absorbance of treated to untreated cells. The $IC_{50}$ values for the inhibition of cell growth were determined by fitting the plot of the logarithmic percentage of surviving cells against the logarithm of the drug concentration using a linear regression function.

### *9.3.2 Diruthenium-1*

Due to the poor solubility of *diruthenium-1* in water, a co-solvent in an amount close to the upper limit of acceptance (0.77 ml of propane-1,2-diol/kg of body weight) had to be added to saline, which is the reason why the i.p. route of administration was chosen rather than the i.v. way.

**Animals and Tumor Model**

Female outbred mice (NMRI) obtained from Masaryk University (Brno, Czech Republic) were used for this study. Animal care was conform to EU recommendations and in accordance with the European convention for the protection of vertebrate animals used for experimental and other scientific purposes; it was approved by the Ethical Commission of the Medical Faculty in Hradec Králové (Nr. MSMT-56249/2012-310). For the MTD assessment, two or three healthy mice per group were observed for weight loss over 14 days after injection of the solution. For the *in vivo* activity study, 98 NMRI female mice weighting in the average 33.5 g (SD = 3.42) were fed a standard diet and water *ad libitum*. A solid Ehrlich tumor was purchased from the Research Institute for Pharmacy and Biochemistry (VUFB) in Prague, and then maintained in NMRI mice by periodical transplantations. The homogenized tumor tissue was inoculated subcutaneously into all mice on day 0, using 0.2 ml of 1/1 (v/v) homogenate freshly prepared in isotonic glucose solution. The tumor-bearing mice were then divided into 7 groups of 14 animals as follows: a control group treated with the pure solvent, 5 groups of animals treated with *diruthenium-1* in doses of 0.2, 0.4, 0.6, 1.0, or 2.0 mg/kg i.p. and a positive control receiving 5 mg/kg cisplatin i.p. (cisplatin 50 ml/25 mg, EBEWE Pharma, Austria) [211]. The solutions were administered on days 1 and 7 in volumes of 0.2 ml per 20 g body weight.

**Statistical Analysis**

One-Way Analysis of Variance with post-hoc Dunnetts's multiple comparison test was used to detect differences in tumor weight. Kaplan-Meier curves and logrank tests were used to compare survival times in groups. Here, the level of significance was $\alpha = 0.05$. MS Excel 2003 and NCSS software were used for the calculations and statistical evaluations.

**Inductively Coupled Plasma-Mass Spectrometry of Ruthenium**

Tissue samples were cut with the aid of a ceramic knife. Approx. 20 mg of sample were weighed into pre-cleaned glass vials. Then 0.3 mL ultrapure double sub-boiled $HNO_3$ conc. and 0.1

mL ultrapure $H_2O_2$ (VWR) was added. After 5 min reaction time 0.05 mL ultrapure sub-boiled HCl conc. was added, the vessels were closed and digested employing closed vessel microwave digestion (Microwave 3000, Anton Paar) with Rotor 64MG5 (64 positions) applying the digestion program as follows: 750 W/15 min (5 min ramp), 600 W/15 min, 0 W/15 min. $T_{max}$ of the IR sensor was set to 140°C. After digestion the clear samples were quantitatively transferred into a pre-cleaned polyethylene tube and filled to approximately 5 g using ultrapure sub-boiled water. The solutions were stored at 4°C until measurement. Ruthenium analysis was carried out at *m/z* = 101 on an Element 2 sector field ICP-MS (Thermo Electron, Bremen, Germany) combined with a PFA-ST microflow nebulizer and a cyclonic spray chamber operated at 4°C (Elemental Scientific, ESI, Omaha, NE, USA). Quantification was performed with external calibration (internal standardization with indium) in a working range of 0.06 – 23.30 µg $L^{-1}$. The procedural limit of detection of Ru was 0.2 ng/g wet weight.

**Cell Isolation and Cultivation**

MCF-7 and BT-549 (ATCC, USA) breast carcinoma cells were cultured in 5% $CO_2$ atmosphere under 37°C in Dulbecco´s modified Eagle´s medium (Sigma, St Louis, MO, USA) supplemented with 10% FCS (PAA, Dartmouth, MA, USA), 1% glutamine (Gibco, Paisley, UK), penicillin/streptomycin (Gibco), only for MCF-7 1% non-essential amino acids (Sigma) and only for BT-549 0.01% insulin (Sigma). Cells were dissociated and reseeded using trypsin-EDTA (Gibco). In all experiments early passages (< 10 passages) of the cells were used and each of the passage reached approximately 70% confluence.

**Treatment of Cells**

Stock solution of *diruthenium-1* was prepared by dissolving 1 mg of the substance in 1 ml of DMSO (Sigma) and diluted by distilled water to reach the concentration of 50 µM. For the experiments, the stock solution was diluted by cultivation medium to final concentrations from 50 nM to 800 nM.

**WST-1 Cssay and LDH Cytotoxicity Assay**

For both the assays, MCF-7 and BT-549 cells were seeded in 96-well plates at a concentration of $1x10^3$ cells/well in 200 µl of culture medium. Cells were allowed to settle overnight at 37 °C in 5% $CO_2$. Cultures were exposed to *diruthenium-1* in concentrations 50, 100, 200, 400 and 800 nmol/l for 72 hours. Then, WST-1 (Roche, Switzerland) was used according to manufactures

instruction. Absorbance was measured with Tecan SpectraFluor Plus Spectrometer (Tecan Austria GmbH, Grodig, Austria) and corresponds to metabolic transformation of WST-1 in mitochondria of viable cells. Data are expressed as ratio of each sample absorbance againts control (100%). To measure LDH release, LDH cytotoxicity detection kit (Roche, Switzerland) according to manufactures instruction was used. LDH release corresponds to absorbance detected by Tecan SpectraFluor Plus Spectrometer (Tecan). Data represent the ratio of free LDH in medium and total LDH (free in medium plus intracellular released after cell lysis) of appropriate samples.

**Lactate**

The concentration of lactate in cultivation medium was measured on Modular PP (Roche Diagnostics, Mannheim, Germany) by the kit Lactate Cobas® (Roche Diagnostics GmbH, Germany) according to the manufacturer's instructions.

**Determination of ATP Levels**

ATP content in breast carcinoma cells MCF-7 and BT-549 was measured by ATP colorimetric assay kit by Bio Vision (Baria, Prague, Czech Republic). Briefly, treated and control cells were harvested at 24 h and 72 h and lysed on ice. Afterwards, 100 µl of ATP lysing buffer was added and lysates were deproteinized using Deproteinization Sample Preparation Kit. Then, 25 µl of sample were added to a 96-well plate, adjusted to 50 µl volume/well with ATP Assay Buffer. After addition of ATP standard and reaction mix (total volume 50 µl/well), plates were incubated at room temperature for 30 min, protected from light. Absorbance was measured at (OD 570 nm) in a microplate reader TECAN SpectraFluor Plus (TECAN Austria GmbH, Grödig, Austria). ATP content was calculated from a standard curve derived from known concentrations of ATP and was expressed as a percentage of control.

**Electrophoresis and Western Blotting**

Samples for protein analysis were obtained either from cancer tissue using an Ultra-turrax T10 Basic Disperser (IKA-Werke GmbH & Co.KG, Germany) and RIPA buffer (Sigma-Aldrich) or from cells, that were treated with increasing concentration of *diruthenium-1* for 72 hours and then whole cell lysates were prepared. The protein concentration was determined with BCA Protein Assay Kit (Pierce). Proteins were separated by SDS-PAGE, transferred to a PVDF membrane (Millipore), washed, and incubated with primary antibody (anti-PCNA, β-actin, anti-CD3 - Sigma-Aldrich; p53 - Exbio; p53_S15 - Calbiochem-Merck; ERK, p_ERK, p_p38 - Cell Signaling

Technology) at 4°C overnight. Then, the membrane was incubated with polyclonal anti-mouse or anti-rabbit secondary antibody (DakoCytomation, CZE). For the signal detection a chemiluminescent detection kit (Roche, CZE) was used. Densitometry was performed using a ScanMaker i900 (UMAX) and the QuantityOne imaging software (BioRad).

**Quantification of Glutathione**

For the measurement of individual GSSG and GSH glutathione forms in the cell homogenate, a selective HPLC method was used [212]. It is based on the derivatization of GSH with *o*-phthalaldehyde yielding a fluorescent product. For the selective measurement of GSSG, GSH in the samples were blocked by *N*-ethylmaleimide prior to *o*-phthalaldehyde derivatization.

**Measurement of Oxygen Consumption**

The experiment was performed on adult Wistar male rats with body weight of 220 g. Liver mitochondria were isolated by differential centrifugation [213]. Oxygen consumption by mitochondria was measured at 30°C using High Resolution Oxygraph2K (Oroboros, Austria). Mitochondria were incubated in K medium (80 mM KCl, 10 mM Tris-HCl, 5 mM K-phosphate, 3 mM $MgCl_2$, 1 mM EDTA, pH = 7.2), with substrates for complex I or complex II. Cytochrome c was added to evaluate the state of the outer mitochondrial membrane. The respirations were inhibited by 0.8 μM *diruthenium-1* for the period of 10 minutes.

## 9.4 Syntheses and Characterizations

### 9.4.1 Monothiolato Complexes 1 – 4

**Synthesis of 1**: $[(\eta^6\text{-}p\text{-}MeC_6H_4Pr^i)_2Ru_2Cl_2(\mu\text{-}Cl)_2]$ (100 mg, 0.163 mmol) was dissolved in 50 mL of ethanol. The mixture was cooled down to - 25°C and benzylthiol (0.25 mmol, 29 µL) was added dropwise. The mixture was stirred for two hours at - 25°C and then concentrated to 5 mL. The product was precipitated by addition of diethylether, separated by filtration and dried *in vacuo*. The product was a mixture of **1** and $[(\eta^6\text{-}p\text{-}MeC_6H_4Pr^i)_2Ru_2Cl_2(\mu\text{-}SCH_2C_6H_5)_2]$ [115], estimated to approximately 3 : 1 on the basis of the NMR spectra.

**Data for 1**: Yield: 108 mg (95%). $C_{27}H_{35}Cl_3Ru_2S$ (699.96): ESI-MS ($MeOH/CH_2Cl_2$): 665.6 $[M]^+$. $^1H$ NMR (400 MHz, $CDCl_3$): δ = 7.61 (d, $^3J$ = 7 Hz, 2 H, $SCH_2C_6\mathit{H}_5$), 7.30 (m, 3 H, $SCH_2C_6\mathit{H}_5$), 4.93 [m, 8 H, $p\text{-}CH_3C_6\mathit{H}_4CH(CH_3)_2$], 4.41 (d, $^3J$ = 11 Hz, 1 H, $SC\mathit{H}_2C_6H_4$), 3.71 (d, $^3J$ = 11 Hz, 1 H, $SC\mathit{H}_2C_6H_4$), 2.15 [m, 2H, $p\text{-}CH_3C_6H_4C\mathit{H}(CH_3)_2$], 1.85 [s, 6 H, $p\text{-}C\mathit{H}_3C_6H_4CH(CH_3)_2$], 1.20 [d, $^3J$ = 7 Hz, 12 H, $p\text{-}C\mathit{H}_3C_6H_4CH(C\mathit{H}_3)_2$] ppm, $^{13}C$ NMR (100 MHz, $CDCl_3$): δ = 130.4, 128.0, 86.7, 83.0, 37.9, 37.6, 30.5, 22.4, 19.3 ppm.

**Synthesis and Isolation of 2:** 100 mg of $[(\eta^6\text{-}p\text{-}MeC_6H_4Pr^i)_2Ru_2Cl_2(\mu\text{-}Cl)_2]$ (0.163 mmol) were dissolved in 10 mL of dichloromethane and 29.0 mg of 4-nitrobenzylthiol (0.163 mmol) were added as a solution in 5 mL of $CH_2Cl_2$. The mixture was stirred at room temperature for 4 hours. Afterwards the solvent was evaporated under reduced pressure and the product was precipitated, filtered, washed with hexane and dried *in vacuo*.

**Data for 2**: Yield: 107 mg (93%). $C_{27}H_{34}Cl_3NO_2Ru_2S \cdot 0.25\ CH_2Cl_2$ (765.93): calcd. C 42.71, H 4.54, N 1.83; found C 42.94, H 4.52, N 1.93. ESI-MS ($MeOH/CH_2Cl_2$): *m/z* = 709.9 $[M]^+$. $^1H$ NMR (400 MHz, $CDCl_3$): δ = 8.18 (d, $^3J$ = 8 Hz, 2 H $SCH_2C_6\mathit{H}_4NO_2$), 7.81 (d, $^3J$ = 8 Hz, 2 H, $SCH_2C_6\mathit{H}_4NO_2$), 5.16 [m, 8 H, $p\text{-}CH_3C_6\mathit{H}_4CH(CH_3)_2$], 4.67 (d, $^3J$ = 11 Hz, 1 H, $SC\mathit{H}_2C_6H_4NO_2$), 3.67 (d, $^3J$ = 11 Hz, 1 H, $SC\mathit{H}_2C_6H_4NO_2$), 2.84 [m, 2 H, $p\text{-}CH_3C_6H_4C\mathit{H}(CH_3)_2$], 2.17 [s, 6 H, $p\text{-}C\mathit{H}_3C_6H_4CH(CH_3)_2$], 1.23 [m, 12 H, $p\text{-}C\mathit{H}_3C_6H_4CH(C\mathit{H}_3)_2$] ppm, $^{13}C$ NMR (100 MHz, $CDCl_3$): δ = 131.2, 123.1, 85.5, 83.2, 36.3, 30.3, 22.2, 19.0 ppm.

**Synthesis of 3:** 100 mg of $[(\eta^6\text{-}p\text{-}MeC_6H_4Pr^i)_2Ru_2Cl_2(\mu\text{-}Cl)_2]$ (0.163 mmol) were dissolved in 40 mL of ethanol and the 1-adamantylthiol (57.7 mg, 0.326 mmol) was added dropwise as a solution in 10 mL of EtOH. The mixture was stirred at room temperature for 3 days. The solvent

was evaporated and the product was isolated by preparative TLC on silica ($CH_2Cl_2$/EtOH 7 : 1), extracted from the orange main band with EtOH and dried *in vacuo*. The product was a mixture of **3** and [(*p*-$MeC_6H_4{}^{i}Pr)_2Ru_2Cl_4$] (approximately 8 : 1 based on the NMR data).

**Data for 3**: Yield: 64 mg (53%). $C_{30}H_{43}Cl_3Ru_2S$ (744.02): ESI-MS ($MeOH/CH_2Cl_2$): *m/z* = 709.30 $[M]^+$. $^1$H NMR (400 MHz, $CDCl_3$): δ = 5.78 [d, $^3J$ = 6 Hz, 4 H, $CH_3C_6H_4CH(CH_3)_2$], 5.66, [d, $^3J$ = 6 Hz, 4 H, $CH_3C_6H_4CH(CH_3)_2$], 2.59 [sept, $^3J$ = 7 Hz, 2 H, $CH_3C_6H_4CH(CH_3)_2$], 2.18 (m, 15 H, $SC_{10}H_{15}$), 1.81 [s, 6 H, $CH_3C_6H_4CH(CH_3)_2$], 1.25 [m, 12 H, $CH_3C_6H_4CH(CH_3)_2$] ppm, $^{13}$C NMR (100 MHz, $CDCl_3$): δ = 98.3, 49.6, 46.7, 36.2, 30.9, 30.2, 22.38, 18.27 ppm.

**Synthesis and Isolation of 4:** [($\eta^6$-*p*-$MeC_6H_4Pr^i)_2Ru_2Cl_2(\mu\text{-}Cl)_2$] (100 mg, 0.163 mmol) was dissolved in 20 mL of ethanol and *m*-carborane-9-thiol (86.3 mg, 0.489 mmol) was added dropwise as a solution in 5 mL of EtOH. The mixture was stirred for 5 days at 40°C, then the solvent was evaporated and the product isolated by preparative TLC on silica ($CH_2Cl_2$/EtOH 7 : 1), extracted from the main red band with EtOH and dried *in vacuo*.

**Data for 4**: Yield: 79 mg (64%). $C_{22}H_{38}B_{10}Cl_3Ru_2S \cdot HCl$ (789.05): calcd. C 33.50, H 5.11; found C 33.93, H 5.38. ESI-MS ($MeOH/CH_2Cl_2$): *m/z* = 717.9 $[M]^+$. $^1$H NMR (400 MHz, $CDCl_3$): δ = 5.62 [d, $^3J$ = 5 Hz, 4 H, $CH_3C_6H_4CH(CH_3)_2$], 5.42 [d, $^3J$ = 5 Hz, 4 H, $CH_3C_6H_4CH(CH_3)_2$], 3.75 – 1.65 (m, 11 H, $C_2H_{11}B_{10}$), 2.63 [sept, $^3J$ = 7Hz, 2H, $CH_3C_6H_4CH(CH_3)_2$], 2.14 [s, 6 H, $CH_3C_6H_4CH(CH_3)_2$], 1.22 [d, $^3J$ = 7 Hz, 12 H, $CH_3C_6H_4CH(CH_3)_2$] ppm, $^{13}$C NMR (100 MHz, $CDCl_3$): δ 81.7, 55.9, 29.8, 22.4, 19.2 ppm.

### 9.4.2 Dithiolato Complexes 5, 7 and 10

The attempts to synthesize complexes **5**, **7**, and **10** using the previously reported synthesis [115] led to the discovery of monothiolato complexes and to the findings presented in the Chapter 2.1. Therefore, a new procedure had to be developed for the synthesis of dithiolato complexes that were needed for the synthesis of conjugates.

The products **5** and **7** were prepared by the following procedure: 0.16 mmol of [(*p*-$MeC_6H_4Pr^i)_2Ru_2Cl_4$] were dissolved in EtOH (10 mL). When the compound had completely dissolved, the corresponding thiol RSH (2 equivalents, 0.32 mmol) was added dropwise as the solution in 5 mL of ethanol. The reaction was stirred at rt for 3 h, the volume was then reduced to 5

mL and diethyl ether (30 mL) was added to precipitate the products. The filtration and washing of the solid 2 times with 20 mL of diethylether afforded the products as orange crystalline powders. The products were dried under vacuum and analyzed by NMR and ESI-MS. The spectra were identical to those reported for the dithiolato products [(*p*-$MeC_6H_4Pr^i$)$_2Ru_2$(μ-$SC_2H_4Ph$)$Cl_2$] and [(*p*-$MeC_6H_4Pr^i$)$_2Ru_2$(μ-S-*p*-$CH_2C_6H_4Bu^t$)$Cl_2$] [115].

The product **10** was prepared by the following procedure: 0.16 mmol of [(*p*-$MeC_6H_4Pr^i$)$_2Ru_2Cl_4$] were dissolved in $CH_2Cl_2$ (10 mL). When the compound had completely dissolved, the benzyl thiol (0.32 mmol) was added dropwise as the solution in 5 mL of ethanol. The reaction was stirred at rt for 3 h, the volume was then reduced to 5 mL and hexane (30 mL) was added to precipitate the product. The filtration and washing of the solid 2 times with 20 mL of hexane afforded the product as orange crystalline powder, which was dried under vacuum and analyzed by NMR and ESI-MS. The spectra were identical to those reported for the dithiolato product [(*p*-$MeC_6H_4Pr^i$)$_2Ru_2$(μ-$SCH_2Ph$)$Cl_2$] [115].

### 9.4.3 Dithiolato Complex 6 and the Corresponding Trithiolato Complex 30

**Synthesis and data for 6:** In a 100 mL reaction flask, 100 mg (0.163 mmol) of [($\eta^6$-*p*-Me-$C_6H_4{}^iPr$)$_2Ru_2Cl_4$] was dissolved in 45 mL of EtOH. 50.3 μL (0.343 mmol) 4-methoxy-α-toluenthiol, dissolved in 5 mL of EtOH were added dropwise by a glass pipet. The solution was heated to 50°C overnight. Afterwards the solvent was reduced to 2 mL *in vacuo*, and the product was precipitated by adding hexane. The solid was filtered, washed with hexane and dried *in vacuo* to give the product as a light orange powder. Yield: 124.2 mg (89%), ESI-MS: (MeOH + $CH_2Cl_2$): *m/z* = 822.8 $[M]^+$. $C_{36}H_{46}Cl_2O_2Ru_2S_2$: calcd. C, 50.99; H, 5.47; found C, 50.76; H, 5.46. $^1$H NMR (400 MHz, $CDCl_3$): δ = 7.49 (d, $^3J$ = 8 Hz, 2H, $SCH_2C_6H_4$-*p*-$OCH_3$), 6.85 (d, $^3J$ = 8 Hz, 2H, $SCH_2C_6H_4$-*p*-$OCH_3$), 5.15 – 4.89 [m, 8H, *p*-$CH_3C_6H_4CH(CH_3)_2$], 4.15 (d, $^3J$ = 11 Hz, 2H, $SCH_2C_6H_4$-*p*-$OCH_3$), 3.83 (s, 6H, $SCH_2C_6H_4$-*p*-$OCH_3$), 3.26 (d, $^3J$ = 11 Hz, 2H, $SCH_2C_6H_4$-*p*-$OCH_3$), 2.86 [sept, $^3J$ = 8 Hz, 2H, *p*-$CH_3C_6H_4CH(CH_3)_2$], 1.89 [s, 6H, *p*-$CH_3C_6H_4CH(CH_3)_2$], 1.2 [s, 12H, *p*-$CH_3C_6H_4CH(CH_3)_2$] ppm, $^{13}$C NMR (100 MHz, $CDCl_3$): δ = 133.03, 131.71, 113.05, 86.49, 78.75, 55.36, 35.93, 29.73, 23.69, 21.29, 18.81 ppm.

**Synthesis and data for 30[Cl]:** Complex **6** (100 mg, 0.118 mmol) was dissolved in EtOH (50 mL). Then 46 mg (0.354 mmol) of 4-hydroxythiophenol, dissolved in 10 mL of EtOH, were added

to this solution dropwise by a pipet, and the solution was refluxed overnight. The solution was concentrated to dryness, the residue dissolved in $CH_2Cl_2$ (1 mL) and subjected to column chromatography on silica gel (solvent system $CH_2Cl_2$/EtOH 7 : 1). The reddish band was collected and evaporated to dryness to give the product as an orange powder. Yield: 110.6 mg (89%), ESI-MS: (MeOH + $CH_2Cl_2$): *m/z* = 903.1 $[M]^+$. $C_{42}H_{51}ClO_3Ru_2S_3$: calcd. C, 53.80; H 5.48; found C, 53.42; H, 5.34. $^1$H NMR (400 MHz, $CDCl_3$): δ = 10.30 (s, 1H, $SC_6H_4$-*p*-O*H*), 7.48 (d, 2H, $^3J$ = 8 Hz, $SC_6H_4$-*p*-OH), 7.42 (t, $^3J$ = 7 Hz, 4H, $SCH_2C_6H_4$-*p*-$OCH_3$), 7.22 (d, 2H, $^3J$ = 8 Hz, $SC_6H_4$-*p*-OH), 6.98 (t, $^3J$ = 9 Hz, 4H, $SCH_2C_6H_4$-*p*-$OCH_3$), 5.03 [d, 2H, $^3J$ = 6 Hz, *p*-$CH_3C_6H_4CH(CH_3)_2$], 4.91 [d, 2H, $^3J$ = 6 Hz, *p*-$CH_3C_6H_4CH(CH_3)_2$], 4.71 [t, $^3J$ = 6 Hz, 4H, *p*-$CH_3C_6H_4CH(CH_3)_2$], 3.88 (d, 6H, $^3J$ = 6 Hz, $SCH_2C_6H_4$-*p*-$OCH_3$), 3.53 (s, 2H, $SCH_2C_6H_4$-*p*-$OCH_3$), 3.34 (s, 2H, $SCH_2C_6H_4$-*p*-$OCH_3$), 2.02 [sept, $^3J$ = 7 Hz, 2H, *p*-$CH_3C_6H_4CH(CH_3)_2$], 1.69 [s, 6H, *p*-$CH_3C_6H_4CH(CH_3)_2$], 1.03 [d, $^3J$ = 7 Hz, 6H, *p*-$CH_3C_6H_4CH(CH_3)_2$], 0.97 [d, $^3J$ = 7 Hz, 6H, *p*-$CH_3C_6H_4CH(CH_3)_2$] ppm, $^{13}$C NMR (100 MHz, $CDCl_3$): δ = 159.44, 159.32, 157.81, 133.88, 131.69, 130.6, 130.40, 115.38, 114.00, 113.85, 106.95, 99.97, 83.72, 83.59, 82.28, 55.99, 55.46, 39.51, 39.27, 30.87, 23.15, 22.42, 17.99 ppm.

### 9.4.4 Cysteinato-Bridged Trithiolato Complex 8

**Synthesis and data for [8][$BF_4$]:** The dithiolato complex [($\eta^6$-*p*-$MeC_6H_4Pr^i$)$_2Ru_2Cl_2$(μ-$SC_6H_4$-*p*-$Bu^t$)$_2$] (**5)** (0.056 mmol) was dissolved in 25 mL of methanol. To this solution, cysteine (10 eq, 0.560 mmol) was added dropwise as a solution in 15 mL of distilled water. The mixture was stirred at room temperature for two days. 10 equivalents of $NaBF_4$ were then added and the suspension was stirred overnight. The solution was filtered and methanol was evaporated at room temperature; the light orange solid that precipitated during the evaporation was washed thoroughly with water and redissolved in MeOH/$H_2O$ 9 : 1 mixture. The product was isolated by size exclusion chromatography on Sephadex® LH20 from the yellow band. The solvents were evaporated *in vacuo*, yielding a yellow powder. Yield: 52.4 mg (95%), ESI-MS (MeOH): *m/z* = 950.0 $[M]^+$, $C_{45}H_{64}BF_4NO_2Ru_2S_3 \cdot H_2O$, calcd. C, 51.27; H, 6.31; N, 1.33, found C, 51.33; H, 6.15; N, 1.39; $^1$H NMR (400 MHz, $CDCl_3$): δ = 7.56 – 7.41 [m, 8H, $SCH_2C_6H_4$-*p*-$C(CH_3)_3$], 5.57 [broad, 1H, *p*-$CH_3C_6H_4CH(CH_3)_2$], 5.49 [broad, 1H, *p*-$CH_3C_6H_4CH(CH_3)_2$], 5.46 [d, $^3J$ = 5 Hz, 1H, *p*-$CH_3C_6H_4$-$CH(CH_3)_2$], 5.32 [d, $^3J$ = 5 Hz, 1H, *p*-$CH_3C_6H_4CH(CH_3)_2$], 5.22 [broad, 1H, *p*-$CH_3C_6H_4CH(CH_3)_2$], 5.17 [broad, 1H, *p*-$CH_3C_6H_4CH(CH_3)_2$], 5.02 [broad, 1H, *p*-$CH_3C_6H_4CH(CH_3)_2$], 4.95 [broad, 1H,

*p*-$CH_3C_6H_4CH(CH_3)_2$], 3.77 [m, 1H, $SCH_2CH(NH_2)COOH$], 3.73 – 3.42 [m, 4H, $SCH_2C_6H_5$-*p*-$C(CH_3)_3$], 3.01 [d, $^3J$ = 12 Hz, 1H, $SCH_2CH(NH_2)COOH$], 2.75 [m, 1H, $SCH_2CH(NH_2)COOH$], 2.23 [m, *p*-$CH_3C_6H_4CH(CH_3)_2$], 2.03 [m, 6H, *p*-$CH_3C_6H_4CH(CH_3)_2$], 1.37 (s, 18H, $SCH_2C_6H_5$-*p*-$C(CH_3)_3$] 1.14 – 1.00 [m, 12H, *p*-$CH_3C_6H_4CH(CH_3)_2$] ppm, $^{13}$C NMR (100 MHz, $CDCl_3$): δ = 170.55, 151.29, 129.01, 125.31, 107.18, 84.36, 83.66, 83.42, 83.22, 82.84, 82.48, 56.73, 48.63, 41.66, 40.42, 38.97, 34.20, 31.39, 22.94, 17.49 ppm.

### 9.4.5 *Diruthenium-1* ([9]Cl)

The compound [(*p*-$MeC_6H_4Pr^i)_2Ru_2(SC_6H_4$-*p*-$Bu^t)_3$]Cl *(diruthenium-1)* was synthesized by a slight variation of the published method [111] and isolated as HCl adduct [(*p*-$MeC_6H_4Pr^i)_2Ru_2$-$(SC_6H_4$-*p*-$Bu^t)_3$]Cl · 0.8 HCl; the purity was verified by NMR spectroscopy and by correct carbon and hydrogen elemental analysis prior to use for the biological study. Microanalyses were carried out by the Mikroelementaranalytisches Laboratorium, ETH Zürich (Switzerland).

**Synthesis and Data of *Diruthenium-1*:** 100 mg (0.16 mmol) of [($\eta^6$-*p*-$MeC_6H_4Pr^i$)$RuCl_2]_2$ were dissolved in 50 mL of ethanol *puriss.* The solution was heated to 60°C; as soon as the starting material was completely dissolved, a solution of 174 µL (1.01 mmol) *p*-$Bu^tC_6H_4SH$ in 5 mL ethanol *puriss.* was added dropwise to the hot solution. The resulting mixture was refluxed for 18 h. After cooling to 20°C, the solvent was removed under reduced pressure. The red oil obtained was purified by column chromatography on silica gel using a mixture of dichloromethane and ethanol (7 : 1) as the eluent. The product was isolated from the main fraction as air-stable red crystalline solid and dried *in vacuo*. Yield: 150 mg (89%) $C_{50}H_{67}Ru_2S_3Cl$ · 0.8 HCl (1031.00): calcd. C 58.25, H 6.63; found C 58.27, H 6.63. ESI-MS (MeOH): *m/z* = 967.4 $[M]^+$. $^1$H NMR (400 MHz, $CDCl_3$): δ = 7.78 (d, $^3J$ = 8.0 Hz, 6H, $SC_6H_4C(CH_3)_3$), 7.38 (d, $^3J$ = 8 Hz, 6H, $SC_6H_4C(CH_3)_3$), 5.41 (d, $^3J$ = 6 Hz, 2H, $MeC_6H_4Pr^i$), 5.20 (d, $^3J$ = 6 Hz, 2H, $MeC_6H_4Pr^i$), 5.12 (d, $^3J$ = 6 Hz, 2H, $MeC_6H_4Pr^i$), 5.06 (d, $^3J$ = 6 Hz, 2H, $MeC_6H_4Pr^i$), 1.84 (sept, $^3J$ = 7 Hz, 2H, $CH(CH_3)_2$), 1.65 (s, 6H, $CH_3$), 1.35 (s, 27H, $SC_6H_4C(CH_3)_3$), 0.86 (d, $^3J$ = 7 Hz, 6H, $CH(CH_3)_2$), 0.69 (d, $^3J$ = 7 Hz, 6H, $CH(CH_3)_2$) ppm, $^{13}$C NMR (100 MHz, $CDCl_3$): δ = 151.9, 134.5, 132.3, 126.2, 106.5, 100.7, 85.1, 84.6, 84.1, 84.0, 58.6, 34.9, 31.3, 30.4, 22.5, 22.0, 17.8 ppm.

### 9.4.6 Complexes with Fluorinated Side-Chains 11 – 13

**Synthesis of 11 – 13:** 0.153 mmol (93.8 mg) of the ruthenium *p*-cymene dichloride dimer were introduced in a Schlenk tube and dissolved in 20 mL of distilled methanol. 0.919 mmol of the corresponding thiol were dissolved in 10 mL of distilled MeOH and introduced dropwise into the Schlenk tube. The reaction mixture was refluxed under inert atmosphere for 40 hours (for compounds **11** and **13**) or for 5 days (for compound **12**). Afterwards the solvent was evaporated *in vacuo* and the mixture was separated by column chromatography on silicagel (solvent system $CH_2Cl_2$/EtOH 7 : 1). The red band was collected, solvents evaporated *in vacuo* and the product was recrystallized from $CH_2Cl_2$/pentane mixture. Resulting orange crystals were collected and dried under reduced pressure.

**Data for [11]Cl:** Yield: 267.9 mg (90%). $C_{50}H_{40}ClF_{51}Ru_2S_3$ (1943.56): calcd. C, 30.90; H, 2.07; found C, 30.62; H, 1.94. ESI-MS: (MeOH + $CH_2Cl_2$): *m/z* = 1908.1 $[M]^+$, $^1$H NMR (400 MHz, $CDCl_3$): δ = 5.72 – 5.48 [broad, 8H, *p*-$CH_3C_6H_4$CH$(CH_3)_2$], 2.84 – 2.47 [broad, 12H, S-$C_2H_4C_8F_{17}$, 2H, *p*-$CH_3C_6H_4CH(CH_3)_2$], 2.22 [s, 6H, *p*-$CH_3C_6H_4CH(CH_3)_2$], 1.27 [m, 12H, *p*-$CH_3C_6H_4CH(CH_3)_2$] ppm, $^{13}$C NMR (100 MHz, $CDCl_3$): δ = 108.03, 101.92, 84.02, 83.72, 83.52, 33.55, 31.72, 29.13, 23.52, 22.37, 18.31 ppm.

**Data for [12]Cl:** Yield: 75.3 mg (34%). $C_{38}H_{40}ClF_{27}Ru_2S_3$ (1343.46): calcd. C, 33.37; H, 2.98; found C, 33.47; H, 2.85. ESI-MS: (MeOH + $CH_2Cl_2$): *m/z* = 1308.7 $[M]^+$, $^1$H NMR (400 MHz, $CDCl_3$): δ = 5.72 – 5.48 [broad, 8H, *p*-$CH_3C_6H_4$CH$(CH_3)_2$], 2.84 – 2.47 [broad, 12H, S-$C_2H_4C_8F_{17}$, 2H, *p*-$CH_3C_6H_4CH(CH_3)_2$], 2.22 [s, 6H, *p*-$CH_3C_6H_4CH(CH_3)_2$], 1.27 [m, 12H, *p*-$CH_3C_6H_4CH(CH_3)_2$] ppm, $^{13}$C NMR (100 MHz, $CDCl_3$): δ = 108.03, 101.92, 84.02, 83.72, 83.52, 33.55, 31.72, 29.13, 23.52, 22.37, 18.31 ppm.

**Data for [13]Cl:** Yield: 236.6 mg (94%). $C_{44}H_{40}ClF_{39}Ru_2S_3$ (1643.51): calcd. C, 31.70; H, 2.45; found C, 31.73; H, 2.16. ESI-MS: (MeOH + $CH_2Cl_2$): *m/z* = 1608.98 $[M]^+$, $^1$H NMR (400 MHz, $CDCl_3$): δ = 5.72 – 5.48 [broad, 8H, *p*-$CH_3C_6H_4$CH$(CH_3)_2$], 2.84 – 2.47 [broad, 12H, S-$C_2H_4C_8F_{17}$, 2H, *p*-$CH_3C_6H_4CH(CH_3)_2$], 2.22 [s, 6H, *p*-$CH_3C_6H_4CH(CH_3)_2$], 1.27 [m, 12H, *p*-$CH_3C_6H_4CH(CH_3)_2$] ppm, $^{13}$C NMR (100 MHz, $CDCl_3$): δ = 108.03, 101.92, 84.02, 83.72, 83.52, 33.55, 31.72, 29.13, 23.52, 22.37, 18.31 ppm.

**Synthesis and data for [14]Cl:** 0.153 mmol (93.8 mg) of the ruthenium *p*-cymene dichloride dimer were introduced in a Schlenk tube and dissolved in 20 mL of distilled methanol. 1.632 mmol

of the 1-octanethiol were dissolved in 10 mL of distilled MeOH and introduced dropwise into the reaction mixture. The mixture was refluxed under inert atmosphere for 7 days. Afterwards, 1.5 grams of activated charcoal were added, the suspension was stirred for 1 hour and it was then filtered. The solvent was evaporated *in vacuo* and the mixture was separated by column chromatography on silicagel (solvent system $CH_2Cl_2$/EtOH 9 : 1). The red band was collected, solvent evaporated *in vacuo* and the product washed thoroughly with diethylether and pentane. Resulting orange powder was dried under reduced pressure. Yield: 40.4 mg (28%). $C_{44}H_{79}ClRu_2S_3 \cdot 0.75\ CH_2Cl_2 \cdot 0.5\ C_5H_{12}$ (1041.66): calcd. C, 54.48; H, 8.37 found C, 54.58; H, 8.65 ESI-MS: (MeOH + $CH_2Cl_2$): *m/z* = 906.20 $[M]^+$, $^1$H NMR (400 MHz, $CDCl_3$): δ = 5.46 [t, $^3J$ = 6 Hz, 4H, *p*-$CH_3C_6H_4CH(CH_3)_2$], 5.32 [d, $^3J$ = 5 Hz, 2H, *p*-$CH_3C_6H_4CH(CH_3)_2$], 5.24 [d, 5 Hz, 2H, *p*-$CH_3C_6H_4CH(CH_3)_2$], 2.55 [sept, $^3J$ = 7 Hz, 2H, *p*-$CH_3C_6H_4CH(CH_3)_2$], 2.34 [m, 6H, S-$C_8H_{17}$], 2.17 [s, 6H, *p*-$CH_3C_6H_4CH(CH_3)_2$], 1.79 – 1.62 [m, 6H, S-$C_8H_{17}$], 1.54 – 1.42 [m, 6H, S-$C_8H_{17}$], 1.40 – 1.26 [m, 24H, S-$C_8H_{17}$], 1.29 [d, $^3J$ = 7 Hz, 6H, *p*-$CH_3C_6H_4CH(CH_3)_2$], 1.23 [d, $^3J$ = 7 Hz, 6H, *p*-$CH_3C_6H_4CH(CH_3)_2$], 0.95 – 0.86 [m, 9H, S-$C_8H_{17}$] ppm, $^{13}$C NMR (100 MHz, $CDCl_3$): δ = 106.41, 101.27, 83.60, 83.14, 82.98, 82.87, 77.30, 76.98, 76.66, 38.96, 32.78, 31.73, 31.52, 29.34, 29.14, 23.89, 22.58, 22.36, 18.14, 14.02.ppm.

### 9.4.7 Complexes with Halido Substituents 15 – 20

**General procedure for the synthesis of 15 – 17:** 0.16 mmol of [(*p*-$MeC_6H_4Pr^i$)$_2Ru_2Cl_4$] were dissolved in EtOH (10 mL). When the compound had completely dissolved, the corresponding thiol RSH (0.32 mmol) was added dropwise as the solution in 5 mL of ethanol. The reaction was stirred at 50°C overnight, the volume of the mixture was then reduced to 5 mL and diethyl ether (30 mL) was added to fully precipitate the products. The filtration and washing of the solid 2 times with 20 mL of diethylether afforded the products as orange crystalline powders. The products were dried under vacuum and analyzed**.**

**Data for 15:** Yield: 132.9 mg (95%), ESI-MS (MeOH): *m/z* = 822.80 $[M]^+$, $C_{34}H_{40}Cl_4Ru_2S_2 \cdot 0.25\ Et_2O$: calcd. C, 48.03; H, 4.89; found C, 48.03; H, 4.74, $^1$H NMR (400 MHz, $CDCl_3$): δ = 7.51 (m, 4H, $SCH_2C_6H_4$-*p*-Cl), 7.29 (m, 4H, $SCH_2C_6H_4$-*p*-Cl), 5.02 – 4.76 [m, 8H, *p*-$CH_3C_6H_4CH(CH_3)_2$], 4.20 (d, $^3J$ = 11 Hz, $SCH_2C_6H_4$-*p*-Cl), 3.24 (d, $^3J$ = 11 Hz, $SCH_2C_6H_4$-*p*-Cl), 2.84 [sept, $^3J$ = 7 Hz, 2H, *p*-$CH_3C_6H_4CH(CH_3)_2$], 1.90 [s, 6H, *p*-$CH_3C_6H_4CH(CH_3)_2$], 1.20 [m, 12H, *p*-$CH_3C_6H_4CH(CH_3)_2$] ppm.

**Data for 16:** Yield: 146.7 mg (95%), ESI-MS (MeOH): *m/z* = 910.70 $[M]^+$, $C_{34}H_{40}Br_2Cl_2Ru_2S_2$: calcd. C, 43.52; H, 4.41; found C, 43.59; H, 4.14, $^1$H NMR (400 MHz, $CDCl_3$): δ = 7.45 (m, 8H, $SCH_2C_6H_4$-*p*-Br), 5.02 – 4.78 [m, 8H, *p*-$CH_3C_6H_4CH(CH_3)_2$], 4.19 (d, $^3J$ = 11 Hz, $SCH_2C_6H_4$-*p*-Br), 3.22 (d, $^3J$ = 11 Hz, $SCH_2C_6H_4$-*p*-Br), 2.85 [sept, $^3J$ = 7 Hz, 2H, *p*-$CH_3C_6H_4CH(CH_3)_2$], 1.90 [s, 6H, *p*-$CH_3C_6H_4CH(CH_3)_2$], 1.21 [m, 12H, *p*-$CH_3C_6H_4CH(CH_3)_2$] ppm.

**Data for 17:** Yield: 122.4 mg (91%), ESI-MS (MeOH): *m/z* = 788.70 $[M]^+$, $C_{34}H_{40}Cl_2F_2Ru_2S_2 \cdot 0.25\ CH_2Cl_2$: calcd. C, 48.68; H, 4.83; found C, 48.81; H, 4.87, $^1$H NMR (400 MHz, $CDCl_3$): δ = 7.55 (m, 4H, $SCH_2C_6H_4$-*p*-F), 7.01 (m, 8H, $SCH_2C_6H_4$-*p*-F), 5.02 – 4.77 [m, 8H, *p*-$CH_3C_6H_4CH(CH_3)_2$], 4.20 (d, $^3J$ = 11 Hz, $SCH_2C_6H_4$-*p*-F), 3.26 (d, $^3J$ = 11 Hz, $SCH_2C_6H_4$-*p*-F), 2.85 [sept, $^3J$ = 7 Hz, 2H, *p*-$CH_3C_6H_4CH(CH_3)_2$], 1.90 [s, 6H, *p*-$CH_3C_6H_4CH(CH_3)_2$], 1.20 [m, 12H, *p*-$CH_3C_6H_4CH(CH_3)_2$] ppm.

**General procedure for the synthesis of 18 – 20:** Complexes **15** – **17** (100 mg) were dissolved in EtOH (50 mL). Then 3 equivalents of 4-hydroxythiophenol, dissolved in 10 mL of EtOH, were added to this solution dropwise by a pipet, and the solution was refluxed overnight. The solution was concentrated to dryness, the residue dissolved in $CH_2Cl_2$ (1 mL) and subjected to column chromatography on silica gel (solvent system $CH_2Cl_2$/EtOH 7 : 1). The reddish band was collected and evaporated to dryness to give the products as orange powders.

**Data for [18]Cl:** Yield: 88.3 mg (83%), ESI-MS (MeOH): *m/z* = 910.80 $[M^+]$, $C_{40}H_{45}Cl_3ORu_2S_3 \cdot 0.25\ CH_2Cl_2$: calcd. C, 49.96; H, 4.74; found C, 49.75; H, 4.82, $^1$H NMR (400 MHz, $CDCl_3$): δ = 10.42 (s, 1H, $SC_6H_4$-*p*-O*H*), 7.53 – 7.39 (m, 2H, $SC_6H_4$-*p*-OH, 8H, $SCH_2C_6H_4$-*p*-Cl), 7.22 (d, 2H, $^3J$ = 8 Hz, $SC_6H_4$-*p*-OH), 5.08 [d, 2H, $^3J$ = 6 Hz, *p*-$CH_3C_6H_4CH(CH_3)_2$], 4.97 [d, 2H, $^3J$ = 6 Hz, *p*-$CH_3C_6H_4CH(CH_3)_2$], 4.71 [d, $^3J$ = 6 Hz, 4H, *p*-$CH_3C_6H_4CH(CH_3)_2$], 3.58 (s, 2H, $SCH_2C_6H_4$-*p*-Cl), 3.41 (s, 2H, $SCH_2C_6H_4$-*p*-Cl), 2.01 [sept, $^3J$ = 7 Hz, 2H, *p*-$CH_3C_6H_4CH(CH_3)_2$], 1.70 [s, 6H, *p*-$CH_3C_6H_4CH(CH_3)_2$], 1.04 [d, $^3J$ = 7 Hz, 6H, *p*-$CH_3C_6H_4CH(CH_3)_2$], 0.98 [d, $^3J$ = 7 Hz, 6H, *p*-$CH_3C_6H_4CH(CH_3)_2$] ppm, $^{13}$C NMR (100 MHz, $CDCl_3$): δ = 159.88, 138.33, 138.21, 133.86, 133.76, 133.38, 130.74, 130.48, 128.89, 128.77, 123.72, 117.12, 107.63, 99.85, 84.20, 83.75, 83.20, 81.97, 30.96, 23.11, 22.65, 17.94 ppm.

**Data for [19]Cl:** Yield: 108.2 mg (99%), ESI-MS (MeOH): *m/z* = 878.90 $[M^+]$, $C_{40}H_{45}ClF_2ORu_2S_3 \cdot 0.75CH_2Cl_2$: calcd. C, 50.08; H, 4.80; found C, 50.16; H, 4.66, $^1$H NMR (400 MHz, $CDCl_3$): δ = 10.39 (s, 1H, $SC_6H_4$-*p*-O*H*), 7.54 – 7.44 (m, 2H, $SC_6H_4$-*p*-OH, 4H, $SCH_2C_6H_4$-*p*-F), 7.28 (m, 2H, $SC_6H_4$-*p*-OH), 7.16 (q, 4H, $^3J$ = 9 Hz, $SCH_2C_6H_4$-*p*-F), 5.06 [d, 2H, $^3J$ = 4 Hz, *p*-

$CH_3C_6H_4CH(CH_3)_2$], 4.94 [d, 2H, $^3J$ = 4 Hz, *p*-$CH_3C_6H_4CH(CH_3)_2$], 4.74 [d, $^3J$ = 4 Hz, 4H, *p*-$CH_3C_6H_4CH(CH_3)_2$], 3.57 (s, 2H, $SCH_2C_6H_4$-*p*-F), 3.40 (s, 2H, $SCH_2C_6H_4$-*p*-F), 2.02 [sept, $^3J$ = 7 Hz, 2H, *p*-$CH_3C_6H_4CH(CH_3)_2$], 1.60 [s, 6H, *p*-$CH_3C_6H_4CH(CH_3)_2$], 1.04 [d, $^3J$ = 7 Hz, 6H, *p*-$CH_3C_6H_4CH(CH_3)_2$], 0.98 [d, $^3J$ = 7 Hz, 6H, *p*-$CH_3C_6H_4CH(CH_3)_2$] ppm, $^{13}$C NMR (100 MHz, $CDCl_3$): δ = 160.11, 133.26, 130.90, 130.72, 130.64, 123.42, 117.26, 115.61, 107.58, 99.90, 84.12, 83.65, 83.23, 34.07, 31.00, 23.17, 22.63, 22.29, 17.95, 14.02 ppm.

**Data for [20]Cl:** Yield: 79.9 mg (72%), ESI-MS (MeOH): *m/z* = 1000.70 [$M^+$], $C_{40}H_{45}Br_2ClORu_2S_3$: calcd. C, 46.40; H, 4.38; found C, 43.21; H, 4.24 – possible degradation. $^1$H NMR (400 MHz, $CDCl_3$): δ = 10.48 (s, 1H, $SC_6H_4$-*p*-O*H*), 7.64 – 7.55 (m, 4H, $SCH_2C_6H_4$-*p*-Br), 7.50 – 7.39 (m, 2H, $SC_6H_4$-*p*-OH, 4H, $SCH_2C_6H_4$-*p*-Br), 7.26 (m, 2H,$SC_6H_4$-*p*-OH), 5.07 [d, 2H, $^3J$ = 6 Hz, *p*-$CH_3C_6H_4CH(CH_3)_2$], 4.96 [d, 2H, $^3J$ = 6 Hz, *p*-$CH_3C_6H_4CH(CH_3)_2$], 4.77 [d, $^3J$ = 6 Hz, 4H, *p*-$CH_3C_6H_4CH(CH_3)_2$], 3.56 (s, 2H, $SCH_2C_6H_4$-*p*-Br), 3.39 (s, 2H, $SCH_2C_6H_4$-*p*-Br), 2.00 [sept, $^3J$ = 7 Hz, 2H, *p*-$CH_3C_6H_4CH(CH_3)_2$], 1.63 [s, 6H, *p*-$CH_3C_6H_4CH(CH_3)_2$], 1.04 [d, $^3J$ = 7 Hz, 6H, *p*-$CH_3C_6H_4CH(CH_3)_2$], 0.98 [d, $^3J$ = 7 Hz, 6H, *p*-$CH_3C_6H_4CH(CH_3)_2$] ppm, $^{13}$C NMR (100 MHz, $CDCl_3$): δ = 159.77, 138.88, 133.39, 131.83, 131.70, 131.13, 130.85, 123.88, 121.76, 121.66, 117.03, 107.62, 99.82, 84.21, 83.78, 83.19, 81.98, 39.43, 39.08, 30.91, 23.09, 22.65, 17.95 ppm.

### 9.4.8 Amido Group-Containing Trithiolato Derivatives 21 – 23

**General synthesis for products 21 – 23:** 100 mg of the ruthenium dithiolato precursor were introduced in a Schlenk tube and dissolved in 40 mL of ethanol. 3 equivalents of the 4-aminothiophenol were dissolved in 10 mL of EtOH and introduced dropwise into the Schlenk tube. The reaction mixture was refluxed for 16 hours. Afterwards the solvent was evaporated *in vacuo* and the mixture was separated by column chromatography on silicagel (solvent system $CH_2Cl_2$/EtOH 5 : 1). The orange band was collected, solvent evaporated *in vacuo* and the product was dried under reduced pressure.

**Data for [21]Cl:** Yield: 91 mg (92%), ESI-MS: (MeOH): *m/z* = 869.6 [$M]^+$. $^1$H NMR (400 MHz, $CDCl_3$): δ = 7.45 – 7.36 (m, 2H, *p*-$SC_6H_4NH_2$, 4H, $SC_2H_4C_6H_5$), 7.31 (m, 6H, $SC_2H_4C_6H_5$), 6.63 (d, $^3J$ = 8 Hz, 2H, *p*-$SC_6H_4NH_2$), 5.18 [d, $^3J$ = 6 Hz, 2H, *p*-$CH_3C_6H_4CH(CH_3)_2$], 5.16 [d, $^3J$ = 6 Hz, 2H, *p*-$CH_3C_6H_4CH(CH_3)_2$], 5.11 [d, $^3J$ = 6 Hz, 2H, *p*-$CH_3C_6H_4CH(CH_3)_2$], 5.04 [d, $^3J$ = 6 Hz, 2H, *p*-$CH_3C_6H_4CH(CH_3)_2$], 3.06 (m, 4H, $SC_2H_4C_6H_5$), 2.81 (t, $^3J$ = 7 Hz, 2H, $SC_2H_4C_6H_5$), 2.62 (t,

$^{3}J$ = 7 Hz, 2H, $SC_2H_4C_6H_5$), 2.17 [sept, $^{3}J$ = 7 Hz, 2H, *p*-$CH_3C_6H_4CH(CH_3)_2$], 1.81 [s, 6H, *p*-$CH_3C_6H_4CH(CH_3)_2$], 1.11 – 1.04 [m, 12H, *p*-$CH_3C_6H_4CH(CH_3)_2$] ppm, $^{13}$C NMR (100 MHz, $CDCl_3$): δ = 204.3, 148.47, 139.71, 139.69, 133.41, 128.73, 128.71, 128.61, 128.55, 126.83, 123.28, 115.24, 107.07, 99.91, 84.31, 83.87, 83.26, 82.78, 57.89, 40.36, 39.81, 38.72, 38.63, 30.85, 23.09, 22.55, 18.28, 17.75 ppm.

**Data for [22]Cl:** Yield: 98.2 mg (89%), ESI-MS: (MeOH): *m/z* = 953.2 $[M]^+$. $^1$H NMR (400 MHz, $CDCl_3$): δ = 7.50 – 7.38 (m, 2H, *p*-$SC_6H_4NH_2$, 8H, *p*-$SCH_2C_6H_4$-$Bu^t$), 7.67 (d, $^{3}J$ = 8 Hz, 2H, *p*-$SC_6H_4NH_2$), 5.03 [d, $^{3}J$ = 6 Hz, 2H, *p*-$CH_3C_6H_4CH(CH_3)_2$], 4.92 [d, $^{3}J$ = 6 Hz, 2H, *p*-$CH_3C_6H_4CH(CH_3)_2$], 4.76 [d, $^{3}J$ = 6 Hz, 2H, *p*-$CH_3C_6H_4CH(CH_3)_2$], 4.61 [d, $^{3}J$ = 6 Hz, 2H, *p*-$CH_3C_6H_4CH(CH_3)_2$], 3.56 (s, 2H, *p*-$SCH_2C_6H_4$-$Bu^t$), 3.39 (s, 2H, *p*-$SCH_2C_6H_4$-$Bu^t$), 2.00 [sept, $^{3}J$ = 7 Hz, 2H, *p*-$CH_3C_6H_4CH(CH_3)_2$], 1.72 [s, 6H, *p*-$CH_3C_6H_4CH(CH_3)_2$], 0.99 [d, $^{3}J$ = 6 Hz, 6H, *p*-$CH_3C_6H_4CH(CH_3)_2$], 0.94 [d, $^{3}J$ = 6 Hz, 6H, *p*-$CH_3C_6H_4CH(CH_3)_2$] ppm.

**Data for [23]Cl:** Yield: 80.8 mg (83%), ESI-MS: (MeOH): *m/z* = 842.11 $[M]^+$, $^1$H NMR (400 MHz, $CDCl_3$): δ = 7.57 – 7.34 (m, 2H, *p*-$SC_6H_4NH_2$, 8H, $SCH_2C_6H_5$), 6.66 (d, $^{3}J$ = 8 Hz, 2H, *p*-$SC_6H_4NH_2$), 5.06 [d, $^{3}J$ = 6 Hz, 2H, *p*-$CH_3C_6H_4CH(CH_3)_2$], 4.93 [d, $^{3}J$ = 6 Hz, 2H, *p*-$CH_3C_6H_4CH(CH_3)_2$], 4.73 [d, $^{3}J$ = 6 Hz, 2H, *p*-$CH_3C_6H_4CH(CH_3)_2$], 4.67 [d, $^{3}J$ = 6 Hz, 2H, *p*-$CH_3C_6H_4CH(CH_3)_2$], 3.56 (s, 2H, $SCH_2C_6H_5$), 3.42 (s, 2H, $SCH_2C_6H_5$), 2.00 [sept, $^{3}J$ = 7 Hz, 2H, *p*-$CH_3C_6H_4CH(CH_3)_2$], 1.72 [s, 6H, *p*-$CH_3C_6H_4CH(CH_3)_2$], 1.01 [d, $^{3}J$ = 6 Hz, 6H, *p*-$CH_3C_6H_4CH(CH_3)_2$], 0.95 [d, $^{3}J$ = 6 Hz, 6H, *p*-$CH_3C_6H_4CH(CH_3)_2$] ppm.

### 9.4.9 Carboxylic Acid-Containing Trithiolato Derivatives 24 – 26

**General synthesis for products 24 and 25:** 400 mg of the ruthenium dithiolato precursor were introduced in a Schlenk tube and dissolved in 100 mL of ethanol. 3 equivalents of the 4-mercaptobenzoic acid were dissolved in 20 mL of EtOH and introduced dropwise into the Schlenk tube. The reaction mixture was refluxed for 16 hours. Afterwards the solvent was evaporated *in vacuo* and the mixture was separated by column chromatography on silicagel (solvent system $CH_2Cl_2$/EtOH 5 : 1). The second orange band was collected, solvent evaporated *in vacuo* and the product was dried under reduced pressure.

**Data for [24]Cl:** Yield: 64.6 mg (14%), ESI-MS: (MeOH): *m/z* = 898.11 $[M]^+$. $^1$H NMR (400 MHz, $CDCl_3$): δ = 8.17 (d, $^{3}J$ = 8 Hz, 2H, *p*-$SC_6H_4COOH$), 7.61 (d, $^{3}J$ = 8 Hz, 2H, *p*-

$SC_6H_4COOH$), 7.41 (m, 4H, $SC_2H_5C_6H_5$), 7.32 (m, 6H, $SC_2H_4C_6H_5$), 5.18 [d, $^3J$ = 6 Hz, 2H, *p*-$CH_3C_6H_4CH(CH_3)_2$], 5.12 [d, $^3J$ = 6 Hz, 2H, *p*-$CH_3C_6H_4CH(CH_3)_2$], 5.09 [d, $^3J$ = 6 Hz, 2H, *p*-$CH_3C_6H_4CH(CH_3)_2$], 5.03 [d, $^3J$ = 6 Hz, 2H, *p*-$CH_3C_6H_4CH(CH_3)_2$], 3.06 (m, 4H, $SC_2H_4C_6H_5$), 2.83 (t, $^3J$ = 7 Hz, 2H, $SC_2H_4C_6H_5$), 2.64 (t, $^3J$ = 7 Hz, 2H, $SC_2H_4C_6H_5$), 2.15 [m, 2H, *p*-$CH_3C_6H_4CH(CH_3)_2$], 1.80 [s, 6H, *p*-$CH_3C_6H_4CH(CH_3)_2$], 1.07 [d, $^3J$ = 6 Hz, 6H, *p*-$CH_3C_6H_4CH(CH_3)_2$], 1.07 [d, $^3J$ = 6 Hz, 6H, *p*-$CH_3C_6H_4CH(CH_3)_2$] ppm.

**Data for [25]Cl:** Yield: 49.8 mg (11%), ESI-MS: (MeOH): *m/z* = 871.08 $[M]^+$. $^1$H NMR (400 MHz, $CDCl_3$): δ = 8.21 (d, $^3J$ = 8 Hz, 2H, *p*-$SC_6H_4COOH$), 7.79 (d, $^3J$ = 8 Hz, 2H, *p*-$SC_6H_4COOH$), 7.50 (m, 4H, $SCH_2C_6H_5$), 7.46 – 7.29 (m, 6H, $SCH_2C_6H_5$), 5.12 [d, $^3J$ = 5 Hz, 2H, *p*-$CH_3C_6H_4CH(CH_3)_2$], 5.00 [d, $^3J$ = 5 Hz, 2H, *p*-$CH_3C_6H_4CH(CH_3)_2$], 4.84 [d, $^3J$ = 6 Hz, 2H, *p*-$CH_3C_6H_4CH(CH_3)_2$], 4.71 [d, $^3J$ = 6 Hz, 2H, *p*-$CH_3C_6H_4CH(CH_3)_2$], 3.62 (s, 2H, $SCH_2C_6H_5$), 3.44 (s, 2H, $SCH_2C_6H_5$), 1.96 [sept, $^3J$ = 6 Hz, 2H, *p*-$CH_3C_6H_4CH(CH_3)_2$], 1.67 [s, 6H, *p*-$CH_3C_6H_4CH(CH_3)_2$], 0.96 [d, $^3J$ = 6 Hz, 6H, *p*-$CH_3C_6H_4CH(CH_3)_2$], 0.89 [d, $^3J$ = 6 Hz, 6H, *p*-$CH_3C_6H_4CH(CH_3)_2$] ppm.

**Synthesis and data for product [26]Cl:** 0.327 mmol of the ruthenium *p*-cymene dichloride dimer were introduced in a Schlenk tube and dissolved in 130 mL of distilled ethanol. 1.96 mmol of the 4-mercaptobenzoic acid were dissolved in 20 mL of distilled EtOH and introduced dropwise into the Schlenk tube. The reaction mixture was refluxed for 16 hours. Afterwards the solvent was evaporated *in vacuo* and the mixture was separated by column chromatography on silicagel (solvent system $CH_2Cl_2$/EtOH 1 : 1 with 0.1% of HCOOH). The red band was collected, solvent evaporated *in vacuo* and the product was recrystallized from MeOH/$Et_2O$ mixture. Resulting orange crystals were collected by filtration and dried under reduced pressure. Yield: 300 mg (95%), ESI-MS: (MeOH): *m/z* = 930.9 $[M]^+$. $C_{41}H_{43}ClO_6Ru_2S_3 \cdot 0.75H_2O$ (979.07): calcd. C, 50.30; H, 4.58; found C, 50.25; H, 4.66. $^1$H NMR (400 MHz, $CDCl_3$): δ = 8.01 (d, $^3J$ = 8 Hz, 6H, *p*-$SC_6H_4COOH$), 7.94 (d, $^3J$ = 8 Hz, 6H, *p*-$SC_6H_4COOH$), 5.83 [d, $^3J$ = 5 Hz, 2H, *p*-$CH_3C_6H_4CH(CH_3)_2$], 5.60 [d, $^3J$ = 5 Hz, 2H, *p*-$CH_3C_6H_4CH(CH_3)_2$], 5.43 [d, $^3J$ = 5 Hz, 2H, *p*-$CH_3C_6H_4CH(CH_3)_2$], 5.39 [d, $^3J$ = 5 Hz, 2H, *p*-$CH_3C_6H_4CH(CH_3)_2$], 1.91 [sept, $^3J$ = 7 Hz, 2H, *p*-$CH_3C_6H_4CH(CH_3)_2$], 1.55 [s, 6H, *p*-$CH_3C_6H_4CH(CH_3)_2$], 0.80 [d, $^3J$ = 6 Hz, 6H, *p*-$CH_3C_6H_4CH(CH_3)_2$], 0.67 [d, $^3J$ = 5 Hz, 6H, *p*-$CH_3C_6H_4CH(CH_3)_2$] ppm, $^{13}$C NMR (100 MHz, $CDCl_3$): δ = 167.38, 144.12, 133.22, 130.20, 130.04, 107.40, 100.60, 85.79, 85.02, 84.25, 30.75, 22.64, 21.64, 17.54 ppm.

### 9.4.1 Propargyl Derivatives 31 – 34

**General procedure for the synthesis of 31 – 34:** 0.052 mmol of the starting trithiolato complex was dissolved in DMF. The solution of propargyl bromide (30 equivalents) was added to this solution, followed by 30 equivalents of potassium carbonate. The suspension was stirred at room temperature for 3 days, after which the solvent was evaporated, the mixture redissolved in dichloromethane, filtered and the product was separated by the column chromatography on silica gel (solvent system dichloromethane/acetone 7 : 1). The product eluted in the second orange band. After the evaporation of the solvent, the resulting orange powder was washed with pentane and dried *in vacuo*.

**Data for [31][$BF_4$]:** Yield: 28.7 mg (57%), ESI-MS (MeOH): *m/z* = 879.90 $[M]^+$. IR: 2110.5 $cm^{-1}$ C≡C stretch, $C_{43}H_{49}BF_4ORu_2S_3$: calcd. C, 53.41; H, 5.11; found C, 53.36, H, 5.12. $^1$H NMR (400 MHz, $CDCl_3$): δ = 7.74 (d, 2H, $^3J$ = 8 Hz, $SC_6H_4$-*p*-$OCH_2CCH$), 7.54 (t, $^3J$ = 8 Hz, 4H, $SCH_2C_6H_5$), 7.35 – 7.05 (m, 6H, $SCH_2C_6H_5$), 6.96 (d, 2H, $^3J$ = 8 Hz, $SC_6H_4$-*p*-$OCH_2CCH$), 5.16 [d, 2H, $^3J$ = 6 Hz, *p*-$CH_3C_6H_4CH(CH_3)_2$], 5.03 [d, 2H, $^3J$ = 6 Hz, *p*-$CH_3C_6H_4CH(CH_3)_2$], 4.87 [d, 2H, $^3J$ = 6 Hz, *p*-$CH_3C_6H_4CH(CH_3)_2$], 4.74 [m, 2H, *p*-$CH_3C_6H_4CH(CH_3)_2$, 2H, $SC_6H_4$-*p*-$OCH_2CCH$], 3.66 (s, 2H, $SCH_2C_6H_5$), 3.50 (s, 2H, $SCH_2C_6H_5$), 2.56 (t, 1H, $^3J$ = 2 Hz, $SC_6H_4$-*p*-$OCH_2CCH$), 1.93 [sept, $^3J$ = 7 Hz, 2H, *p*-$CH_3C_6H_4CH(CH_3)_2$], 1.75 [s, 6H, *p*-$CH_3C_6H_4CH(CH_3)_2$], 0.98 [d, $^3J$ = 7 Hz, 6H, *p*-$CH_3C_6H_4CH(CH_3)_2$], 0.92 [d, $^3J$ = 7 Hz, 6H, *p*-$CH_3C_6H_4CH(CH_3)_2$] ppm, $^{13}$C NMR (100 MHz, $CDCl_3$): δ = 157.86, 139.82, 139.76, 133.90, 129.52, 129.36, 128.74, 128.56, 128.13, 128.01, 115.47, 107.05, 100.02, 83.89, 83.80, 83.71, 82.34, 78.02, 77.28, 77.17, 76.97, 76.65, 75.86, 56.04, 40.15, 39.87, 30.84, 23.16, 22.47, 18.05 ppm.

**Data for [32][$BF_4$]:** Yield: 21.2 mg (41%), ESI-MS (MeOH): *m/z* = 908.60 $[M]^+$. IR: 2118.7 $cm^{-1}$ C≡C stretch, $C_{45}H_{53}BF_4ORu_2S_3$: calcd. C, 54.32; H, 5.37; found C, 54.54; H, 5.37, $^1$H NMR (400 MHz, $CDCl_3$): δ = 7.65 (d, 2H, $^3J$ = 8 Hz, $SC_6H_4$-*p*-$OCH_2CCH$), 7.43 – 7.27 (m, 6H, $SC_2H_4C_6H_5$), 6.92 (d, 2H, $^3J$ = 8 Hz, $SC_6H_4$-*p*-$OCH_2CCH$), 5.23 – 5.17 [m, 4H, *p*-$CH_3C_6H_4CH(CH_3)_2$], 5.15 [d, 2H, $^3J$ = 6 Hz, *p*-$CH_3C_6H_4CH(CH_3)_2$], 5.09 [d, 2H, $^3J$ = 6 Hz, *p*-$CH_3C_6H_4CH(CH_3)_2$], 4.74 [d, 2H, $^3J$ = 2 Hz, $SC_6H_4$-*p*-$OCH_2CCH$], 3.12 – 3.02 (m, 4H, $SC_2H_4C_6H_5$), 2.86 (t, 2H, $^3J$ = 7 Hz, $SC_2H_4C_6H_5$), 2.63 (t, 2H, $^3J$ = 7 Hz, $SC_2H_4C_6H_5$), 2.56 (t, 1H, $^3J$ = 2 Hz, $SC_6H_4$-*p*-$OCH_2CCH$), 2.10 [sept, $^3J$ = 7 Hz, 2H, *p*-$CH_3C_6H_4CH(CH_3)_2$], 1.81 [s, 6H, *p*-$CH_3C_6H_4CH(CH_3)_2$], 1.05 [t, $^3J$ = 7 Hz, 12H, *p*-$CH_3C_6H_4CH(CH_3)_2$] ppm, $^{13}$C NMR (100 MHz, $CDCl_3$): δ = 157.85,

139.86, 133.83, 129.83, 128.81, 126.80, 115.36, 106.97, 100.22, 84.25, 83.85, 83.73, 83.09, 55.97, 40.96, 39.99, 38.66, 38.59, 30.87, 23.15, 22.44, 17.76 ppm.

**Data for [33][$BF_4$]:** Yield: 40.4 mg (72%), ESI-MS (MeOH): *m/z* = 993.0 $[M]^+$. IR: 2119 $cm^{-1}$ C≡C stretch, $C_{51}H_{65}BF_4ORu_2S_3 \cdot 0.1\ C_5H_{12}$: calcd. C, 56.94; H, 6.14; found C, 57.15; H, 5.94. $^1H$ NMR (400 MHz, $CDCl_3$): δ = 7.72 (d, 2H, $^3J$ = 8 Hz, $SC_6H_4$-*p*-$OCH_2CCH$), 7.52 – 7.40 [m, 8H, $SCH_2C_6H_4$-*p*-$C(CH_3)_3$], 6.95 (d, 2H, $^3J$ = 8 Hz, $SC_6H_4$-*p*-$OCH_2CCH$), 5.09 [d, 2H, $^3J$ = 6 Hz, *p*-$CH_3C_6H_4CH(CH_3)_2$], 4.96 [d, 2H, $^3J$ = 6 Hz, *p*-$CH_3C_6H_4CH(CH_3)_2$], 4.86 [d, 2H, $^3J$ = 6 Hz, *p*-$CH_3C_6H_4CH(CH_3)_2$], 4.74 [d, 2H, $^3J$ = 2 Hz, $SC_6H_4$-*p*-$OCH_2CCH$], 4.59 [d, 2H, $^3J$ = 6 Hz, *p*-$CH_3C_6H_4CH(CH_3)_2$], 3.60 (s, 2H, $SCH_2C_6H_4$-*p*- $C(CH_3)_3$), 3.40 (s, 2H, $SCH_2C_6H_4$-*p*- $C(CH_3)_3$), 2.56 (t, 1H, $^3J$ = 2 Hz, $SC_6H_4$-*p*-$OCH_2CCH$), 1.89 [sept, $^3J$ = 7 Hz, 2H, *p*-$CH_3C_6H_4CH(CH_3)_2$], 1.74 [s, 6H, *p*-$CH_3C_6H_4CH(CH_3)_2$], 1.35 [d, 18H, $^3J$ = 12 Hz, $SCH_2C_6H_4$-*p*-$C(CH_3)_3$], 0.94 [d, $^3J$ = 7 Hz, 6H, *p*-$CH_3C_6H_4CH(CH_3)_2$], 0.90 [d, $^3J$ = 7 Hz, 6H, *p*-$CH_3C_6H_4CH(CH_3)_2$] ppm, $^{13}C$ NMR (100 MHz, $CDCl_3$): δ = 157.83, 151.64, 136.70, 133.87, 129.44, 129.25, 129.07, 125.49, 125.30, 115.44, 106.85, 100.34, 84.00, 83.61, 83.55, 82.37, 56.05, 34.74, 34.70, 31.38, 30.77, 23.05, 22.60, 18.13 ppm.

**Data for [34][$BF_4$]:** Yield: 32.1 mg (60%), ESI-MS (MeOH): *m/z* = 940.9 $[M]^+$. IR: 2117.7 $cm^{-1}$ C≡C stretch, $C_{45}H_{53}BF_4O_3Ru_2S_3$: calcd. C, 52.63; H, 5.20; found C, 52.58; H, 5.41. $^1H$ NMR (400 MHz, $CDCl_3$): δ = 7.72 (d, 2H, $^3J$ = 8 Hz, $SC_6H_4$-*p*-$OCH_2CCH$), 7.44 (t, 4H, $SCH_2C_6H_4$-*p*-$OCH_3$), 7.00 (d, 2H, $^3J$ = 8 Hz, $SC_6H_4$-*p*-$OCH_2CCH$), 6.95 (t, 4H, $SCH_2C_6H_4$-*p*-$OCH_3$), 5.11 [d, 2H, $^3J$ = 6 Hz, *p*-$CH_3C_6H_4CH(CH_3)_2$], 4.99 [d, 2H, $^3J$ = 6 Hz, *p*-$CH_3C_6H_4CH(CH_3)_2$], 4.84 [d, 2H, $^3J$ = 6 Hz, *p*-$CH_3C_6H_4CH(CH_3)_2$], 4.74 [m, 4H, *p*-$CH_3C_6H_4CH(CH_3)_2$, 2H, $SC_6H_4$-*p*-$OCH_2CCH$], 3.87 (d, 6H, $^3J$ = 10 Hz, $SCH_2C_6H_4$-*p*-$OCH_3$), 3.57 (s, 2H, $SCH_2C_6H_4$-*p*-$OCH_3$), 3.38 (s, 2H, $SCH_2C_6H_4$-*p*-$OCH_3$), 2.56 (t, 1H, $^3J$ = 2 Hz, $SC_6H_4$-*p*-$OCH_2CCH$), 1.93 [sept, $^3J$ = 7 Hz, 2H, *p*-$CH_3C_6H_4CH(CH_3)_2$], 1.74 [s, 6H, *p*-$CH_3C_6H_4CH(CH_3)_2$], 0.99 [d, $^3J$ = 7 Hz, 6H, *p*-$CH_3C_6H_4CH(CH_3)_2$], 0.93 [d, $^3J$ = 7 Hz, 6H, *p*-$CH_3C_6H_4CH(CH_3)_2$] ppm, $^{13}C$ NMR (100 MHz, $CDCl_3$): δ = 159.45, 159.33, 157.81, 133.88, 131.69, 130.60, 130.40, 115.38, 114.01, 113.85, 106.97, 99.96, 83.71, 83.60, 82.28, 55.99, 55.51, 55.45, 39.51, 39.23, 30.86, 23.15, 22.42, 17.99 ppm.

### 9.4.1 Ibuprofen Conjugates 35 – 38

**General procedure for the synthesis of complexes 35 – 38:** All the ibuprofen conjugates were synthesized using standard Schlenk techniques. The dinuclear trithiolato complex (0.314 mmol),

(±)-ibuprofen (2.0 eq.) and DMAP (1.0 eq.) were dissolved in distilled $CH_2Cl_2$ (4 mL). A solution of DCC (2.0 eq.) in the distilled $CH_2Cl_2$ (3 mL) was added dropwise and the reaction was stirred at room temperature for 16 hours. The solvent was removed under reduced pressure and the mixture was redissolved in cold acetonitrile. The white precipitate was filtered off by a syringe filter (PTFE, 0.22 µm) and the filtrate was evaporated and chromatographed on silica (solvent system $CH_2Cl_2$/Acetone 7 : 1). The main orange band was collected, the solvent evaporated to dryness and the solid was washed several times with pentane and dried *in vacuo*.

**Data for [35][$BF_4$]:** Yield: 27.7 mg (79%), ESI-MS (MeOH/$CH_2Cl_2$): *m/z* = 1031.5 $[M]^+$. $C_{53}H_{63}BF_4O_2Ru_2S_3$: calcd. C, 56.98; H, 5.68, found C, 57.12; H, 5.72. $^1$H NMR (400 MHz, $CDCl_3$): δ = 7.78 (d, $^3J$ = 8 Hz, 2H, $SC_6H_4$-*p*-O), 7.57 – 7.35 [m, 10H, $SCH_2C_6H_5$], 7.31 [d, $^3J$ = 8 Hz, 2H, $OCC(CH_3)C_6H_4CH_2CH(CH_3)_2$], 7.18 [d, $^3J$ = 8 Hz, 2H, $OCC(CH_3)C_6H_4CH_2CH(CH_3)_2$], 6.97 (d, $^3J$ = 8 Hz, 2H, $SC_6H_4$-*p*-O), 5.12 [d, $^3J$ = 6 Hz, 2H, *p*-$CH_3C_6H_4CH(CH_3)_2$], 4.98 [d, $^3J$ = 6 Hz, 2H, *p*-$CH_3C_6H_4CH(CH_3)_2$], 4.82 [t, $^3J$ = 6 Hz, 2H, *p*-$CH_3C_6H_4CH(CH_3)_2$], 4.70 [d, $^3J$ = 6 Hz, 2H, *p*-$CH_3C_6H_4CH(CH_3)_2$], 3.96 [q, $^3J$ = 7 Hz, 1H, $OCCH(CH_3)C_6H_4CH_2CH(CH_3)_2$], 3.65 [s, 2H, $SCH_2C_6H_5$], 3.45 [s, 2H, $SCH_2C_6H_5$], 2.49 [d, $^3J$ = 7 Hz, 2H, $OCCH(CH_3)C_6H_4CH_2CH(CH_3)_2$], 1.90 [m, 2H, *p*-$CH_3C_6H_4CH(CH_3)_2$; 1H, $OCCH(CH_3)C_6H_4CH_2CH(CH_3)_2$], 1.73 [s, 6H, *p*-$CH_3C_6H_4$-$CH(CH_3)_2$], 1.62 [d, $^3J$ = 7 Hz, 3H, $OCCH(CH_3)C_6H_4CH_2CH(CH_3)_2$], 0.98 [d, $^3J$ = 7 Hz, 6H, $OCCH(CH_3)C_6H_4CH_2CH(CH_3)_2$], 0.92 [m, 12H, *p*-$CH_3C_6H_4CH(CH_3)_2$] ppm. $^{13}$C NMR (100 MHz, $CDCl_3$): δ = 204.31, 173.01, 151.14, 140.91, 139.72, 136.99, 133.53, 129.55, 129.33, 128.75, 128.58, 128.12, 128.02, 127.15, 122.15, 107.24, 100.13, 83.81, 82.40, 45.19, 40.09, 30.88, 30.15, 25.36, 23.12, 22.44, 22.37, 18.51, 17.97, 15.23 ppm.

**Data for [36][$BF_4$]:** Yield: 25.8 mg (72%), ESI-MS (MeOH/$CH_2Cl_2$): *m/z* = 1058.8 $[M]^+$. $C_{55}H_{67}BF_4O_2Ru_2S_3$: calcd. C, 57.68; H, 5.90, found C, 57.43; H, 5.92. $^1$H NMR (400 MHz, $CDCl_3$): δ = 7.69 (d, $^3J$ = 8 Hz, 2H, $SC_6H_4$-*p*-O), 7.43 – 7.28 [m, 10H, $SC_2H_4C_6H_5$; 2H, $OCCH(CH_3)C_6H_4CH_2CH(CH_3)_2$], 7.18 [d, $^3J$ = 8 Hz, 2H, $OCC(CH_3)C_6H_4CH_2CH(CH_3)_2$], 6.94 (d, $^3J$ = 8 Hz, 2H, $SC_6H_4$-*p*-O), 5.20 [m, 2H, *p*-$CH_3C_6H_4CH(CH_3)_2$], 5.18 – 5.10 [m, 4H, *p*-$CH_3C_6H_4$-$CH(CH_3)_2$], 5.07 [m, 2H, *p*-$CH_3C_6H_4CH(CH_3)_2$], 3.96 [q, $^3J$ = 7 Hz, 1H, $OCCH(CH_3)C_6H_4CH_2CH(CH_3)_2$], 3.13 – 3.00 (m, 4H, $SC_2H_4C_6H_5$), 2.87 (t, $^3J$ = 7 Hz, 2H, $SC_2H_4C_6H_5$), 2.64 (t, $^3J$ = 7 Hz, 2H, $SC_2H_4C_6H_5$), 2.49 [d, $^3J$ = 7 Hz, 2H, $OCCH(CH_3)C_6H_4CH_2CH(CH_3)_2$], 2.07 [sept, $^3J$ = 7 Hz, 2H, *p*-$CH_3C_6H_4CH(CH_3)_2$], 1.89 [sept, $^3J$ = 7 Hz, 1H, $OCCH(CH_3)C_6H_4CH_2CH(CH_3)_2$], 1.81 [s, 6H, *p*-$CH_3C_6H_4CH(CH_3)_2$], 1.62 [d, $^3J$ = 7 Hz, 3H, $OCCH(CH_3)C_6H_4CH_2CH(CH_3)_2$], 1.04 [t, $^3J$ = 7 Hz, 12H, *p*-$CH_3C_6H_4CH(CH_3)_2$], 0.93 [d, $^3J$ =

7 Hz, 6H, OCCH($CH_3$)$C_6H_4CH_2CH(CH_3)_2$] ppm. $^{13}$C NMR (100 MHz, $CDCl_3$): δ = 204.30, 173.01, 151.08, 140.39, 139.87, 136.96, 135.49, 133.48, 129.55, 128.86, 128.79, 128.75, 128.72, 127.15, 126.80, 122.01, 107.12, 100.28, 84.27, 84.01, 83.83, 83.14, 58.43, 45.19, 45.01, 41.17, 40.19, 38.63, 38.54, 30.88, 30.16, 23.15, 22.41, 22.37, 18.49, 17.77 ppm.

**Data for [37][$BF_4$]:** Yield: 24.7 mg (64%), ESI-MS ($MeOH/CH_2Cl_2$): *m/z* = 1143.7 $[M]^+$. $C_{61}H_{79}BF_4O_2Ru_2S_3$: calcd. C, 59.59; H, 6.48, found C, 59.77; H, 6.73. $^1$H NMR (400 MHz, $CDCl_3$): δ = 7.77 (d, $^3J$ = 8 Hz, 2H, $SC_6H_4$-*p*-O), 7.44 [m, 8H, $SCH_2C_6H_4$-*p*-$C(CH_3)_3$], 7.31 [d, $^3J$ = 8 Hz, 2H, $OCC(CH_3)C_6H_4CH_2CH(CH_3)_2$], 7.17 [d, $^3J$ = 8 Hz, 2H, $OCC(CH_3)C_6H_4CH_2CH(CH_3)_2$], 6.97 (d, $^3J$ = 8 Hz, 2H, $SC_6H_4$-*p*-O), 5.09 [d, $^3J$ = 6 Hz, 2H, *p*-$CH_3C_6H_4CH(CH_3)_2$], 4.97 [d, $^3J$ = 6 Hz, 2H, *p*-$CH_3C_6H_4CH(CH_3)_2$], 4.86 [m, 2H, *p*-$CH_3C_6H_4CH(CH_3)_2$], 4.61 [d, $^3J$ = 6 Hz, 2H, *p*-$CH_3C_6H_4CH(CH_3)_2$], 3.96 [q, $^3J$ = 7 Hz, 1H, $OCCH(CH_3)C_6H_4CH_2CH(CH_3)_2$], 3.60 [s, 2H, $SCH_2C_6H_4$-*p*-$C(CH_3)_3$], 3.40 [s, 2H, $SCH_2C_6H_4$-*p*-$C(CH_3)_3$], 2.49 [d, $^3J$ = 7 Hz, 2H, $OCCH(CH_3)C_6H_4CH_2CH(CH_3)_2$], 1.89 [m, 2H, *p*-$CH_3C_6H_4CH(CH_3)_2$; 1H, $OCCH(CH_3)C_6H_4CH_2CH(CH_3)_2$], 1.73 [s, 6H, *p*-$CH_3C_6H_4CH(CH_3)_2$], 1.62 [d, $^3J$ = 7 Hz, 3H, $OCCH(CH_3)C_6H_4CH_2CH(CH_3)_2$], 0.99 – 0.82 [m, 12H, *p*-$CH_3C_6H_4CH(CH_3)_2$; 6H, $OCCH(CH_3)C_6H_4CH_2CH(CH_3)_2$] ppm. $^{13}$C NMR (100 MHz, $CDCl_3$): δ = 204.30, 173.02, 151.62, 151.49, 151.11, 140.91, 136.99, 136.65, 135.00, 133.47, 129.55, 129.25, 129.03, 127.15, 125.50, 125.32, 122.12, 107.06, 100.43, 83.97, 83.89, 83.63, 83.60, 82.40, 45.18, 45.01, 39.85, 39.40, 34.73, 34.68, 33.46, 31.38, 30.79, 30.15, 25.44, 24.78, 22.97, 22.57, 22.37, 18.50, 18.02 ppm.

**Data for [38][$BF_4$]:** Yield: 26.9 mg (73%), ESI-MS ($MeOH/CH_2Cl_2$): *m/z* = 1091.5 $[M]^+$. $C_{55}H_{67}BF_4O_4Ru_2S_3 \cdot 0.75C_5H_{12}$: calcd. C, 57.31; H, 6.22, found C, 57.43; H, 6.17. $^1$H NMR (400 MHz, $CDCl_3$): δ = 7.76 (d, $^3J$ = 8 Hz, 2H, $SC_6H_4$-*p*-O), 7.43 [m, 4H, $SCH_2C_6H_4$-*p*-$OCH_3$], 7.31 [d, $^3J$ = 8 Hz, 2H, $OCC(CH_3)C_6H_4CH_2CH(CH_3)_2$], 7.17 [d, $^3J$ = 8 Hz, 2H, $OCC(CH_3)C_6H_4CH_2CH(CH_3)_2$], 7.00 (d, $^3J$ = 8 Hz, 2H, $SC_6H_4$-*p*-O), 6.95 [m, 4H, $SCH_2C_6H_4$-*p*-$OCH_3$], 5.17 [d, $^3J$ = 6 Hz, 2H, *p*-$CH_3C_6H_4CH(CH_3)_2$], 4.99 [d, $^3J$ = 6 Hz, 2H, *p*-$CH_3C_6H_4CH(CH_3)_2$], 4.83 [m, 2H, *p*-$CH_3C_6H_4CH(CH_3)_2$], 4.75 [d, $^3J$ = 6 Hz, 2H, *p*-$CH_3C_6H_4CH(CH_3)_2$], 3.95 [q, $^3J$ = 7 Hz, 1H, $OCCH(CH_3)C_6H_4CH_2CH(CH_3)_2$], 3.86 [d, 6H, $^3J$ = 10 Hz, $SCH_2C_6H_4$-*p*-$OCH_3$], 3.56 [s, 2H, $SCH_2C_6H_4$-*p*-$OCH_3$], 3.37 [s, 2H, $SCH_2C_6H_4$-*p*-$OCH_3$], 2.49 [d, $^3J$ = 7 Hz, 2H, $OCCH(CH_3)C_6H_4CH_2CH(CH_3)_2$], 1.89 [m, 2H, *p*-$CH_3C_6H_4CH(CH_3)_2$; 1H, $OCCH(CH_3)C_6H_4CH_2CH(CH_3)_2$], 1.73 [s, 6H, *p*-$CH_3C_6H_4CH(CH_3)_2$], 1.62 [d, $^3J$ = 7 Hz, 3H, $OCCH(CH_3)C_6H_4CH_2CH(CH_3)_2$], 0.98 [d, $^3J$ = 7 Hz, 6H, $OCCH(CH_3)C_6H_4CH_2CH(CH_3)_2$], 0.92 [m, 12H, *p*-$CH_3C_6H_4CH(CH_3)_2$] ppm. $^{13}$C NMR (100 MHz, $CDCl_3$): δ = 204.31, 173.00, 159.34,

151.10, 140.91, 136.99, 133.49, 131.59, 130.62, 130.38, 129.55, 127.15, 122.09, 114.04, 113.87, 107.23, 107.19, 99.97, 99.92, 83.75, 82.33, 55.51, 45.19, 45.01, 39.56, 33.27, 30.89, 30.15, 23.11, 22.43, 22.40, 18.51, 17.97 ppm.

### 9.4.2 Chlorambucil Conjugates 39 – 43

**General Procedure for the Synthesis of 39 – 43:** In a Schlenk tube, 30 mg of [($\eta^6$-*p*-$MeC_6H_4{}^{i}Pr)_2Ru_2(SCH_2R)_2(SC_6H_4$-*p*-OH)]Cl (R = Ph 0.032 mmol, R = $CH_2Ph$ 0.032 mmol, R = $C_6H_4$-*p*-$^{t}$Bu 0.029 mmol, R = $C_6H_4$-*p*-OMe 0.030 mmol) were dissolved in distilled dichloromethane (10 mL), 10 equivalents of $NaBF_4$ were added, and the mixture was stirred at room temperature for 12 hours. Then the solution was filtered through a syringe filter (0.22 µm), passed through a small plug of silica gel (solvent system $CH_2Cl_2$/acetone 7 : 1) and transferred into another Schlenk tube containing a solution of chlorambucil (2.0 equivalents) and 4-(dimethyl-amino)pyridine (1.0 equivalent) in $CH_2Cl_2$ (5 mL). A solution of dicyclohexylcarbodiimide (2.0 molar equivalents) in the $CH_2Cl_2$ (5 mL) was added dropwise to this mixture. The reaction was stirred at room temperature under nitrogen atmosphere for 16 hours. The solvent was then removed under reduced pressure, the residue dissolved in cold acetonitrile, filtered through a syringe filter, evaporated to dryness and chromatographed on silica gel (solvent system $CH_2Cl_2$/acetone 7 : 1). The first orange band was collected and evaporated to give the products as orange powders. Product **43** required a thorough washing with pentane to remove all the remaining impurities.

**Data for [39][$BF_4$]:** Yield: 29.7 mg (84%), ESI-MS (MeOH/ $CH_2Cl_2$): *m/z* = 1128.4 $[M]^+$. $C_{54}H_{64}BCl_2F_4NO_2Ru_2S_3 \cdot 0.75CH_2Cl_2$: calcd. C 51.42; H 5.16; N 1.10; found C 51.64; H 5.18; N 1.15. $^1$H NMR (400 MHz, $CDCl_3$): δ = 7.82 (d, $^3J$ = 8 Hz, 2H, $SC_6H_4$-*p*-O), 7.59 – 7.35 (m, 10H, $SCH_2C_6H_5$), 7.15 [d, $^3J$ = 8 Hz, 2H, $OCC_3H_6$-*p*-$C_6H_4N(C_2H_4Cl)_2$ ], 7.05 (d, 2H, $^3J$ = 8 Hz, *p*-$SC_6H_4O$), 6.76 [d, $^3J$ = 8 Hz, 2H, $OCC_3H_6$-*p*-$C_6H_4N(C_2H_4Cl)_2$], 5.15 [d, $^3J$ = 5 Hz, 2H, , *p*-$CH_3C_6H_4CH(CH_3)_2$], 4.99 [d, $^3J$ = 5 Hz, 2H, *p*-$CH_3C_6H_4CH(CH_3)_2$], 4.86 [d, $^3J$ = 5 Hz, 2H, *p*-$CH_3C_6H_4CH(CH_3)_2$], 4.71 [d, $^3J$ = 5 Hz, 2H, *p*-$CH_3C_6H_4CH(CH_3)_2$], 3.75 [m, 4H, $OCC_3H_6$-*p*-$C_6H_4N(C_2H_4Cl)_2$], 3.66 [m, 4H, $OCC_3H_6$-*p*-$C_6H_4N(C_2H_4Cl)_2$, 2H, $SCH_2C_6H_5$], 3.46 (s, 2H, $SCH_2C_6H_5$), 2.68 [t, $^3J$ = 7 Hz, 2H, $OCC_3H_6$-*p*-$C_6H_4N(C_2H_4Cl)_2$], 2.59 [t, $^3J$ = 7 Hz, 2H, $OCC_3H_6$-*p*-$C_6H_4N(C_2H_4Cl)_2$], 2.05 [quint, $^3J$ = 7 Hz, 2H, $OCC_3H_6$-*p*-$C_6H_4N(C_2H_4Cl)_2$], 1.92 [sept, $^3J$ = 7 Hz, 2H, *p*-$CH_3C_6H_4CH(CH_3)_2$], 1.76 [s, 6H, *p*-$CH_3C_6H_4CH(CH_3)_2$], 0.99 [d, $^3J$ = 7 Hz, 6H, *p*-$CH_3C_6H_4$-$CH(CH_3)_2$], 0.92 [d, $^3J$ = 7 Hz, 6H, *p*-$CH_3C_6H_4CH(CH_3)_2$] ppm, $^{13}$C NMR (100 MHz, $CDCl_3$): δ =

150.96, 139.73, 133.59, 129.93, 129.53, 129.35, 128.77, 128.61, 128.15, 122.30, 107.06, 100.27, 84.11, 83.62, 82.46, 40.09, 39.91, 30.88, 23.20, 22.36, 18.00 ppm.

**Data for [40][$BF_4$]:** Yield: 31.5 mg (81%), ESI-MS (MeOH/$CH_2Cl_2$): *m/z* = 1158.0 $[M]^+$. $C_{56}H_{68}BCl_2F_4NO_2Ru_2S_3$: calcd. C 54.10; H 5.51; N 1.13; found C 53.71; H 5.53; N 1.23. $^1$H NMR (400 MHz, $CDCl_3$): δ = 7.73 (d, $^3J$ = 8 Hz, 2H, $SC_6H_4$-*p*-O), 7.45 – 7.27 (m, 10H, $SC_2H_4C_6H_5$), 7.13 [d, $^3J$ = 8 Hz, 2H, $OCC_3H_6$-*p*-$C_6H_4N(C_2H_4Cl)_2$ ], 7.01 (d, 2H, $^3J$ = 8 Hz, $SC_6H_4$-*p*-O), 6.68 [d, $^3J$ = 8 Hz, 2H, $OCC_3H_6$-*p*-$C_6H_4N(C_2H_4Cl)_2$], 5.23 [d, $^3J$ = 5 Hz, 2H, , *p*-$CH_3C_6H_4CH(CH_3)_2$], 5.19 [d, $^3J$ = 5 Hz, 2H, *p*-$CH_3C_6H_4CH(CH_3)_2$], 5.15 [d, $^3J$ = 5 Hz, 2H, *p*-$CH_3C_6H_4CH(CH_3)_2$], 5.10 [d, $^3J$ = 5 Hz, 2H, *p*-$CH_3C_6H_4CH(CH_3)_2$], 3.72 [m, 4H, $OCC_3H_6$-*p*-$C_6H_4N(C_2H_4Cl)_2$], 3.65 [m, 4H, $OCC_3H_6$-*p*-$C_6H_4N(C_2H_4Cl)_2$, 2H, $SCH_2C_6H_5$], 3.08 (m, 4H, $SC_2H_4C_6H_5$), 2.88 (m, 2H, $SC_2H_4C_6H_5$), 2.66, [m, 4H, $OCC_3H_6$-*p*-$C_6H_4N(C_2H_4Cl)_2$], 2.59 (t, $^3J$ = 8 Hz, 2H, $SC_2H_4C_6H_5$), 2.06 [m, 2H, $OCC_3H_6$-*p*-$C_6H_4N(C_2H_4Cl)_2$, 2H, *p*-$CH_3C_6H_4CH(CH_3)_2$], 1.83 [s, 6H, *p*-$CH_3C_6H_4CH$-$(CH_3)_2$], 1.05 [t, $^3J$ = 7 Hz, 12H, *p*-$CH_3C_6H_4CH(CH_3)_2$] ppm, $^{13}$C NMR (100 MHz, $CDCl_3$): δ = 171.72, 150.92, 139.85, 133.53, 129.75, 128.85, 128.77, 128.72, 126.82, 122.15, 112.49, 107.03, 100.37, 84.18, 83.95, 83.19, 41.17, 40.41, 40.19, 38.67, 38.55, 33.87, 33.54, 30.88, 26.51, 23.21, 22.38, 17.80 ppm.

**Data for [41][$BF_4$]:**. Yield: 28.0 mg (79%), ESI-MS (MeOH/$CH_2Cl_2$): *m/z* = 1240.6 $[M]^+$. $C_{62}H_{80}BCl_2F_4NO_2Ru_2S_3$: calcd. C 56.10; H 6.07; N 1.06; found C 56.19; H 6.17; N 1.05. $^1$H NMR (400 MHz, $CDCl_3$): δ = 7.80 (d, $^3J$ = 8 Hz, 2H, $SC_6H_4$-*p*-O), 7.45 [m, 8H, $SCH_2C_6H_4$-*p*-$C(CH_3)_3$], 7.14 [d, $^3J$ = 8 Hz, 2H, $OCC_3H_6$-*p*-$C_6H_4N(C_2H_4Cl)_2$ ], 7.04 (d, $^3J$ = 8 Hz, 2H, $SC_6H_4$-*p*-O), 6.73 [d, $^3J$ = 8 Hz, 2H, $OCC_3H_6$-*p*-$C_6H_4N(C_2H_4Cl)_2$], 5.11 [d, $^3J$ = 6 Hz, 2H, , *p*-$CH_3C_6H_4CH(CH_3)_2$], 4.97 [d, $^3J$ = 6 Hz, 2H, *p*-$CH_3C_6H_4CH(CH_3)_2$], 4.89 [d, $^3J$ = 6 Hz, 2H, *p*-$CH_3C_6H_4CH(CH_3)_2$], 4.60 [d, $^3J$ = 6 Hz, 2H, *p*-$CH_3C_6H_4CH(CH_3)_2$], 3.74 [m, 4H, $OCC_3H_6$-*p*-$C_6H_4N(C_2H_4Cl)_2$], 3.66 [m, 4H, $OCC_3H_6$-*p*-$C_6H_4N(C_2H_4Cl)_2$], 3.61 [s, 2H, $SCH_2C_6H_4$-*p*-$C(CH_3)_3$], 3.41 [s, 2H, $SCH_2C_6H_4$-*p*-$C(CH_3)_3$], 2.67 [t, $^3J$ = 7 Hz, 2H, $OCC_3H_6$-*p*-$C_6H_4N(C_2H_4Cl)_2$], 2.58 [t, $^3J$ = 7 Hz, 2H, $OCC_3H_6$-*p*-$C_6H_4N(C_2H_4Cl)_2$], 2.05 [quint, $^3J$ = 7 Hz, 2H, $OCC_3H_6$-*p*-$C_6H_4N(C_2H_4Cl)_2$], 1.89 [sept, $^3J$ = 7 Hz, 2H, *p*-$CH_3C_6H_4CH(CH_3)_2$], 1.76 [s, 6H, *p*-$CH_3C_6H_4CH(CH_3)_2$], 1.37 [s, 9H, $SCH_2C_6H_4$-*p*-$C(CH_3)_3$], 1.33 [s, 9H, $SCH_2C_6H_4$-*p*-$C(CH_3)_3$], 0.94 [d, $^3J$ = 7 Hz, 6H, *p*-$CH_3C_6H_4CH(CH_3)_2$], 0.89 [d, $^3J$ = 7 Hz, 6H, *p*-$CH_3C_6H_4CH(CH_3)_2$] ppm, $^{13}$C NMR (100 MHz, $CDCl_3$): δ = 171.66, 151.57, 150.87, 136.68, 133.53, 129.88, 129.06, 125.51, 125.34, 122.25, 106.89, 100.54, 84.17, 83.47, 82.46, 39.94, 39.38, 34.74, 33.88, 33.45, 31.34, 30.79, 26.36, 23.05, 22.52, 18.07 ppm.

**Data for [42][$BF_4$]:** Yield: 21.7 mg (53%). $C_{56}H_{68}BCl_2F_4NO_4Ru_2S_3$: calcd. C 52.75; H 5.37; N 1.10; found C 52.61; H 5.40; N 1.11. ESI-MS ($MeOH/CH_2Cl_2$): *m/z* = 1189.6 $[M]^+$. $^1H$ NMR (400 MHz, $CDCl_3$): δ = 7.80 (d, $^3J$ = 8 Hz, 2H, $SC_6H_4$-*p*-O), 7.44 (m, 4H, $SCH_2C_6H_4$-*p*-$OCH_3$), 7.12 [d, $^3J$ = 8 Hz, 2H, $OCC_3H_6$-*p*-$C_6H_4N(C_2H_4Cl)_2$ ], 7.02 (m, 2H, $SC_6H_4$-*p*-O, 2H, $SCH_2C_6H_4$-*p*-$OCH_3$), 6.95 (d, $^3J$ = 8 Hz, 2H, $SCH_2C_6H_4$-*p*-$OCH_3$), 6.67 [d, $^3J$ = 8 Hz, 2H, $OCC_3H_6$-*p*-$C_6H_4N(C_2H_4Cl)_2$], 5.14 [d, $^3J$ = 5 Hz, 2H, , *p*-$CH_3C_6H_4CH(CH_3)_2$], 5.00 [d, $^3J$ = 5 Hz, 2H, *p*-$CH_3C_6H_4CH(CH_3)_2$], 4.87 [d, $^3J$ = 5 Hz, 2H, *p*-$CH_3C_6H_4CH(CH_3)_2$], 4.77 [d, $^3J$ = 5 Hz, 2H, *p*-$CH_3C_6H_4CH(CH_3)_2$], 3.86 (d, $^3J$ = 11 Hz, 6H, $SCH_2C_6H_4$-*p*-$OCH_3$), 3.72 [m, 4H, $OCC_3H_6$-*p*-$C_6H_4N(C_2H_4Cl)_2$], 3.65 [m, 4H, $OCC_3H_6$-*p*-$C_6H_4N(C_2H_4Cl)_2$], 3.59 (s, 2H, $SCH_2C_6H_4$-*p*-$OCH_3$), 3.39 (s, 2H, $SCH_2C_6H_4$-*p*-$OCH_3$), 2.67 [t, $^3J$ = 7 Hz, 2H, $OCC_3H_6$-*p*-$C_6H_4N(C_2H_4Cl)_2$], 2.58 [t, $^3J$ = 7 Hz, 2H, $OCC_3H_6$-*p*-$C_6H_4N(C_2H_4Cl)_2$], 2.05 [m, 2H, $OCC_3H_6$-*p*-$C_6H_4N(C_2H_4Cl)_2$], 1.92 [m, 2H, *p*-$CH_3C_6H_4CH(CH_3)_2$], 1.76 [s, 6H, *p*-$CH_3C_6H_4CH(CH_3)_2$], 0.99 [d, $^3J$ = 6 Hz, 6H, *p*-$CH_3C_6H_4CH(CH_3)_2$], 0.93 [d, $^3J$ = 6 Hz, 6H, *p*-$CH_3C_6H_4CH(CH_3)_2$] ppm, $^{13}C$ NMR (100 MHz, $CDCl_3$): δ = 204.305, 171.29, 159.36, 150.9, 144.45, 134.95, 133.56, 131.64, 130.61, 130.40, 130.18, 123.70, 122.19, 114.05, 113.88, 112.24, 109.93, 107.10, 100.09, 83.87, 83.65, 82.40, 55.50, 55.44, 53.59, 40.55, 33.86, 33.55, 30.87, 26.53, 23.16, 22.34, 17.97 ppm.

**Data for [43][$BF_4$]:** Yield: 26.8 mg (70%). $C_{54}H_{62}BCl_4F_4NO_2Ru_2S_3 \cdot 0.5C_5H_{12}$: calcd. C 51.41; H 5.19; N 1.06; found C 51.51; H 5.06; N 1.36. ESI-MS ($MeOH/CH_2Cl_2$): *m/z* = 1197.8 $[M]^+$. $^1H$ NMR (400 MHz, $CDCl_3$): δ = 7.81 (d, $^3J$ = 8 Hz, 2H, $SC_6H_4$-*p*-O), 7.52 (m, 4H, S-*p*-$CH_2C_6H_4$-Cl), 7.45 (d, $^3J$ = 8 Hz, 2H, , S-*p*-$CH_2C_6H_4$-Cl), 7.39 (d, $^3J$ = 8 Hz, 2H, , S-*p*-$CH_2C_6H_4$-Cl), 7.12 [d, $^3J$ = 8 Hz, 2H, $OCC_3H_6$-*p*-$C_6H_4N(C_2H_4Cl)_2$ ], 7.04 (d, 2H, $^3J$ = 8 Hz, *p*-$SC_6H_4O$), 6.66 [d, $^3J$ = 8 Hz, 2H, $OCC_3H_6$-*p*-$C_6H_4N(C_2H_4Cl)_2$], 5.19 [d, $^3J$ = 6 Hz, 2H, , *p*-$CH_3C_6H_4CH(CH_3)_2$], 5.06 [d, $^3J$ = 6 Hz, 2H, *p*-$CH_3C_6H_4CH(CH_3)_2$], 4.94 [d, $^3J$ = 6 Hz, 2H, *p*-$CH_3C_6H_4CH(CH_3)_2$], 4.82 [d, $^3J$ = 6 Hz, 2H, *p*-$CH_3C_6H_4CH(CH_3)_2$], 3.72 [m, 4H, $OCC_3H_6$-*p*-$C_6H_4N(C_2H_4Cl)_2$], 3.65 [m, 4H, $OCC_3H_6$-*p*-$C_6H_4N(C_2H_4Cl)_2$, 2H, S-*p*-$CH_2C_6H_4$-Cl], 3.46 (s, 2H, $SCH_2C_6H_5$), 2.66 [t, $^3J$ = 7 Hz, 2H, $OCC_3H_6$-*p*-$C_6H_4N(C_2H_4Cl)_2$], 2.57 [t, $^3J$ = 7 Hz, 2H, $OCC_3H_6$-*p*-$C_6H_4N(C_2H_4Cl)_2$], 2.04 [quint, $^3J$ = 7 Hz, 2H, $OCC_3H_6$-*p*-$C_6H_4N(C_2H_4Cl)_2$], 1.90 [sept, $^3J$ = 7 Hz, 2H, *p*-$CH_3C_6H_4CH(CH_3)_2$], 1.76 [s, 6H, *p*-$CH_3C_6H_4CH(CH_3)_2$], 0.99 [d, $^3J$ = 7 Hz, 6H, *p*-$CH_3C_6H_4CH(CH_3)_2$], 0.92 [d, $^3J$ = 7 Hz, 6H, *p*-$CH_3C_6H_4CH(CH_3)_2$] ppm, $^{13}C$ NMR (100 MHz, $CDCl_3$): δ = 144.43, 138.39, 133.63, 130.70, 129.71, 128.87, 122.32, 112.17, 107.26, 100.30, 84.03, 83.74, 82.41, 53.56, 40.52, 33.85, 30.85, 23.19, 22.33, 17.97 ppm.

# References


1. R. Weinberg, *The Biology of Cancer*, Garland Science, **2014**, 960 pages.
2. J.S. Bertram, *Molecular aspects of medicine*, **2001**, 21, 167-223.
3. http://www.nature.com/scitable/topicpage/cell-division-and-cancer-14046590, consulted 22.05.**2015**.
4. G.M. Cooper, *The Cell: A Molecular Approach*. Sunderland (MA): Sinauer Associates, Inc., **2000**, 689 pages.
5. B.W. Stewart, C.P. Wild, *World Cancer Report 2014*, Lyon: International Agency for Research on Cancer, **2014**, 630 pages.
6. American Cancer Society, *Cancer Facts & Figures 2014*, Atlanta: American Cancer Society; **2014**, 70 pages.
7. http://www.cancer.gov/cancertopics/what-is-cancer#types-of-cancer, consulted 23.05.**2015**.
8. E. Boyland, *British Journal of Industrial Medicine*, **1985**, 42, 716-718.
9. F. Hampl, S. Rádl, J. Paleček, *Farmakochemie*, Praha: Vydavatelství VŠCHT Praha, **2007**, 450 pages.
10. V.T DeVita, E. Chu, *Cancer Research*, **2008,** 68, 21, 8643-8653.
11. R.T. Skeel, *Handbook of Cancer Chemotherapy*, Philadephia: Lippincott Williams & Wilkins, **2007**, 817 pages.
12. http://www.cancer.org/treatment, consulted 20.05.**2015**.
13. P. Keating, *Cancer on Trial: Oncology as a New Style of Practice*, Chicago: University Of Chicago Press, **2012**, 424 pages.
14. http://news.harvard.edu/gazette/story/2012/07/transforming-cancer-treatment/, consulted 23.05.**2015**.
15. A.K. Haldar, P. Sen, S. Roy, *Molecular Biology International*, **2011,** Volume 2011, 23 pages.
16. C. Orvig, M.J. Abrams, *Chemical Reviews*, **1999**, 99, 2201-2204.
17. P. J Sadler, *Advances in Inorganic Chemistry*, **1991**, 36, 1-48.
18. B.M. Sutton in *Platinum, Gold, and Other Metal Chemotherapeutic Agents;* S.J. Lippard (Ed.), ACS Symposium series 209, Washington, D.C: American Chemical Society, **1983**, pages 355-369.
19. B. Rosenberg, L. VanCamp, T. Krigas, *Nature*, **1965**, 205, 698-699.

20. G.H. Smith, *Nurse Practitioner*, **1979**, 4, 35-41.
21. G. Sava, A. Bergamo in *Platinum and Other Heavy Metal Compounds in Cancer Chemotherapy*, A. Bonetti, R. Leone, F.M. Muggia, S.B. Howell (Eds.), Humana Press, **2009**, pages 57-66.
22. T.C. Johnstone, K. Suntharalingam, S.J. Lippard, *Philosophical Transactions of the Royal Society A*, **2015**, 373, 1-12.
23. S. van Rijt, P.J. Sadler, *Drug Discovery Today*, **2009**, 14, 1089-1097.
24. N.P.E. Barry, P.J. Sadler, *Chemical Communications*, **2013**, 49, 5106-5131.
25. http://www.rsc.org/periodic-table/element/78/platinum, consulted 5.6.**2015**.
26. M.E. Weeks, Discovery of the Elements ($7^{th}$ ed.), *Journal of Chemical Education*, **1968**, 896 pages.
27. http://www.platinum.matthey.com/about-pgm/history-of-pgm, consulted 5.6.**2015**.
28. P.J. Loferski, *Platinum-Group Metals*, **2010**, Minerals Yearbook, USGS 2010.
29. *Martindale: The Complete Drug Reference*, S.C. Sweetman (Ed.), London: Pharmaceutical Press, $35^{th}$ edition, **2007**, 4596 pages.
30. M. Watson, A. Barrett, R. Spence, C. Twelves, *Oncology*, Oxford: Oxford University Press, $2^{nd}$ edition, **2006**, 212 pages.
31. G.J. Bosl, D.F. Bajorin, J. Sheinfeld, R.J. Motzer, R.S.K. Chaganti in: V.T.J. DeVita, S. Hellman, S.A. Rosenberg (Eds.), *Cancer of the testis*, Philadelphia: Lippincott, Williams&Wilkins, **2001**, pages 1491-1518.
32. N.J. Wheate, S. Walker, G.E. Craig, R. Oun, Dalton Transactions, **2003**, 39, 35, 8113-8127.
33. J.J. Wilson, S.J. Lippard, *Chemical Reviews*, **2014**, 114, 4470-4495.
34. D.J. Stewart, *Critical Reviews in Oncology/Hematology*, **2007**, 63, 1, 12-31.
35. M. Mishima, G. Samimi, A. Kondo, X. Lin, S.B. Howell, *European Journal of Cancer*, 38, 10, **2002**, 1405-1412.
36. S. B. Fricker, *Dalton Transactions*, **2007**, 4903-4917.
37. I. Kostova, *Current Medicinal Chemistry*, **2006**, 13, 1085-1107.
38. N.V. Pitchkov, *Platinum Metal Reviews*, **1996**, 40, 181-188.
39. http://www.ciaaw.org/atomic-weights.htm, consulted 3.6.**2015**.
40. D.R. Lide, (Ed.), *CRC Handbook of Chemistry and Physics*, Internet Version 2005, <http://www.hbcpnetbase.com>, Boca Raton, FL: CRC Press, **2005**, 2660 pages.

41. J. Emsley (Ed.), *Nature's Building Blocks: An A-Z Guide to the Elements*. Oxford, England, UK: Oxford University Press, **2003**, 538 pages.
42. S. Murahashi (Ed.), *Ruthenium in Organic Synthesis*, Weinheim: WILEY-VCH Verlag GmbH & Co. KGaA, **2004**, 383 pages.
43. R.B. Heslop, P.L. Robinson, *Inorganic chemistry*, 2nd edition, Amsterdam: Elsevier, **1960**, page 503.
44. F. P. Dwyer, E. C. Gyarfas, W. P. Rogers, J. H. Koch, *Nature*, **1952**, 170, 4318, 190-191.
45. B. Therrien, J. Furrer, *Advances in Chemistry*, **2014**, 1-20.
46. M.J. Clarke, *Metal Ions in Biological System*, **1980**, 11, 231-283.
47. G. Süss-Fink, *Dalton Transactions*, **2010**, 39, 1673-1688.
48. J. Reedijk, *Platinum Metals Review*, **2008**, 52, 1, 1-9.
49. G. Sava, A. Bergamo, S. Zorzet, B. Gava, C. Casarsa, M. Cocchietto, A. Furlani, V. Scarcia, B. Serli, E. Iengo, E. Alessio, G. Mestroni, *European Journal of Cancer*, **2002**, 38, 427-435.
50. M. Groessl, E. Reisner, C.G. Hartinger, R. Eichinger, O. Semenova, A.R. Timerbaev, M.A. Jakupec, V.B. Arion, B.K. Keppler, *Journal of Medicinal Chemistry*, **2007**, 50, 2185-2193.
51. M.A. Jakupec, M. Galanski, V.B. Arion, C.G. Hartinger, B.K. Keppler, *Dalton Transactions*, **2008**, 183-194.
52. P.J. Dyson, G. Sava, *Dalton Transactions*, **2006**, 16, 1929-1933.
53. G. Sava, S. Zorzet, C. Turrin, F. Vita, M.R. Soranzo, G. Zabucchi, M. Cocchietto, A. Bergamo, S. DiGiovine, G. Pezzoni, L. Sartor, S. Garbisa, *Clinical Cancer Research*, **2003**, 9, 1898-1905.
54. M. Bacac, A.C.G. Hotze, K. van der Schilden, J.G. Haasnoot, S. Pacor, E. Alessio, G. Sava, J. Reedijk, *Journal of Inorganic Biochemistry*, **2004**, 98, 402-412.
55. A. Bergamo, B. Gava, E. Alessio, G. Mestroni, B. Serli, M. Cocchietto, S. Zorzet, G. Sava, *International Journal of Oncology*, **2002**, 21, 1331-1338.
56. A. Bergamo, G. Sava, *Dalton Transactions*, **2007**, 1267-1272.
57. I. Bratsos, A. Bergamo, G. Sava, T. Gianferrara, E. Zangrando, E. Alessio, *Journal of Inorganic Biochemistry*, **2008**, 102, 606-617.

58. B. Gava, S. Zorzet, P. Spessotto, M. Cocchietto, G. Sava, *Journal of Pharmacology and Experimental Therapeutics*, **2006**, 317, 284-291.
59. G. Sava, F. Frausin, M. Cocchietto, F. Vita, E. Podda, P. Spessotto, A. Furlani, V. Scarcia, G. Zabucchi, *European Journal of Cancer*, **2004**, 40, 1383-1396.
60. C. Casarsa, M. T. Mischis, G. Sava, *Journal of Inorganic Biochemistry*, **2004**, 98, 1648-1654.
61. a) G. Sava, S. Zorzet, C. Turrin, F. Vita, M. Soranzo, G. Zabucchi, M. Cocchietto, A. Bergamo, S. DiGiovine, G. Pezzoni, L. Sartor, S. Garbisa, *Clinical Cancer Research*, **2003**, 9, 1898-1905.
    b) A. Levina, A. Mitra, P.A. Lay, *Metallomics*, 2009, 1, 458-470.
62. S. Leijen, S.A. Burgers, P. Baas, D. Pluim, M. Tibben, E. van Werkhoven, E. Alessio, G. Sava, J.H. Beijnen, J.H.M. Schellens, *Investigational New Drugs* **2015**, 33, 201-214.
63. H. Keller, B.K. Keppler, US Patent, **1989**, 4843069.
64. B.K. Keppler, K.G. Lipponer, B. Stenzel, F. Kratzin, in B.K. Keppler (Ed.), *Metal Complexes in Cancer Chemotherapy*, VCH, Weinheim, **1993**, page 187.
65. P. Heffeter, K. Böck, B. Atil, M.A.R. Hoda, W. Körner, C. Bartel, U. Jungwirth, B.K. Keppler, M. Micksche, W. Berger, G. Koellensperger, *Journal of Biological Inorganic Chemistry*, **2010**, 15, 5, 737-748.
66. C.G. Hartinger, M.A. Jakupec, S. Zorbas-Seifried, M. Groessl, A. Egger, W. Berger, H. Zorbas, P.J. Dyson, B.K. Keppler, *Chemistry & Biodiversity*, **2008**, 5, 2140-2155.
67. R. Trondl, P. Heffeter, C.R. Kowol, M.A. Jakupec, W. Berger, B.K. Keppler, *Chemical Science*, **2014**, 5, 2925-2932.
68. G. Wilkinson, The Long Search for Stable Transition Metal Alkyls (Nobel Lecture), *Science*, **1974**, 185, 109-112.
69. T. M. Zydowsky, *Chemometrics and Intelligent Laboratory Systems*, **2000**, 29-34.
70. E.O. Fischer, W. Hafner, *Zeitschrift für Naturforschung B*, **1955**, 10, 665-668.
71. H. Werner, *Angewandte Chemie International Edition*, **2012**, 51, 2-9.
72. D. Seyferth, *Organometallics*, **2002**, 21, 1520-1530.
73. http://www.nobelprize.org/nobel_prizes/chemistry/laureates/1973/press.html, consulted 03.06.**2015**.
74. G. Winkhaus, H. Singer, *Journal of Organometalic Chemistry*, **1967**, 7, 487-491.

75. R.A. Zelonka, M. C. Baird, *Canadian Journal of Chemistry*, **1972**, 50, 3063-3072.
76. J. W. Kang, K. Moseley, P. M. Maitlis, *Journal of the American Chemical Society*, **1969**, 91, 5970-5977.
77. M.A. Bennett, A.K. Smith, *Journal of the Chemical Society, Dalton Transactions*, **1974**, 233-241.
78. B. Therrien, *Coordination Chemistry Reviews*, **2009**, 253, 493-519.
79. L.D. Dale, J.H. Tocher, T.M. Dyson, D.I. Edwards, D.A. Tocher, *Anti-Cancer Drug Design*, **1992**, 7, 3-14.
80. C.S. Allardyce, P.J. Dyson, D.J. Ellis, S.L. Heath, *Chemical Communications*, **2001**, 1396-1397.
81. R.E. Morris, R.E. Aird, P.D. Murdoch, H.M. Chen, J. Cummings, N.D. Hughes, S. Parsons, A. Parkin, G. Boyd, D.I. Jodrell, P.J. Sadler, *Journal of Medicinal Chemistry*, **2001**, 44, 3616-3621.
82. C. Scolaro, A. Bergamo, L. Brescacin, R. Delfino, M. Cocchietto, G. Laurenczy, T.J. Geldbach, G. Sava, P.J. Dyson, *Journal of Medicinal Chemistry*, **2005**, 48, 4161-4171.
83. S. Chatterjee, S. Kundu, A. Bhattacharyya, C.G. Hartinger, P.J. Dyson, *Journal of Biological Inorganic Chemistry*, **2008**, 13, 1149-1155.
84. W.H. Ang, P.J. Dyson, *European Journal of Inorganic Chemistry*, **2006**, 4003-4018.
85. B. Dutta, C. Scolaro, R. Scopelliti, P.J. Dyson, K. Severin, *Organometallics*, **2008**, 27, 1355-1357.
86. C.S. Allardyce, P.J. Dyson, D.E. Ellis, P.A. Salter, R. Sopelliti, *Journal of Organometalic Chemistry*, **2003**, 668, 35-42.
87. C.A. Vock, A.K. Renfrew, R. Scopelliti, L. Juillerat-Jeanneret, P.J. Dyson, *European Journal of Inorganic Chemistry*, **2008**, 1661-1671.
88. P.J. Dyson, Chimia, **2007**, 61, 698-703.
89. W.H. Ang, A. Casini, G. Sava, P.J. Dyson, *Journal of Organometallic Chemistry*, **2011**, 696, 989-998.
90. W.H. Ang, E. Daldini, L. Juillerat-Jeanneret, P.J. Dyson, *Inorganic Chemistry*, **2007**, 46, 9048-9050.

91. R.E. Morris, R.E. Aird, P.D.S. Murdoch, H. Chen, J. Cummings, N.D. Hughes, S. Pearsons, A. Parkin, G. Boyd, D.I. Jodrell, P.J. Sadler, *Journal of Medicinal Chemistry*, **2001**, 44, 3616-3621.
92. H. Chen, J.A. Parkinson, S. Parsons, R.A. Coxall, R.O. Gould, P.J. Sadler, *Journal of the American Chemical Society*, **2002**, 124, 3064-3082.
93. O. Novakova, H. Chen, O. Vrana, A. Rodger, P.J. Sadler, V. Brabec, *Biochemistry*, **2003**, 42, 11544-11554.
94. F. Wang, H. Chen, J.A. Parkinson, P.del S. Murdoch, P.J. Sadler, *Inorganic Chemistry*, **2002**, 41, 4509-4523.
95. F. Wang, J. Bella, J.A. Parkinson, P.J. Sadler, *Journal of Biological Inorganic Chemistry*, **2005**, 10, 147-155.
96. F. Wang, J. Xu, A. Habtemariam, J. Bella, P.J Sadler, *Journal of the American Chemical Society*, **2005**, 127, 17734-17743.
97. H. Chen, J.A. Parkinson, R.E. Morris, P.J. Sadler, *Journal of the American Chemical Society*, **2003**, 125, 173-186.
98. F. Wang, A. Habtemariam, E.P.L. van der Geer, R. Fernández, M. Melchart, R.J. Deeth, R. Aird, S. Guichard, F.P.A. Fabbiani, P. Lozano-Casal, I.D.H. Oswald, D.I. Jodrell, S. Parsons, P.J. Sadler, *Proceedings of the National Academy of Sciences*, **2005**, 102, 51, 18269-18274.
99. M.-G. Mendoza-Ferri, C.G. Hartinger, R.E. Eichinger, N. Stolyarova, K. Severin, M.A. Jakupec, A.A. Nazarov, B.K. Keppler, *Organometallics*, **2008**, 27, 2405-2407.
100. S.W. Magennis, A. Habtemariam, O.Novakova, J.B. Henry, S. Meier, S. Parsons, I.D.H. Oswald, V. Brabec, P.J. Sadler, *Inorganic Chemistry*, **2007**, 46, 5059-5068.
101. B. Therrien, W.H. Ang, F. Chérioux, L. Vieille-Petit, L. Juillerat-Jeanneret, G. Süss-Fink, P.J. Dyson, *Journal of Cluster Science*, **2007**, 18, 741-752.
102. F. Schmitt, P. Govindaswamy, G. Süss-Fink, W.H. Ang, P.J. Dyson, L. Juillerat-Jeanneret, B. Therrien, *Journal of Medicinal Chemistry*, **2008**, 51, 1811-1816.
103. F. Schmitt, P. Govindaswamy, O. Zava, G. Süss-Fink, L. Juillerat-Jeanneret, B. Therrien, *Journal of Biological Inorganic Chemistry*, **2009**, 14, 101-109.
104. H.T. Schacht, R.C. Haltiwanger, M. Rakovoski Dubois, *Inorganic Chemistry*, **1992**, 31, 1728-1730.
105. K. Mashima, A. Mikami, A. Nakamura, *Chemical Letters*, **1992**, 1795-1798.

106. F. Chérioux, B. Therrien, G. Süss-Fink, *European Journal of Inorganic Chemistry*, **2003**, 1043-1047.
107. F. Chérioux, B. Therrien, G. Süss-Fink, *Inorganica Chimica Acta*, **2004**, 357, 834-838.
108. F. Chérioux, C.M. Thomas, T. Monnier, G. Süss-Fink, *Polyhedron*, **2003**, 22, 543-548.
109. M. Gras, B. Therrien, G. Süss-Fink, O. Zava, P.J. Dyson, *Dalton Transactions*, **2010**, 39, 10305-10313.
110. S.J. Dougan, P.J. Sadler, *Chimia*, **2007**, 61, 704-715.
111. F. Giannini, J. Furrer, A.-F. Ibao, G. Süss-Fink, B. Therrien, O. Zava, M. Baquie, P.J. Dyson, P. Štěpnička, *Journal of Biological Inorganic Chemistry*, **2012**, 17, 951-960.
112. F. Giannini, J. Furrer, G. Süss-Fink, C.M. Clavel, P.J. Dyson, *Journal of Organometalic Chemistry*, **2013**, 744, 41-48.
113. F. Giannini, L.E.H. Paul, J. Furrer, B. Therrien, G. Süss-Fink, *New Journal of Chemistry*, **2013**, 37, 3503-3511.
114. F. Giannini, G. Süss-Fink, J. Furrer, *Inorganic Chemistry*, **2011**, 50, 10552-10554.
115. A.-F. Ibao, M. Gras, B. Therrien, G. Süss-Fink, O. Zava, P.J. Dyson, *European Journal of Inorganic Chemistry*, **2012**, 9, 1531-1535.
116. F. Chérioux, B. Therrien, G. Süss-Fink, *European Journal of Inorganic Chemistry*, **2003**, 1043-1047.
117. M. Gras, B. Therrien, G. Süss-Fink, O. Zava, P.J. Dyson, *Dalton Transactions*, **2010**, 39, 10305-10313.
118. J.M. Estrela, A. Ortega, E. Obrador, *Critical Reviews in Clinical Laboratory Sciences*, 2006, 43, 2, 143-181.
119. T. Schnelldorfer, S. Gansauge, F. Gansauge, S. Schlosser, H.G. Beger, A.K. Nussler, *Cancer*, **1989**, 7, 1440-1447.
120. W.S. Sheldrick, C. Landgrafe, *Inorganica Chimica Acta*, **1993**, 208, 145-151.
121. M. Ito, A. Watanabe, Y. Shibata, T. Ikariya, *Organometallics*, **2010**, 29, 4584-4592.
122. M.J.-L. Tschan, F. Chérioux, B. Therrien, G. Süss-Fink, *European Journal of Inorganic Chemistry*, **2004**, 2405-2411.

123. Y. Miyake, S. Endo, M. Yuki, Y. Tanabe, Y. Nishibayashi, *Organometallics*, **2008**, 27, 6039-6042.

124. M. Nishio, H. Matsuzaka, Y. Mizobe, T. Tanase, M. Hidai, *Organometallics*, **1994**, 13, 4214-4226.

125. S.J. Dougan, A. Habtemariam, S.E. McHale, S. Parsons, P.J. Sadler, *Proceedings of the National Academy of Sciences*, **2008**, 105, 11628-11633.

126. Y. Jung, S.J. Lippard, *Chemical Reviews*, **2007**, 105, 1387-1407.

127. M. Bacac, A.C.G. Hotze, K. van der Schilden, J.G. Haasnoot, S. Pacor, E. Alessio, G. Sava, J. Reedijk, *Journal of Inorganic Biochemistry*, **2004**, 98, 402-412.

128. R.E. Morris, R.E. Aird, P.D.S. Murdoch, H. Chen, J. Cummings, N.D. Hughes, S. Pearsons, A. Parkin, G. Boyd, D.I. Jodrell, P.J. Sadler, *Journal of Medicinal Chemistry*, **2001**, 44, 3616-3621.

129. F. Kratz, M. Hartmann, B.K. Keppler, L. Messori, *Journal of Biological Chemistry*, **1994**, 269, 2581-2588.

130. R.F. Borch, M.E. Pleasants, *Proceedings of the National Academy of Sciences*, **1979**, 76, 6611-6614.

131. L.E.H. Paul, B. Therrien, J. Furrer, *Inorganic Chemistry*, **2012**, 51, 1057-1067.

132. L.E.H. Paul, B. Therrien, J. Furrer, *Journal of Biological Inorganic Chemistry*, **2012**, 17, 1053-1062.

133. A.J. Taylor, M. Wenzel, *Xenobiotica*, **1978**, 8, 107-112.

134. M.M. van Hennik, W.J. van der Vijgh, I. Klein, F. Elferink, J.B. Vermorken, B. Winograd, H.M. Pinedo, *Cancer Research*, **1987**, 47, 6297-301.

135. J.C. Schuh, *Toxicologic Pathology*, **2004**, 32, Suppl. 1, 53-66.

136. C. Scolaro, A. Bergamo, L. Brescacin, R. Defino, M. Cocchietto, G. Laurenczy, T.J. Geldbach, G. Sava, P.J. Dyson, *Journal of Medicinal Chemistry*, **2005**, 48, 4161-4171.

137. M. Pernot, T. Bastogne, N.P.E. Barry, B. Therrien, G. Koellensperger, S. Hann, V. Reshetov, M. Barberi-Heyob, *Journal of Photochemistry and Photobiology B*, **2012**, 117, 80-89.

138. A.J. Taylor, M. Wenzel, *Xenobiotica*, **1978**, 8, 107-112.

139. M.M. van Hennik, W.J. van der Vijgh, I. Klein, F. Elferink, J.B. Vermorken, B. Winograd , H.M. Pinedo, *Cancer Research*, **1987**, 47, 6297-301.

140. M.V. Céspedes, I. Casanova, M. Parreño, R. Mangues, *Clinical and Translational Oncology*, **2006**, 8, 318-329.

141. D. Li, J.I. Williams, R.J. Pietras, *Oncogene*, **2002**, 21, 2805-2814.

142. A.J. Litterman, D.M. Zellmer, K.L. Grinnen, M.A. Hunt, A.Z. Dudek, A.M. Salazar, J.R. Ohlfest, *Journal of Immunology*, **2013**, 190, 6259-6268.

143. J.A. Segura, L.G. Barbero, J. Márquez, *FEBS Letters*, **1997**, 414, 1-6.

144. J.F. Turrens, *Journal of Physiology*, **2003**, 552, 335-344.

145. Y. Chen, M.Y. Qin, L. Wang, H. Chao, L.N. Ji, A.L. Xu., *Biochimie*, **2013**, 95, 2050-2059.

146. Z. Zhao, Z. Luo, Q. Wu, W. Zheng, Y. Feng, T. Chen., *Dalton Transactions*, **2014**, 43, 17017-17028.

147. I. Ojima (Ed.), *Fluorine in Medicinal Chemistry and Chemical Biology*, John Wiley & Sons, **2009**, 640 pages.

148. K. Müller, C. Faeh, F. Diederich, *Science*, **2007**, 317, 5846, 1881-1886.

149. J. Wang, M. Sanchez-Rosello, J. Luis Acena, C. del Pozo, A.E. Sorochinsky, S. Fustero, V.A. Soloshonok, H. Liu, *Chemical Reviews*, **2014**, 114, 2432-2506.

150. G.A. Patani, E.J. LaVoie, *Chemical Reviews*, **1996**, 96, 3147-3176.

151. W.C. Black, C.I. Bayly, D.E. Davis, S. Desmarais, J.-P. Falgueyret, S. Léger, C. S. Li, F. Massé, D.J. McKay, J.T. Palmer, M.D. Percival, J. Robichaud, N. Tsou, R. Zamboni, *Bioorganic & Medicinal Chemistry Letters*, **2005**, 15, 4741-4744.

152. J.-P. Bégué, D. Bonnet-Delpon, *Bioorganic and Medicinal Chemistry of Fluorine*, Wiley-Interscience, **2008**, 366 pages.

153. For reviews see for example: a) P. Rai, S. Mallidi, X. Zheng, R. Rahmanzadeh, Y. Mir, S. Elrington, A. Khurshid, T. Hasan, *Advanced Drug Delivery Reviews*, **2010**, 62, 1094-1124; b) Z. Huang, *Technology in Cancer Research & Treatment*, **2005**, 4, 283-293; c) Q. Shao, B. Xing, *Chemical Society Reviews*, **2010**, 39, 2835-2845.

154. For reviews see for example: a) A. Hervault, N.T.K. Thanh, *Nanoscale*, **2014**, 6, 11553-11573; b) A.J. Giustini, A.A. Petryk, S.M. Cassim, J.A. Tate, I. Baker, P.J. Hoopes, *Nano Life*, **2010**, 1, 17-32; c) T. Kobayashi, *Biotechnology Journal*, **2011**, 6, 1342-1347.

155. For reviews see for example: a) M. Urano, M. Kuroda, Y. Nishimura, *International Journal of Hyperthermia*, **1999**, 15, 79-107; b) M.A. Ward, T.K. Georgiou,

*Polymers*, **2011**, 3, 1215-1242; c) J.R. McDaniel, M.W. Dewhirst, A. Chilkoti, *International Journal of Hyperthermia*, **2013**, 29, 501-510.

156. C.M. Clavel, O. Zava, F. Schmitt, B.H. Kenzaoui, A.A. Nazarov, L. Juillerat-Jeanneret, P.J. Dyson, *Angewandte Chemie International Edition*, **2011**, 50, 7124-7127.
157. C.M. Clavel, E. Paunescu, P. Nowak-Sliwinska, P.J. Dyson, *Chemical Science*, **2014**, 5, 1097-1101.
158. C.M. Clavel, P. Nowak-Sliwinska, E. Paunescu, A. W. Griffioen, P. J. Dyson, *Chemical Science*, **2015**, 6, 2795-2801.
159. A. Choudhary, R.T. Raines, *ChemBioChem*, **2011**, 12, 1801-1807.
160. A. Kurzwernhart, W. Kandioller, S. Bächler, C. Bartel, S. Martic, M. Buczkowska, G. Mühlgassner, M.A. Jakupec, H.-B. Kraatz, P.J. Bednarski, V.B. Arion, D. Marko, B.K. Keppler, C.G. Hartinger, *Journal of Medicinal Chemistry*, **2012**, 55, 10512-10522.
161. H.C. Kolb, M.G. Finn, K.B. Sharpless, *Angewandte Chemie International Edition*, **2001**, 40, 2004-2021.
162. V.V. Rostovtsev, L.G. Green, Valery V. Fokin, K.B. Sharpless, *Angewandte Chemie International Edition*, **2002**, 41, 2596-2599.
163. F. Himo, T. Lovell, R. Hilgraf, V.V. Rostovtsev, L. Noodleman, K.B. Sharpless, V.V. Fokin, *Journal of the American Chemical Society*, **2005**, 127, 210-216.
164. M. Arseneault, C. Wafer, J.-F. Morin, *Molecules*, **2015**, 20, 9263-9294.
165. E. Lallana, A. Sousa-Herves, F. Fernandez-Trillo, R. Riguera, E. Fernandez-Megia, *Pharmaceutical Research*, **2012**, 29, 1-34.
166. S. Mischler, S. Guerra, R. Deschenaux, *Chemical Communications*, **2012**, 48, 2183-2185.
167. S. Campidelli, *Current Organic Chemistry*, **2011**, 15, 1151-1159.
168. T.J. Del Castillo, S. Sarkar, K.A. Abboud, A.S. Veige, *Dalton Transactions*, **2011**, 40, 8140-8144.
169. http://www.sigmaaldrich.com/catalog/product/aldrich/712760; http://www.sigmaaldrich.com/catalog/product/aldrich/712752; http://www.sigmaaldrich.com/catalog/product/aldrich/762024, consulted 13.07.**2015**

170. T. Farooq, L.K. Sydnes, K.W. Törnroosa, B.E. Haug, *Synthesis*, **2012**, 44, 2070-2078.

171. G. Tripodo, D. Mandracchia, S. Collina, M. Rui, D. Rossi, *Medicinal Chemistry*, **2014**, S1, 004, 1-8.

172. S.Y. Kim, S.H. Cho, Y.M. Lee, L.-Y. Chu, *Macromolecular Research*, **2007**, 15, 646-655.

173. H.F. Dvorak, *New England Journal of Medicine*, **1986**, 315, 1650-1659.

174. S.E. Grivenikov, F.R. Greten, M. Karin, *Cell*, **2010**, 140, 883-899.

175. A. Mantovani, P. Allavena, A. Sica, F. Balkwill, *Nature*, **2008**, 454, 436-444.

176. C. de Martel, S. Franceschi, *Critical Reviews in Oncology/Hematology*, **2009**, 70, 183-194.

177. H. Takahashi, H. Ogata, R. Nishigaki, D.H. Broide, M. Karin, *Cancer Cell*, **2010**, 17, 89-97.

178. J.R. Brown, R.N. DuBois, *Journal of Clinical Oncology*, **2005**, 2840-2855.

179. S. Tomozawa, N.H. Tsuno, E. Sunami, K. Hatano, J. Kitayama, T. Osada, S. Saito, T. Tsuruo, Y. Shibata, H. Nagawa, *British Journal of Cancer*, **2000**, 83, 324-328.

180. B. Singh, J.A. Berry, A. Shoher, V. Ramakrishnan, A. Lucci, *International Journal of Oncology*, **2005**, 26, 1393-1399.

181. F.M. Giardiello, G.J. Offerhaus, R.N. DuBois, *European Journal of Cancer*, **1995**, 31A, 1071-1076.

182. L.J. Hixson, D.S. Alberts, M. Krutzsch, J. Einsphar, K. Brendel, P.H. Gross, N.S. Paranka, M. Baier, S. Emerson, R. Pamukcu, R.W. Burt, *Cancer Epidemiology, Biomarkers & Prevention*, **1994**, 3, 433-438.

183. S.J. Shiff, M.I. Koutsos, L. Qiao, B. Rigas, *Experimetal Cell Research*, **1996**, 222, 179-188.

184. M. Jaattela, *Experimental Cell Research*, **1999**, 248, 30-43.

185. A. Aghdassi, P. Phillips, V. Dudeja, D. Dhaulakhandi, R. Sharif, R. Dawra, M.M. Lerch, A. Saluja, *Cancer Research*, **2007**, 67, 616-625.

186. H. Endo, M. Yano, Y. Okumura, H. Kido, *Cell Death and Disease*, **2014**, 5, 1-10.

187. A.C. Pinto, J.N. Moreira, S. Simoes in *Current Cancer Treatment - Novel Beyond Conventional Approaches*, O. Ozdemir (Ed.), InTech **2011**, 810 pages.

188. W. Neumann, B.C. Crews, M.B. Sárosi, C.M. Daniel, K. Ghebreselasie, M.S. Scholz, L.J. Marnett, E. Hey-Hawkins, *ChemMedChem*, **2015**, 10, 183-192.

189. Q. Cheng, H. Shi, H. Wang, Y. Min, J. Wang, Y. Liu, *Chemical Communications*, **2014**, 50, 7427-7430.

190. W. Neumann, B.C. Crews, L.J. Marnett, E. Hey-Hawkins, *ChemMedChem*, **2014**, 9, 1150-1153.

191. F. Aman, M. Hanif, W.A. Siddiqui, A. Ashraf, L.K. Filak, J. Reynisson, T. Söhnel, S.M.F. Jamieson, C.G. Hartinger, *Organometallics*, **2014**, 33, 5546-5553.

192. W.H. Ang, L.J. Parker, A. De Luca, L. Juillerat-Jeanneret, C.J. Morton, M. Lo Bello, M.W. Parker, P.J. Dyson, *Angewandte Chemie International Edition*, **2009**, 21, 3912-3915.

193. S.J. Lippard, Y. Song, K. Suntharalingam, Patent US 20140274988 A1 (18. September **2014**).

194. F. Giannini, M. Bartoloni, L.E.H. Paul, G. Süss-Fink, J.-L. Reymond, J. Furrer, *MedChemComm*, **2015**, 6, 347-350.

195. D. Catovsky, M. Else, S. Richards, *Clinical Lymphoma Myeloma and Leukemia*, **2011**, 11, S2-S6.

196. D. Mohamed, S. Mowaka, J. Thomale, M.W. Linscheid, *Chemical Research in Toxicology*, **2009**, 22, 1435-1446.

197. A.A. Nazarov, S.M. Meier, O. Zava, Y.N. Nosova, E.R. Milaeva, C.G. Hartinger, P.J. Dyson, *Dalton Transactions*, **2015**, 44, 3614-3623.

198. C.M. Clavel, O. Zava, F. Schmitt, B.H. Kenzaoui, A.A. Nazarov, L. Juillerat-Jeanneret, P.J. Dyson, *Angewandte Chemie International Edition*, **2011**, 50, 7124-7127.

199. G.C. Kundu, J.R. Schullek, I.B. Wilson, *Pharmacology Biochemistry and Behavior*, **1994**, 49, 621-624.

200. L. Panasci, J.-P. Paiment, G. Christodoulopoulos, A. Belenkov, A. Malapetsa, R. Aloyz, *Clinical Cancer Research*, **2001**, 7, 454-461.

201. M.A. Bennett, T.-N. Huang, T.W. Matheson, A.K. Smith, *Inorganic Syntheses*, **1982**, 21, 74-78.

202. G.M. Sheldrick, *Acta Crystallographica*, **2008**, A64, 112-122.

203. L.J. Farrugia, *Journal of Applied Crystallography*, **1997**, 30, 565.

204. G. M. Sheldrick, *Acta Crystallographica*, **1990**, A46, 467.

205. G. M. Sheldrick, SHELXL-97, University of Göttingen, Göttingen, Germany, **1999**.

206. K.F. Morris, C.S. Johnson, *Journal of the American Chemical Society*, **1992**, 114, 3139-3141.

207. G.A. Morris, In: D.M. Grant, R.K. Harris (Eds.) *Encyclopedia of nuclear magnetic resonance*, **2002**, Wiley, Chichester, pp 35-44.

208. P.K. Glasoe, F.A. Long, *Journal of Physical Chemistry*, **1960**, 64, 188-190.

209. K. Mikkelsen, S.O. Nielsen, *Journal of Physical Chemistry*, **1960**, 64, 632-637.

210. J.R. van Beijnum, P. Nowak-Sliwinska, E. van den Boezem, P. Hautvast, W.A. Buurman, A.W. Griffioen, *Oncogene*, **2013**, 17, 363-374.

211. Since diruthenium-1 was used as HCl adduct (0.8 eq), the exact concentration values are: 0.19, 0.39, 0.58, 0.97 and 1.94 mg/kg.

212. R. Kand'ár, P. Záková, H. Lotková, O. Kucera, Z. Cervinková, *Journal of Pharmaceutical and Biomedical Analysis*, **2007**, 43, 1382-1387.

213. E. Bustamante, J.W. Soper, P.L. Pedersen, *Analytical Biochemistry*, **1977**, 80, 401-408.

# Abbreviations

| | |
|---|---|
| A | adenosine |
| acac | acetylacetone |
| al | aliphatic substituent |
| Ala | L-Alanine |
| ar | aromatic substituent |
| ATP | adenosine triphosphate |
| Asp | L-Aspartic acid |
| Bcl-2 | B-cell lymphoma 2 |
| bip | bipyridine |
| $Bu^t$ | *tert*-butyl group |
| BW | body weight |
| bz | benzene |
| C | cytidine |
| Cys | L-Cysteine |
| COX | cyclooxygenase |
| dha | dihydroanthracene |
| dmso | dimethyl sulfoxide |
| DNA | deoxyribonucleic acid |
| DOSY | Diffusion-ordered spectroscopy |
| dpp | 2,3-bis(2-pyridyl)pyrazine |
| en | ethylenediammine |
| EPR | electron paramagnetic resonance spectroscopy |
| ERK | extracellular signal-regulated kinases |
| ESI-MS | electrospray ionization mass spectroscopy |
| G | guanosine |
| GSH | reduced form of glutathione |
| GSSG | oxidized form of glutathione |
| His | L-Histidine |
| hmb | hexamethylbenzene |
| HSP70 | heat shock protein 70 |
| I | integral (in Chapter 9) |

| | |
|---|---|
| $IC_{50}$ | inhibitory concentration of 50% of cells |
| ICP-MS | inductively coupled plasma mass spectroscopy |
| im | imidazole |
| ind | indazole |
| inda | indane |
| i.p. | intraperitoneal administration |
| i.v. | intravenous administration |
| LDH | lactate dehydrogenase |
| MAP | mitogen-activated protein |
| MTD | maximal tolerated dose |
| MTT | 3(4,5dimethyl-2-thiazolyl)-2,5-diphenyl-2H-tetrazolium bromide) |
| MS | mass spectroscopy |
| NCI | National Cancer Institute |
| NMR | nuclear magnetic resonance spectroscopy |
| NSAID | non-steroid anti-inflammatory drug |
| p.o. | per oral administration |
| *p*-cym | *para*-cymene |
| PCNA | proliferating cell nuclear antigen |
| $Pr^i$ | isopropyl group |
| pta | 1,3,5-triaza-7-phosphatricyclo-[3.3.1.$1^{3,7}$]decane |
| rt | room temperature |
| SD | standard deviation |
| SEM | standard error of the mean |
| T | thymidine |
| tha | tetrahydroanthracene |
| THF | tetrahydrofuran |

# List of Structures

Complexes already known are marked by an asterisk.

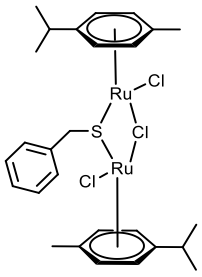


**1**

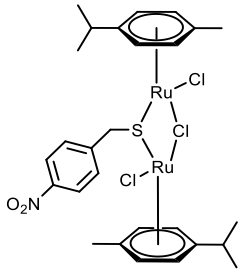


**2**

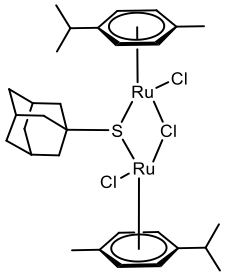


**3**

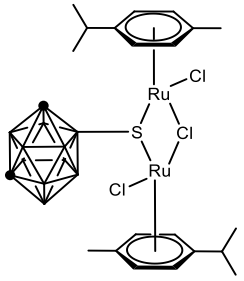


**4**

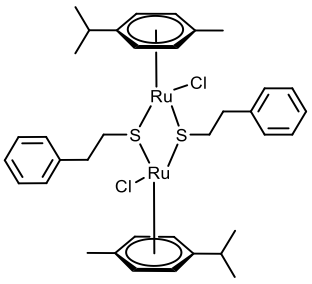


**5***

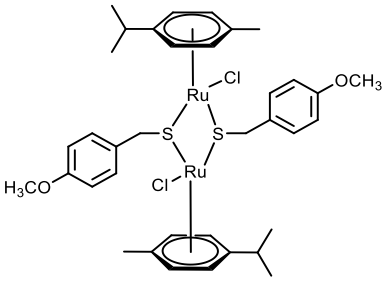


**6**

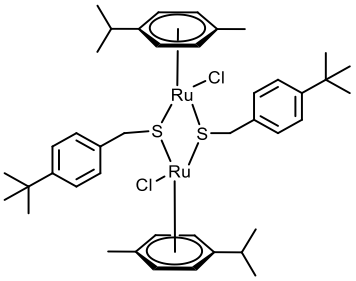


**7***

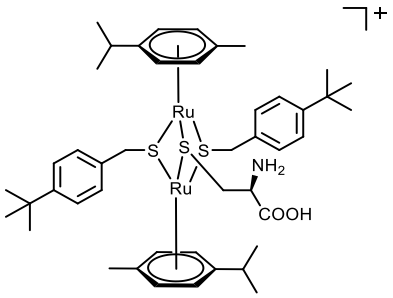


**8**

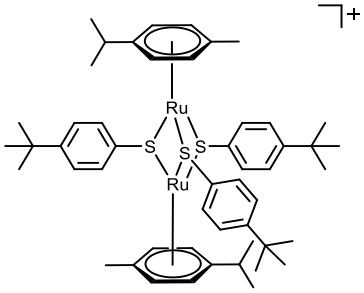


**9***

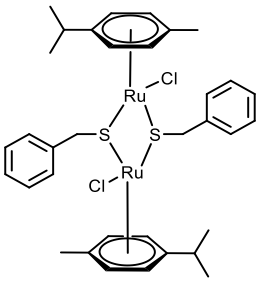


**10***

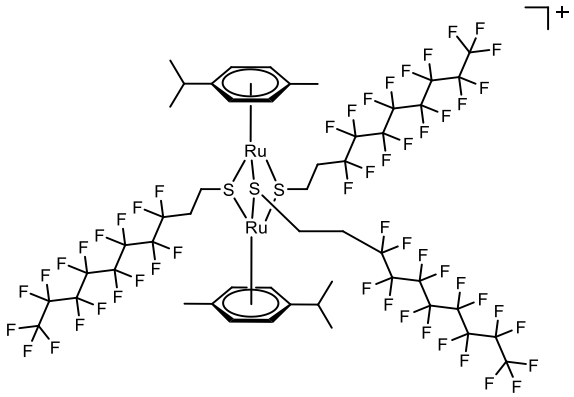


**11**

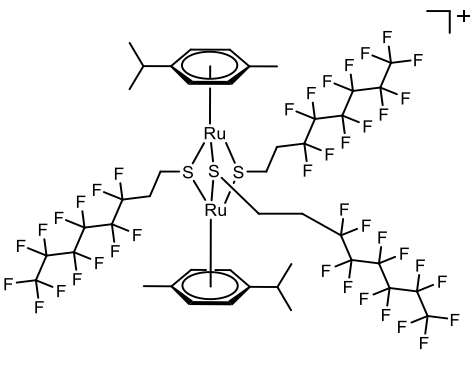


**12**

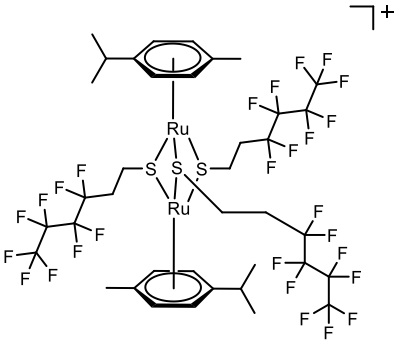

**13**

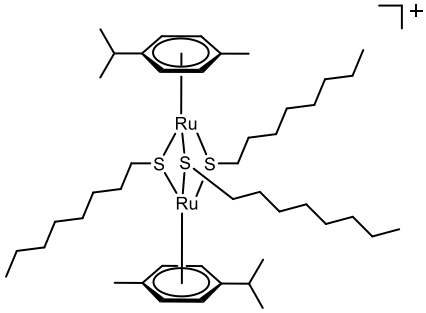

**14**

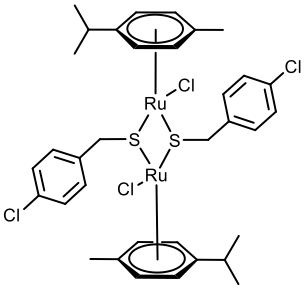

**15**

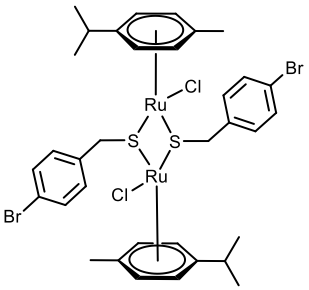

**16**

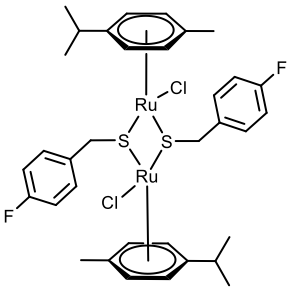

**17**

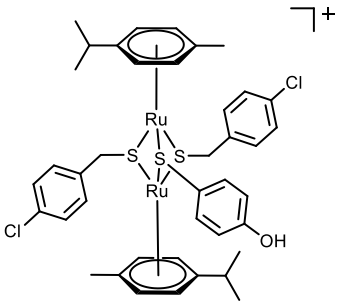

**18**

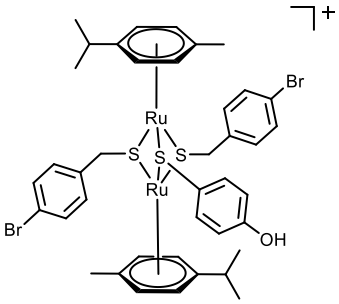

**19**

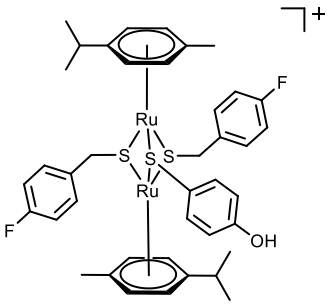

**20**

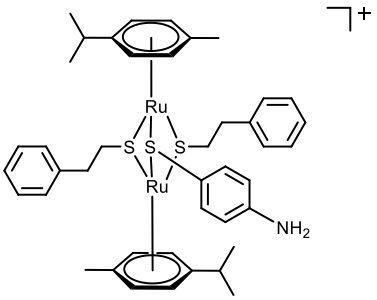

**21**

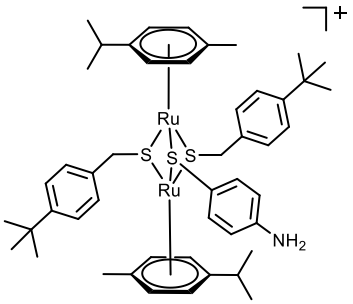

**22**

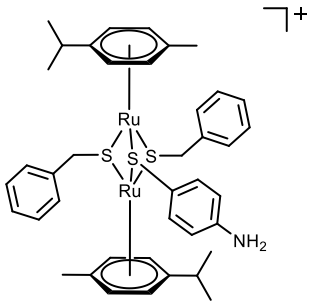

**23**

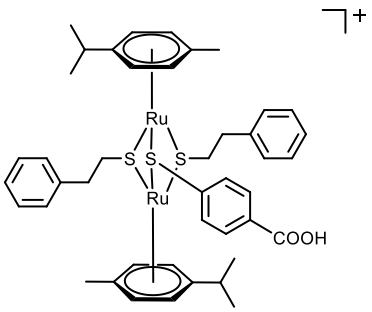

**24**

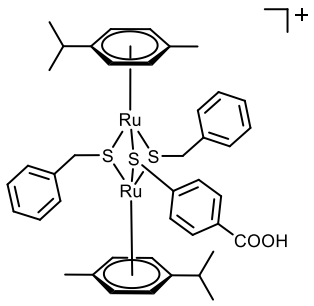


**25**

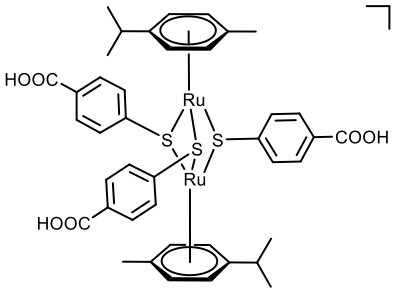


**26**

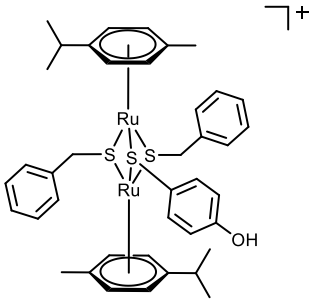


**27***

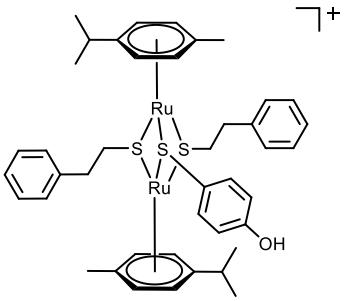


**28***

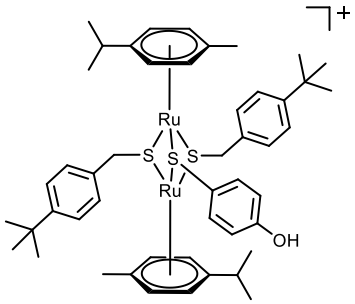


**29***

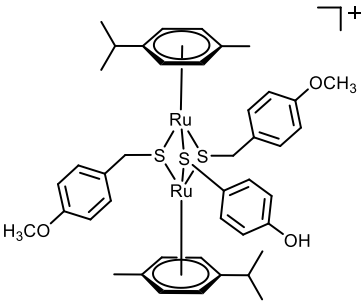


**30**

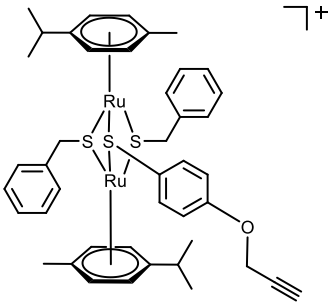


**31**

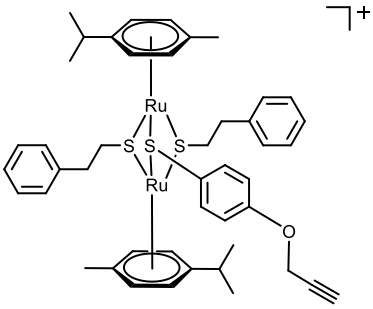


**32**

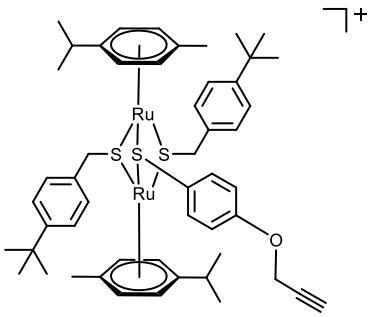


**33**

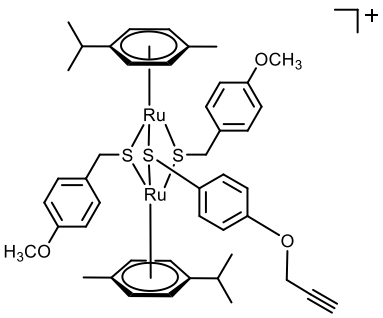


**34**

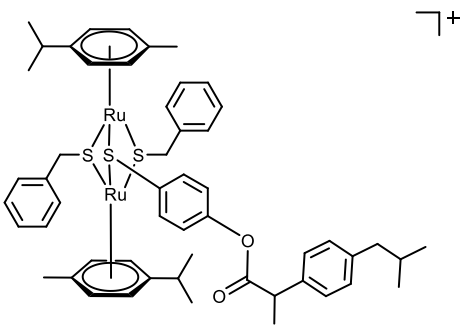


**35**

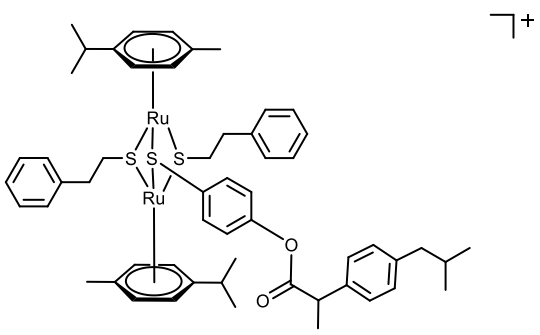

**36**

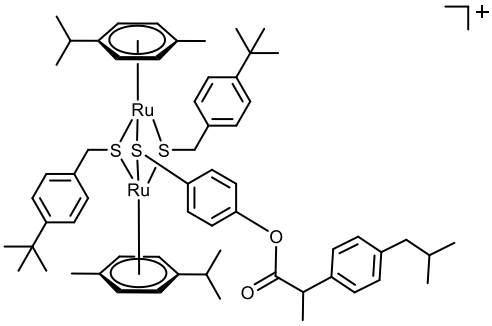

**37**

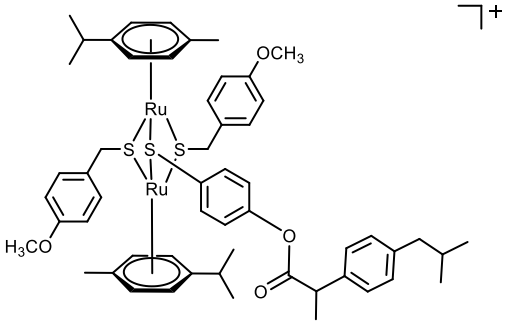

**38**

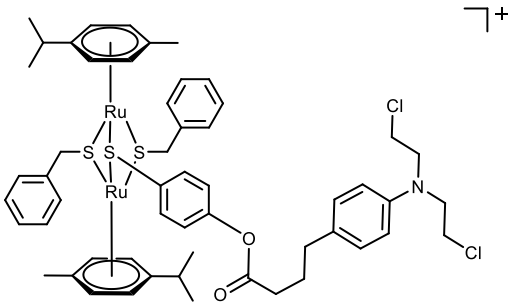

**39**

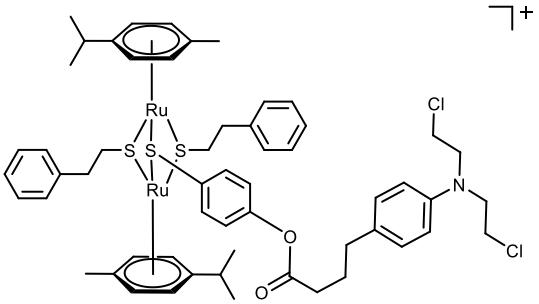

**40**

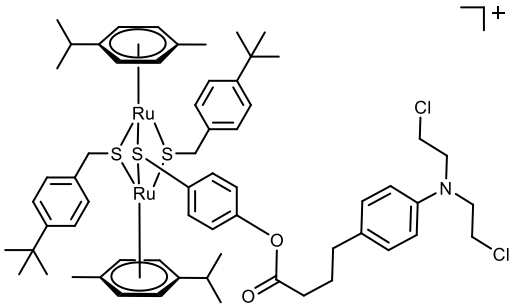

**41**

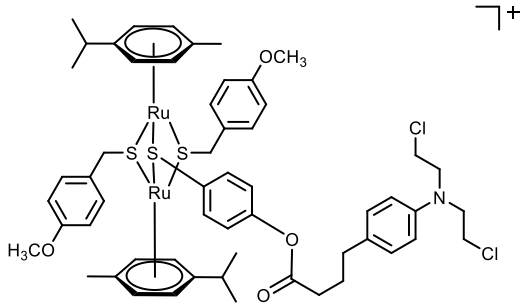

**42**

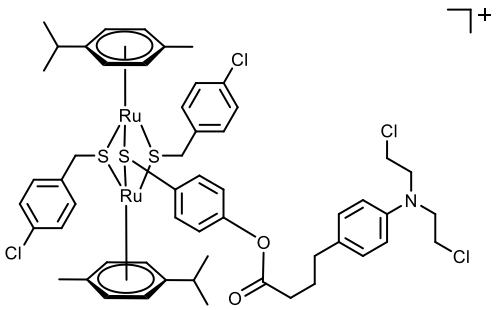

**43**

# List of Figures

# List of Schemes



# List of Tables

# List of Publications and Conference Contributions

**Publications during the PhD studies:**

1. P. Tomšík, D. Muthná, **D. Stíbal**, V. Kasilingam, E. Čermáková, M. Řezáčová, B. Therrien, G. Süss-Fink, *In Vitro* and *In Vivo* Evaluation of the Anticancer Activity of *Diruthenium-2,* a New Trithiolato Arene Ruthenium Complex [($\eta^6$-*p*-$MeC_6H_4$-$Pr^i$)$_2Ru_2$(μ-S-*p*-$C_6H_4OH)_3$]Cl, **in preparation**
2. **D. Stíbal**, B. Therrien, T. Riedel, P.J. Dyson, G. Süss-Fink, Dinuclear arene ruthenium thiolato complexes with fluorinated side-chains, *Inorganica Chimica Acta*, **in preparation.**
3. **D. Stíbal**, F. Giannini, B. Therrien, J. Furrer, G. Süss-Fink, Interactions between dinuclear thiolato-bridged arene ruthenium complexes and biological ligands, *Journal of Bioinorganic Chemistry*, **in preparation.**
4. **D. Stíbal**, B. Therrien, G. Süss-Fink, P. Nowak-Sliwinska, P.J. Dyson, E. Čermáková, M. Řezáčová, P. Tomšík, Chlorambucil Conjugates of Dinuclear *P*-cymene Ruthenium Trithiolato Complexes as Dual Target Anticancer Compounds, *Journal of Medicinal Chemistry*, **in preparation**.
5. **D. Stíbal**, G. Süss-Fink, B. Therrien, Di-(*μ*-phenylmethanethiolato-$\kappa^2$*S*:*S*)-(*μ*-4-hydroxybenzenethiolato-$\kappa^2$*S*:*S*)bis[($\eta^6$-1-isopropyl-4-methylbenzene)ruthenium(II)] tetrafluoroborate, *Acta Crystallogaphica. Section E. - Structure Reports Online*, **submitted**.
6. M.-N. Jeckelmann, **D. Stíbal**, Complexes Cytotoxiques Hydrosolubles De Type [$(arene)_2Ru_2(SR^{al})2(SR^{ar})]^+$ Comme Agents Anticancéreux, *Bulletin de la Société des Enseignants Neuchâtelois de Sciences*, n°46, Hiver 2014-15, Chimie.
7. P. Tomšík, D. Muthná, M. Řezáčová, S. Mičuda, J. Ćmielová, M. Hroch, R. Endlicher, Z. Červinková, E. Rudolf, S. Hanne, **D. Stíbal**, B. Therrien, G. Süss-Fink, [(*p*-$MeC_6H_4Pr^i$)$_2Ru_2$($SC_6H_4$-*p*-$Bu^t)_3$]Cl (*diruthenium-1*), a dinuclear arene ruthenium compound with very high anticancer activity: An *in vitro* and *in vivo* study, *Journal of Organometallic Chemistry*, **2015**, 782, 42-51.
8. **D. Stíbal,** B. Therrien, F. Giannini, L.E.H. Paul, J. Furrer, G. Süss-Fink, Monothiolato-Bridged Dinuclear Arene Ruthenium Complexes: The Missing Link in the Reaction of

Arene Ruthenium Dichloride Dimers with Thiols, *European Journal of Inorganic Chemistry*, **2014,** 34, 5925-5931.

**Previous work:**

1. **D. Stíbal**, J. Sa, J.A. van Bokhoven, One-pot photo-reductive N-alkylation of aniline and nitroarene derivatives with primary alcohols over Au-$TiO_2$, *Catalysis Science & Technology*, **2013**, 94-98.
2. J. Švrček, K. Syslová, **D. Stíbal,** M. Kuzma, P. Kačer, Degradation of biologically active substances by vapor-phase hydrogen peroxide, *Research on Chemical Intermediates,* **2013**, 619-626.
3. **D. Stibal, D**, K. Syslova, P. Kacer, Structural Characterization of Analytic Products Decontamination of Platinum Cytostatics using Hydrogen Peroxide Vapor, *Chemické Listy*, **2012**, 106, S1, S119-S122.

**Conference Contributions**

1) **SCS Fall Meeting 2015**, Lausanne, Switzerland, 4.9.2015, **Poster**
2) **ICBIC17**, Beijing, China, 20. – 24.7.2015, **Flash presentation + Poster**
3) **IABC13**, Galway, Ireland, 12. – 15.06.2015, **Flash presentation + Poster**
4) **SCS Fall Meeting 2014**, Zurich, Switzerland, 9.9.2014, **Poster**
5) **ISBOMC14**, Vienna, Austria, 22. – 25. 6.2014, **Poster**
6) **SCS Fall Meeting 2013**, Lausanne, Switzerland, 6.11.2013, **Poster**
7) **Swiss Summer School in Synthesis and Catalysis 2013**, Villars, Switzerland, 12. – 16.7. 2013, **Poster**
8) **Subject Days** "Modern synthetic methods and their application in the context of Natural products", Neuchâtel, Switzerland, 10 – 11.6.2013, **Oral presentation**

The goal of the presented thesis was to investigate the properties of dinuclear arene ruthenium thiolato-bridged complexes and to establish their potential as anticancer drugs. In the first part of the thesis, several monothiolato, dithiolato and trithiolato complexes were synthesized and evaluated for their stability and reactivity with biological substrates. The results were correlated with the *in vitro* anticancer activity of the three types of complexes and showed the most stable trithiolato complexes to be the most active against ovarian cancer cell lines. Subsequently, the most active trithiolato derivative, *diruthenium-1*, was thoroughly investigated *in vitro* and *in vivo* to establish the mode of action of this complex, showing its promising ability to influence the tumor growth and to prolong the survival of tumor-bearing mice.

In the second part of this thesis, three series of conjugates of the mixed trithiolato complexes were synthesized to demonstrate the potential of the coupling of dinuclear arene ruthenium complexes with biologically active organic molecules. Thus, the thiolato-bridged complexes were coupled with propargyl bromide, the resulting conjugates being available for the 1,3-Huisgen addition with tumor targeting compounds. Conjugates with ibuprofen were synthesized to investigate the effect of the antiinflamatory agent on the activity and selectivity of the resulting complexes towards cancer cells. Finally, conjugates of dinuclear trithiolato arene ruthenium complexes with alkylating agent chlorambucil were synthesized to show the effect of the two different modes of action of the conjugates on their activity *in vitro* and *in vivo*.

These results show the potential of the dinuclear thiolato-bridged arene ruthenium complexes as a versatile platform for the synthesis of anticancer agents with variable biological properties and modes of action.